

The Volcanoes of the Island of Hawaii

Field Trip Guide

Institute on Lake Superior Geology Special Publication 3

Allan MacTavish, M.Sc., P.Geo.

George Hudak III, Ph.D., P.Geo.

December 2023

Table of Contents

1. Introduction 2
1.1. Field Stop and Information Sources: 2
1.2. Field Trip Overview: 3
1.3. 2022 Mauna Loa Eruption: 4
1.4. Acknowledgements: 4
1.5. Photo Credits for Field Guide Cover: 4
1.6. Important Notes on Spelling, Location, Distance, and Units of Volume: 4
2. Geology of the Hawai‘ian Islands 9
2.1. Volcano Descriptions 15
3. Field Trip Stops 40
3.1. Day 1: Kailua-Kona to Hawai‘i Volcanoes National Park 40
3.2. Day 2: Highway 11 and South Point 45
3.3. Day 3 (Part 1): Mauna Loa Road and Mauna Loa Strip 49
3.3. Day 3 (Part 2): Mauna Iki Trail/Ka‘ū Desert Trail and the Southwest Rift Zone 53
3.4. Day 4: Kīlauea Caldera, Kīlauea Iki, Hilina Pali 63
3.4. Day 4 (Part 1): Kīlauea Caldera 64
3.4. Day 4 (Part 2): Koa‘i Fault Zone and Hilina Pali 79
3.5. Day 5 – Chain of Craters Road, Napaū/Mauna Ulu Trail, Hōlei Pali 84
3.5. Day 5 (Part 2) – Chain of Craters Road 102
3.6. Day 5 (Part 1): Helicopter Flight over Kīlauea (Morning) 107
3.6. Day 6 (Part 2): Kīlauea Lower East Rift Zone (afternoon) 110
3.7. Day 7 (Mauna Loa) and Day 8 (Mauna Kea) 119
3.7. Day 7 (Part 1) – Hilo Area 120
3.7. Day 7 (Part 2): Saddle Road (Highway 220) and Mauna Loa Observatory Road 123
3.8. Day 8 – Mauna Kea Summit Road 129
3.9. Day 9: Mamalahoa Highway (Hawai‘i Belt Road; Hāmākua Coast) 133
3.10. Day 10 – Kohala Volcano – Waimea to Hāwī 138
3.11. Day 11 – Waimea to Kailua-Kona 146
4.1. Glossary References 168
5. Field Guide References 172

1. Introduction

The original version of this field guide was written to accompany the successful Institute on Lake Superior Geology (ILSG)-sponsored 'Volcanoes of the Island of Hawai'i' Field Trip' that took place between February 11 and 21, 2020. The aims of the field trip were to observe the characteristics of modern volcanoes in an intra-plate, non-rift environment (*see* Figure 1) and to provide contrast and comparison with modern and ancient rift environments (i.e. North American Mid-Continent Rift (MCR); Mid-Altlantic Rift in Iceland).

The 9 main Hawai'ian Islands are shown in Figure 2. This field trip is confined to the Island of Hawai'i, which is the easternmost and largest island of the chain and is host to 5 extinct, dormant, or active volcanoes (*see* Figure 3). Short volcano descriptions are given within this introductory section immediately below (USGS HVO website); whereas longer descriptions, including 2 associated submarine volcanoes, will be presented in the 'Volcano Descriptions' sub-section of the 'Geology of the Hawai'ian Islands' section, also below:

1) ***Kīlauea*** (4009ft, 1222m), is the most active subaerial (exposed above sea level) volcano on earth and was continuously active between 1983 and 2018, mainly in the vicinity of the Pu'u Ō'ō vent; however, the 35-year eruption ended after a caldera subsidence event and a voluminous 3-month eruption from the Lower East Rift Zone occurred between April 30 and August 9, 2018. After the 2020 field trip there have been three successive eruptions at the volcano's summit, all consisting of a lava lake that began infilling the 2018 caldera subsidence crater centred on Halema'uma'u Crater. The first eruption began on December 20, 2020 and ceased on May 13, 2021; the second commenced on September 29, 2021 and ended on December 9, 2022; and the third began less than a month later on January 5, 2023 and is ongoing.
2) ***Mauna Loa*** (13,681ft, 4170m) is active and the largest, most massive volcano on earth; after last erupting in 1984 Mauna Loa began erupting from fissures within its summit caldera on November 27, 2022. The vigorous eruption migrated north to several fissures located on the upper Northeast Rift Zone on the 28th where lava continued to flow until the eruption was declared over on December 10, 2022 (USGS HVO Website).
3) ***Mauna Kea*** (13,803ft, 4207m) is considered by some to be active, but is presently within the waning stages of activity (i.e., dormant); Mauna Kea last erupted at ~3300 BP (Before Present);
4) ***Hualālai*** (8278ft, 2523m) is in its waning stages of activity and last erupted in between 1801 and 1802; and
5) **Kohala** (5480 ft, 1670m) is considered extinct; it is deeply eroded with its last eruption occurring at ~100,000 BP.

This version of the guide is no longer designed to be used by a specific field trip group (i.e. the 2020 group) and has been modified to be used by anyone, or any group, who so wishes to examine the volcanology of the island. Since the primary author (AM) is very visual-centric this guide contains a large number of photographs and maps. This is primarily to help those using the guide to more readily find and identify field trip outcrops and other described features. Also, the guide has, in some ways, become a travelogue of the 2020 field trip with many of the included photos taken during that trip and an earlier field field trip reconnaissance completed by the primary author (AM) in August 2019.

1.1. Field Stop and Information Sources:

Several excellent, pre-existing geological field guides, written by experienced and knowledgeable authors, and publications available from the US National Park Service (NPS) were critical to the preparation of this guide. Those used (in no particular order) were: Hazlett (2014); Hazlett and Hyndman (2007 edition of 1996 book); Easton and Easton (1995); Robinson (2010, 2012); Merguerian and Okulewicz (2007); Tilling et. al. (2010); and the NPS Mauna Ulu Eruption and Kilauea Iki Trail guides.

Full source citations are listed in the reference section of this guide. Some field stops were generated, and others discarded, after a field reconnaissance using a preliminary version of the guide was completed by AM during the summer of 2019. Also, several field stops were added after the 2020 field trip using descriptions and locations discovered and then generated by AM during the field trip.

Both the satellite and street views of Google Earth Professional were of inestimable use for planning, locating, and examining field stops proposed for the original version of the guide. AM cannot stress how important it was to have the ability, within a few minutes to examine, download a high resolution image, and obtain a UTM location of a proposed stop while sitting in front of a computer located over 4100mi (6600km) away in northwestern Ontario. Google Earth is an incredible resource, particularly Google Earth Street View.

1.2. Field Trip Overview:

This 11-day field trip consists of 96 stops and 49 sub-stops. The suggested daily field trip routes are shown in Figure 4; however, those using this guide do not have to stick to the routes or visit all of the stops shown. The daily routes were designed to decrease daily driving distances and radiate, or extend linearly from the accommodations used during the 2020 field trip. One recommended variation of the routes given would be to modify the days such that the shortest hikes are done first and the longest hikes are done last. This allows participants to a build-up a conditioning level over the course of the field trip making each successive hike easier to complete. Experience during the 2019 summer reconnaissance by AM clearly showed that reordering the hikes from shortest to longest with 1 or 2 non-hiking days between hikes worked well during the 2020 trip, particularly for the older participants.

The helicopter tour completed on the morning of Day 6 of the 2020 field trip provided an excellent overview of the structure and eruptive activity of Kīlauea, helped add perspective and scale to the surface visits, and hopefully tied the many Kīlauea stops into a cohesive whole. Those using this guide do not have to take a helicopter tour, or if taking a tour, even to use the route shown in Figure 4. The authors strongly recommend taking a helicopter tour if your trip budget allows. It is surprisingly affordable and well worth the cost, particularly if you can fill the helicopter with your group. There are several tour companies operating out of the International Airports in Hilo and Kailua-Kona that offer packaged aerial tours over Kīlauea. The 2020 field trip chartered 2 Bell 407 aircraft from Paradise Helicopters in Hilo who, since we chartered the helicopters rather than booking an existing fixed tour, allowed us to tailor the specific route flown within the chartered time-frame (paid by the hour rather than by a per/person cost. Over the last 15 years AM has taken many helicopter flights over the islands and volcanoes of Hawai'i and every flight was well worth the cost.

Participants of the 2020 field trip mainly stayed in budget accommodation in order to keep field trip costs within a reasonable range. These accommodations included the Kīlauea Military Camp (dormitory accommodations, 8 nights), the Kamuela Inn in Waimea (2 nights), and the Marriott Courtyard King Kamehameha's Kona Beach Hotel (Kailua-Kona, 1 night). Of course, users of this guide can stay where-ever they wish, again depending upon their trip budget.

For the most part, meals were not provided during the 2020 trip. The Kīlauea Military Camp has restaurant facilities for breakfast and dinner meals. The food is relatively basic, but quite good and bag lunches are available for purchase with notice given the night before.

This guide initially contained daily road logs; however, those logs were cumbersome and took up a lot of space. After the 2019 reconnaissance trip it was decided to drop the road logs and state all stop locations in the appropriate UTM GPS co-ordinates. Most people now own, and can effectively use, handheld GPS units (particularly geologists) and many rental vehicles now have built-in GPS units.

1.3. 2022 Mauna Loa Eruption:

With impeccable timing the most recent eruption of Mauna Loa (November 27 to December 10, 2022) began just as final edits were being completed on this guide. This obviously threw a major spanner (wrench to American readers) into the works, particularly the field trip stops planned for the afternoon of Day 7. This required a revision of the Mauna Loa information, including the addition of a short history of the new eruption (with maps and photographs) and the inclusion of a new stop where the road was truncated by the new 2022 flow field (USGS HVO website). None of the originally planned stops were destroyed by the advancing flows; however, the upper 2 stops became inaccessible once the upper half of the road was cut off by 2022 Fissure 3 and 4 flows. Some of the stops planned for the lower half of the road are probably now unnecessary (and probably less interesting) with the presence of a nearby new flow field, but have been left in the guide as contrast to the flows from the new eruption. Therefore, the afternoon of Day 7 was modified to fit the current conditions.

The authors cannot in good conscience add other new stops to the guide without visiting the potential sites beforehand, either in person or using Google Earth, other than the point where the easternmost flow of the eruption (a single Fissure 4 flow) cut the Observatory Road. Google Earth will not complete a ground resurvey the Mauna Loa Observatory Road until access is restored to the observatory, which could be several years. However, we do recommend driving the Mauna Loa Observatory Road as far as is allowed, or is possible, to examine the new flow field at your leisure. The existing stops past where the road was truncated have been left in the guide so that they can be visited once the road is re-established.

1.4. Acknowledgements:

There are 2 people who need to be gratefully acknowledged for their contribution to the success of the 2020 field trip and ultimately, this final, albeit revised version of the field guide:

- **Peter Hinz, H.B.Sc., P.Geo.** (Ontario Geological Survey, retired) who, along with AM (the field trip leader) was co-organizer of the trip. The trip would not have happened, or proceeded in such a relatively flawless manner, without his considerable input, his wonder and fascination with the rocks, and his constant good humour.
- **Dr. Prajukti (Juk) Bhattacharyya** (Professor of Geology, University of Wisconsin, Whitewater). Juk had registered for the originally planned August 2019 field trip, but could not participate after it was postponed to February 2020. She graciously agreed to be AM's extremely overqualified "field assistant" for the 2-week field reconnaissance completed in July and August 2019. The resulting trip would not have been as successful without her help.

1.5. Photo Credits for Field Guide Cover:

Clockwise from the upper left: Pu'u Pua'i cinder cone and Kīlauea Iki crater, A.D. MacTavish (2008); lava falls entering the Pacific Ocean, south flank Kīlauea, A.D. MacTavish (2011); 'a'ā flow crossing Makamae Street, Leilani Estates, May 6, 2018, Lower East Rift Zone, USGS HVO website; steam escaping from mostly buried lava tube within the active Pu'u Ō'ō flow field, A.D. MacTavish (2008).

1.6. Important Notes on Spelling, Location, Distance, and Units of Volume:

- Since the primary author (AM) is Canadian all spelling within the body of the guide is British/Canadian standard. The exception is the 'Glossary of Volcanic Terms' compiled by the guide's co-author, George Hudak in 2020. He used US standard spelling practices.
- The GPS datum for all locations stated is UTM Zone Q5, WGS84.
- Distance and volume units are stated initially in imperial units (US standard) followed by the corresponding metric units (world standard) in brackets; i.e., 100ft (33m).

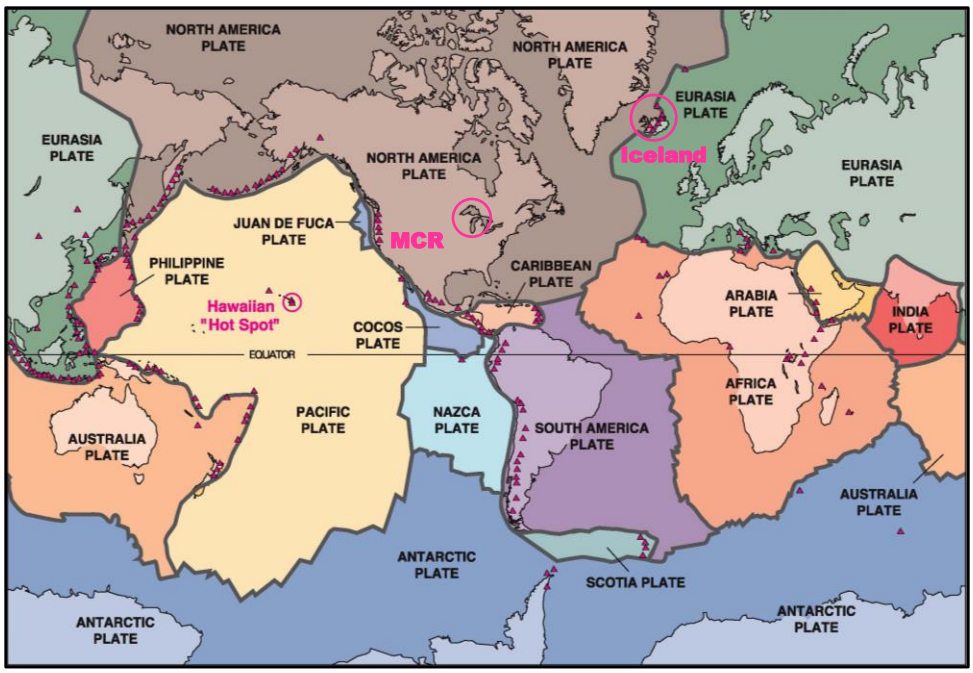


Figure 1: Location of the Hawai'ian Islands with respect to world tectonic plates, the MCR, and Iceland. Modified after Tilling et al., 2010.

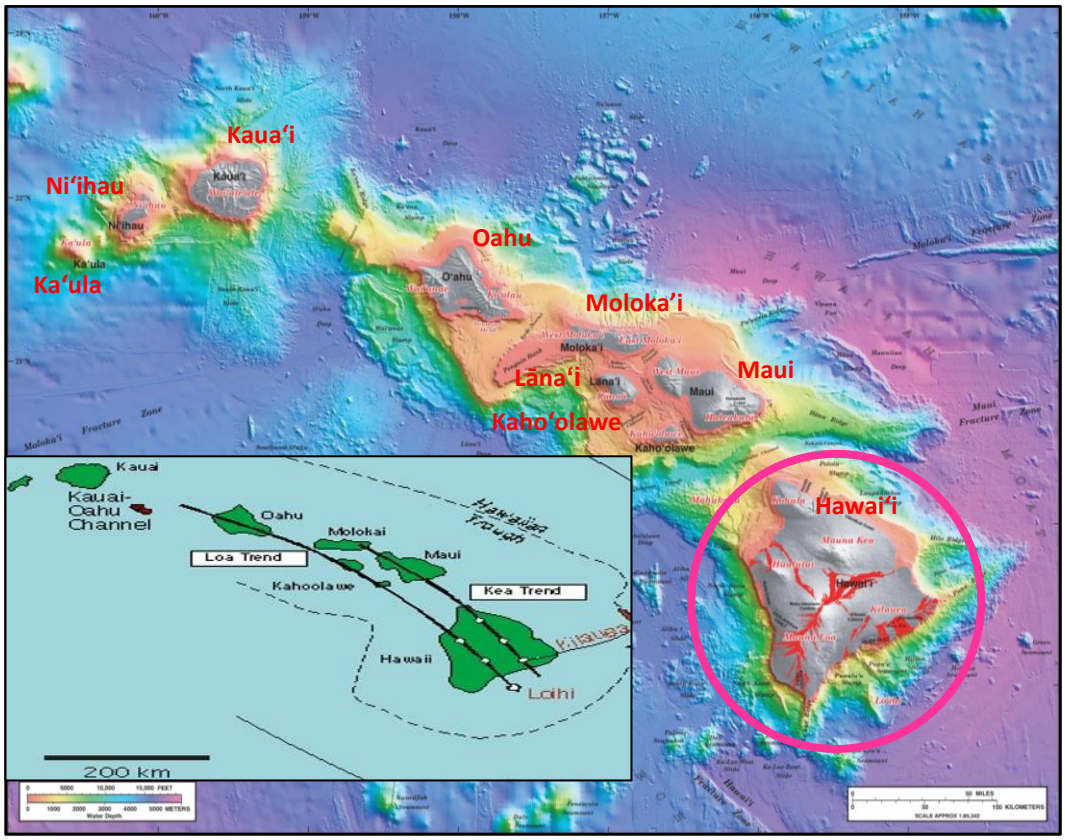


Figure 2: Topographic relief and bathymetric map of the nine main Hawai'ian Islands. Modified from Easton et al., 2003. The inset shows the Kea and Loa volcanic trends first postulated by Dana in the 1840's (Figure modified from Gazdar, 2003).

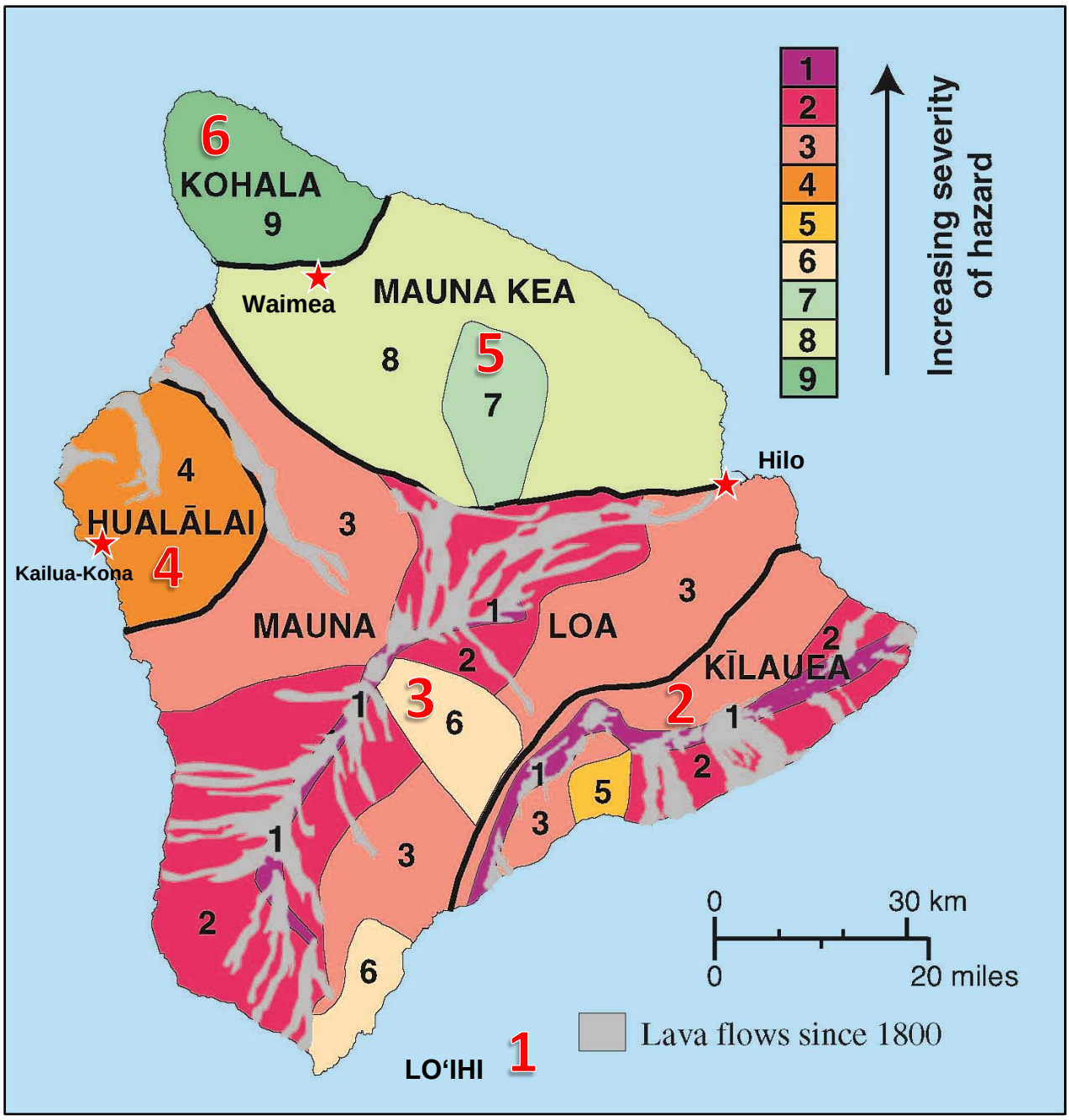


Figure 3: Volcanic Hazard Map of the Island of Hawai‘i. Each volcano associated with the island is named and numbered (in red) according to age from youngest, Lo‘ihi (1) to the oldest, Kohala (6). Volcanic hazard severity is shown by the smaller black numbers with the hazard key at the top right of the figure. The estimated location of Lo‘ihi is shown by the #1. Figure modified after USGS Volcanic Hazard Map from Lava Flows (2010) downloaded from temblor.net website.

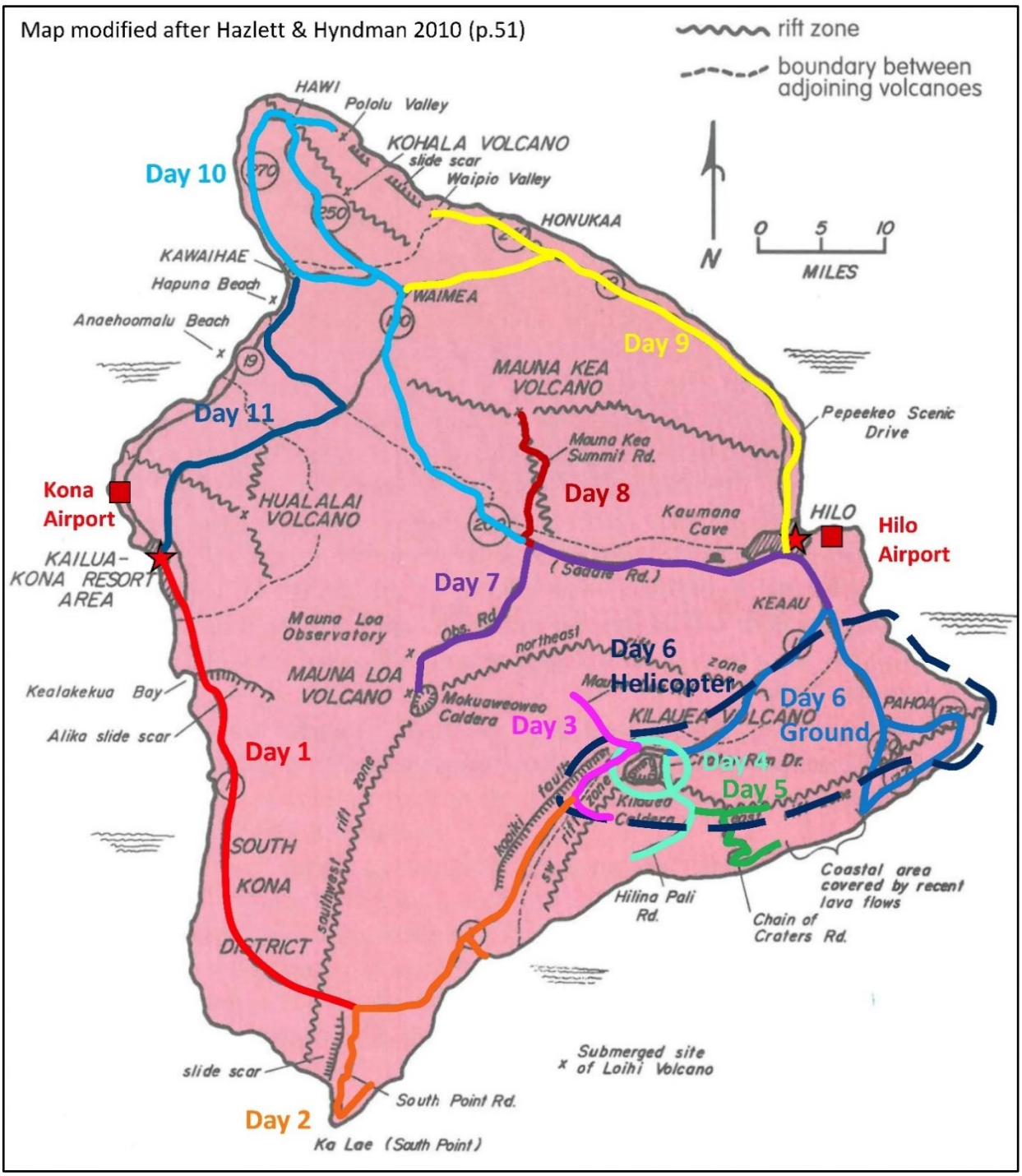


Figure 4: The 11 planned daily field trip routes for the Island of Hawai'i presented within this guide. Modified from Hazlett and Hyndman, 2007 (p.50).

Table 1: Suggested Field Trip Itinerary

Day	Suggested Accommodation and Location	Activity Summary	Planned Stops
0	Kailua-Kona; there are a variety of hotels, condos, or B&Bs available	Night before start of the field trip	None
1	Kīlauea and Volcano; Kīlauea Military Camp (KMC); Volcano House Hotel; or B&Bs in the Village of Volcano	Drive to Kīlauea; geology of Mauna Loa southern flank; Kealakekua Bay and pali; Puʻuhonua o Hōnaunau (Place of Refuge)	D1-1 to D1-7
2	Same as Above	Punaluʻu Black Sand Beach; Ka Lea (South Point); Pāhala Ash; and Papakōlea green sand beaches	D2-8 to D2-9b
3	Same as Above	Part 1: Mauna Loa Road and Scenic Lookout; Part 2: Kīlauea Southwest Rift Zone; Kaʻū Desert trail; Keanakākoʻi Ash; fossilized footprints; Mauna Iki shield	Part 1: D3-10 to D3-14 Part 2: D3-15 to D3-25
4	Same as Above	Part 1: Kīlauea Caldera; Kīlauea Iki trail; Devastation Trail; Keanakākoʻi Crater; Part 2: Koaʻi Fault Zone; Hilina Pali Road	Part 1: D4-26 to D4-32 Part 2: D4-33 to D4-38
5	Same as Above	Part 1: Chain of Craters Road; Na Paū Trail; Puʻu Huluhulu; perched lava lake; Mauna Ulu summit and lava channels Part 2: Hōlei Pali; Puʻu Loa trail and Puʻu Loa Petroglyphs; Hōlei Sea Arches; Roads End; and Puʻu Oʻo flow field	Part 1: D5-39 to D5-41 Part 2: D5-42 to D5-49
6	Same as Above	Part 1: Guided helicopter tour of Kīlauea summit caldera, Southwest and East Rift zones, Mauna Ulu, Puʻu Oʻo Lower East Rift Zone (LERZ); southern coastline Part 2: June 27th Flow (Pāhoa); New Kaimu Black Sand Beach, MacKenzie State Park; 2018 LERZ eruption flow fields; Rifts 8, 9, 12; 20,21 (Leilani Estates)	Part 1: D6-50 Part 2: D6-51 to D6-58
7	Same as Above; alternate hotels and B&Bs in Waimea	Part 1: Hilo area; Coconut Island Park; Tsunami Park; Rainbow Falls; Kaūmanu Cave Part 2: Saddle Road; Puʻu Huluhulu; Mauna Loa Observatory Road; 2022 Mauna Loa flows; multicoloured flows, Mauna Loa Observatory, & lava flow diversion barriers if Mauna Load Road has re-opened	Part 1: D7-59 to D7-61 Part 2: D7-62 to D7-68
8	Same as Above; or alternatively hotels and B&Bs in Waimea	Mauna Kea Summit Road; Puʻu Kalapeamoa cinder cone; Mauna Kea Visitors Centre; Ellison B. Onizuka Astronomical Complex; Lake Waiau Trail; Mauna Kea Observatories; and summit	D8-69 to D8-75
9	Waimea; Kamuela Inn or other area hotels and B&Bs	Mamaloa Highway from Hilo to Waipio Valley and Waimea; NE coast Mauna Kea geology; Hawaiʻi Tropical Botanical Gardens; ʻAkaka Falls; Lauapāhoehoe flows; Waipiʻo Valley; Kohala Saddle	D9-76 to D9-81
10	Waimea; Kamuela Inn or other area hotels and B&Bs	Kohala Volcano; Puʻu Kawaiwai cinder cone; benmoreite flows; Pololu Valley; residual boulders; Moʻokini Luakini and King Kamehameha birthplace; Lapakahi State Park; Mugearite flows; pseudodykes	D10-82 to D10-91
11	Kailua-Kona, Hawai'i; there are many hotels, condos and B&B's available	Last field trip day; Mauna Kea West Rift Zone and cinder cone field; Hapuna Beach basaltic ankaramite lave; Hualālai and 1959 Mauna Loa flows contact; Hualālai trachyte flows; Pu'u Waʻawaʻa trachytic cinder cone; Kaʻūpūlehu flow Scenic Lookout; Hualālai Northwest Rift Zone	D11-92 to D11-96

2. Geology of the Hawai‘ian Islands

The Hawai‘ian Islands are the best-known examples of oceanic intraplate volcanoes (those which lie within tectonic plates). Another oceanic example would be the Canary Islands. Not all intraplate volcanoes are oceanic, many are continental such as the volcanoes of the Yellowstone volcanic system in North America and the Quaternary volcanic fields of the Eifel Region in Germany (Schmincke, 2004). About 25% of the world's volcanoes are of the intraplate variety (Lockwood and Hazlett, 2010) and are thought to be related to 'hot spots', also referred to as 'melting sources' (Lockwood and Hazlett, 2010) and 'mantle plumes' (Morgan, 1971).

According to Foulger and Anderson (2006) the Hawai‘ian Islands are part of the ~70 million-year-- old, ~3230mi (5200km) long Hawai‘ian-Emperor Chain comprising more than 100 individual seamounts, atolls, islands, and volcanoes. From the Island of Hawai‘i the chain extends west-northwestward for ~1680 mi (2700km) to Yuryaku Seamount (near Midway Atoll) as the Hawai‘ian Ridge, where it abruptly bends north-northwestward and extends for another ~1550mi (2500km) to the western end of the Aleutian Trench as the Emperor Seamount Chain (Lockwood and Hazlett, 2010). The oldest island in the Hawai‘an chain is ~25-million-year-old Kure Atoll and the youngest is the still forming Island of Hawai‘i (commonly referred to as the Big Island).

The distinctive northwest-southeast alignment of the Hawai‘ian chain was known to the early Hawaiians. Their legends clearly reveal that they recognized that the islands were progressively younger from the northwest to the southeast.

The first geologic study of the Hawaiian Islands (1840-1841) was directed by James Dwight Dana (Dana, 1890) who deduced that the islands young to the southeast from the differences in their degree of erosion. He also suggested that other island chains in the Pacific showed a similar general decrease in age from northwest to southeast.

The 9 main islands of the Hawaiian chain are composed of 15 volcanoes apparently comprising two strands of volcanoes located along distinct but parallel curving pathways. Multiple volcanoes line up to form each strand. Dana (1890) coined the terms Loa and Kea series for the two prominent trends. The Kea trend includes Kīlauea, Mauna Kea, Kohala, East Maui (Haleakalā), and West Maui volcanoes. The Loa trend includes Kama‘ehuakanaloa (Lō‘ihi), Mauna Loa, Hualālai, Mahukona (a submerged volcano and the original volcano comprising the Big Island), Kaho`olawe, Lana`i, West Moloka`i, and possibly Kaua‘i (Figure 2). The pair of volcano trends may exist all the way along the Hawaiian and Emperor chains, though this is less clear amongst the older islands and seamounts (Clague and Dalrymple, 1987).

Relative age of an island or atoll can be determined based on its state of growth or erosion (Mattox, 1994). The Hawaiian archipelago rides on the northwesterly moving Pacific Plate. The oldest islands of the archipelago are located far to the northwest of the main Hawaiian Islands. The youngest member of the chain, Kama‘ehuakanaloa (Lō‘ihi), is presently forming as a submarine seamount ~ 19mi (30km) south of the southern coastline of the Island of Hawai‘i. The Big Island is approaching mid-life, while Lō‘ihi is still submerged. By contrast, Kure and Midway atolls are in the final stages of the life cycle of an island. The formation of fringing reefs combined with gradual sinking and erosion of an island causes it to eventually disappear from the surface of the ocean. During this process, reefs grow vertically (upward) and begin to surround the island, eventually becoming separated from the island by a lagoon. If sinking continues, the island disappears and only a circular reef remains - an atoll. Eventually, once the reef sinks below the surface, the original island becomes a submerged, flat-topped guyot. Most of the ancient volcanoes comprising the northwestern Hawai‘ian and Emperor chains are now guyots.

Physically, Hawai‘ian volcanoes exhibit distinct developmental eruptive stages and, from birth to the post-shield/declining stage, their life-span is usually <1,000,000 years. The available references rarely agree on the number of stages and the various lists contain between 4 and 10 stages and substages. The most common listings comprise between 6 and 8 distinct stages. The stages below are a fusion of data from Moore and Clague (1992), Clague and Sherrod (2014), Mattox (1994), and Seach (2022) and consists of 7 stages with the shield stage split into 3 sub-stages:

1. ***Initial Deep Submarine Pre-Shield Stage:*** This initial stage of Hawai‘ian volcano growth is characterized by infrequent, small-volume, effusive alkalic eruptions with pillowed lava flows forming an unstable edifice with up to 45^{o} slopes and a summit caldera (*see* Figure 5-1). Rock-types comprise basanite, alkalic basalt, and transitional basalt. The steep slopes are due to the alkalic composition of the flows which is more viscous than shield stage tholeiitic basalt. Inherently unstable, steep-sided seamounts composed of immense piles of uncemented, watermelon-shaped lava pillows tend to collapse many times before reaching the ocean surface. The only Hawai‘ian volcano presently at this stage is Lō’ihi which has recently been renamed Kama‘ehuakanaloa .
2. ***Shield Stage:*** This is the most voluminous stage of Hawaiian volcanism where more than 95% of the volume of the tholeiitic basalt of a Hawaiian volcano is erupted over a period that may last up to 2 million years. The oceanic crust of the Pacific Plate, unaccustomed to the enormous weight of the volcanoes building atop it, subsides greatly during this stage, as much as 3mm per year. Mauna Loa and Kīlauea are both within this stage of development. Mattox (1994) splits the shield building stage into Stage 2 Submarine, Stage 3 Sea Level (termed emergent above), and Stage 4 Subaerial stages. Clague and Dixon (2000) place Kīlauea into a shield explosive phase (low-elevation subaerial shield) where the volcano exhibits effusive, strombolian, and Hawaiian eruption styles interspersed with phreatomagmatic explosive episodes. Possible examples of this were the phreatomagmatic explosions that accompanied the recent 2018 Kīlauea summit caldera collapse.
    a. ***Submarine Shield Sub-stage:*** Early shield-building eruptions are entirely underwater during this stage (*see* Figure 5-1) and occurs after the switch from alkalic to tholeiitic volcanism. After the switch in chemistry the rate of growth of the volcano exceeds the rate of subsidence due to the increase in eruptive volume. The bulk of the material produced is tholeiitic in composition with voluminous eruptions of pillowed flows. Volcanic edifice slopes during this stage are in the 10 to 20^{o} range There is no explosive eruptive activity due to water depth.
    b. ***Emergent or Sea-level Shield Sub-stage (none at this present time):*** Eventually the volcano approaches, and then emerges, above sea level with a combination of effusive, Hawaiian, and strombolian volcanism, interspersed with explosive phreatomagmatic eruptions due to the decrease of confining water pressure. At this point an island begins to form (*see* Figure 5-2). Phreatomagmatic pyroclastic debris (known as hyaloclastite) covers the submarine sub-stage pillowed flows and steepens the flanks of the emerging volcanic island to between 10 and 15^{o} (Figure 5-2). Wikipedia refers to this as the *explosive phase* which lasts to when the volcano has sufficient mass and height (1000m or 3000ft) and the interaction between sea water and lava finally fades.
    c. ***Subaerial Shield Sub-stage:*** This is the dominant above sea level growth stage and results in the formation of a permanent island by very frequent (almost continuous), voluminous, central- and rift effusive Hawaiian eruptions and the production of ‘a‘ā and pāhoehoe flows (*see* Figure 5-3). Calderas and pit craters form repeatedly, continued submarine and sea level eruptions expand the volcano outwards and with time only a

small percentage of tephra erupts from the volcano. The slopes of the volcano during the subaerial shield stage vary between 3 and 10^{o} and are responsible for the characteristic shape of a shield volcano. The cover of fluid, very thin, but dense flows produced during this stage sits precariously upon the weak support of the underlying pillowed flows and hyaloclastites. This weak, unstable base often results in large blocks of the island sliding into the sea and causing enormous, extremely destructive tsunamis with wave heights that can exceed 350m.

3. ***Post-shield, Capping, or Declining Stage:*** During this stage eruption volumes decrease and the summit magma chamber solidifies. Transition to post-tholeiitic volcanism is gradual and can last up to 100,000 years with post-shield lavas comprising only a small part of the total erupted volume. The eruption rate usually decreases to zero over a span of between 500,000 and 1 million years. The short-lived, periodic eruptions of this stage tend to cap the volcano with a steep, hummocky carapace of short-length alkaline lava flows and clusters of steep-sided cinder cones (*see* Figure 5-4, Declining Stage). These lavas typically consist of alkalic basalt, hawaiite, and trachyte and commonly fill and overflow the shield-stage caldera. Explosive eruptions become more common because alkaline flows are more viscous in nature.
4. ***Erosional Stage:*** The post-shield stage is followed by a stage where erosion and subsidence are dominant over lava production. During this stage deep canyons and sea cliffs may form along the flanks of the volcano (*see* Figure 5-5; e.g., Kohala volcano) and the island begins to shrink in size. As the volcanic islands erode and subside, fringing coral reefs grow.
5. ***Post-Erosional or Rejuvenated (Renewed) Stage:*** Volcanism of this stage is characterized by strongly alkaline, strombolian to effusive, sometimes phreatomagmatic, volcanism (*see* Figure 5-6). Rock-types produced include melilitite, nephelinite, basanite, and alkalic basalt. This stage is characterized by low eruption rates with sporadic activity that may occur over several million years and comprise much less than 1% to the cumulative eruptive volume of a volcano. Most Hawaiian volcanoes do not pass through this stage; however, those that do exhibit periods of erosion that may precede or be interspersed with the eruptions. Lavas commonly erupt through reefs that form offshore as erosion progresses or near the shoreline to produce volcanic maars (e.g., Diamond Head on O‘ahu). There are no Hawai‘ian volcanoes presently within this stage; however, Haleakalā is thought by some to represent an early form of the stage. This stage may be related to remelting of still hot rocks at depth beneath the volcano due to decompression caused by uplift accompanying erosion of the volcanic edifice.
6. ***Atoll Stage:*** This stage occurs after erosional processes and subsidence due to the increasing weight of the cooling seafloor eventually lowers the surface of a subaerial volcano to sea level forming flat islands surrounded by coral reefs (*see* Figure 5-7). Midway and Kure Islands are examples of Hawai‘ian atolls. As the island continues to subside the reefs grow further and further away from the volcanic edifice forming broad lagoon-like planes.
7. ***Late Seamount or Guyot Stage:*** Erosional processes and subsidence eventually overtake reef building and the island sinks below the ocean’s surface to form an elevated flat-topped submarine seamount surrounded by, and capped by, dead, submerged coral reef remnants (*see* Figure 5-8). This type of seamount is referred to as a *guyot*.

Walker (1990) has described four styles of Hawai‘ian volcanic activity which are summarized below:

1. ***Hawai‘ian:*** This is the most common style and is characterized by fountains of gas-rich foamy lava (pumice) spurting from a fissure and being torn into tatters as it flies through the air. Fountain height depends upon lava volumetric discharge rate and gas content and ranges from <5m to >500m (Head and Wilson, 1989). Most of the lava erupted by this style forms pyroclastic spatter deposits such as spatter cones, rings, or ramparts of various heights, diameters, or lengths. If the fountain is concentrated enough some of the lava will flow away. Most of the modern eruptions from Kīlauea are of this style.
2. ***Strombolian:*** This style results from both higher gas content and viscosity when compared to Hawai‘ian-style and results in a higher eruptive column and a more highly fragmented lava producing scoria or cinders that cool significantly before landing. This activity forms cinder cones ranging from 50 to 200m in height, with 100 to 200m diameter craters, and extensive cinder deposits located around or downwind of the cones. This style characterizes the declining as well as rejuvenated volcanism stages. Examples include the spectacular-coloured cinder cones within the erosional summit crater of Haleakalā and the slopes and summit of Mauna Kea.
3. ***Surtseyan:*** Surtseyan eruptions occur in shallow water (emergent sub-stage) or along sea coasts where large amounts of water interact violently with ascending lava within the vent. This results in a characteristic large, ascending, steam cloud (eruption column) producing highly fragmented lava in the range of sandy and glassy ash. This material accumulates around the vent forming an ash ring which, with time, form indurated tuff rings such as Diamond Head (on O‘ahu) and Kapoho Crater (on the Big Island).
4. ***Phreatic:*** Phreatic steam-flash eruptions are very violent and sometimes occur at the summit of Kīlauea when lava drains back into the magma conduit system and interacts with hot groundwater trapped within the conduits. This eruption-style was responsible for the explosive eruptions and spectacular, debris-laden eruption columns that were produced from Kīlauea’s summit caldera between May and August 2018 after the 10yr old lava lake resident within Halema‘uma‘u crater drained away. After the magma drained away the subsidence into the void left by its disappearance resulted in a summit caldera collapse. When eruption columns collapse, they can generate pyroclastic base surges. It is thought that a base surge of this type killed part of the Hawai‘ian war-party that made the fossilized footprints in freshly fallen Keanakāko‘i Ash erupted from Kīlauea in 1790 (*see* field trip Stop D3-19, below).

Petrochemically Hawai‘ian volcanoes exhibit 4 well-documented eruptive stages (Clague and Dalrymple, 1987; Clague and Dixon, 2000) consisting of:

1. An alkalic submarine pre-shield stage;
2. A main tholeiitic stage that dominates submarine, emergent, and subaerial shield growth;
3. An alkalic post-shield stage; and
4. A strongly alkalic post-erosional or rejuvenated stage.

The Island of Hawai‘i hosts 2 active (Mauna Loa, Kīlauea), 2 dormant (Mauna Kea, Hualālai), and 1 extinct volcano (Kohala). The submerged remains of Mahukona, the precursor volcano to Kohala, are located a short distance northwest of the Big Island (Moore and Clague, 1992). The order of volcano growth that makes up the island and its submarine base are: Mahukona; Kohala; Mauna Kea; Hualālai; Mauna Loa, Kīlauea, and Lō’ihi (*see* Figure 6). Mahukona started the formation of the Island of Hawai‘i over 500,000 years ago and after extinction slid into the sea about 300,000 years ago (Moore and Clague, 1992). The youngest active volcano in the chain is the Lō’ihi seamount and is located ~20mi (30km) south of Kilauea at a little over 1000m water depth. The stages of growth, with approximate ages, of the Island of Hawai‘i are graphically depicted in Figure 6, below.

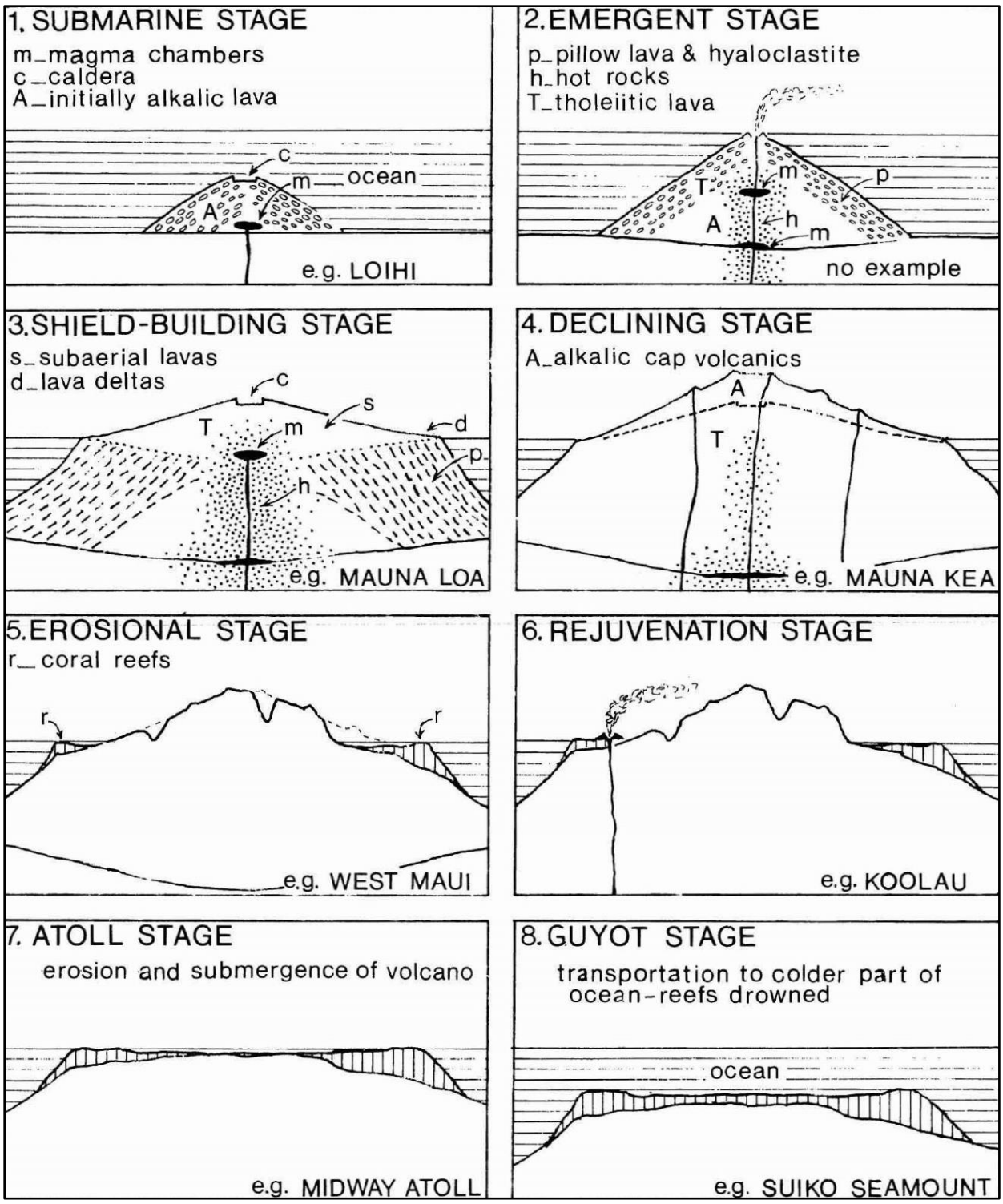


Figure 5. The 8 volcanic growth stages of the Hawai'ian islands are shown in this composite diagram modified by Walker (1990) after Stearns (1946), Macdonald et al. (1983), and Peterson and Moore (1987). Not all of the stages represented in the written descriptions above are shown in this figure with the Shield stage beginning during the Submarine stage and including the Emergent stage. The Declining stage in this diagram is equivalent to the Capping or Post-shield stage described in the written text.

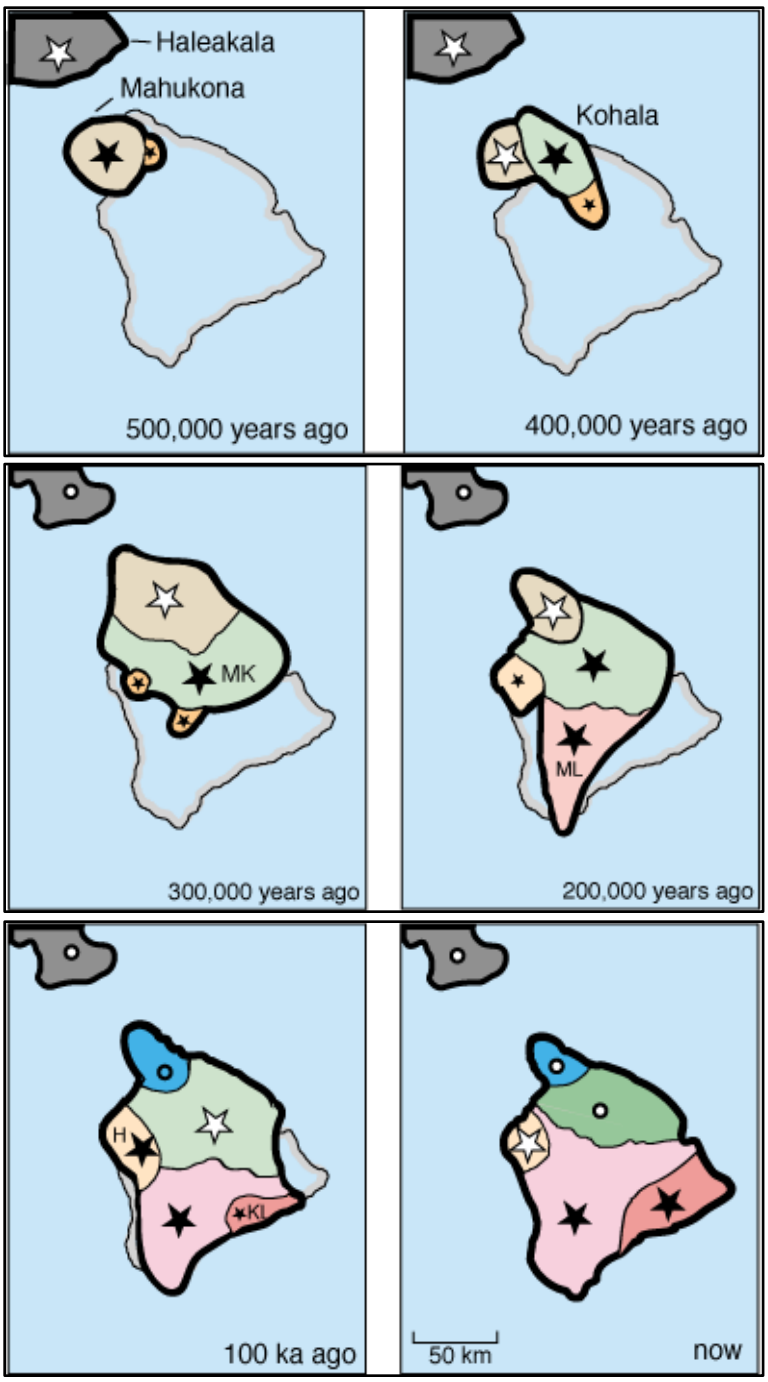


Figure 6. This figure graphically shows the growth of the island of Hawai'i over the past half million years. The growth is shown at 100,000-year (100ka) intervals with shoreline and volcano boundaries (heavy shaded lines), vigorous subaerial volcanic centers (solid stars), waning subaerial volcanic centers (open stars), and dormant or feebly active subaerial volcanic centers (open circles). Volcano shortform notations are: Kohala (KO); Mahukona (M); Hualālai (H); Mauna Kea (MK); Mauna Loa (ML); and Kilauea (KI). The diagram is modified after Moore and Clague (1992).

2.1. Volcano Descriptions

The individual volcano descriptions for the Island of Hawai'i are presented in order of decreasing age and, along with the 5 subaerial volcanoes on the island, will also include the submerged, extinct Mahukona volcano, which is thought to be the precursor volcano for the island, and the youngest active volcano, Kama'ehuakanaloa (Lō'ihi), which is located south of the island.

2.1.1. Mahukona:

The extinct submarine volcano Mahukona was discovered in 1987 and is located ~30mi (50km) west of Kohala volcano (*see* Figures 6 and 7). It was first identified and named by Garcia et al (1990) who later showed (Garcia et al, 2012) that it is a chemically distinct and separate volcano and not part of another volcanic edifice such as Kohala or Hualālai. Mahukona's existence was predicted by Dana (1890) based on an interpreted gap in the Loa trend of his then hypothesised, subparallel Loa and Kea volcanic trends (*see* Figure 8) that comprise the Hawai'ian volcanic chain.

Mahukona is interpreted by some as the precursor volcano to the Island of Hawai'i and is thought to have begun forming between 1.5 and 1.0 million years ago (Clague and Sherrod, 2014) and to have ceased erupting ~350,000 years ago (Garcia et al, 2012). Earlier researchers (Clague and Moore, 1991; Moore and Clague, 1992) interpreted that the volcano became subaerial ~800,000 years ago and ceased shield-building ~463,000 years ago; whereas, later researchers (Garcia et. al., 2012) believe that it never emerged above sea level (ASL) although they agree on the timing of the growth stages.

Mohukona is small compared to most other Hawai'ian volcanoes with a volume of ~1440mi^3 (6000km^3), a height above the sea floor of ~9500ft, a cone diameter of ~ 2.5mi (4km), and a summit that is ~3600ft (1100m) below sea level (BSL) (Robinson and Eakins, 2006). Garcia et al (1990 and 2012) have shown that the surface lavas of the cone are weakly alkalic.

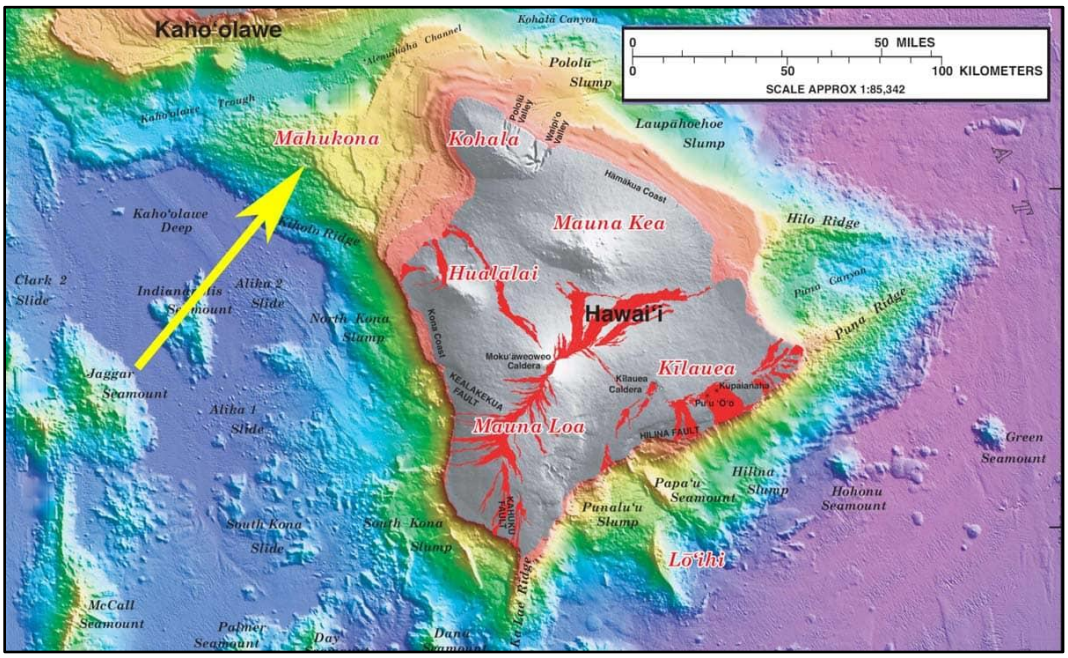


Figure 7: This bathymetric map shows the approximate location of extinct submarine volcano Mahukona (identified by the yellow arrow) located ~50km west of the extinct, subaerial Kohala volcano. This figure was downloaded from lovebigisland.com who modified it from a publicly available map on the USGS website. The map also shows, in red, the locations of flows erupted on the island between 1800 and 2018.

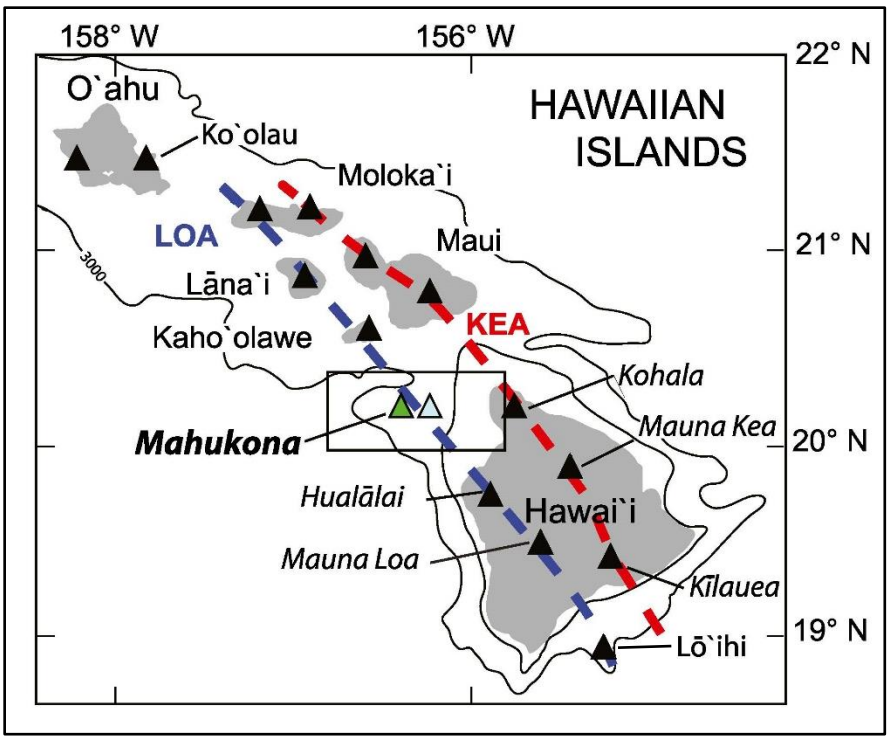


Figure 8: Map of the Hawai'ian Islands showing the Loa and Kea trends originally hypothesized by Dana (1890) and now almost universally accepted. The location of Mahukona is highlighted by the box in the centre of the figure, the bold text and the green triangle. Figure from Garcia et al. (1990).

2.1.2. Kohala:

Kohala Mountain is described by Robinson (2010) as a 20mi (32km) long, extinct volcano that forms the large, ridge-shaped northern peninsula of the Island of Hawai'i. It is the oldest volcano on the island at ~1,000,000 years of age, emerged ASL ~500,000 years ago, entered the post-shield stage and began erupting alkalic lavas ~280,000 years ago, and last erupted ~60,000 years ago (Moore and Clague, 1992). Robinson (2010) further states that Kohala is presently transitioning between the post-shield and erosional stages, and, at its greatest areal extent, was thought to be at least twice its present size with a length of >50km. The youngest eruptive activity on Kohala was contemporaneous with the shield-building stage on Mauna Kea (Easton and Easton, 1995).

Kohala is presently 5479ft (1670m) high, has an area of 235mi^2 (609km^2), a volume of ~3400mi^3 (14,172km^3), and was at least 5300ft (1615m) higher when it last erupted (Robinson, 2010; Hazlett and Hyndman, 2007). The volcano has a dominant northwest-trending rift zone and a shorter southeast-trending rift zone. It is mainly veneered by alkalic cinder cones and lava flows of the Hāwī Formation which is underlain by the older, late shield stage Pololū Formation (~400,000 years old). The oldest exposed Kohala lavas are the also the oldest on the island and have been dated at ~460,000yrs. The southern flank of Kohala is buried beneath Mauna Kea and Mauna Loa flows (Robinson, 2010). The geology of Kohala is shown in Figure 9. The western flank of Kohala is thought to partially overlie the eastern flank of Mahukona.

Erosion has had a dramatic effect on Kohala, particularly its northeastern coastline, where canyons as deep as 2460ft (750m), including the Waipi'o Valley, have been cut into the mountain. The seven prominent deep canyons incised into the northeast coast cut deeply through the capping alkalic (hawaiitic to trachytic) lavas into the underlying shield-stage tholeiitic lavas and have subsequently been partially infilled by alluvial sediments (Walker, 1990). This section of coast is also characterized by a

relatively straight, fault-controlled line of ~1970ft (600m) high cliffs that form the headwall of the mainly submarine Pololū debris avalanche (Moore et. al., 1989). Hazlett and Hyndman (2007) state that this slide occurred somewhere between 400,000 and 150,00 years ago and resulted in much of the northeastern flank of Kohala sliding into the ocean and travelling for about 80mi (130km) along the seafloor. Robinson (2010) estimates that the slide was ~12.4mi (~20km) wide at the shoreline and extended back to Kohala's summit.

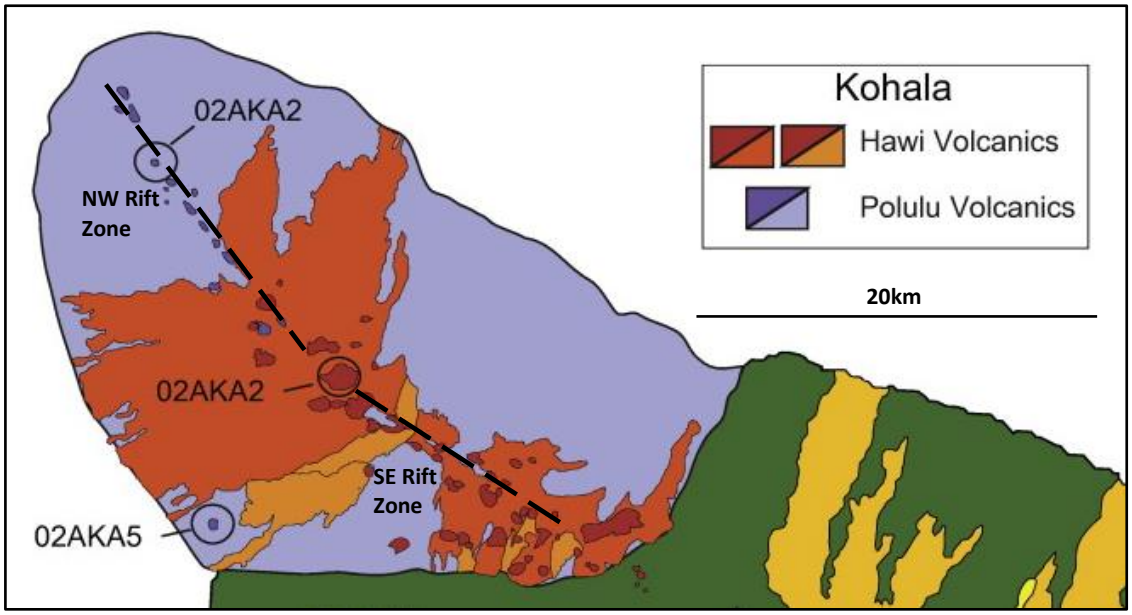


Figure 9: The Geology of Kohala volcano. Dashed black lines show the locations of the northwest (NW) and the southeast (SE) rift zones. Modified from Aciego et. al. (2010). The numbered circles are where samples were taken for dating purposes, but those results are not included within this guide.

2.1.3. Mauna Kea:

The following description is modified from Robinson (2010); Hazlett and Hyndman (2007); and the USGS HVO website.

Dormant Mauna Kea volcano is the tallest mountain on earth, if measured from its base at 19,678ft (5998m) below sea level (BSL) to its highest point at 13,796ft (4205m) ASL at the top of the Pu'u Wekiu cinder cone. Measured in this way Mauna Kea is 33,474ft (10,203m) high. The volume of the volcano is 10,075mi^3 (42,000 km^3), which is about 55% less than the 22,800mi^3 (95,000 km^3) of Mauna Loa.

Mauna Kea, like dormant Hualālai and extinct Kohala, has evolved past the shield-building stage into the hawaiitic substage of advanced post-shield stage, as indicated by (from Hazlett and Hyndman, 2007 and the HVO website):

- Very low eruption rates compared to Kīlauea and Mauna Loa;
- The absence of a summit caldera and elongated fissure vents that radiate from its summit;
- Steeper and more irregular topography; i.e., the upper flanks of the volcano are twice as steep as those of Mauna Loa; and
- The different chemical compositions of the lava, which are now alkalic.

In part, these differences are due to a low magma supply rate that produces occasional eruptions from isolated, small batches of magma that rise periodically into the volcano and then solidify without producing continuously active summit reservoirs. The lavas produced are more viscous, with a higher

volatile content, which produces thick flows that steepen the sides of the volcano and explosive eruptions that build large cinder cones. The generalized geology of Mauna Kea is in Figures 10 and 11.

Mauna Kea is presently dormant and last erupted ~4500 years ago. It is likely to erupt again since the volcano's quiescent periods are long compared to: the more active late-stage Hualālai, which last erupted in the late 1700's and early 1800's; the much more active Mauna Loa which erupts every few years to tens of years; and the extremely active Kilauea which erupts every few years.

The oldest dated rocks exposed on the flanks of Mauna Kea are 237,000±31,000 years BP. The volcano is estimated be ~1,000,000 years old, with its shield stage lasting ~800,000 years, and it is estimated to have begun the post-shield stage somewhere between 200,000 and 250,000 years ago.

Mauna Kea and Mauna Loa are often snow-covered between November and March and on 3 occasions during the Pleistocene Mauna Kea hosted permanent ice-caps and summit glaciers. The ice cap on Mauna Kea reached to below the 11,000ft ASL level (*see* Figure 12). The preserved glacial moraines and glacial outwash formed on 2 occasions from between 70,000 years ago and 40,000 to 13,000 years ago. Mauna Loa also probably hosted and ice-cap, but any evidence has long been buried by younger lava flows.

The Mauna Kea summit road was closed in early August 2019 due to political and indigenous Hawai'ian protestors against the building of another telescope at the summit astronomical observatory. Negotiations with various state, federal, and observatory officials lead to the protestors temporarily removing the blockade just before the February 2020 Field Trip and allowed the field trip to drive the summit access road and reach the summit of the volcano. As of December, 2022 access to the summit of the mountain is again allowed.

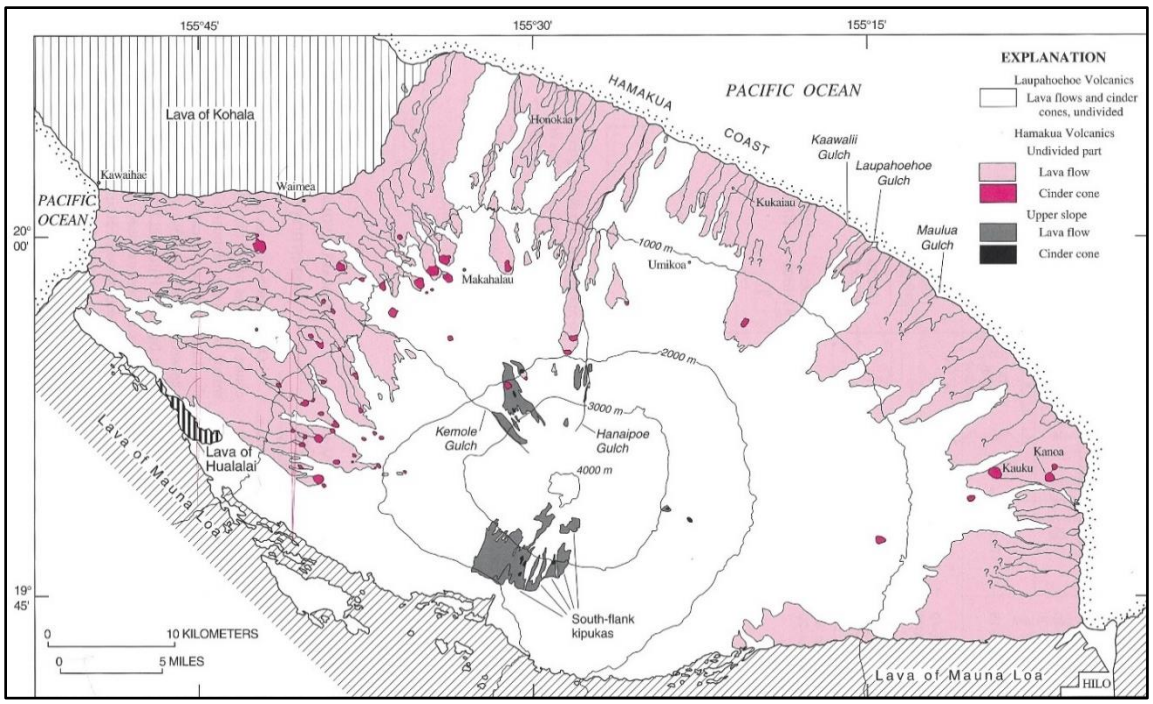


Figure 10: This geological map of Mauna Kea shows the generalized surface distribution of the Hamakua Volcanics. The younger Lauapāhoehoe Volcanics are inferred to overlie a vast area of Hamakua Volcanics on the upper flanks and summit. Map downloaded from the HVO website.

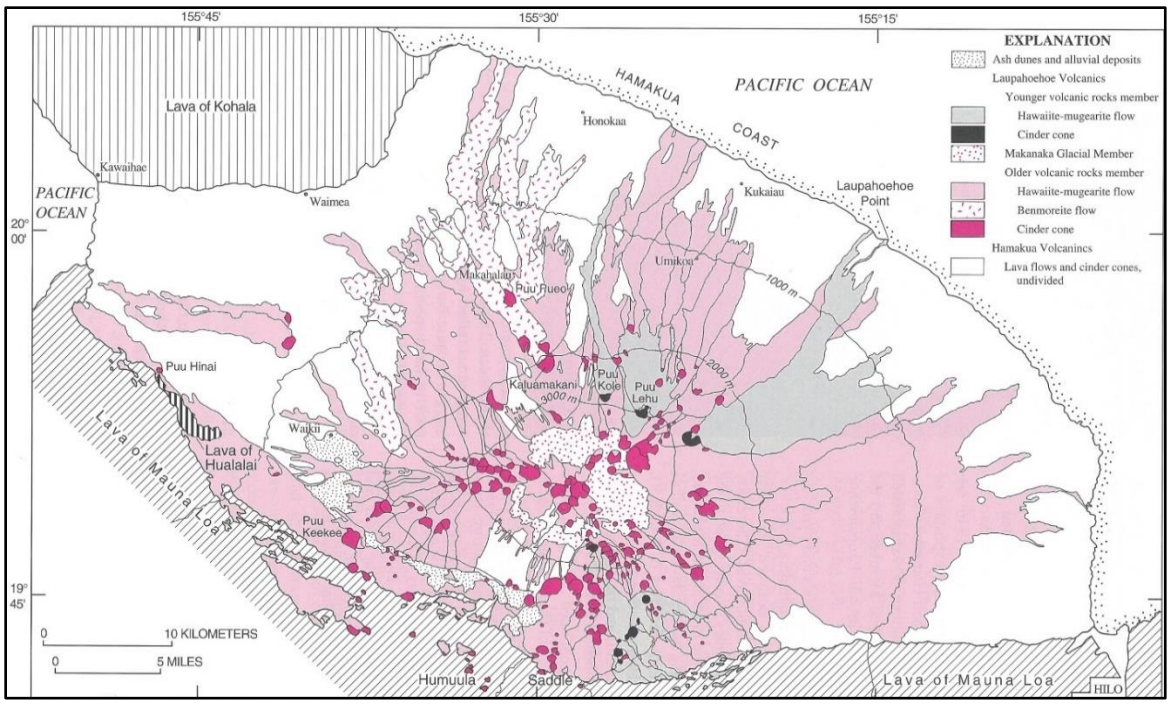


Figure 11: This geology map of Mauna Kea shows the generalized surface distribution of the lava flows, cinder cones, and glacial deposits of the Lauapāhoehoe Volcanics. Map downloaded from the HVO website.

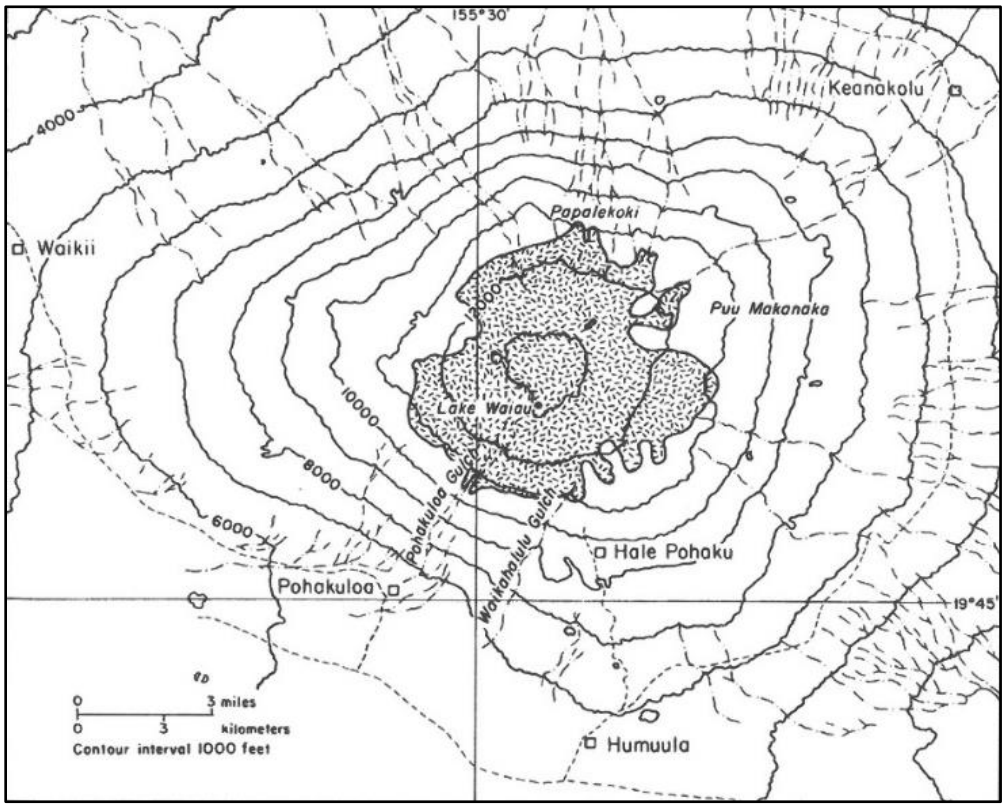


Figure 12: Map of Mauna Kea showing the extent of the summit icecap during the Pleistocene. From Merguerian and Okulewicz (2007, p.75) who took the figure from Macdonald et al (1983, Figure 13.3, p.257).

2.1.4. Hualālai:

Hualālai is an 8300ft (2530m) high, post-shield stage volcano with a volume of 2,975 mi^3 (12,400 km^3) and an area of 290mi^2 (751 km^2) (Robinson, 2010). The mountain has well-defined northwest (NW) and southeast (SE) rift zones and a poorly-developed north rift zone (*see* Figure 13).

Hualālai is thought to have emerged above sea level on the southwest flank of Mauna Kea ~300,000 years ago. Shield building tapered off about 130,000 years ago (Moore and Clague, 1992). The oldest exposed surface rocks on Hualālai are dated at ~128,000 years old with geological mapping indicating that 95% of its surface is covered by flows that are <10,000 years old. Of those flows most are <5000 years old. This suggests that eruptions can at times be quite common and that the mountain could potentially pose a considerable hazard to the large number of people presently living on or around it (i.e., Kailua-Kona and surroundings).

Estimations on the growth of Hualālai are uncertain due to the burial of parts of the volcano by Mauna Loa lavas and because of a gravitational failure (slump) of the southwest flank of the mountain that produced the North Kona Landslide before 130,000 years ago (Moore and Clague, 1992). This slide produced a >40km wide up to 4km high scarp that extended into the shield to the northwest rift zone. (Moore and Clague (1992).

Hualālai is the third youngest volcano on the island and has erupted from at least 7 different vents during the last 2100 years (Walker, 1990). Sometime between 1200 and 1400 AD (the timing is uncertain) the large Wahapele eruption was active for a few weeks or months, possibly as long as several years. Flows from the Wahapele eruption reached the sea about 10mi (16km) south of Kailua-Kona (USGS HVO website) in the Keauhou Bay area. The mountain's last eruptions were in the late 1700's (the dates are uncertain) and between 1800 and 1801, where flows issued from 6 vents. Two flows erupted during 1800 and 1801 reached the sea (USGS HVO website). Flows active in 1801 form the southernmost expression of this eruption and underlie Keahole-Kona International Airport located 7mi (11km) north of the City of Kailua-Kona (USGS HVO website). The flows comprising the 1800 to 1801 eruption are viewed at Stop D11-96.

The 1800 Hualālai flows contain large numbers of dunitic and gabbroic xenoliths/blocks that are thought to be sourced from intrusions that core the volcano (Walker, 1990, Kirby and Green, 1980; and Jackson et al., 1981)

Hualālai presently erupts viscous alkaline lavas, including alkalic olivine basalt and trachyte, with the entire subaerial surface of the volcano covered with flows of alkalic composition. In a similar manner as Mauna Kea, the viscosity of these alkaline lavas, particularly trachyte, has steepened the volcano's flanks and covered its summit and northwest and southeast rift zones with cinder cones and pit craters. Trachyte forms the large Puʻu Waʻawaʻa cone and the 330 to 660ft (100 to 200m) thick flow that emerged from it (Walker, 1990). The viscous, alkalic eruptions during the Wahapele period included a powerfully explosive phase that spread pyroclastic material over a large area. This again underscores the potential danger that Hualālai volcano poses to those who live on, or near, the mountain.

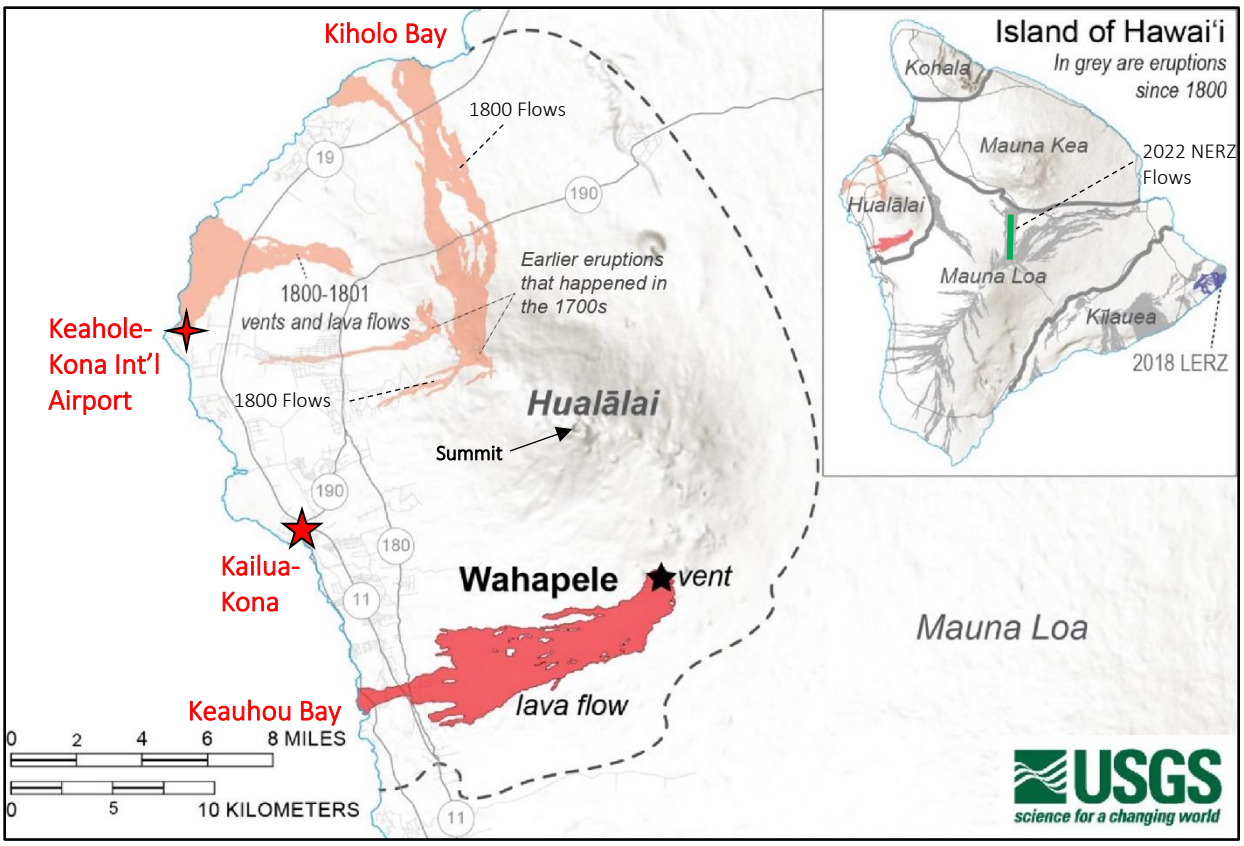


Figure 13: Modified USGS relief map showing Hualālai volcano and the lava flows extruded from a series of vents over that last 1000 years. The Wahapele flows (pink) are thought to have been erupted sometime between 1200 and 1400AD, but did not come from a vent located on either of the rift zones. The salmon-coloured flows were erupted during the late 1700's and 1800 to 1801. The NW and SE rift zones are defined by black dashed lines. The inset map shows the surface expression of the 5 volcanoes comprising the island and the lava flows erupted from Mauna Loa and Kīlauea since 1800AD, including the rough location of the 2022 Mauna Loa flows (green). Figure was downloaded from the USGS HVO website and then modified.

2.1.5. Mauna Loa:

The following description is modified from information provided by Robinson, 2010; Hazlett and Hyndman, 2007; and the USGS HVO website.

Mauna Loa (Hawai'ian for 'Long Mountain') is the largest and most massive volcano on earth, but not the highest, which is Mauna Kea (*see* Day 8, below). It dominates just over half of the Big Island; has an area of 2035mi^2 (5271km^2); reaches to a height of 13,678ft (4169m) ASL; has a volume of 19,000mi^3 (79,195km^3); and a weight of 207 x 10^6 tons (188 x 10^6 tonnes). This immense weight greatly depresses the sea floor around the island and results in a base to summit elevation of ~31,000ft (9449m).

Mauna Loa first erupted on the seafloor along the flanks of either Hualālai or Mauna Kea between ~1,000,000 and 600,000 years ago and emerged above sea level ~300,000 years ago. The oldest exposed flows on the volcano are between 100,000 and 200,000 years old with ~98% of those exposed lavas <10,000 years old. The volcano is less active than Kīlauea, but it characteristically produces greater lava volumes over shorter periods of time because it is fed from a much larger magma chamber than the one beneath Kīlauea.

The Mauna Loa summit hosts the elongated, northeast-southwest-orientated Moku'āweoweo caldera, with dimensions of 2.8 by 1.6mi (4.5 by 2.5km), including the summit collapse pits. The caldera floor, is

~180 m (590 ft) below the volcano's summit, which is located on the western rim of the caldera. Three rift zones radiate down the flanks of the volcano from the caldera. The southwest rift zone enters the ocean west of Ka Lae (South Point); the northeast rift zone arcs down the slope of the mountain ending in rain forest 15mi (24km) south of Hilo; and the third, diffuse northwest rift zone traverses the flank of the volcano and extends to the foot of Mauna Kea located 20mi (32km) north of Mauna Loa.

Geological mapping and radio-carbon dating of flows produced during the last 4000 years shows that vent locations have cycled twice between summit-dominant and rift-dominant vents. Rift-dominant eruptions have dominated the last 700 to 800 years, whereas the last summit-dominant stage occurred between ~200AD and 1200AD, a period of almost 1000years. HVO geologists suggest that the decline of summit-dominant eruptions and the increase in rift-dominant activity was related to the summit collapse that led to the formation of Moku'āweoweo Caldera. Once the caldera formed the lava flows erupted within it were trapped and were then usually unable to overflow the caldera rim. There are several possible causes for the transition from summit-dominant to rift zone-dominant eruptions such as: significant changes in the magma supply or reservoir plumbing system of the volcano leading to the formation of the summit caldera; the advent of explosive activity; and/or flank instability.

HVO scientists refer to five broad areas on the volcano where eruptions occur: the summit area, which is that part of the volcano above 12,000 ft (3,660m) ASL and includes Moku'āweoweo Caldera and the uppermost parts of the northeast and southwest rift zones; the northeast and southwest rift zones below the summit area; and the southeast, north, and west flanks (considered as one). At least 33 radial vents have been mapped in the north and west sectors signifying that lava can erupt from these sectors in addition to the rift zones and summit area.

The volcano is in the closing part of its shield stage and has erupted 34 times since 1843, making it one of the earth's most active volcanoes (*see* Figure 14). Mauna Loa's large, voluminous, basalt flow eruptions have reached the ocean 8 times since 1868. Previous to November 27, 2022 the next to last eruption began on March 24, 1984 and continued until April 15, 1984 (23 days). During that short period of time lava flows from the eruption approached to within 4mi (6.4km) of the City of Hilo.

Hazlett and Hyndman (2007) state that Mauna Loa may be the most threatening Hawai'ian volcano, mainly due to the volume and length of erupted flows which have threatened Hilo on 7 occasions since its founding. Lava flow hazard zones are shown in the lower right of Figure 14.

2.1.5.1. 2022 Mauna Loa Eruption:

The most recent eruption of Mauna Loa began at 1130PM on Sunday November 27, 2022 within Moku'āweoweo Caldera where lava initially issued from fissures quickly covered much of the caldera floor. By the morning of the 28th lava was issuing from several active fissures to the southwest of the caldera and within the upper northeast rift zone (NERZ). By mid-day of the 28th activity to the southwest and within the caldera had ceased and lava fountains up to 200ft (60m) high were observed issuing from Fissures 3 and 4 (F3 and F4, *see* Figure 15) located downslope from the caldera within the upper part of the NERZ. F3, at an elevation of ~11,500ft (3510m) ASL, quickly became the dominant vent source. Flows from F3 first cut the Mauna Loa Weather Observatory Road, located ~3.9mi (6.3km) downslope from the vent, in 2 places on the 28th. F4, located 1mi (1.6km) northeast of F3, continued to extrude flows until December 2nd and associated flows again cut the Mauna Loa Observatory Road on December 1st. By December 5th the access road had been further cut multiple times over a wide area by flows from F3, after it had become the only active vent. By December 5, 2022 flows had advanced a further 6.2mi (10.0km) downslope to reach the relatively flat plateau (the Saddle) that occupies the area between Mauna Loa, Mauna Kea, and Hualālai at ~ 6500 (1829m) ASL. The flatter slopes of the saddle caused the flows to slow, spread out, inflate, and split into several separate sub-flows, some of which were channelized, and small overflows from main channels were common. Lava fountains from the vent

attained heights of >330ft or 100m (higher than at the beginning of the eruption) and were feeding a >10.5mi (16.70km) long lava flow. Eruptive activity at the F3 vent began to decrease over the night of December 7 and 8. By the morning of the 8th flow volume was much reduced causing the flow front on the saddle to stall ~1.7mi (2.8km) south of, and before reaching, the Daniel K. Inouye Highway (Saddle Road). The height of the F3 spatter cone, when eruptive volume began to decrease on the 8th, was 98ft (29.9m). Eruptive activity continued to wane with lava volumes decreasing such that by the morning of the 10th only a few weak flows were active. These flows were fed by a lava lake within the vent rather than the fountains which typified the eruption to this point. By the morning of the 11th all activity on the flow field appeared to have ceased; however, the main flow still glowed and inched forward on occasion as it settled. The F3 vent was still incandescent at night. The eruption was deemed over late on December 10, 2022 (USGS HVO website) after being active for 12 days. The location of flows and fissures associated with the 2022 eruption are summarized on Figure 15.

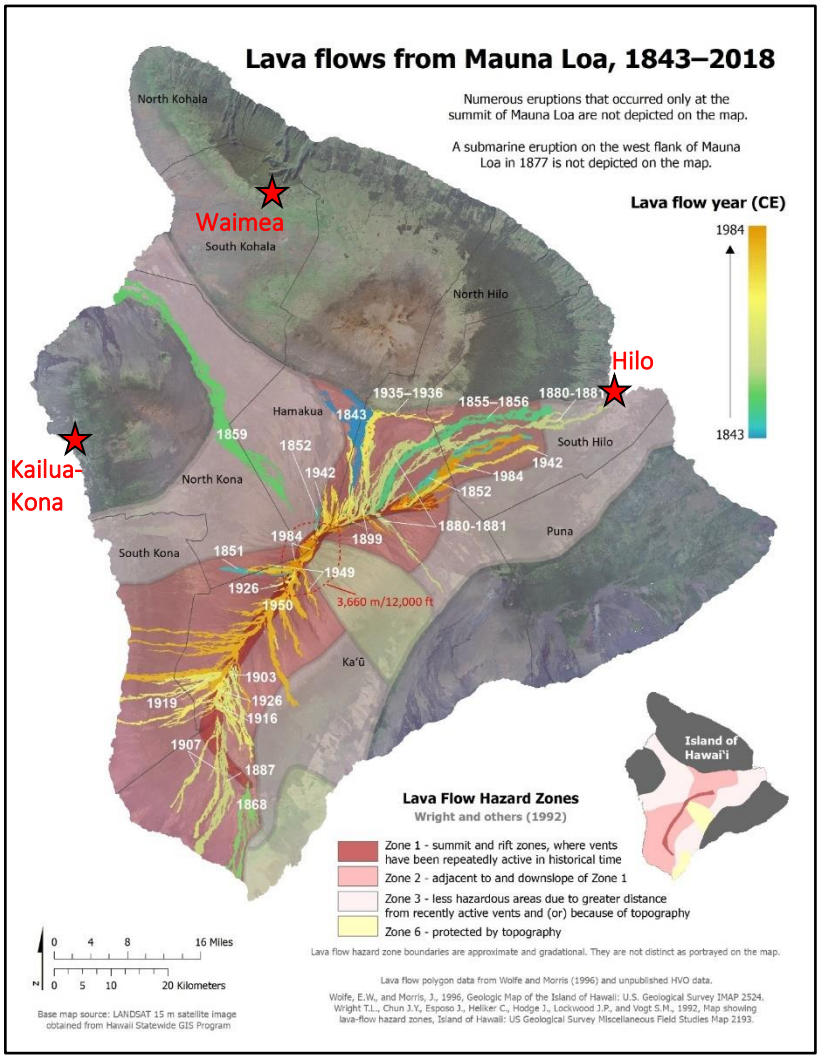


Figure 14: Map showing the extent of historic Mauna Loa lava flows; hazard zones are designated by the USGS. The 2022 flows are located about where the 1843 flows are shown. Map downloaded from the HVO website.

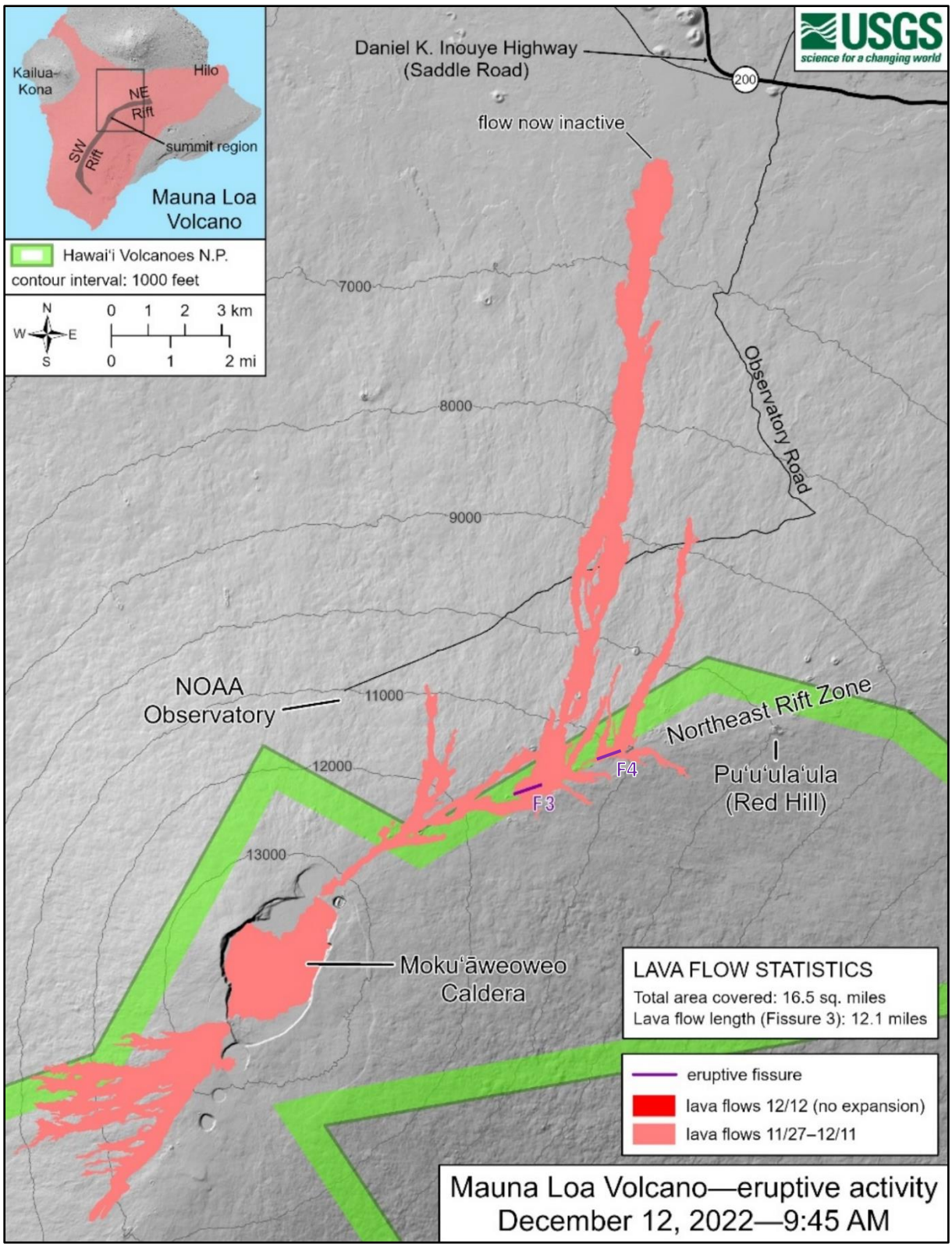


Figure 15: Map showing the lava flows erupted from Mauna Loa's summit caldera and the Upper Northeast Rift Zone during the November 27 and December 10, 2022 eruption. Map downloaded from the USGS HVO website.

2.1.6. Kīlauea (description after Hazlett, 2014; the USGS HVO Website, 2022):

Kīlauea is the most active volcano on earth and has the appearance of a bulge on the southeastern flank of Mauna Loa. For a long time it was thought to be a satellite of Mauna Loa; however, research shows that Kīlauea has a distinct and deep magma-plumbing system that extends into the earth for >60km. Eruptive activity for Kīlauea since 1790 is shown in Figure 16.

The first alkali-basalt lava flows of Kīlauea's submarine pre-shield stage erupted onto the seafloor on the southeastern flank of Mauna Loa between 210,000 and 280,000 years ago. It transitioned to the submarine shield-building stage about 155,000 years ago and emerged above sea level between 50,000 and 100,000 years ago. The oldest exposed surface lavas are the Hilina basalt formation which is exposed along various Hilina fault scarps on Kīlauea's central south flank. These flows are the oldest found above sea level and erupted between 50,000 and 70,000 years ago. >90% of the remaining surface flows are <1000 years old, and 70% of those are <600 years old. The summit of the volcano is located at 4080ft (1240m) ASL.

Research and mapping clearly show that Kīlauea exhibits cycles of explosive and non-explosive (effusive) eruptions that individually last for prolonged periods of time. This pattern of activity has persisted for at least the last 2500 years and possibly longer, but since the surface of Kīlauea is very young it is difficult to accurately determine the eruption record earlier than that time.

The known eruption record shows that effusive (non-explosive eruptions) were the norm up to ~2200 years ago. At this time the Powers Caldera, which is the precursor to the present caldera, formed by a collapse of the crater floor to a depth of at least 2030ft (620m) where magma and external water interacted to trigger powerful phreatomagmatic eruptions. Tephra from the many explosive (pyroclastic) eruptions that occurred over the next 1,200 years produced the Uwekahuna tephra. The most powerful known explosive eruption from Kīlauea occurred between 850 and 950CE and sent golf ball-sized rocks as far away as the southern coast of the island, a distance of 11mi (18km).

Effusive activity began again ~1000 years ago and completely filled the summit caldera to where it overflowed to form the Observatory Shield. Eruptions were also frequent along the east and southwest rift zones. Observatory Shield construction ended ~1400CE when activity migrated to the east and over the next 60years produced the longest-lasting flow ever witnessed in Hawai'i. This Ailā'au flow covered much of Kīlauea from the summit to the coast on the north side of the East Rift Zone.

The Ailā'au eruption ended ~1470CE and the collapse after the withdrawal of lava from the summit formed the present-day Kīlauea Caldera. The Keanakāko'i explosive eruption period began ~1500CE when the caldera floor dropped to a depth of ~1970ft (600m) and had a diameter of 2.2mi (3.5km) by 1.9mi (3 km). The Keanakāko'i period ended in ~1800CE after at least 4 strong explosive eruptions over a 300yr period ejected ash over a broad area east of the volcano and deposited the 35ft (11m) thick Keanakāko'i tephra (ash bed). In 1790, near the end of the period, a series of strong explosive eruptions produced several pyroclastic base surges, which are a type of turbulent, very hot (>100^{o}C), fast-moving, low-density pyroclastic density currents that can sweep over ridges, hills, and other topographic boundaries and are almost impossible to escape, particularly on foot. These surges seared down the west side of the summit area killing several hundred, possibly several thousand, indigenous Hawai'ians (*see* The Footprints Trail, Field Trip Day 2). This is the deadliest known eruption of a volcano on U.S. soil.

The control on this explosive-effusive cycle may be magma supply. High volumes of magma will allow the caldera to fill, as well as feed large amounts of magma to summit lava flows and rift zone vents. When the magma supply drops the caldera will collapse. If the floor of the crater drops sufficiently to approach or cross the water table then that water interacts with the magma in the vent to produce phreatomagmatic (magma-steam) explosions. When the magma supply again increases to allow

effusive eruptions to dominate then the cycle begins again. Research strongly suggests that a caldera is necessary for prolonged periods of explosive summit eruptions and it is estimated that a deep caldera has existed at the summit for ~60% of the last 2,500 years.

Before the end of April 2018, the summit caldera (*see* Figure 18A, B, C, and D) was 541ft (165m) deep with an outermost diameter of 3.7mi (5.95km) and an elongate, north-northeast-trending main depression measuring 3.1mi by 1.9mi (4.99km by 3.06km). As mentioned above this caldera largely formed between 400 and 500 years ago with lesser collapses leading up to ~1790CE when pyroclastic eruptions deposited the thick, complex Keanakāko'i Ash over a wide area. This ash is best observed along the Footprints Trail (Day 2).

Also, before the end of April 2018, the Kīlauea summit caldera hosted the 0.62mi (1km) diameter Halemaʻumaʻu Crater (*see* Figures 17 and 19) which represented the top of a low-lying lava shield within the greater caldera. Halemaʻumaʻu Crater began forming in July 1894 when the original lava shield collapsed. The crater reached its pre-2018 size and shape in 1924 when a long-lived lava lake (1905 to 1924) contained within an earlier, smaller version of the crater drained away. Over a 9-day period between April 29, 1924 and May 7, 1924, a series of collapses and steam-blast eruptions roughly doubled the size of the crater to its pre-May 2018 dimensions. The most recent pre-2018 effusive summit eruption, began on March 19, 2008 with an explosion blew a narrow subvertical vent into the bottom of Halemaʻumaʻu Crater near its southern margin. This vent initially emitted sulphur-dioxide-rich (SO_2) gasses and eventually hosted a lava lake that occasionally overflowed onto the crater floor.

A protracted Central East Rift Zone (CERZ) eruption (*see* Figure 20A, B, C, D) began on January 3, 1983 as a series of localized fissure eruptions and by June 1983 had focussed on the Puʻu Ōʻō vent. The eruption focussed there for ~3 years until it shifted 1.8mi (3km) east down-rift to the Kupaianaha vent. The next 5½ years were a period of almost continuous and destructive eruption from the Kupaianaha vent that destroyed many homes and the communities of Kapaʻahu and Kalapana. In February 1992 eruptive activity shifted west up-rift via a series of fissure eruptions that culminated in a fissure eruption on the west flank of Puʻu Ōʻō. The eruption focus stayed near, Puʻu Ōʻō for the next 26 years (*see* Figure 21). The only community threatened during this time was the town of Pahoa, located ~12mi (20km) east of Puʻu Ōʻō on Highway 130, between July and December 2014 (*see* Figure 22).

Eruption from Puʻu Ōʻō and vicinity was continuous until April 30, 2018 when, after a series of earthquakes, the magma moved from Puʻu Ōʻō and the eruptive vent collapsed. The magma was observed by seismic monitoring to move >20km east to the Lower East Rift Zone (LERZ). Vigorous eruption began on May 3rd via a series of 24 fissures along a 14km segment of the LERZ and continued until August 9th. Also, in early May the 10yr old summit lava lake within Halemaʻumaʻu Crater began to drain away and by May 10th had disappeared from view. Once the supporting magma beneath Halemaʻumaʻu disappeared the area around the crater began to dramatically subside. This caldera collapse was accompanied by numerous steam-generated pyroclastic eruptions and Halemaʻumaʻu Crater was eventually replaced by a much larger and deeper crater 1.7mi (3km) in length, 0.93mi (1.5km) in width, and >1640ft (500m) in depth. A small lake was present at the bottom of the crater in February 2020 (*see* Figure D6-3, right). Since the February 2020 field trip and the final edit of this Guide there were 3 summit eruptions within the new Halemaʻumaʻu Crater. The deep, cone-shape crater that formed in mid-2018 has been partially infilled by lava lakes formed during the 3 eruptions. The first eruption, between December 20, 2020 and May 26, 2021, partially infilled the crater by 732ft (223m) bringing the base of the crater up to 2431ft (743m) ASL. The second eruption began September 29, 2021 and ended on December 9, 2022. The third eruption commenced on January 5, 2023 and was ongoing by the completion of this guide in February 2023.

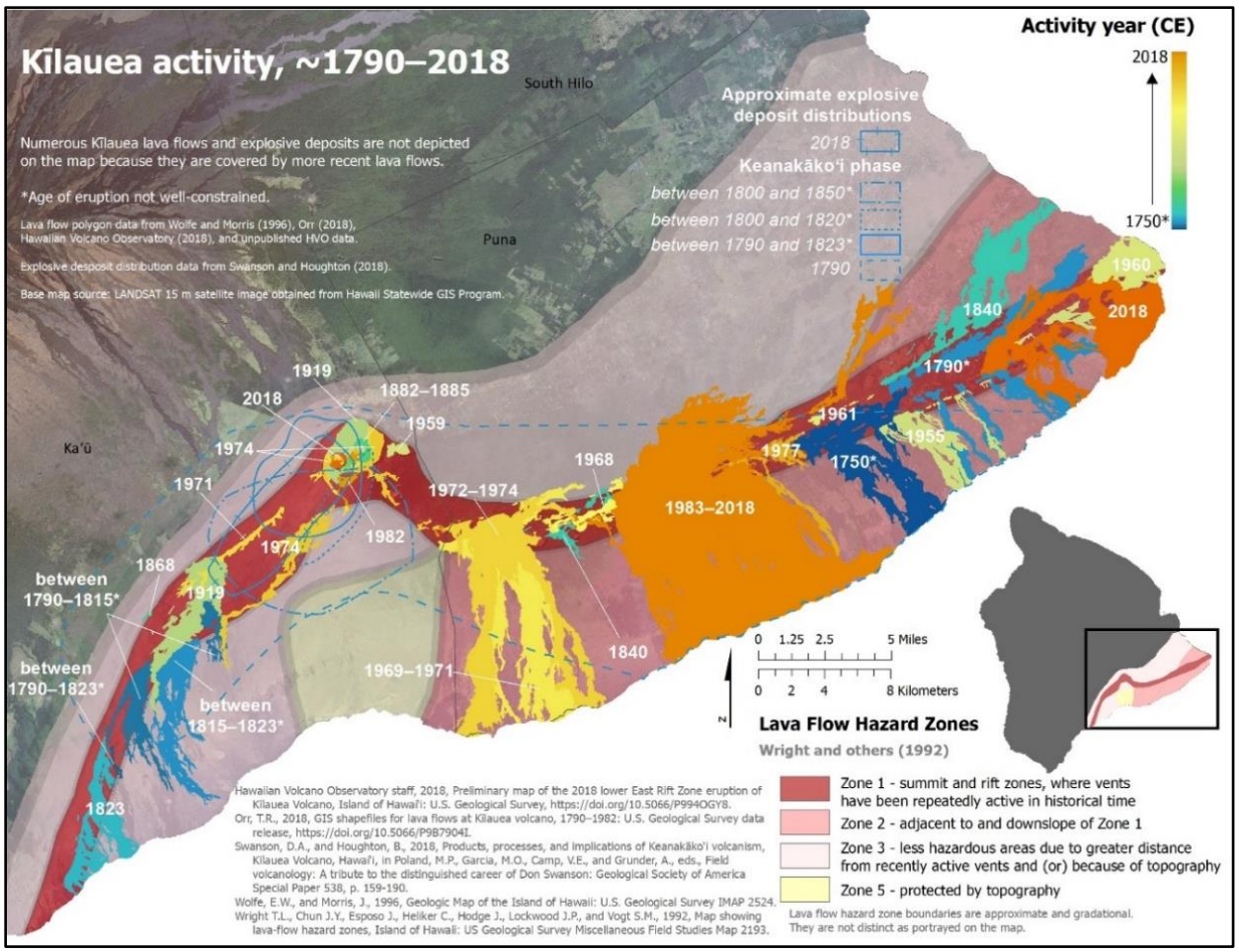
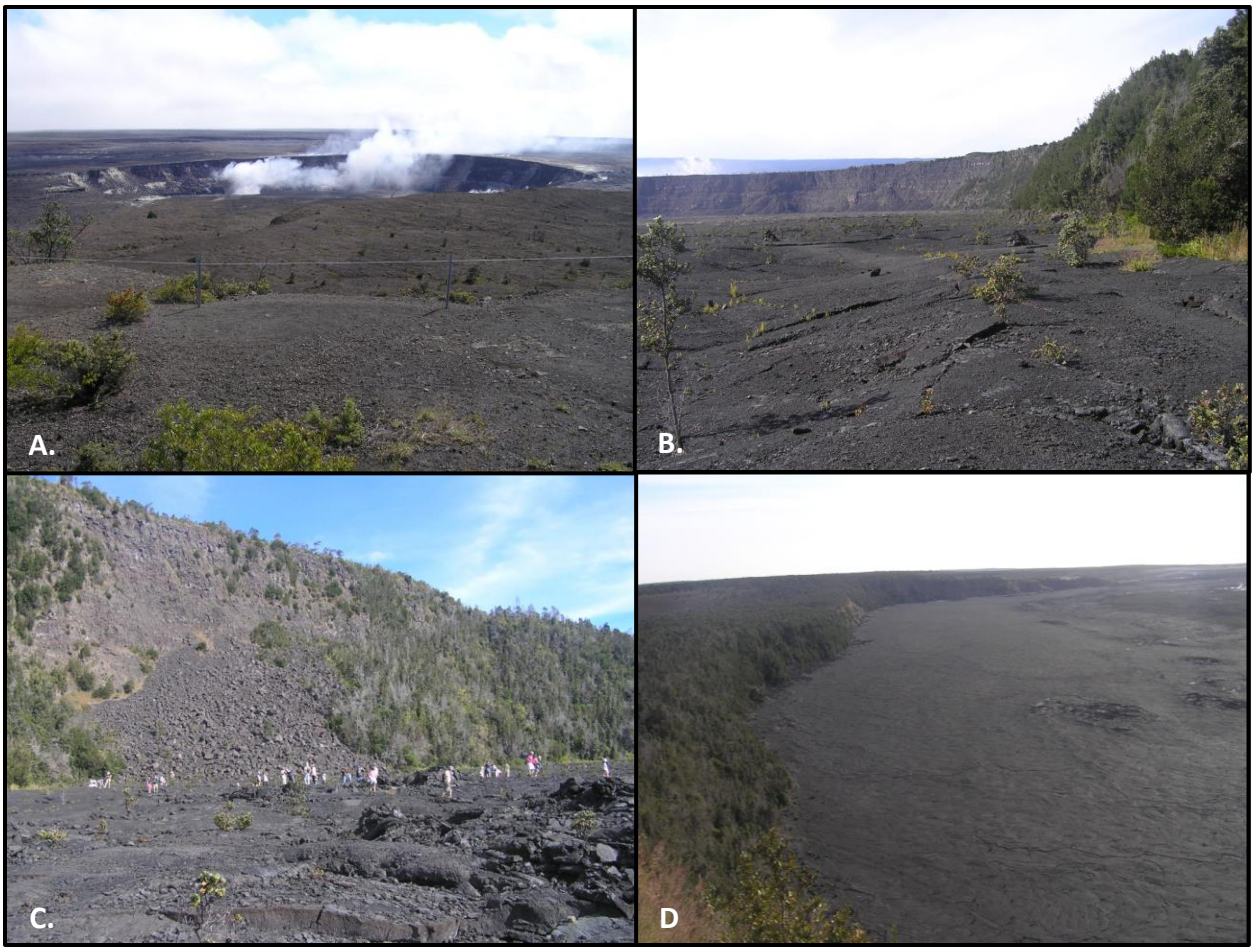


Figure 16: Map of Kīlauea volcano showing subaerial extent of historic lava flows extruded between 1790 and 2018; hazard zones are designated by the USGS. Map downloaded from the HVO website.



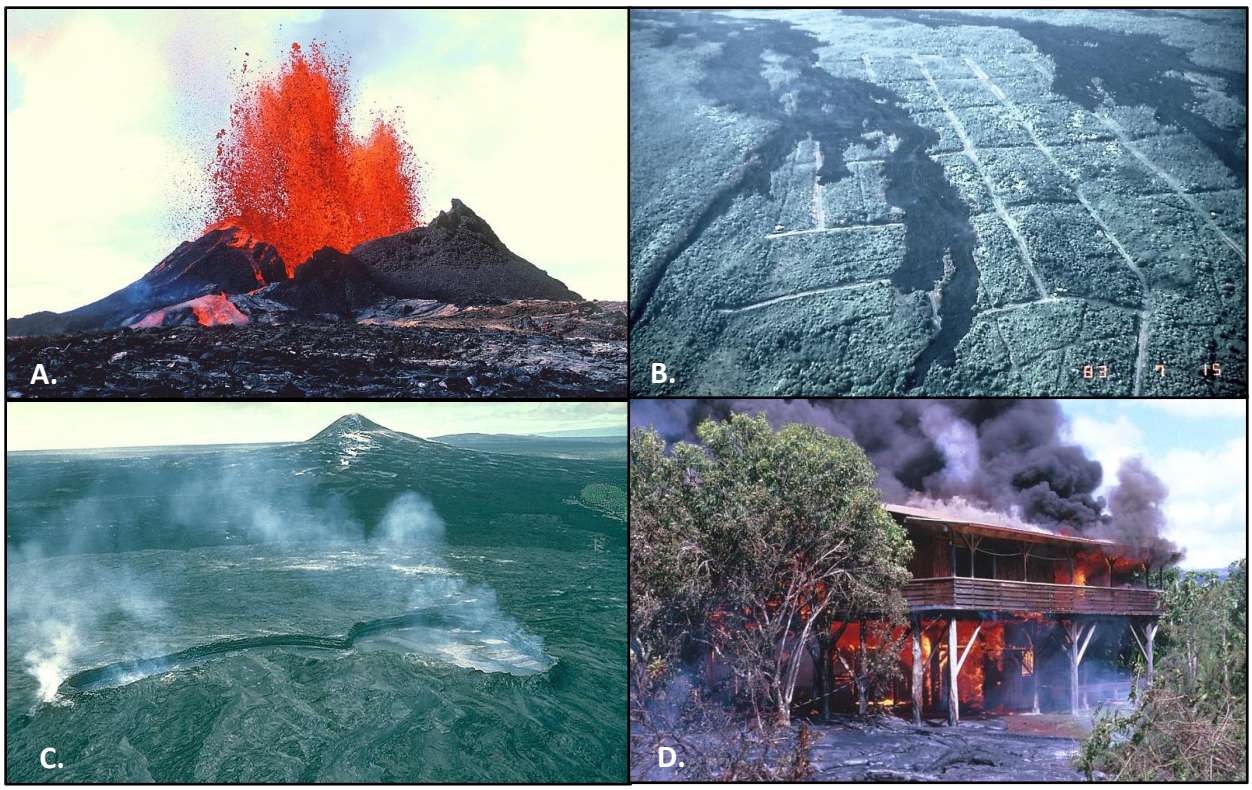
Figure 17: Incandescent volcanic ash and lava fragments are blasted from the Halemaʻumaʻu Crater vent at Kīlauea's summit during an explosive eruption on October 12, 2008 (left). The volcanic-gas plume emitted from that vent a month later in November 2008 on the right. Photographs by Janet L. Babb from Tilling et. al. (2011), USGS General Information Product 135 that were downloaded from the USGS HVO website.



Figures 18A, B, C, and D: Kīlauea Caldera as it appeared before May, 2018: **A.** Halemaʻumaʻu Crater viewed from the now closed Jagger Museum observation deck with the vase plume from the lava lake clearly visible; **B.** Northwest caldera rim from the caldera floor below the Volcano House Hotel; **C.** Northeast caldera rim from the caldera floor; and **D.** Eastern Caldera rim from northern caldera rim. Photos by A.D. MacTavish (2009).



Figures 19: These 2 photos are close-ups of Halemaʻumaʻu Crater and the lava lake that was resident within the crater between 2008 to 2018: **A.** Aerial view of Halemaʻumaʻu Crater with lava lake/gas vent (2010); **B.** Halemaʻumaʻu lava lake at night (2012). Photos downloaded from the HVO Website.



Figures 20A, B, C, and D: Kīlauea's Central East Rift Zone eruption began in January 1983 and ended in May 2018. Photos of the earlier stages of this eruption can be seen here: **A.** Lava fountain at Pu'u Ō'ō (1983); **B.** A'ā flows from Pu'u Ō'ō vent passing through the Royal Gardens Subdivision located about 4km southeast of the vent (1983); **C.** Kupaianaha vent and perched lava pond with the Pu'u 'Ō'ō cone in background (1986); and **D.** Flows from the Kupaianaha Vent destroying a house in Kalapana (1990). All photos downloaded from the HVO Website.



Figures 21: These 2 photos show eruptive activity associated with Pu'u Ō'ō: The left photo shows a perched lava channel with Pu'u Ō'ō in the background (2007); the right photos show the Kamomoa lava fountains with Pu'u Ō'ō in the background (2011). Photos downloaded from the HVO Website.



Figure 22: These photos show the Pu‘u Ō‘ō ‘June 27th Flow’ threatening the town of Pahoa in 2014: Lava flows from Pu‘u Ō‘ō are approaching Pahoa (left); a pāhoehoe lava flow advancing west of Pahoa between the town and the Waste Transfer Station on Apa‘a Street (right). Photos downloaded from the USGS HVO Website.

2.1.6.1. 2018 Kīlauea LERZ Eruption and Halema‘uma‘u Summit Caldera Collapse

The description within this sub-section was modified and summarized from publicly available data on the USGS HVO website.

During late April 2018 the focus of the 35-year Kīlauea eruption shifted from Pu‘u Ō‘ō on the Central East Rift Zone (CERZ) and the volcano’s summit (Halema‘uma‘u lava lake) to the Lower East Rift Zone (LERZ) after the collapse of the long-term Pu‘u Ō‘ō crater on April 30, 2018. On May 2nd this collapse was followed by a series of strong earthquakes and the opening of the first ground cracks along the LERZ and the dropping of the level of the 10yr old Halema‘uma‘u summit lava lake.

The LERZ fissure eruption began on May 3rd with one vent (Fissure 1) opening in the area of Mohala and Leilani Streets in the Leilani Estates subdivision. By the next day there were 6 open fissures, with lava issuing from Fissure 2 and a magnitude 6.9 earthquake on south flank of Kīlauea.

On May 8th there was a pause in eruptive activity after 15 new LERZ fissures opened. On May 10th the Halema‘uma‘u lava lake had disappeared from view and on May 11th Hawai‘i Volcanoes National Park was closed to the public.

After 4 days of inactivity Fissure 16 opened on May 12th and by May 14th Fissures 17, 18, and 19 were open with flows issuing from Fissures 16 and 17.

On May 15th a 12,000ft (3660m) ash plume issued from Halema‘uma‘u after a rock fall and subsequent explosions. On the same day Fissure 20 opened in the Lanipuna Gardens Subdivision, located <0.6mi (1km) SE of Leilani Estates, and a slow, narrow flow from Fissure 17 was creeping toward the ocean.

Explosive events at the Kīlauea summit commenced on May 16th with ash clouds rising up to 30,000ft ASL. The Hawai‘i Volcano Observatory (HVO) building was evacuated and subsequently permanently closed, and cracks were observed on Highway 11, a short distance northeast of the Park Entrance (between mile markers 28 and 29). Explosive events of various sizes continued at the summit until early August with caldera subsidence beneath Halema‘uma‘u beginning on May 25th.

By May 19th fountaining from Fissures 16 through 20 had merged into the single, continuous fissure referred to as Fissure 20. Lava from this fissure entered the ocean near the MacKenzie State Park Recreation Area the same day (this ocean entry lasted about 10 days).

By May 28th there were 24 LERZ fissures with at lava erupting from least 10 of the fissures at the same time. A large, over 100ft (30m) high, spatter rampart had been built around Fissure 7 by lava fountains

reaching up to 200ft (45 to 60m) high, that fed a perched, 20 to 40ft (6 to 12m) thick, pāhoehoe flow. On the same day a magnitude 4.1 earthquake occurred on the Koa`e fault zone south of the caldera. Caldera down-drop accelerated with the onset of near-daily summit collapse events with each event releasing energy equivalent to a Magnitude 5.0 earthquake.

By May 31st impressive fountaining from Fissure 8 had formed a broad, levéed, channelized flow. Fissure 8 quickly became the most active and longest acting fissure of the 2018 eruption. On June 2nd the channelized Fissure 8 flow crossed Highway 137, near the junction with Highway 132, advanced into Kapoho Crater, and entered and completely filled up Green Lake within the crater. This voluminous and fast-moving flow entered Kapoho Bay on the Pacific Ocean late the next day after travelling over 8mi (13km) from Fissure 8. The flow immediately began building a lava delta into Kapoho Bay on a 500ft (150m) wide flow front and, by the following morning, the flow had completely infilled the bay. The width of this flow front had expanded to 3.7mi (6km) by July12th.

By July 18th an increase in lava supply from Fissure 8 produced several overflows that destroyed more homes. Explosions were evident near the main ocean entry, which had shifted to near Ahalanui Beach Park. The margin of the flow at the ocean entry continued to extend southwards and advanced to within <575ft (175m) of the Isaac Hale Park boat ramp.

The eruption of lava from Fissure 8 continued vigorously until August 4th when the eruption rates began to decrease. Summit deflation stopped after a single collapse event earlier in the day.

By August 7 the only eruptive activity at Fissure 8 consisted of a small active lava lake within the cone. The lake's surface was located between 15 and 30ft (5 to 10m) below the spillway entrance of the cone. Small, active ooze-outs near the coast on the Kapoho Bay and Ahalanui lava lobes were greatly diminished and active lava remained close to the Pohoiki boat ramp at Isaac Hale Park, but had not advanced significantly toward it. Deformation at the summit had virtually stopped.

From August 9th to 13th the activity and lava output from Fissure 8 remained low with no signs of reactivation or new subsurface intrusion. Up-rift Fissures 9, 10, and 24 and down-rift Fissures 3, 7, 13, and 23 continued to steam. The crusted Fissure 8 lava pond was deep within the cone and on the 10th was about 130ft (40m) below the rim of the cinder cone. On the 11th there were 2 lava ponds – one active and the other stagnant and crusted over. On the 12th the only molten lava visible was oozing into the ocean between the Kapoho Bay and Ahalanui areas; the summit remained quiet except for a few small rock falls.

As of August 16th, Kīlauea volcano had remained quiet for over a week with no collapse events at the summit and, other than a crusted-over lava pond deep within the Fissure 8 cone and a few scattered ocean entries, there was no lava flowing in the Lower East Rift Zone.

On September 22, 2018 Hawai'i Volcanoes National Park partially reopened and the eruption appeared to be over.

Lava from the 2018 LERZ eruption covered >5914 acres and destroyed at least 533 homes. The lava delta built by the Fissure 8 Flow within Kopoho Bay covered an area of over 380 acres and extended out over 0.5mi (800m) from the former shoreline.

Figures 23 through 25 and Figure 30 highlight the 2018 Kīlauea summit caldera collapse beneath Halema'uma'u Crater. Figure 26 shows the 2023 lava lake that now occupies, and has infilled, much of the 2018 crater as the result of the 3 summit eruptions that have occurred between 2019 and February 2023. Figures 27 and 28 highlight various aspects of the 2018 Lower East Rift Zone eruption.

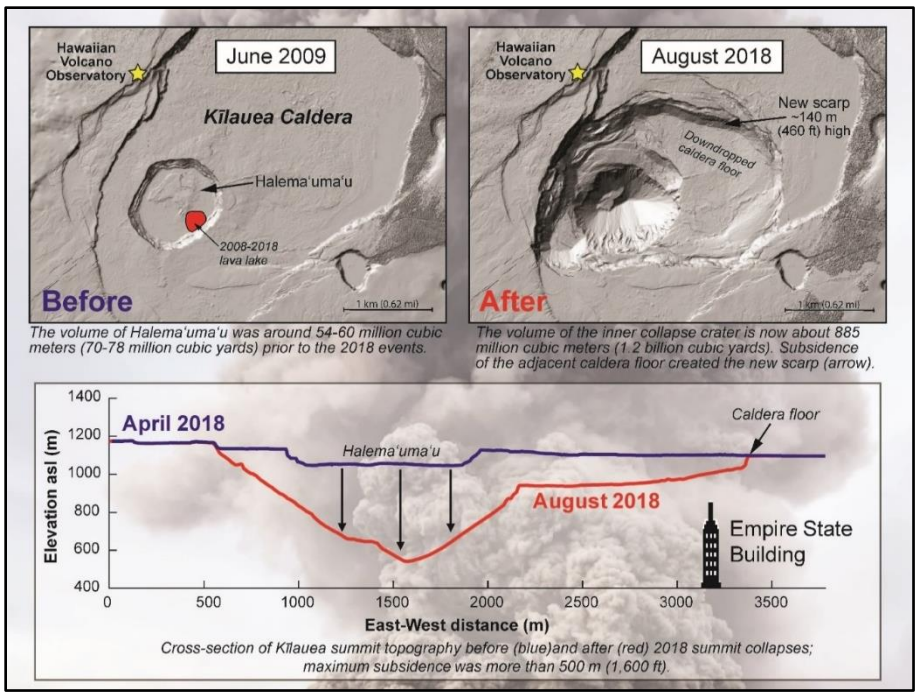


Figure 23: Airborne radar maps (upper 2 panels) of Halemaʻumaʻu Crater and Kīlauea Caldera taken in June 2009 and August 2018 show the changes in the caldera floor before and after the withdrawal of the lava lake that occupied the crater between 2008 and 2018. The lower panel shows a vertical cross-section through the crater showing the over 500m subsidence of the floor of the crater between May and August 2018 (USGS HVO Website).

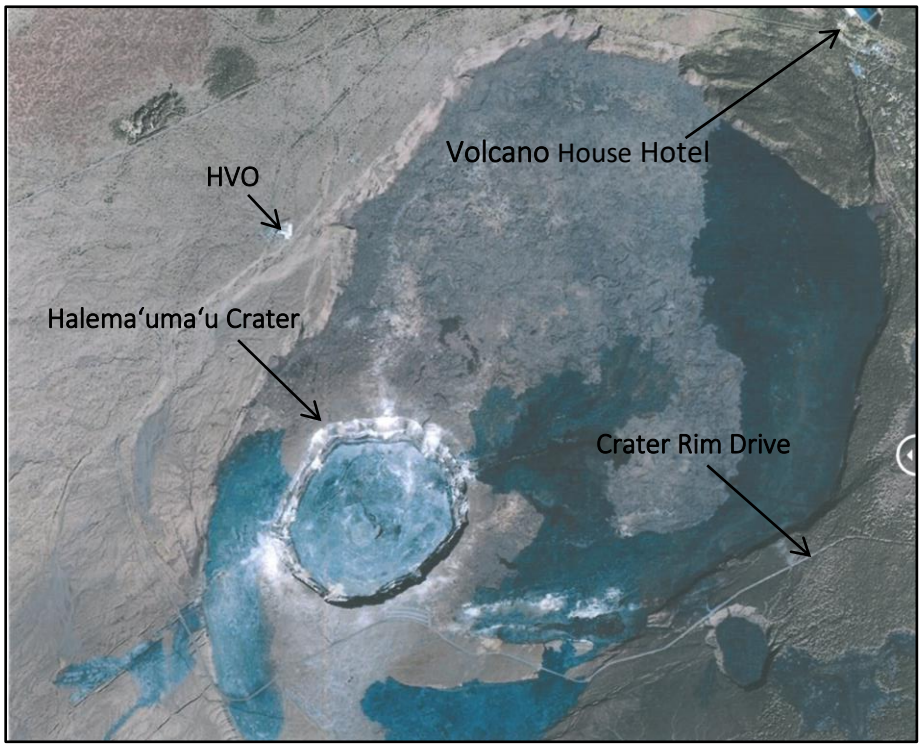


Figure 24: Satellite image of Kīlauea Caldera and Halemaʻumaʻu Crater in January 2003. Photo from USGS HVO Website.

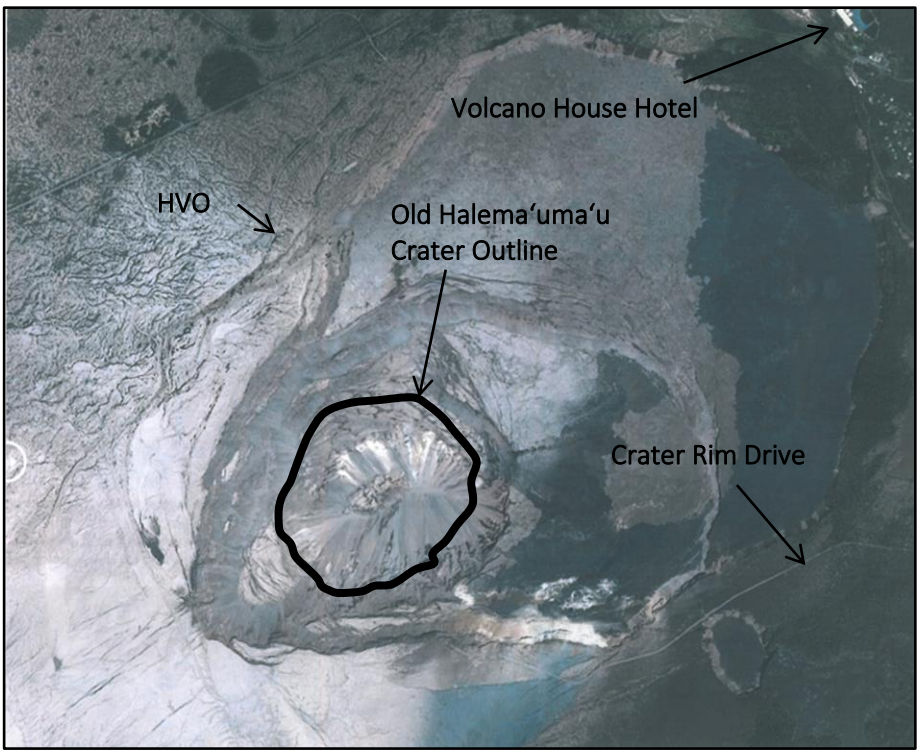


Figure 25: Satellite image of Kīlauea Caldera and Halemaʻumaʻu Crater after the collapse of Halemaʻumaʻu taken on August 11, 2018. Photo from USGS HVO Website.



Figure 26: Aerial photograph of a greatly modified Kīlauea caldera showing the changes, due to the collapse of the caldera floor beneath Halemaʻumaʻu Crater, that took place between May and August 2018. The new crater is ~2.5km by 2km, and 350 to 400m deep. Photo by A.D. MacTavish, August 4, 2019.



Figure 27: The post-2018 Halema‘uma‘u Crater at 645AM January 6, 2023 showing the active lava lake from the Kīlauea summit eruption that began on January 5, 2023. Sunrise-lit Mauna Loa is in the background to the west. Most of the crater formed in 2018 is now infilled with lava. Photo taken from the USGS HVO website.

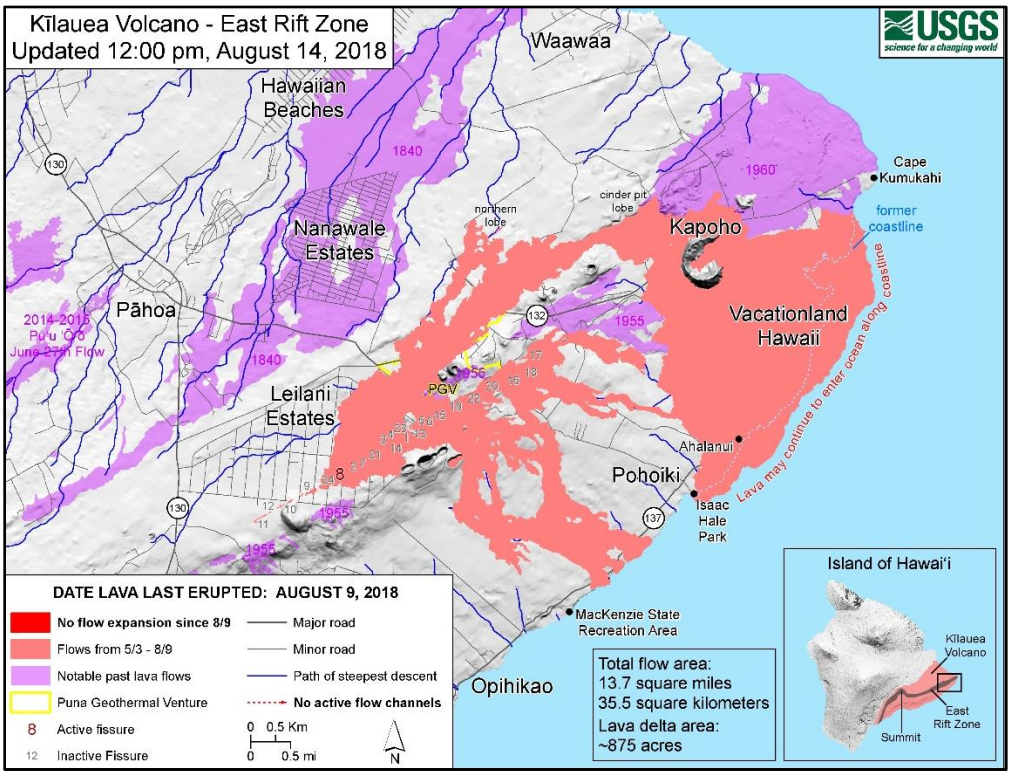


Figure 28: Map showing the flows (represented by the salmon colour) produced by the 2018 Lower East Rift Zone eruption. Figure taken from the USGS HVO website.



Figure 29: 2018 Lower East Rift Zone eruption photos (all photos downloaded from the USGS HVO website): **A.** Leilani Estates, fountaining from a new fissure, May 4, 2018; **B.** ʻAʻā flow crossing Makamae Street, Leilani Estates, May 6, 2018; **C.** Fissure 20 channelized flow, May 19, 2018; **D.** Channelized flows entering the Pacific Ocean, evening May 23, 2018; **E.** Breached spatter cone and fountaining at Fissure 8, June 5, 2018; **F.** Flows entering Kapoho Bay, June 5, 2018; the bay has been completely infilled and the lava delta has extended ~300m outward from the former entrance to the bay.



Figure 30: Kīlauea 2018 Summit Events: **A.** Summit eruption cloud, May 15, 2018; **B.** 'Summit eruption plume, May 23, 2018; **C.** Halemaʻumaʻu Crater subsidence, June 5, 2018; **D.** The new Halemaʻumaʻu Crater, March 6, 2019; **E.** New Halemaʻumaʻu Crater taken from a helicopter overflight on August 4, 2019; the view is to the south. Photos A, B, C, and D from the USGS HVO website; Photo E by A.D. MacTavish (2019).

2.1.7. Lo‘ihi (Kama‘ehuakanaloa):

As mentioned at the beginning of Section 2, above, Lō’ihi is the youngest active volcano associated with the Island of Hawai‘i and has recently been renamed. According to the USGS HVO website the name Lō’ihi was introduced in 1955 to describe the elongated shape of the seamount. More recently, Hawai‘ian scholars have found that stories of “Kama‘ehu” , the red island child of Haumea (earth) and ‘Kanaloa’ (sea) that rises from the deep in the ocean floor, may also be a reference to the submarine volcano, hence the proposal and acceptance of the name ‘Kama‘ehuakanaloa’, which means ‘red island child of the earth and sea’. The name ‘Kama‘ehuakanaloa’ was adopted by the Hawai‘i Board of Geographic Names in 2021 (USGS HVO website) and is not yet in common use, or even known about other than by researchers, and will not be used further in this guide. Lō’ihi, which means ‘long’ in Hawai‘ian, is considerably easier to remember, to spell, and to pronounce (by the author’s at least).

Lō‘ihi is presently forming as a submarine seamount located ~ 19mi (31km) south of the southern coastline of the Island of Hawai’i (*see* Figure 30). It has a volume of 407mi^3 (1,700km^3) with its summit at ~10,100ft (3078m) above the abyssal ocean floor at a water depth of 3235ft (986m).

The seamount comprising Lō’ihi was long thought to be a young submarine volcano, but that was not confirmed until a series of sub-sea earthquake swarms detected by the HVO’s seismic network in 1971, 1972, and 1975 quickly lead to the recovery of fresh, glassy lava samples and the identification of active hydrothermal vents and deposits near the summit (Moore et al., 1979, Frey and Clague, 1983, Garcia et al., 1989; Clague et al., 2019).

According the USGS HVO website the summit of Lō’ihi is nearly flat and marked by a caldera-like depression that is ~1.7mi (2.8km) wide and ~2.3mi (3.7km) long. The southern part of the caldera is host to three collapse pits or craters. The most recent, Pele's Pit, formed during an intense 1996 seismic swarm that was subsequent to an eruption from a shallow magma chamber (Clague et al., 2019). This new crater is about ~1,970 ft (600 m) in diameter with its base ~985ft (300m) below the previous surface. Figure 31 shows a Clague et al. (2019) interpretation of the summit caldera complex and its various pit craters. The volcano has grown from eruptions along distinct northwest and southeast rift zones that extend out from the caldera.

Clague et al (2019) state that the asymmetric, east-west-dipping slopes of the rift zones and the summit platform suggest that the flanks of Lō’ihi have been modified by landslides. They also state that the west flank has been modified by 2 landslides and the eastern flank has been modified by one much larger slide or several merged slides (Malahoff, 1987).

Lō’ihi is nearing the end of its deep submarine, pre-shield stage and is starting to switch from the alkaline-dominant volcanism characteristic of the pre-shield stage to the tholeiitic-dominant volcanism characteristic of the beginnings of the submarine shield sub-stage (Clague and Dixon, 2000). Lō’ihi could emerge above sea level in as little as ~30,000 years or as much as 200,000 years, depending upon eruption rate (USGS HVO website).

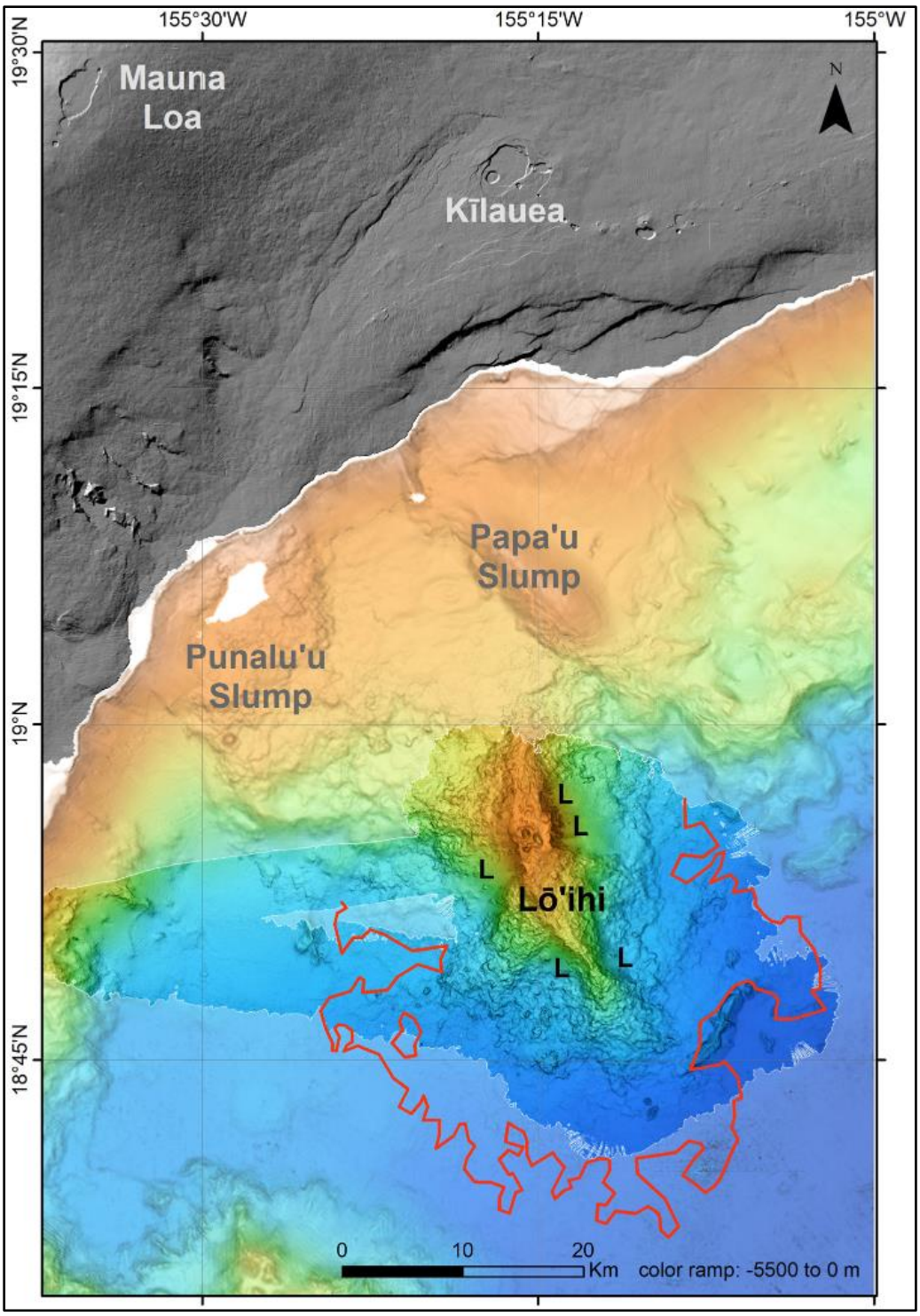


Figure 30: This is a regional map of the Lō‘ihi Seamount, the surrounding seafloor, and the sub-aerial south flank of the island of Hawaii. The summit calderas of Kīlauea and Mauna Loa are labeled, as are the Punalu’u and Papa’u slumps. The red line surrounding Lō‘ihi is the extent of known lava flows. The letter ‘L’ indicates the locations of flank landslides. The color ranges from blue for deep and shallowing through of green and yellow shades into orange for shallow. Figure from Clague et al., 2019.

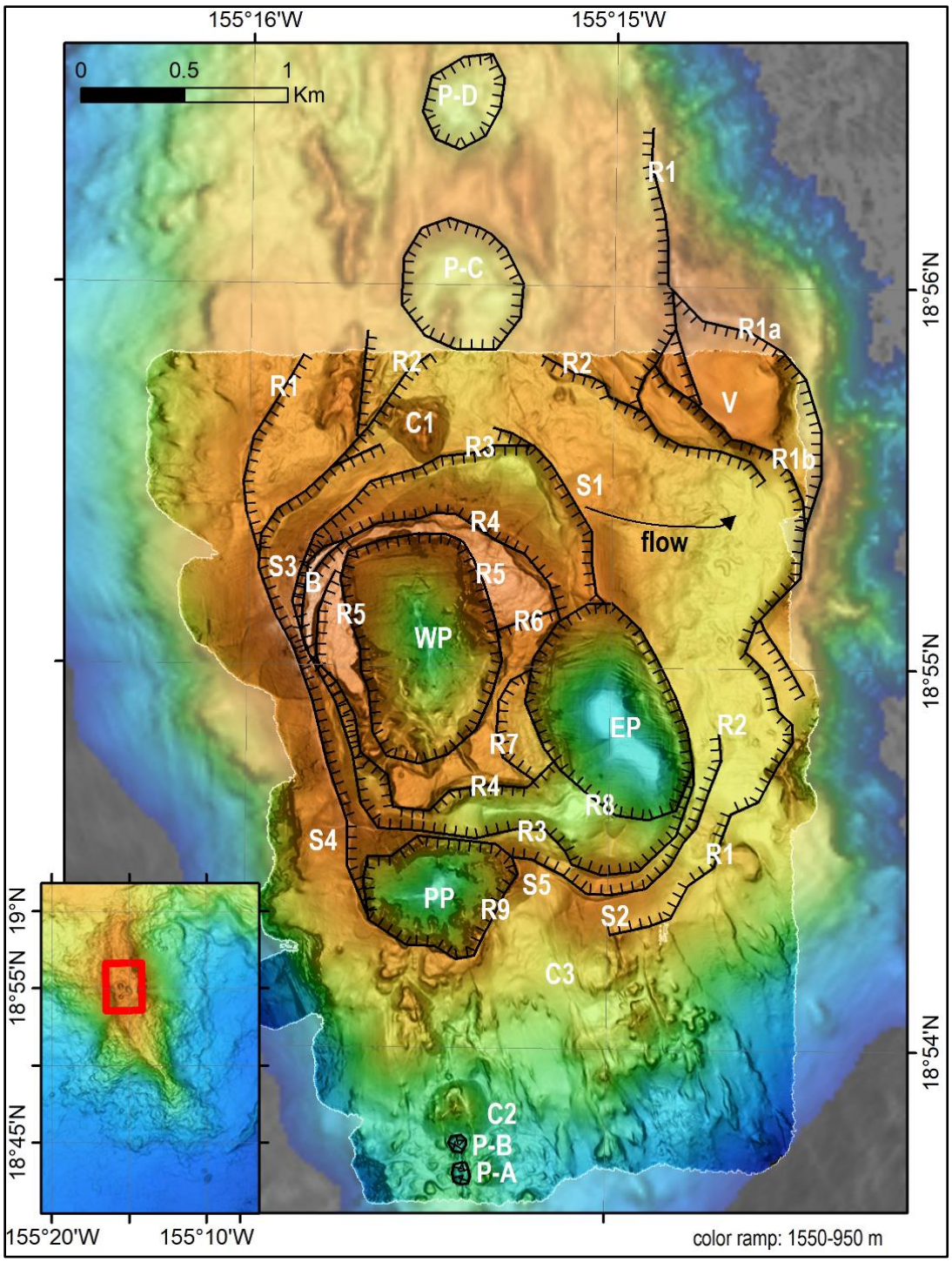


Figure 31: Lōʻihi summit bathymetry with interpretive overlay of caldera- and pit crater-bounding scarps. Hatched lines indicate down-thrown side of the caldera- or pit crater-bounding scarps or ring faults R1 (oldest) to R9 (youngest). The exact sequence of formation for some collapse events could not be determined. P-A to P-D are pit craters. EP is East Pit, WP is West Pit, PP is Pele's Pit, C1 to C3 indicate cones, S1 to S5 indicate the remnants of lava shields, B indicates 1996 basaltic breccia, and V indicates 5-11m thick volcaniclastic sediment with a basal age date of ~5900 years. Arrow labeled "flow" indicates direction of channelized flow from S1 to the east. Figure from Clague et al. (2019).

3. Field Trip Stops

3.1. Day 1: Kailua-Kona to Hawai‘i Volcanoes National Park

The 7 stops planned for Day 1 are located between the city of Kailua-Kona and the junction between Highway 11 and the South Point Road. The stops are listed below and are shown in Figure D1-1:

1. Kealakekua Bay, Kapu o Keōua Pali (fault scarp), and the 1779 Captain Cook landing location monument;
2. Pu‘uhonua o Hōnaunau (Place of Refuge) National Historic Park;
3. The 1950 Mauna Loa Ka‘apuna Flow and Pali Kaholo;
4. 1926 Mauna Loa Ho‘ōpūloa flow at the site of the destroyed village of Ho‘ōpūloa;
5. Old Mauna Loa ‘a‘ā flow infilling an older flow channel and complex lava draping.
6. 1907 flows, view of Ka Lea slide scarp, and coastal littoral cones; massive olivine-porphyritic flow core;
7. 1868 Mauna Loa ‘a‘ā lava channel; columnar jointing; and olivine-rich pāhoehoe basalt flows with lava stalactites, dripstone, a pseudodyke, and horizontal tree moulds.

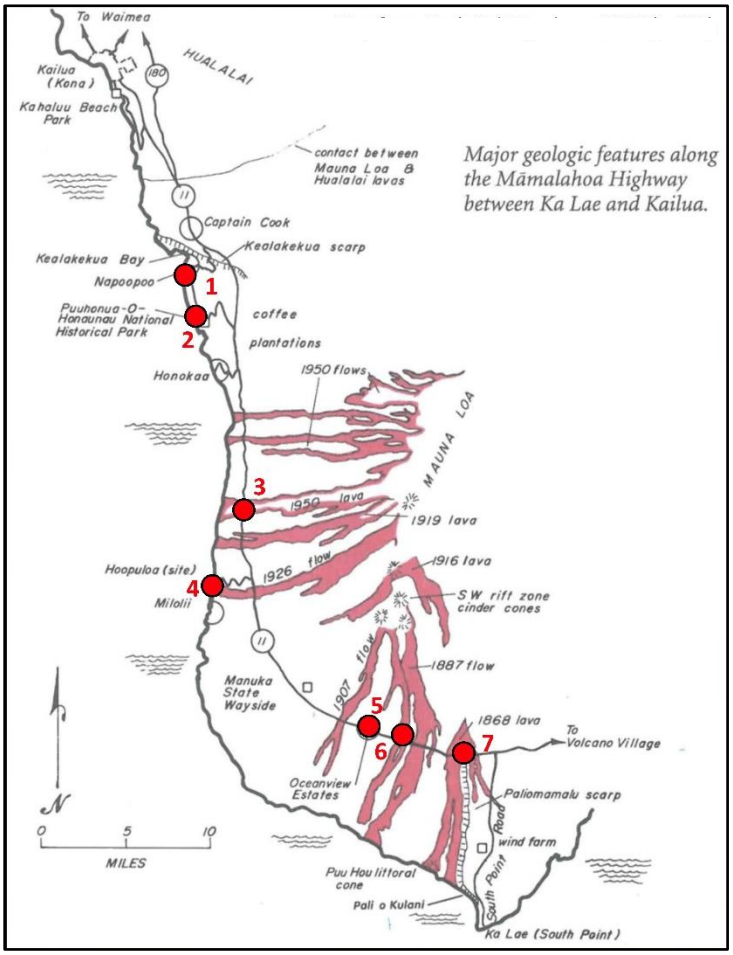


Figure D1-1: Map showing the Day 1 field stops associated with Mamaloa Highway 11 between Kailua-Kona and the South Point (Ka Lae) Road. Map modified from Hazlett and Hyndman (2007, p.102).

Stop D1-1. Kealakekua Bay and Kapu o Keōua Pali (Fault Scarp). Data Source: Robinson (2010).

- **UTM 193505E, 2156045N; several parking areas near the end of, or alongside, the road.**

From the waterfront village of Nāpoʻopoʻo an impressive view of the Kapu o Keōua Pali is possible. This pali, or fault scarp, is thought to have originated during the enormous Alikā landslide that occurred between 100,000 to 150,000 years ago. This landslide may have generated an immense tsunami that scoured the island of Kahoʻolawe to a height of 800ft (243m) and washed blocks of coral as high as 1000ft (305m) up the slopes of the Island of Lānaʻi. Looking closely at the pali (*see* Figure D1-2) will reveal the presence of several old landslide scars.

Captain James Cook landed across the bay in 1779 near the white pylon monument (in the distance south of the pali) and was killed near this spot later in the year during a battle with Hawaiʻians natives.

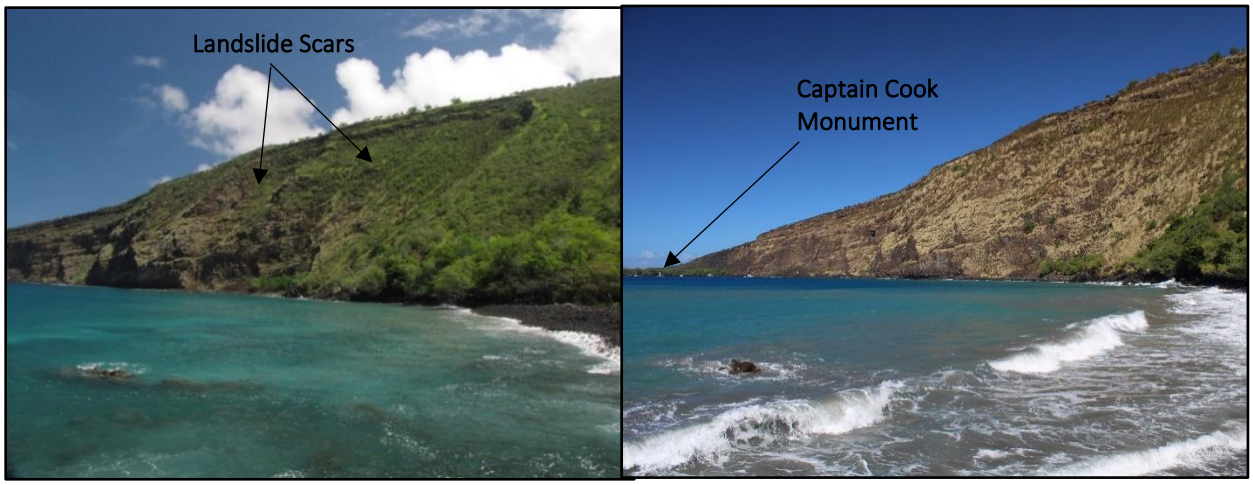


Figure D1-2: Pali Kapu o Keōua (fault scarp) with several old landslide scars (shown left) and the location of the Captain Cook Monument (shown right). Photo Credits: A.D. MacTavish (left, 2019; right 2020).

Stop D1-2. Puʻuhonua o Hōnaunau (Place of Refuge) National Historic Park. Data Source: Robinson (2010).

- **UTM 194405E, 2150110N; park in parking lot.**

The Puʻuhonua o Hōnaunau is an ancient Hawaiʻian religious site built on a 750 to 1500yr old pāhoehoe flow delta and is the best-preserved site of its kind in the islands (*see* Figure D1-3, left). It was originally built about 1650 and was restored in 1968.

A large drystone wall over 1000ft (305m) long, 15ft (4.6m) thick, and 10ft (3m) high (*see* Figure D1-3, right) was built about 1550AD and leads up to the main temple. The wall separated the temple site from the royal grounds on the east side of the wall.

The city was a sacred sanctuary that provided temporary shelter to defeated warriors and kapu (taboo) breakers. If kapu breakers were able to reach the site after swimming through the shark infested ocean they were cleansed during a ceremony of absolution and their lives were spared. During times of war this site was also a place of temporary shelter for women, children, the aged, and defeated warriors.

Every hour on the half hour NPS Park Ranger's present talks in a small amphitheatre near the park entrance building. The talks add detail about the site and its cultural and religious significance.



Figure D1-3: The upper left photo is a silhouette of the Place of Refuge temple. The upper right photo shows the 10ft (3m) high drystone wall built with blocks of lava and no mortar. Some of blocks are greater than 2m in length. Photo Credit: A.D. MacTavish (2012).

Stop D1-3. Kaʻapuna Flow. Data sources: Hazlett and Hyndman (2007); Robinson (2010).

- **UTM 197773E, 2132571N, parking area along shoulder of the Highway.**

At this stop is the very rough Kaʻapuna ʻaʻā flow which is the widest (~1100ft or 640m) and most easily recognizable of the multiple flow tongues formed during the spectacular 1950 Mauna Loa eruption.

The 1950 eruption began when a 15mi (24km) long fissure opened along the southwest rift zone, which is located towards the sea from Mokuʻāweoweo, Mauna Loa's summit caldera. Approximately 491,789,433 cubic yards (491.8×10^6 yd^3) or 376,000,000 cubic metres (376×10^6 m^3) of dark, blocky ʻaʻā erupted from the fissure over a period of a few days. The lava flowed down-slope to the sea at a speed of ~6mph (10km/hour) and buried a community in the process.

Accretionary lava balls can be seen at the north edge of parking area.

The steep slope below and to the west of the highway is Pali Kaholo which is the top of a large slump that cut into the lower western flank of Mauna Loa.

Stop D1-4. 1926 Mauna Loa (or Hoʻōpūloa flow). Data sources: Hazlett and Hyndman (2007); Robinson (2010).

- **UTM 194595E, 2124810N; pull-off area at north side of road.**

This stop is the approximate location of Hoʻōpūloa Village which was destroyed by the underlying Mauna Loa flow in 1926. There has been considerable rebuilding over the old village site.

This channelized ʻaʻā flow (*see* Figure D1-4) is the result of an eruption along the southwest rift of Mauna Loa that began on April 14, 1926 at an elevation of 7478ft (2316m). The eruption lasted 14 days, extruded a volume of at least 130.8×10^6 yd^3 (100×10^6 m^3), and destroyed the Hoʻōpūloa Village.

The Miloli‘i road taken to get to this site traverses down the pali from Highway 11 to the coast in multiple switchbacks comprising >100 turns over a 5mi (8km) distance; the experience of this road is similar in some ways to the much longer, busier, and much more exhausting Hana Road located on the northeast coast of the Island of Maui (which is well worth a careful drive, in good weather).



Figure D1-4: Channelized 1926 ‘a‘ā flow at the former site of Ho‘ōpūloa Village. Photo Credit: Google Earth.

Stop D1-5. Lava Channel, Drape Structures. Data sources: Easton and Easton (1995); MacTavish (2019).

- **UTM 209680E, 2111865N; park 160m to the east-southeast near the entrance to King Kamehameha Boulevard (the safer option) or on the southern road shoulder at the field stop.**

The roadcut on the north side of the road hosts an infilled, 46 to 54ft (14 to 16m) wide ‘a‘ā flow channel occupying a depression within underlying pāhoehoe flows (*see* Figure D1-5, left). These olivine-phyric flows form complex drape structures over the levée margins of channel on both sides of the highway (*see* Figure D1-5, right). The flows infilling the channel were subsequently overlain by a thin columnar-jointed flow.



Figure D1-5: On the left is an ‘a‘ā flow infilling a channel in underlying pāhoehoe flows and overlain by columnar-jointed flow on the north side of the highway. The right photo shows complex drape structures forming a levée to the underlying flow channel infilled by the later ‘a‘ā flow. Photo Credits: A.D. MacTavish (left, 2020; right, 2019).

Stop D1-6. 1907 Mauna Loa flows; Ka Lea slide scarp; littoral cones; massive olivine-porphyritic flow core. Data sources: Easton and Easton (1995); MacTavish (2019).

- **UTM 211515E, 2111125E; scenic overlook (Mile Marker 75).**

A 15-day Mauna Loa eruption began on January 9, 1907 at an elevation of 6200ft (1890m) ASL. The vent, located 8mi (13km) inland, erupted $981x10^6$ yd^3 ($750x10^6$ m^3) of lava over this period. The roadcut at this stop exposes the core of a massive ʻaʻā flow with oxidized top and bottom breccias, and abundant green olivine crystals up to 0.16in (4mm) in diameter. Numerous Mauna Loa Southwest Rift Zone cones and flows are located upslope from this location (not readily visible).

The Pali o Kūlani fault and slump scarp, located west of Ka Lea (South Point), is visible east and south of the overlook (*see* Figure D1-6). This pali formed when a large submarine landslide broke away from Mauna Loa's submerged western slope. In the distance, to the right of the pali at the shoreline, are numerous littoral cinder cones comprising the Puʻu Hoʻu Cone Complex. The largest, most prominent cone is wave-eroded Puʻu Hoʻu, which is located to the left of the smaller cones (Figure D1-6).

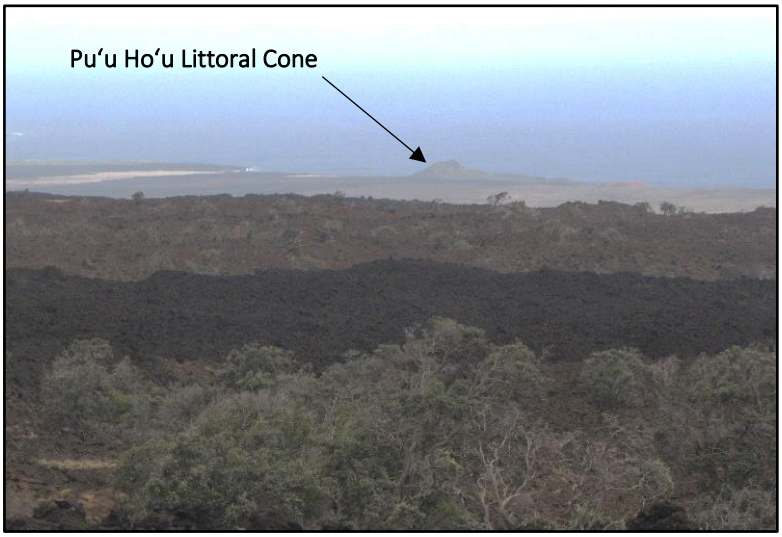


Figure D1-6: 1907 flow (dark-coloured lava) with the Puʻu Hoʻu littoral cone field at the coastline in the distance. Photo Credit: A.D. MacTavish (2019).

Stop D1-7. Olivine-rich 1868 Mauna Loa pāhoehoe basalt flows; lava tubes (pyroducts); and horizontal tree moulds. Data sources: Easton and Easton (1995); Robinson (2010); Hazlett and Hyndman (2007).

- **UTM 216865E, 2109545N; parking on the right (south) side of highway.**

On the north side of the highway the eastern portion of the 1868 Mauna Loa flow is characterized by thin, very vesicular pāhoehoe flows that range from olivine-poor at their base upward through olivine-rich to picritic (very olivine rich with >13 weight % MgO) at their tops (*see* Figure D1-7, left). The cooling units consist of 2 layers, separated by a central cavity (small lava tubes/pyroducts?), contain dripstone (*see* Figure D1-7, right) and occasionally small lava stalactites. Lava drapes are common and there are some small, horizontal tree moulds. On the south side of the highway there is a pseudo-dyke produced by channel overflow from a crack in the 1868 levée. Some volcanologists now using of the term pyroduct instead of lava tube; however, the term lava tube is much more intuitive for non-specialists to understand without a lot of explanation and will continue to be used within this guide.



Figure D1-7: The left photo shows the thin 1868 Mauna Loa pāhoehoe olivine basalt flows. Note the wall built on top of the outcrop from blocks of the thin flows. The right photo shows drip-stone and incipient lava stalactites within the central cavity (small lava tube/pyroduct) of a single cooling unit. Photo Credits: A.D. MacTavish (2019).

3.2. Day 2: Highway 11 and South Point

Note that as you drive southwest along Highway 11 you will be driving back and forth across the contact between the usually well-vegetated and blocky Mauna Loa ‘a‘ā flows and the primarily less vegetated, Kīlauea pāhoehoe flows. For much of the drive the Mauna Loa flows will be to the right and the Kīlauea flows will be to the left. You will also drive past several thin, difficult to see deposits of Pāhala Ash; however, the best exposures are most easily observed at South Point

8. Punalu‘u Black Sand Beach Park and Hawai‘ian green sea turtles.
9. South Point, Pāhala Ash (Stop D2-9a), and green sand beaches (Stop D2-9b).

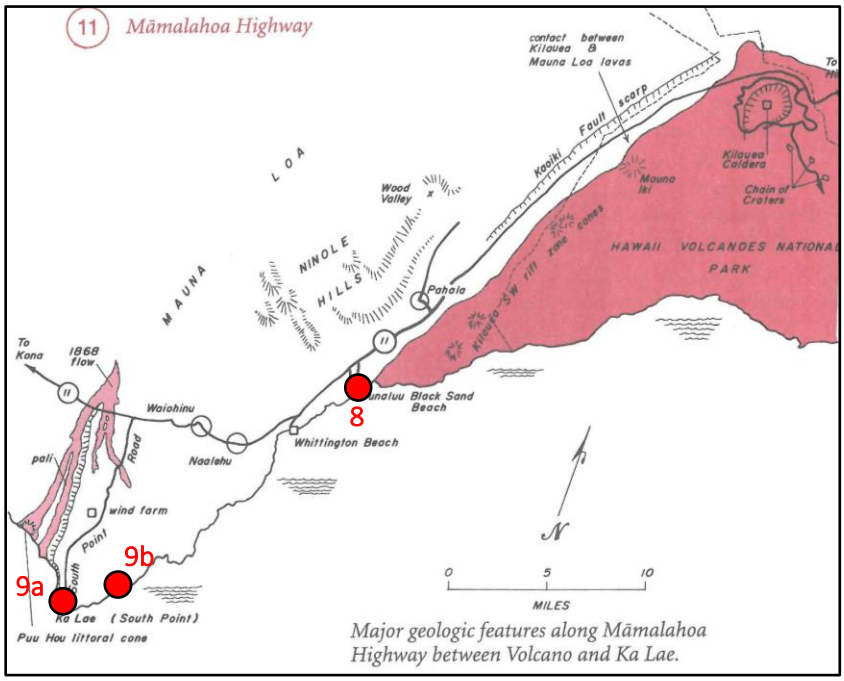


Figure D2-1: Map showing the Day 2 field stops associated with Mamaloa Highway 11, south and west of the town of Pahala and the South Point (Ka Lae) Road. Map modified from Hazlett and Hyndman (2007, p.96).

Stop D2-8. Punalu‘u Black Sand Beach. Data sources: Hazlett and Hyndman (2007); Robinson (2010); MacTavish (2020).

- **UTM 236403E, 2117534N; parking lot.**

The Punalu‘u Beach Park protects a black sand beach (*see* Figure D2-2, left) that is thought to be the site of the first landing in the islands by Polynesians. The sand on the beach was derived from both Mauna Loa and Kīlauea flows and consists of black particles of obsidian (volcanic glass) formed when the lava flows entered the sea, chilled very rapidly, and broke into glassy, sand-sized grains. The beach was larger in the past; however, much of the original sand was removed by a series of tsunami’s that pounded this coastline in 1868, 1960, and 1975.

Hawai‘ian green sea turtles (honu) are often present and sleeping in the beach sand (*see* Figure D2-2). AM has visited this beach 5 times over a twelve-year period and there has always been at least 1 honu sunning itself. **Please do not touch the turtles because the bacteria on our skin is potentially deadly to them**.

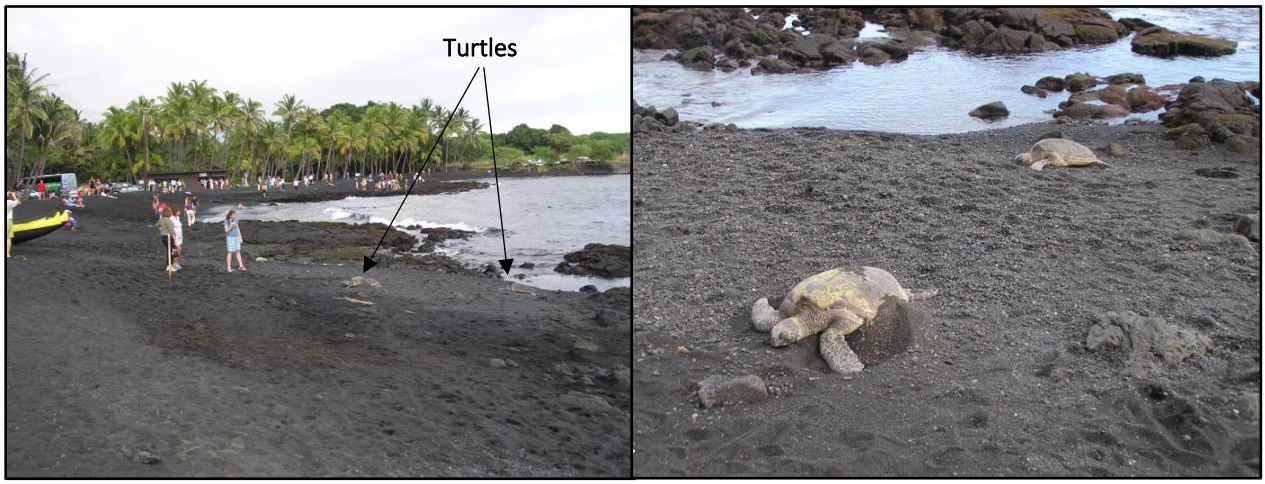


Figure D2-2: The left photo shows the black sand beach at Punalu‘u Beach Park. The right photo is a close-up of 2 Hawaiian green sea turtles (honu) sunning themselves on the beach. Photo credits: A.D. MacTavish (2008).

Stop D2-9a, Ka Lea (South Point) and the Pahala Ash. Data sources: Easton (1978, 1987); Easton and Easton (1995).

- **UTM 217575E, 2093130N; parking lot.**

Ka Lea is the southernmost point in the United States and is the site of one of the island’s oldest settlements, with artifacts dating back to circa 300AD.

Also, at this stop the ~31,000yr old Mauna Loa pāhoehoe flows are overlain by 3.3 to 4.9ft (1 to 1.5m) of >22,000yr old, fine-grained, yellow-brown, palagonatized, wind-reworked Pāhala Ash (*see* Figure D2-3). The Pāhala Ash is an enigmatic, widespread deposit used as a stratigraphic marker despite the uncertainty of its source or age. It is present on Kīlauea, Mauna Loa, Mauna Kea, and Kohala volcanoes. The oldest Pāhala Ash on Mauna Loa and Kīlauea is ~31,000 years old with the youngest ash covered by flows that are between 10,000 and 200 years old. This ash formation may represent a long period where Kīlauea was primarily explosive, possibly due to a period of higher rainfall during the last glacial maximum. This caused more phreatomagmatic (water and magma interaction) summit activity, increased the size of the caldera, and resulted in both explosive and magmatic activity (Easton, 1978).



Figure D2-3: These photos show the 1 to 1.5m thick deposits of well-bedded, but poorly consolidated Pāhala Ash at Ka Lea (South Point). Photo credits: A.D. MacTavish (2019).

The sea cliff (*see* Figure D2-4) that forms South Point's western coastline and eventually heads inland to the north is known as Pali o Kūlani. The cliff is a slump scarp where Mauna Loa's Southwest Rift Zone dropped due to a large slide that broke from the submerged Mauna Loa slope to the south and west. The Puʻu Haʻu Littoral Cone can be seen ~4.35mi (7km) to the northwest (observed first from Stop D1-7) from the top of the western sea cliff (noted by arrow in the upper left of Figure D2-4). The cone marks the location where a tongue of lava from the 1868 Mauna Loa ʻaʻā flow, that erupted from the inland extension of the scarp, entered the ocean. Wave erosion has cut the cone in half.

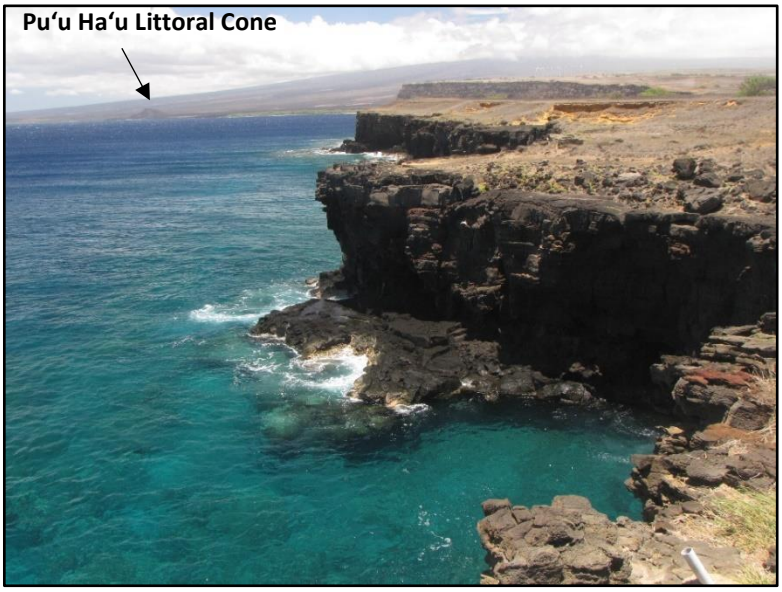


Figure D2-4: The western sea cliff at Ka Lea (South Point) with the Puʻu Haʻu cone in the distance to the northwest at top left. Photo credit: A.D. MacTavish (2019).

Stop D2-9b. Papakōlea Green Sand Beach. Data sources: Easton (1978, 1987); Easton and Easton (1995).

- **UTM 218448E, 2094263N; parking Area.**
- **UTM 221295E, 2095850N; intermediate green sand beach located south of 4x4 road.**
- **UTM 221295E, 2095850N; Papakōlea Green Sand Beach.**

South Point is famous for its green olivine sand beaches. The source of the olivine comprising the beach is the weathered and eroded, olivine-rich, Pu‘u Mahana Littoral Cone.

The at least 2 to 3-hour return hike from the parking lot northeast to the Papakōlea Green Sand Beach is approximately 2mi (3.2km), as the nene flies, and at least 3mi (5km) along a complex series of 4x4 roads incised into the Pāhala Ash. Some field guides, and the present authors, recommend that if you have any trouble walking that you do not attempt the full hike. There are other, smaller, pocket green sand beaches along the shoreline seaward of the route about 2/3 of the distance to the main beach (*see* Figure D2-5), that can be visited if there is not enough time (or energy) to complete the full walk (bring lots of water and snacks and liberally apply sunscreen). This is not an easy walk, even though it is relatively flat. Access to the main beach is difficult so good hiking boots or hiking shoes are a must.

For a fee very rough transportation in the back of 4x4 trucks is available from a group of indigenous Hawai‘ians at the parking lot at the beginning of the access trail. This transportation is not recommended if you have a bad back, knees or neck or suffer from vertigo or motion sickness.

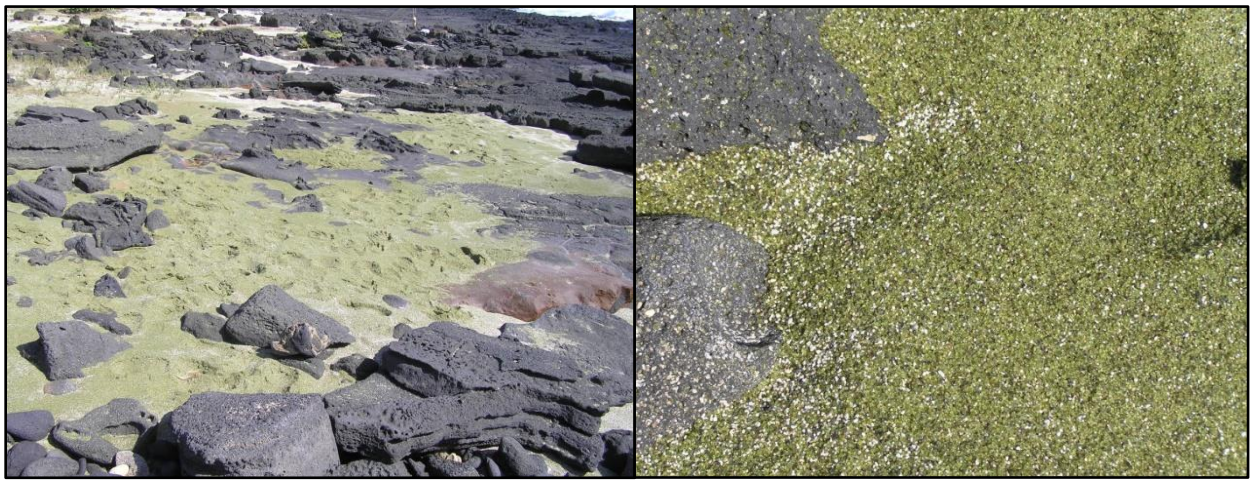


Figure D2-5: The left photo shows a small, pocket green sand beach located along the coastline between South Point and the Papakōlea Green Sand Beach. The right photo shows the small, green, olivine sand grains mixed with small amounts of carbonate sand and some magnetite that comprise the pocket beach in the left photo. Photo credits: A.D. MacTavish (2019).

Robinson (2010) states that the olivine comprising the beach sand was derived by wave erosion of the Pu‘u Mahana Littoral Cone (or tuff ring volcano; *see* Figure D2-6) which formed approximately 28,000 years ago. A tuff ring forms from interaction of magma with shallow groundwater or seawater. Wave action has eroded the seaward side of the tuff ring, formed a small bay, and removed the light grains of ash while leaving the denser and heavier olivine grains behind.

The sides of the cliffs above the beach are quite steep and access to the beach is difficult. **Do not attempt to descend to the beach if you have difficulty walking or climbing**



Figure D2-6: Papakōlea Green Sand Beach from the western crater rim. Please note how small the people on the beach appear, which gives you an idea of the height of the poorly consolidated cliffs. The ash layers comprising the walls of the cone are readily visible in the upper centre of the photo. Photo credit: A.D MacTavish, 2020.

3.3. Day 3 (Part 1): Mauna Loa Road and Mauna Loa Strip

The Mauna Loa Road starts at Highway 11 and ascends up the eastern flank of Mauna Loa for 12mi (19.3km) to an elevation of 6725ft (2050m). This road traverses the 'Mauna Loa Strip' which is the portion of Hawai'i Volcanoes National Park linking the summits of Kīlauea and Mauna Loa (Moku'āweoweo Caldera). The Mauna Loa Strip from the western rim of Kīlauea caldera comprises a narrow, dark green, forested belt enclosed by the grassy, light-coloured grassland that ascends Mauna Loa's eastern flank. This strip of subtropical Hawai'ian upland forest is one of the world's most rare and fragile ecosystems. This forest type was once much more widespread; however, it has been almost completely eliminated due to overgrazing, over-logging, eruptions, and displacement by introduced species (Hazlett 2014).

Since this is a unique, ecologically fragile area with a high fire danger it is recommended that all visitors be especially careful. **PLEASE DO NOT SMOKE FOR ANY REASON**.

Mauna Loa Road Field Trip Stops (*see* Figure D3-1):

10. Large tree moulds.
11. Kīpuka Puaulu; ecologically diversified old land surrounded by younger lavas.
12. Ke'āmuku Flow; thin lobe of a larger composite flow derived from several eruptions that have been grouped together.
13. Ke'āmuku Flow channel; a spectacular and well-developed flow channel.
14. Road's End Scenic Overlook; panoramic view of Kīlauea Caldera, the Ka'ū Desert, and the upper Southwest and East rift zones (on a clear day); this is also the start of the Mauna Loa Trail.

Backtrack from Stop D3-14 to Highway 11 and drive southwest to the Ka'ū Desert Trail (Footprints/Mauna Iki Trail) for Part 2 of Day 3.

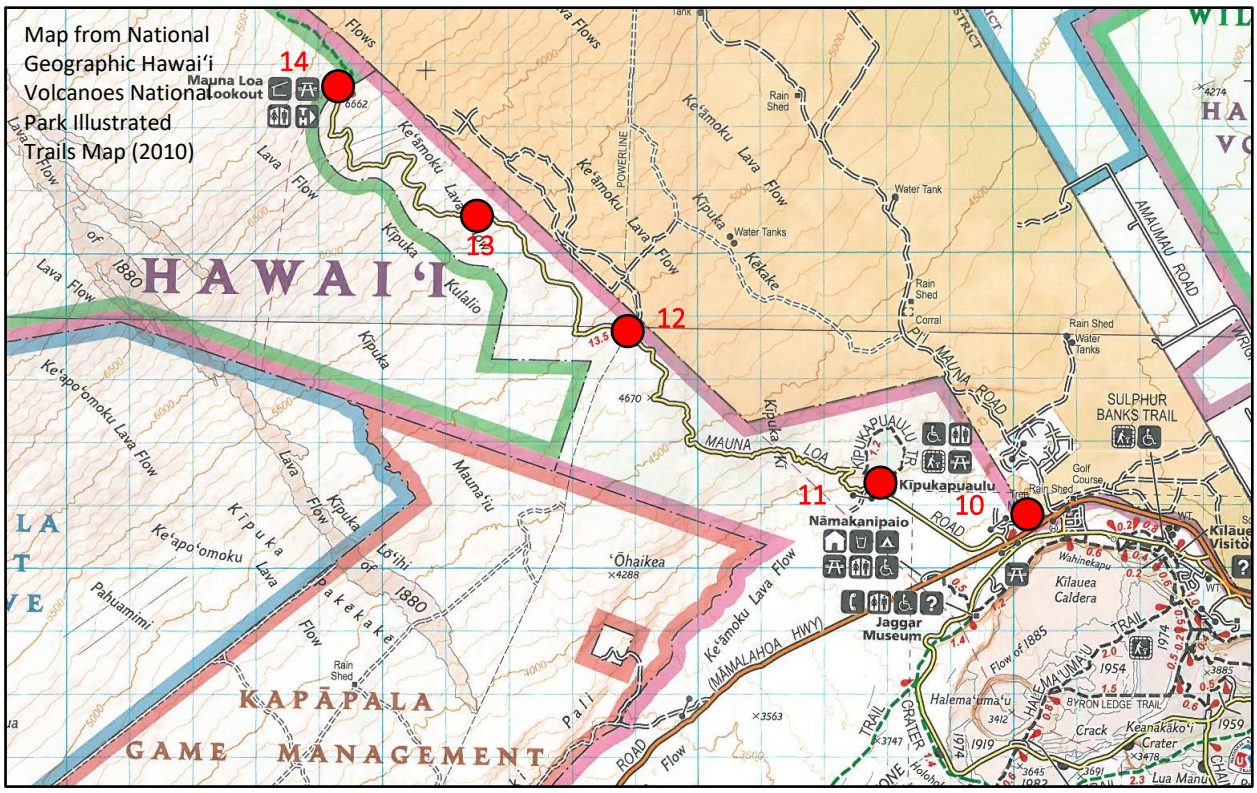


Figure D3-1: Field trip stops on the Mauna Loa Road and within the Mauna Loa Strip. Map taken from the National Geographic Hawai'i Volcanoes National Park Illustrated Trails Map (2010).

Stop D3-10: Lava Tree Moulds Area. Data sources: Hazlett and Hyndman (2007); Hazlett (2014); Easton and Easton (1995); MacTavish (2019).

- **UTM 260480, 2150490; parking area and turnaround located at the end of a 0.4mi (640m) long side road to the right of the Mauna Loa Road.**

The lava tree moulds here are very large, well-preserved, and encased by 700 to 800yr old Kīlauea pāhoehoe lava and according to Hazlett and Hyndman (2007) are:

> '*Among the largest and deepest in Hawai'i and preserve the shapes of mature acacia koa tree trunks*.'

These moulds can exceed ~5ft (1.5m) in diameter with depths of up to 10ft (3m). The largest mould is located to the right of the road about 200ft (60m) west of the parking area (at approximately UTM 260412E, 2150479N) as you are exiting the road loop back to the Mauna Loa Road. Some of the moulds have trees growing out of them or provide a place for roots to grow (*see* Figure D3-2). In all cases at this location there is a well-developed weathering-resistant, up 15cm thick, radially jointed chill margin surrounding each mould (also see Figure D3-2).

Figure D3-3 graphically illustrates how tree moulds and lava trees form.



Figure D3-2: Large fenced lava tree mould with tree root and thick chilled mould rim on the left and the preserved bark pattern in mould wall on the right. Photo credits: A.D. MacTavish (2019).

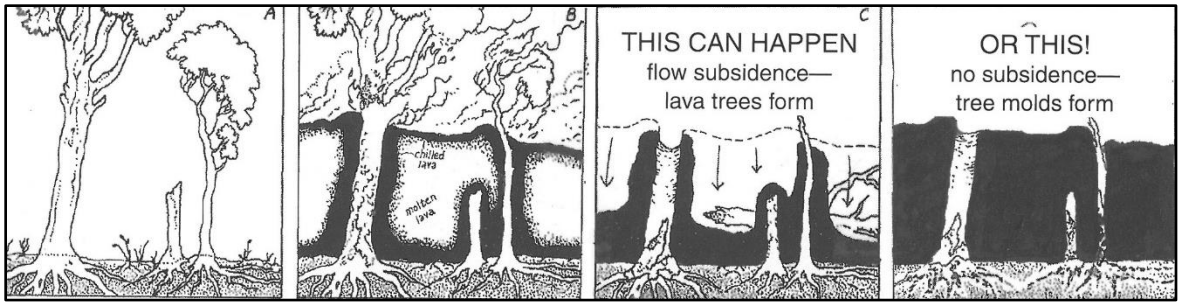


Figure D3-3: Lava trees and tree moulds form when a forest is invaded by a lava flow and the lava surrounds the trees. The lava chills against the tree trunks, the ground, and the top of the flow and forms a solid crust around the trees. As the lava supply diminishes the remaining liquid drains away. 'Tree moulds' are hollow impressions of trees left in the lava that are enveloped, but not instantaneously incinerated by the lava and where the surface of the flow does not drop. If the mould is preserved as a shell rising above the surface of the flow after the flow surface drops it is termed a 'lava tree'. (Hazlett, 2014; Easton and Easton, 1995).

Stop D3-11. Kīpuka Puaulu and self-guided trail. Data sources: Hazlett and Hyndman (2007); Easton and Easton (1995); National Parks Service (NPS) Kipukapuaulu Trail Guide.

- **UTM 258180E, 2150865N; parking area.**

Kīpuka are areas of old, often forested land, that are usually surrounded by unvegetated younger terrain, often flows. There are innumerable kīpuka on the island and they provide isolated habitats for many, often rare, plants, animals, and birds that can be found nowhere else on earth.

The fragile, ecologically diverse Kīpuka Puaulu is located at the base of the long slopes where Kīlauea and Mauna Loa meet. Here the kīpuka is underlain by up to 20ft (6m) of 2200yr old volcanic ash that accumulated as fallout strata and windblown ash on top of older flows. The kīpuka is enclosed on 3 sides by a <500yr old Mauna Loa flow and, at the trail entrance, by a 700-800yr old Kīlauea flow. If time allows the trail may be hiked by those who are interested. Walking the 1mi (1.6km) self-guided nature trail (please keep the gate closed) provides striking contrast in vegetation that corresponds to different ages, compositions, and weathered surfaces along the edge of the kīpuka.

Stop D3-12. Thin southeast offshoot lobe of the composite Keʻāmuku Flow. Data Sources: Hazlett (2014); MacTavish (2019).

- **UTM 254110E, 2153350N; parking area.**
- **UTM 254065E, 2153405; centre of flow lobe ~75m northwest along road from cattleguard.**

This narrow (~330ft or ~100m wide), offshoot ʻaʻā flow lobe from the main composite Keʻāmuku Flow, located to the north, is a weakly-developed levéed channel containing a broken, roughly spherical accretionary lava ball located ~35m (115ft) south (downslope) from the road (*see* Figure D3-4). This lava ball was formed from pieces of solidified lava which were pulled into the stream of the lava channel and rolled along with the current such that the ball eventually accumulated a series of coats of lava in a similar manner to a rolled snowball increasing in size due to added snow.



Figure D3-4: Broken accretionary lava ball within offshoot of the Keʻāmoku Flow. Photo source: Google Earth.

Stop D3-13. Keʻāmuku Flow. Data sources: Lockwood (1979); Hazlett (2014); MacTavish (2019).

- **UTM 251868E, 2155185N; centre of flow.**
- **UTM 251940E, 2155225N; eastern parking area located just before the flow opposite the 5630ft (1730m) ASL sign.**
- **UTM 251697E, 2155250N; western parking area (located ~330ft or ~100m past the flow).**

Flows from several eruptions have been grouped together by the USGS and referred to as the Keʻāmuku Flow. Here this specific ʻaʻā flow exhibits a spectacular, well-developed, levéed lava channel (*see* Figure D3-5) that Lockwood (1979) estimates is between 400 and 500yrs old and was erupted from vents on Mauna Loa's northeast rift zone.

There are numerous, partially buried accretionary lava balls within the channel.



Figure D3-5: Well-developed, levéed, lava channel within the Keʻāmoku Flow. Photo source: A.D. MacTavish (2019).

Stop D3-14. Road's End Scenic Overlook. Data Sources: Hazlett (2014); Easton and Easton (1995).

- **UTM 249630, 2157090; parking area, restrooms, and picnic tables.**

From the road, and the overlook shelter, panoramic views of Kīlauea Caldera and the upper Southwest and East Rift zones are available from an elevation of 6725ft (2046m), if cloud cover permits. This is also the trailhead for the 30.5km (19.0mi) Mauna Loa Trail which leads upslope to Mokuʻāweoweo caldera and the summit of Mauna Loa at 13,677m (an approximate 2-day hike).

3.3. Day 3 (Part 2): Mauna Iki Trail/Kaʻū Desert Trail and the Southwest Rift Zone

Field trip stops along the western portion of the Kaʻū Desert Trail/Mauna Iki Trail (*see* Figure D3-6):

15. Kaʻū Desert Trailhead with a view of Kaʻōiki Pali to the west. The trail starts on the lower Keʻāmoku Flow.
16. Several Large accretionary lava balls similar to those observed earlier at Stops D3-12 and D3-13.
17. Trail drops down from Keʻāmoku ʻaʻā flows onto Kīlauea pāhoehoe flows. Sand dunes, palagonitized Pele's hair, and some ash layers are visible along the trail.
18. Keanakākoʻi Ash with well-developed graded, cross-bedded and laminated ash layers.
19. Fossil footprints in 1790 pisolitic (accretionary lapilli-bearing) Keanakākoʻi Ash. Recent pyroclastic activity from Kīlauea summit (2018) has obscured many of the footprints. However, wind will probably uncover other, presently buried footprints in the future.
20. Accretionary lapilli layer.
21. Pāhoehoe toes formed from small lava breakouts from the base of a small tumulus.
22. Pre-Mauna Iki lava channel with lava level marks visible on the northern levée of the channel.
23. Trail crosses 700yr old pāhoehoe flows covered with drifts of Keanakākoʻi Ash and recent, circa 2018, Pele's hair with a large tumulus rising near the edge of the Mauna Iki shield.
24. The southern edge of the large tumulus hosts the broken and congealed remnants of several small lava falls.
25. Mauna Iki summit which was active in 1919 and 1920. This shield is relatively low topographically.

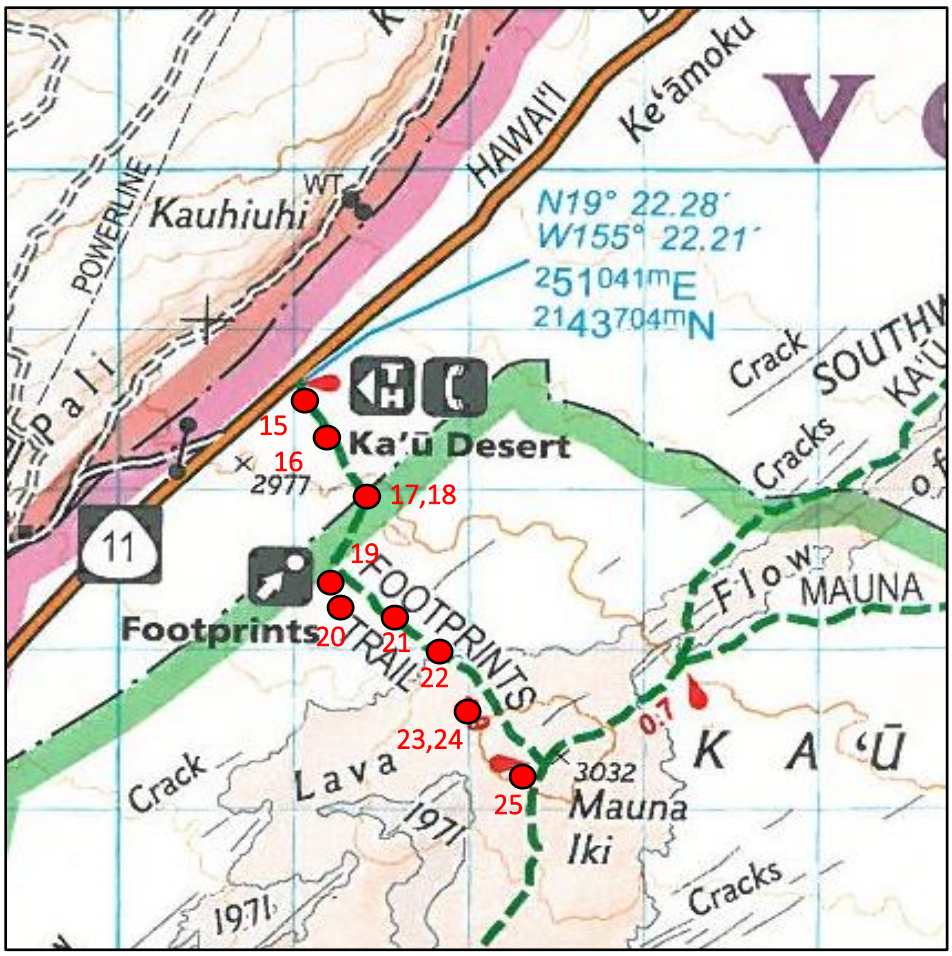


Figure D3-6: Field trip stops along the Ka'ū Desert Trail between Highway 11 and the summit of Mauna Iki. Map taken from National Geographic Hawai'i Volcanoes National Park Illustrated Trails Map (2010).

Stop D3-15, Ka'ū Desert Trailhead. Data Sources: Lockwood (1986); Hazlett (2014); MacTavish (2019).

- **UTM 251315E, 2143330N; turnout (parking area) on left.**

Approximately 1.0km (0.5mi) west of the parking area is Ka'ōiki Pali which is a 100m (325ft) high fault scarp related to the Ka'ōiki fault system. This fault system is a region of recurrent seismic activity along the southeast flank of Mauna Loa (Hazlett, 2014)

The Ka'ū Desert Trail begins on the lower part of the Ke'āmoku Flow visited earlier in the day at Stops D3-12 and D3-13. The 'a'ā flow at this location has been dated at ~500yrs old (Hazlett, 2014); many well-developed accretionary lava balls are present on the surface of the flow. This date was obtained via a 1986 personal communication between Hazlett (2014) with J.P. Lockwood.

Stop D3-16a. Large accretionary lava balls. Data source: MacTavish (2019).

- **UTM 251375E, 2143250N.**

This area has several good examples of large, well-developed, accretionary lava balls (*see* Figure D3-7) that are similar to those observed earlier at Stops D3-12 and D3-13. Some of the best examples are located to the left (east) of the trail near the 2 trail signs at this location.



Figure D3-7: Large well-developed accretionary lava balls on the Lower Keʻāmoku Flow. Photo credit: A.D. MacTavish (2019).

Stop D3-16b, Large, >2m accretionary lava ball. Data source: MacTavish (2019).

- **UTM 251430E, 2143150N**

At this field stop, on the left side of the trail, is a >6.5ft (~2m) diameter accretionary lava ball (*see* Figure D3-8, left). This lava ball has several cavities that show the interior structure of the ball (*see* Figure D3-8, right).



Figure D3-8: The left photo shows a large >2m diameter accretionary lava ball on the north edge the trail (Dr. Juk Bhattacharyya as scale). The right photo shows the interior of the lava ball exposed by a large cavity (lens cap for scale). Photo credits: A.D. MacTavish (2019).

Stop D3-17. Edge of Keʻāmuku Flow. Data sources: Easton and Easton (1995); Hazlett (2014).

- **UTM 251705E, 2142620N**

The trail descends between 20 and 30ft (6 to 9m) from the top of the Keʻāmuku Flow onto the surface of an 800 to 900yr old (Swanson, 2000), ropey Kīlauea pāhoehoe flow (*see* Figure D3-9).

The surface of the flow is locally covered by patches of a dark sandy ash which is the upper part of the Keanakākoʻi Ash erupted from the Kīlauea summit in 1790 (Easton and Easton 1995; Hazlett 2014).

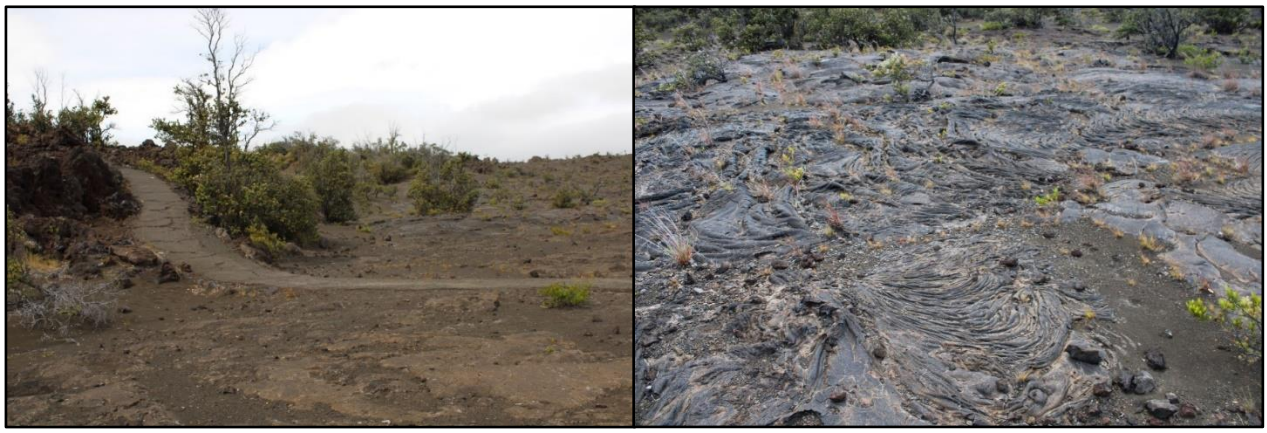


Figure D3-9: In the left photo the Kaʻū Desert Trail descends from the Keʻāmoku Flow onto and older, underlying, ropey Kīlauea pāhoehoe flow, shown in the right photo. Photo credits: A.D. MacTavish (2019).

Stop D3-18. Keanakākoʻi Ash. Data sources: Swanson and Christianson (1973); MacTavish (2019).

- **UTM 251632E, 2142286N; ~30m east (left) of where the paved trail ends.**

This location and its vicinity has several good exposures of finely bedded and laminated, graded, and cross-bedded greyish brown and light grey to yellowish-brown Keanakākoʻi Ash that erupted from the summit of Kīlauea in 1790. This ash is easily eroded and reworked by the wind and varies from weakly lithified to completely unlithified. Partially lithified examples are often preserved in cracks, crevasses, and wind-protected locations such as the lee sides of basalt outcrops and small ridges, or where stabilized by the roots of trees or grass (*see* Figure D3-10). Where more than a few centimetres are preserved it is possible to see that the greyish-coloured ash is unlithified, whereas, the yellowish-coloured ash is partially lithified and more weathering-resistant.

The cross-bedded nature of some of the preserved ash supports the Swanson and Christianson (1973) suggestion that the ash, at least in part, was formed from a series of pyroclastic base surge events.



Figure D3-10: The upper photo shows graded, cross-bedded, finely bedded to laminated Keanakāko‘i Ash of various colours. The buff to tan-coloured layers are the ones that preserve the 1790 fossil footprints hopefully exposed near Stop D3-19. The lower left photo shows ash plastered against an older flow. The lower right photo shows ash preserved in cracks and below overhangs in the older flow. Photo credits: A.D. MacTavish (2019).

Stop D3-19. Fossil footprints in Keanakāko‘i Ash. Data sources: Easton and Easton (1995); Hazlett (2014); Swanson and Christianson (1973).

- **UTM 251562E, 2142195N; NPS Hut.**

The 230yr old fossil footprints (*see* Figure D3-11) are preserved within yellowish-grey, partially lithified beds of Keanakāko‘i Ash erupted from Halema’uma’u crater within the Kīlauea summit caldera in 1790. Many of the unprotected footprints within the yellowish-grey to yellowish-brown beds of Keanakāko‘i Ash have been covered by both windblown 1790’s and 2018 ash and are often very difficult to find and to see. An NPS shelter built on site exhibits moulds of some of the better fossil footprints, but does not cover any of the actual footprints, which are all exposed to outside weather.



Figure D3-11: These photos show some of the footprints preserved in the yellowish-brown variety of Keanakāko'i Ash. Most of these footprints had been covered by windblown 1790 and 2018 vintage ash during AM's visits to the site during the summer of 2019 and winter of 2020 and did not provide any illustrative photographs. Photo credits: Donald A. Swanson, U.S. Geological Survey, Hawaiian Volcano Observatory website.

3.3.1. History of the Footprints Area:

The following description of the events in 1790 that produced the fossil footprints was taken verbatim from Easton and Easton (1995, p.37 and 38; also *see* Figure D3-12) with the spelling of Hawai'ian words as in the original document:

"*Footprints are preserved in indurated ash from the 1790 eruption from Halemaumau. In addition to the footprints at the shelter, other footprints are visible along the trail. The following account of the 1790 eruption is condensed from Swanson and Christianson (1973).*

An army led by King Keoua camped on the northern rim of Kilauea Caldera. That night Kilauea erupted violently. The next day King Keoua was afraid to travel, and Kilauea again erupted explosively that night. The same pattern held for the next day. On the third day, Keoua split his army into three groups of about 80 men (and their families) each, and resumed their march to Kau. The groups left at intervals of about 2 to 4 hours apart. Soon after the second group left, a violent phreatic or phreatomagmatic eruption occurred at Kilauea, and a hot base surge composed mainly of superheated steam spread SW of Kilauea Crater, enveloping the second group of King Keoua's party, suffocating the army [see Figure D3-18]. *The lethal front also overwhelmed the first group, but had dissipated somewhat, and caused only a few injuries or deaths. The third group was in a protected area and quickly joined the first group (after discovering the deaths of the second group) and quickly left the scene. Other base surges probably accompanied the explosions witnessed by Keoua's army on the previous 3 nights, but the encampment was on the high upwind side of the caldera, and the high caldera walls would have served to protect the encampment. The death of part of King Keoua's army has historical significance, since the loss of warriors may have aided Kamehameha in his unification of the Island of Hawaii, and later the archipelago.*

The footprints are preserved in soft ash 7 to 9 km SW of the 1790 eruption site and occur in two ash layers that contain numerous pisoliths (accretionary lapilli) and are separated by 90cm of dune sand. The lower footprint layer contains few footprints, most heading away from Kilauea. The upper footprint layer contains more footprints, most heading to Kilauea Crater. Swanson and Christianson (1973) speculate that the lower footprints were made when the army fled the eruption site, and the upper footprints when the army returned days or weeks later."

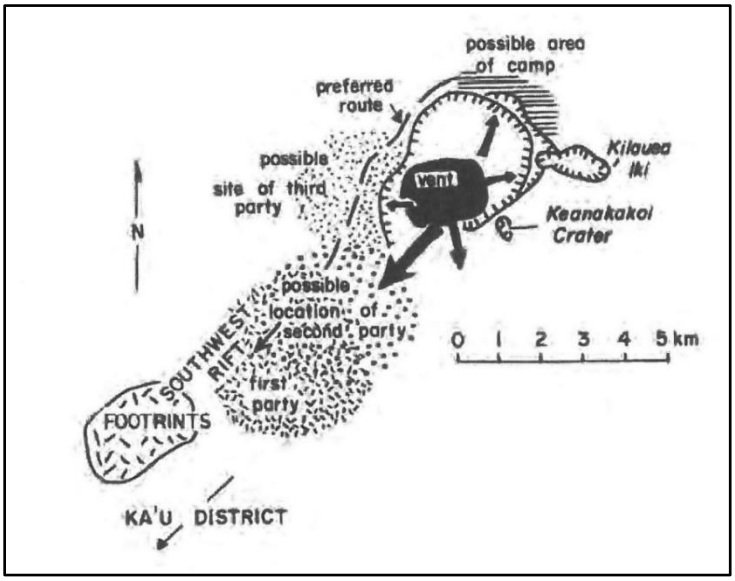


Figure D3-12: Sketch map showing the location of King Keōua's army, the area of the eruption, and the footprint locality. Map after Swanson and Christianson (1973) and taken from Easton and Easton (1995).

Stop D3-20. Accretionary Lapilli/Lapillistone. Data Source: A.D. MacTavish.

- **UTM 251565E, 2142071N; located ~650ft (~200m) south of the Footprints shelter (NPS hut).**

Visible here is a thin, 10-15cm thick, slightly erosion-resistant, weakly-indurated (lithified), brownish-grey lapillistone layer consisting of 3 to 4mm diameter, light brown, accretionary lapilli (pisoliths) concentrated within a light brown ash matrix (*see* D3-13). The lapilli within the layer are marginally matrix-supported.



Figure D3-13: Accretionary lapillistone layer. Left photo shows the surface of the slightly weather-resistant layer. The right photo shows the accretionary lapilli and ash comprising the layer. Photo credits: A.D. MacTavish (2020).

Stop D3-21: Budding of pāhoehoe toes from small tumulus. Data Source: A.D. MacTavish (2020).

- **UTM 251852E, 2141953N.**

This stop shows several small pāhoehoe toes formed from small lava breakouts from the base of a small tumulus (*see* Figure D3-14). These small breakouts only travelled a couple of metres from the tumulus before congealing.



Figure D3-14: Pāhoehoe toes budding from small tumulus. Photo credit: A.D. MacTavish (2020).

Stop D3-22: Lava levels on margins of lava channel. Data Source: A.D. MacTavish (2020).

- **UTM 252041E, 2141725N; Northern levée of the channel.**

The shallow lava channel at this stop has prominent levées with well-preserved, horizontal lava levels that mark the level of lava within the channel when flowing lava was present and lava volume from the source was decreasing (*see* Figure D3-15). This channel is pre-Mauna Iki Shield.



Figure D3-15: The left photo shows a shallow lava channel and its northern levée. The right photo shows the horizontal lava levels progressively marking the top level of the lava within the channel as the volume of lava decreased. Photo credits: A.D. MacTavish (2020).

Stop D3-23. Large fractured tumulus on the margins of the Mauna Iki Shield. Data source: Hazlett (2014).

- **UTM 252285E, 2141518N; located ~215ft (~65m) west of the trail and easily identifiable by its height and size.**

The feature here is the spectacular, very large, fractured, 10 to 12m high tumulus that looms west of the trail near the northern edge of the Mauna Iki shield (*see* Figure D3-16). Mauna Iki sits on Kīlauea's Southwestern Rift Zone about 8.8km southwest of the summit caldera.

Tumuli form when pāhoehoe flows develop a crust on their surface due to cooling in contact with air. A subsequent influx of lava beneath this crust will lift or inflate it. This inflation is not uniform, with some portions of the flow inflating more than others. Tumuli are essentially focused inflation features, whereas areas of arrested inflation (depressions) are referred to as inflation pits (Hazlett 2014). This tumulus is very large compared with most other tumuli observed on this field trip.



Figure D3-16: Large, fractured tumulus with February 2020 tour participants for scale. Photo credit: A.D. MacTavish (2020).

Stop D3-24. Three small lava falls formed from late lava breakouts (?) from tumulus. Data source: A.D. MacTavish (2020).

- **UTM 252287E, 2141497N; located ~80m west of the trail.**

On the south side of the large tumulus observed at Stop D3-23 are 3, possibly syn-tumulus, lava breakouts (buds) that flowed down the side of the tumulus, possibly at the end of its formation. The buds oozed over the broken lip of an earlier pāhoehoe lava tube to form several small lava falls. These small falls are now mostly broken (*see* Figure D3-17). Participants in the February 2020 Field Tour designated these features as 'post-tumulus budding lava ooze blobs', which is an entertaining, somewhat non-geological, description which describes the sense of fun and wonder embodied by the participants of the field trip, if nothing else.



Figure D3-17: 'Post tumulus budding lava ooze blobs' (not a technical term, but entertaining nonetheless) located on south side of the large, fractured tumulus described at Stop D3-23, with a trekking pole for scale. Photo credit: A.D. MacTavish (2020).

Stop D3-25. Summit of Mauna Iki Lava Shield. Data source: Hazlett (2014); Rowland and Munro (1996).

- **UTM 252610E, 2141010N**

This stop is at the summit of the small Mauna Iki lava shield which formed during an 8-month eruption along Kīlauea's Southwest Rift Zone in 1919 and 1920.

During most of the eruption the Mauna Iki summit contained an active lava lake which often overflowed and poured through lava channels and lava tubes down the flanks of the shield. At the same time there was also a lava lake within Halemaʻumaʻu crater at the summit of Kīlauea. It was noted that periods of high-stand within the Halemaʻumaʻu lava lake coincided with vigorous overflow from Mauna Iki. This strongly suggests that a direct connection existed between the 2 vents even though they were geographically separated, northeast to southwest by 5.45mi (8.8km). The shield grew laterally more than vertically which accounts for its relatively low topographic height above the surrounding terrain.

The total volume of lava erupted from Mauna Iki was about 1.23 billion ft^3 (35 million m^3) (Rowland and Munro, 1996).

Safety Note: Please be very careful and remain on the trail when at the summit of Mauna Iki. The summit area is relatively dangerous due to the instability of the crater rim, lava tube skylights, and embankment edges.

3.4. Day 4: Kīlauea Caldera, Kīlauea Iki, Hilina Pali

3.4.1. The Kīlauea East Rift Zone:

Figure D4-1 (*see* below) is a generalized depiction of the structure of Kīlauea Volcano from Hazlett (2014). The East Rift Zone trends east-northeast, except for the relatively short distance between the summit caldera and Pauahi Crater, where the trend is southeast. For some unknown reason the bend in the rift to the east-northeast occurs near Mauna Ulu.

There is a second, limited fissure system extending from Halema‘uma‘u through Kīlauea Iki Crater that may represent an ancient trace of the East Rift Zone, most of which has shifted southward as the volcano has grown.

The ***East Rift Zone*** (Figure D4-1) is informally subdivided into: the ***Upper East Rift Zone*** (UERZ); the ***Central East Rift Zone*** (CERZ); and the ***Lower East Rift Zone*** (LERZ).

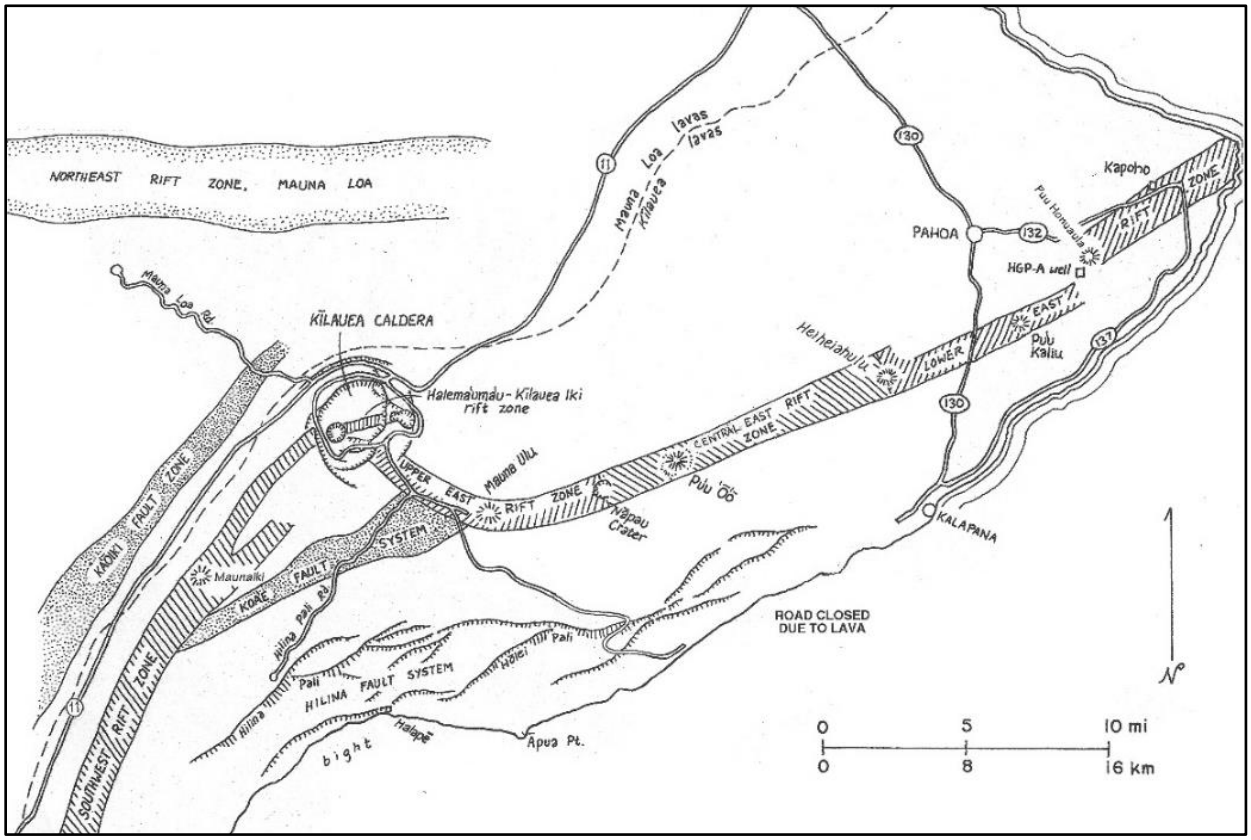


Figure D4-1: Generalized structure of Kīlauea Volcano showing the caldera, the East Rift Zone, Southwest Rift Zone, Kaōiki Fault Zone, Koa‘e Fault System, and Hilina Fault System. Map from Hazlett (2014, p.78).

3.4. Day 4 (Part 1): Kīlauea Caldera

Much of Crater Rim Drive and many Kīlauea Caldera area trails were closed during the 2018 eruption and the caldera collapse of Halemaʻumaʻu Crater. This collapse happened after the withdrawal of the lava lake that had been active within the crater between 2008 and 2018. Most trails were closed during the February 2020 field trip; however, all are now open. Crater Rim Drive is permanently closed from the Jagger Museum/HVO to the junction with the Puʻu Puaʻi/Devastation Trail access road. The National Park Service (NPS) plans on re-routing Crater Rim Drive south of the destroyed central portion of the road. The Uēkahuna Bluff viewpoint located north of the closed Jagger Museum/HVO has reopened.

The Field Trip Stops for Day 4 (Part 1) are (*see* Figure D4-2):

26. Steaming Bluffs Overlook;
27. Volcano House Observation Deck;
28. Kīlauea Visitor Center and park headquarters;
29. Kīlauea Iki Scenic Viewpoint; Kīlauea Iki trailhead;
30. Kīlauea Iki Trail (partially closed in 2020); the portion of this trail leading northwest from Sub-stop D4-30-4 to Waldron Ledge was closed during the 2020 field trip due to the instability of the northeastern caldera wall, but it is now open all the way to Volcano House;
31. Puʻu Puaʻi and Devastation Trail; walk to cinder cone located at the south rim of Kīlauea Iki; and
32. Keanakākoʻi Crater; road access past Crater Rim Drive/Chain of Craters Road junction is blocked to vehicular traffic due to the partial destruction of Crater Rim Drive by caldera subsidence. Access by foot is allowed.

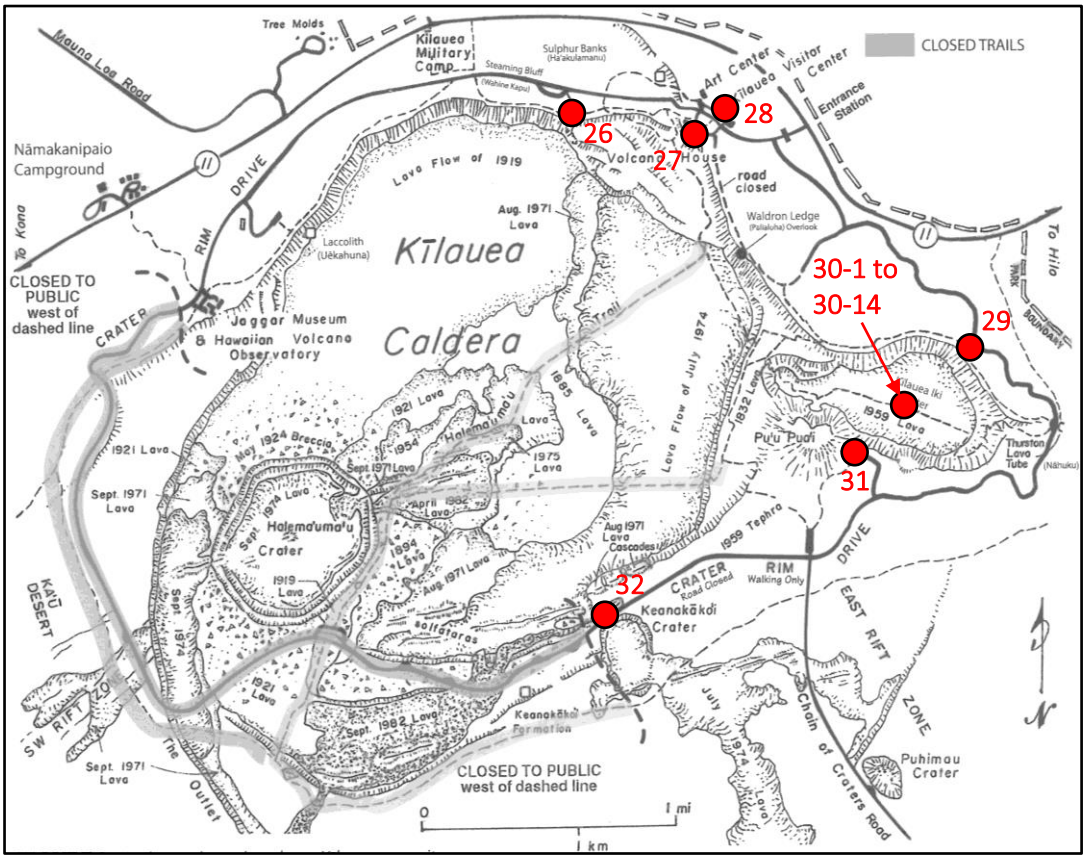


Figure D4-2: Map of Kīlauea Caldera and Kīlauea Iki Crater showing Day 4 (Part 1) field trip stop locations. Map taken from Hazlett (2014, p.28).

Stop D4-26. Steaming Bluffs (Wahinekapu) and Sulphur Banks. Data source: Hazlett (2014).

- **UTM 262875E, 2149795N, parking area.**

The Steaming Bluff Viewpoint is located ~600ft (180m) south of the parking lot along a flat, wide, and well-marked trail.

The Sulphur Banks solfatara are located to the northeast of the parking area and are associated with ring faults occurring along the northern edge of the caldera (low cliff-face observable ~1000-1300ft or 300-400m north). The solfatara can be reached by taking the Sulphur Banks (Haʻakulamanu) Trail starting on the north side of Crater Rim Drive opposite the parking lot. If you look around before moving out of the parking lot you will see numerous steam clouds issuing from steam vents located along various structures flanking the slightly down-dropped caldera block at this location.

To access the Steaming Bluffs Viewpoint, take the viewpoint trail south from the parking area. There are also several steam vents below the viewpoint that issue from one of the faults bounding the main part of the caldera. The viewpoint provides a good view of the Kīlauea Caldera and the new crater formed after the collapse of the caldera floor beneath Halemaʻumaʻu crater in mid-2018.



Figure D4-3: The left photo shows steam issuing from below the Steaming Bluffs Viewpoint. The right photo provides a view of the modified Halemaʻumaʻu Crater within Kīlauea Caldera as seen from the Steaming Bluffs Viewpoint. Photo sources: A.D. MacTavish (2020).

Stop D4-27. Volcano House Hotel, Kīlauea Caldera Viewpoint. Data source: MacTavish (2019).

- **UTM 262875E, 2149795N; parking lot.**

The viewpoint area on the caldera side of the hotel provides another good place to observe Kīlauea Caldera. Features visible from the viewpoint:

- Almost directly ahead (at 1100 o'clock) is the large, crater formed during the 2018 caldera collapse events that swallowed the original Halemaʻumaʻu Crater (*see* Figure D4-4, left);
- To the right is the vertical cliff-face marking one of the northwestern rim faults of the caldera (*see* Figure D4-4, right). This not the northern caldera rim. The northern rim is located a further 2000-2300ft (600 to 700m) to the north and can be easily seen from the Steaming Bluffs;
- On a clear day, in the distance to the west and past the caldera rim, can be seen the mass of Mauna Loa Volcano. Please note the gentle slopes involved. We cannot see the summit from this location since the eastern flank of the volcano bulges somewhat and blocks the view; and

- Visually following the cliff rim further to the left the buildings comprising the Hawaiian Volcano Observatory (HVO) and the Jagger Museum will eventually come into view (just before the cliff face drops down a level). Both are now indefinitely, possibly permanently, closed due to earthquake damage from the violent subsidence of the caldera floor in mid-2018.

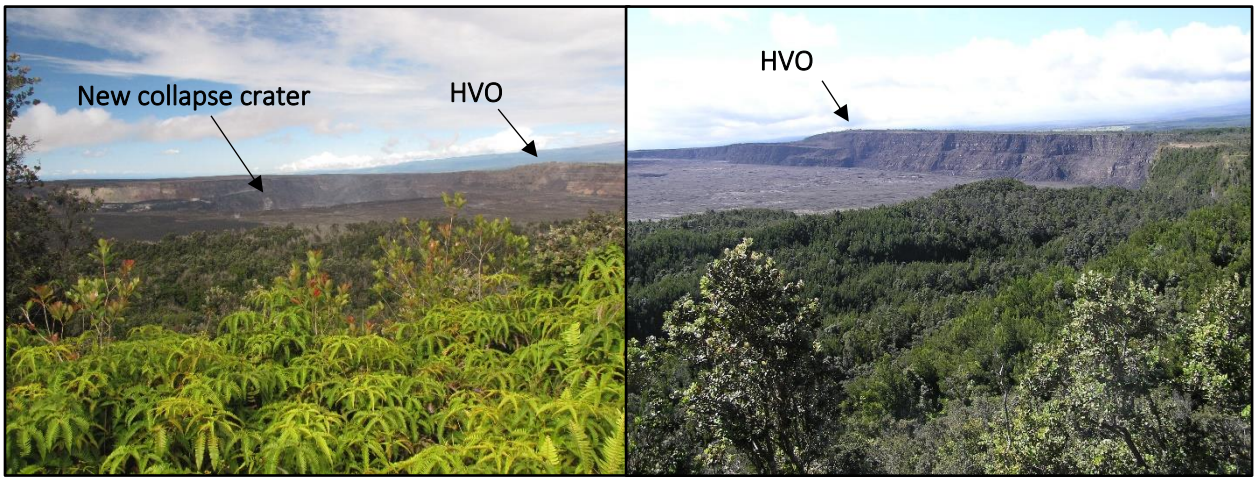


Figure D4-4: The left photo shows the new collapse crater (caldera) that engulfed Halema'uma'u Crater. The right photo allows a good view of the northern rim of Kīlauea Caldera. All photos taken from the Volcano House viewing area. Photo sources: A.D. MacTavish (left photo, 2020, right photo; 2012).

Stop D4-28. Kīlauea Visitor Center.

- **UTM 262995E, 2149900N, parking Lot; this stop will be made on Day 1 or Day 2.**

Maps, books, trail information, weather, T-shirts, washrooms, etc. can be obtained at this visitor's centre. There are usually some park rangers around that will be happy to answer any questions you may have.

Stop D4-29. Kīlauea Iki Viewpoint Trailhead. Data Source: Hazlett (2014).

- **UTM 264475E, 2148490N; parking lot.**

Kīlauea Iki crater (*see* Figures D4-5 and D4-6) is the site of the mid-15th century collapse of the 'Ailā'au lava shield. In 1832 and 1868 eruptions began with crater floor collapse followed by partial lava infill. Prior to 1959 the crater was ~600ft (180m) deep and almost completely forested;

The 1959 eruption began at 808PM on November 14th after a 3-month swarm of earthquakes and summit inflation. The eruption lasted for 36 days, filled the crater to the 400ft (120m) level with a lava lake; produced 17 episodes of lava fountaining (Figure D4-5, right), some reaching heights of 1900ft (580m); and built the Pu'u Pua'i (gushing hill) cinder cone (left centre in both photos in Figure D4-5). The northern flank of the cone has partially collapsed since the eruption; however, parts of the steep, unstable face of Pu'u Pua'i occasionally slid into the lake during the eruption and were rafted across the lake where today they form topographic highs on the floor of the crater.

The volcanic haze ('vase') plume from the lava lake that resided in Halema'uma'u Crater from early 2008 until mid-2018 is visible behind the cinder cone in the background of the left photo in Figure D4-5.

The present crater floor, which is the solidified top of the 1959 lava lake, still steams in places, providing evidence of continuing heat release due to cooling of the crystallized lava at depth.



Figure D4-5: The left photo shows Kīlauea Iki Crater in December 2012 with Pu'u Pua'i cinder cone in the left middle distance. The right photo is a wonderful picture of lava fountaining and the active lava lake within the crater during the 1959 eruption. Both photos were taken from about the same location. Photo sources: The left photo is by A.D. MacTavish (2012); the right photo is by the USGS (1959) and was downloaded from the USGS HVO website.

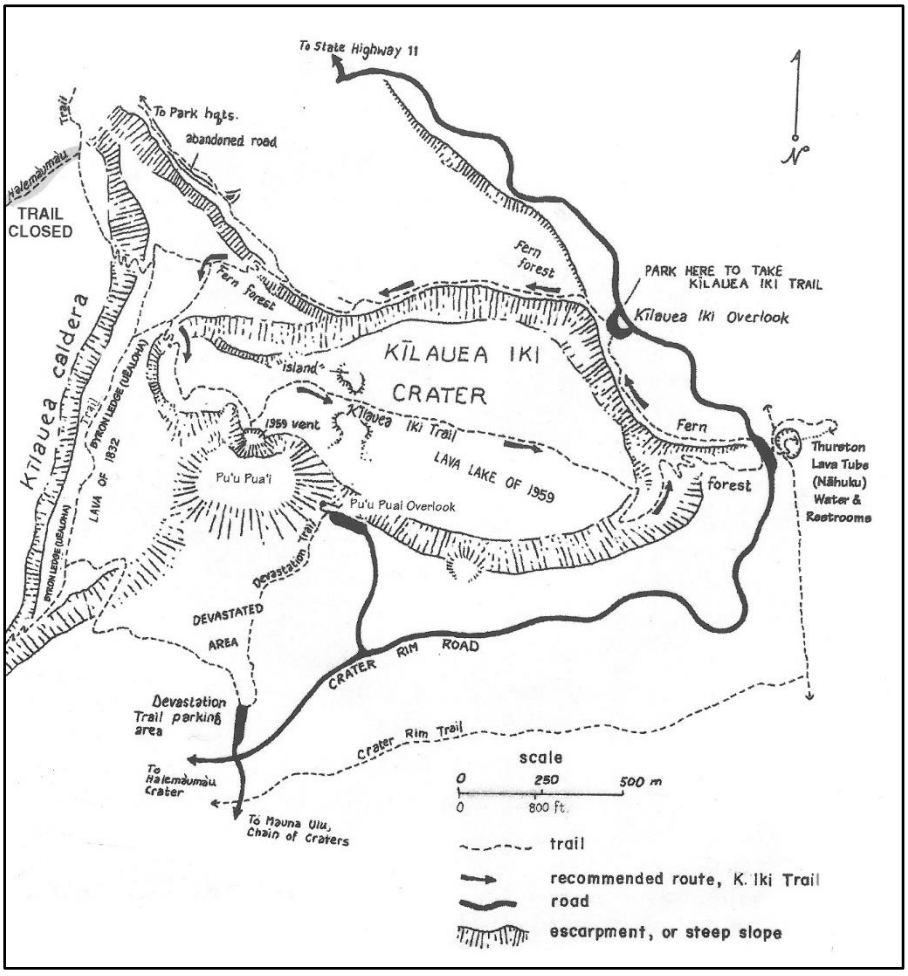


Figure D4-6: Map of Kīlauea Iki Crater and immediate vicinity. Taken from Hazlett (2014, p.66).

Stop D4-30. Kīlauea Iki Trail. Data Sources: Hazlett (2014); NPS Kīlauea Iki Trail Guide.

- **UTM 262995E, 2149900N; parking lot at trailhead and overlook**.

The Kīlauea Iki Trail leaves from the northern end of the Overlook parking lot and heads in an anti-clockwise direction around the crater's north rim, winds down to Byron Ledge (western rim) and down to the crater floor where it proceeds east along the long axis of the crater floor, climbs the eastern crater rim to the Nāhuku (Thurston Lava Tube) parking lot, and then proceeds northwest along the crater rim back to the Overlook parking lot. This 4mi (6.4km), moderate-difficulty hike makes a 440ft (122m) elevation change from 3874ft (1180m) at the eastern rim down to ~3474ft (1060m) on the crater floor. The trail ends at the southern end of the overlook parking lot. Small brown NPS trail markers with yellow numbers mark the trail stops and the 14 D4-30 sub-stops within this field guide match those numbers (*see* Figure D4-7). After the 2018 main caldera subsidence events the northern half of the trail was closed due to instability of the Kīlauea Iki Crater walls; however, it was re-opened just prior to the 2020 field trip and remains open.

While on this trail please abide by the following safety rules:

- Stay on the trail;
- Avoid unstable cliff edges;
- Keep away from ground cracks;
- Wear sturdy walking shoes or hiking boots (flip-flops and sandals are dangerous on this trail);
- Wear sunscreen;
- Bring a raincoat, particularly if you are hiking the trail in the afternoon since, in this part of the island, it rains most afternoons; AM has been rained upon both times he has hiked the trail; and
- Carry plenty of drinking water (it can get very hot within the crater).

Weather conditions can change very quickly so please take protective gear for both rain and sun.

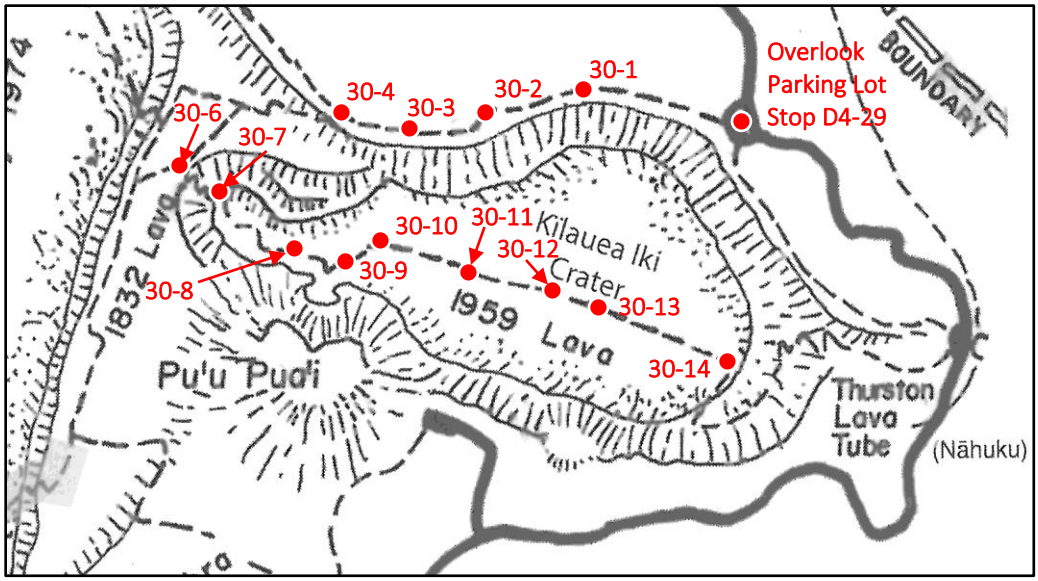


Figure D4-7: Field trip Day 4 sub-stops within Kīlauea Iki Crater. Map modified from Hazlett (2014, p.66).

Stop D4-30-1. Kīlauea Iki Crater, NPS Marker 1. Data source: NPS Kīlauea Iki Trail Guide.

- **Approximate UTM 264250E, 2148540N**.

This location is identified with a brown NPS sign with the yellow #1 at the beginning of the opening. It provides a good view of the Pu‘u Pua‘i cinder cone. The main 1959 eruptive vent (*see* Figure D4-8) is the linear depression/cavity located at the base of the cone. During the eruption this fissure was up to 800m in length. The photo below is the only one available that properly shows the fissure, even though it was taken from the top of the crater wall located across the crater to the south of this stop location.

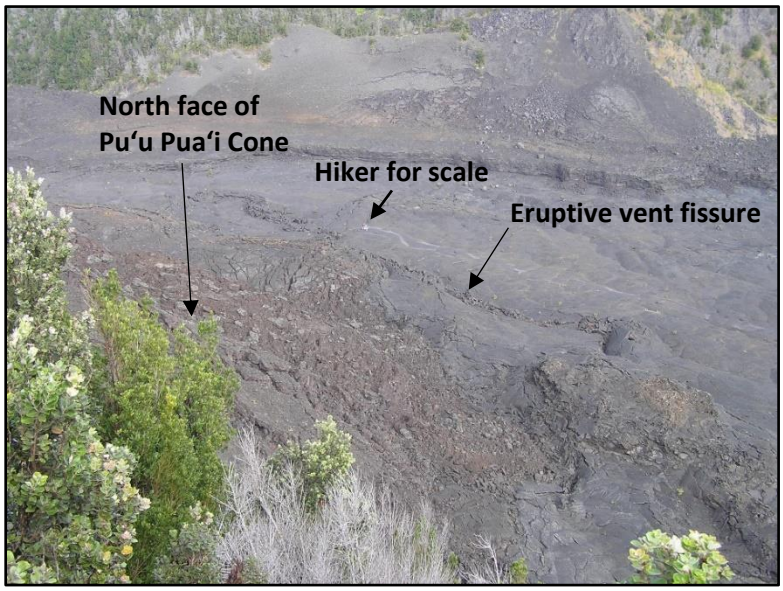


Figure D4-8: The 1959 Kīlauea Iki eruptive vent seen from the top of south wall of the crater on the eastern flank of the cinder cone (the only available photo properly showing the fissure). Photo source: A.D. MacTavish (2019).

Stop D4-30-2. Concrete Trolley Platform, NPS Marker 2. Data source: NPS Kīlauea Iki Trail Guide.

- **Approximate UTM 263820E, 2148505N.**

After the eruption ended in late 1959 USGS scientists used this site to descend into the crater using a trolley system to study and sample the cooling lava lake. The NPS Kīlauea Iki Trail Guide states:

“An old jeep powered the trolley system. Workers suspended a steel cable from a tripod on the crater rim to an A-frame on the crater floor. Rope wrapped around a spool on the rear axle of a Jeep moved the trolley along the cable transporting heavy equipment into and out of the crater.”

As you walk to the next stop you will cross a deep crack formed during the collapse of the crater ~500 years ago. Please stay on the trail to view this crack.

Stop D4-30-3. Lava fountain spatter, NPS Marker 3. Data source: NPS Kīlauea Iki Trail Guide.

- **Approximate UTM 263665E, 2148465N**

During 1 of the 17 fountaining episodes that characterized the 1959 eruption the fountain was deflected to the north by slabs of rock partially blocking the vent. During a 20-minute bombardment the surrounding forest and this spot were completely denuded of vegetation by spatter with blobs up to 3.28ft (1m) in diameter. The surface of the trail here is lumpier than the rock that was previously walked over due to the lumpy spatter surface. This location also provides an excellent view of the cinder cone.

Stop D4-30-4. Byron Ledge and Pu‘u Pua‘i; NPS Marker 4. Data source: NPS Kīlauea Iki Trail Guide.

- **Approximate UTM 263515E, 2148565N**

This stop is <30ft (10m) past the junction with the Crater Rim trail and provides another view of the cinder cone (which will be off to the left) as well as Uwēaloha (Byron Ledge, *see* Figure D4-9) which is a tree-covered ridge that separates Kīlauea Iki Crater from the eastern floor of Kīlauea Caldera. In the distance, to the west, you should be able to see the buildings of the HVO and Jagger Museum perched on the western rim of the caldera and, on a clear day, the massive bulk of Mauna Loa rising up in the distance

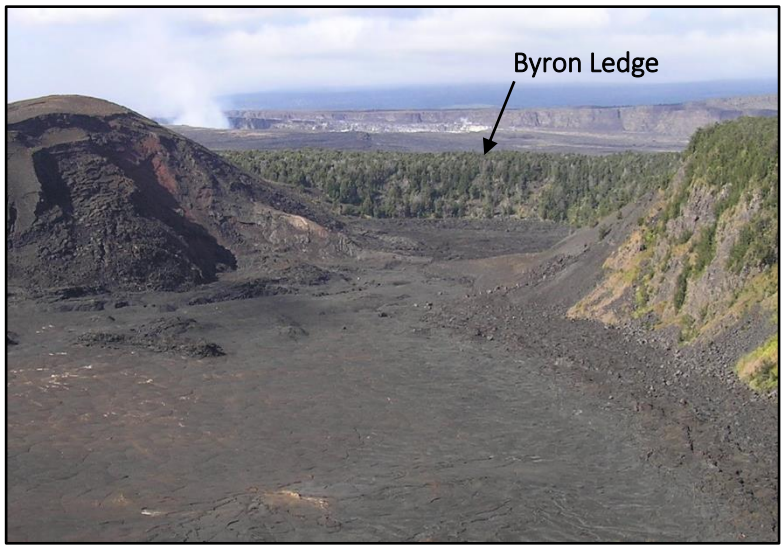


Figure D4-9: Byron Ledge in the middle distance in December 2008. Photo credit: A.D. MacTavish (2008).

Stop D4-30-6. Byron Ledge trail junction, NPS Marker 6 (NPS Marker 5 was skipped). Data source: NPS Kīlauea Iki Trail Guide.

- **Approximate UTM 263142E, 2148392N.**

From this location on Byron Ledge the unobstructed view is to the east along the axis of the crater and the floor of the lava lake. There is also a good view of the western flank of the Pu‘u Pua‘i cinder cone and north flank slump scars. These slump scars formed when over-steepened slabs of congealed spatter occasionally broke loose during the eruption, slid down the side of the cone, and exposed the hot interior of the cone.

Due to irregular steps placed on the trail by the NPS the trail from this point to the crater floor is steep and uneven and makes several switchbacks across the slope as it descends.

Please proceed slowly and be careful of your footing. **The trail becomes slippery when wet.**

Stop D4-30-7. 'Lava subsidence terrace'; NPS Marker 7. Data source: NPS Kīlauea Iki Trail Guide.

- **Approximate UTM 263207E, 2148344N.**

Here the base of Byron Ledge is also near the base of a 'lava subsidence terrace' (or 'volcanic bathtub ring') that marks the high mark of the lava lake at 50ft (15m) above the present surface (*see* Figure D4-10). During the eruption the lake occasionally filled higher than the vent causing the fountains to stop erupting. Lava often drained back into the vent dragging pieces of the lake's crust with it. This drain-back was often up to 4 times faster than during eruption and formed a noisy lava whirlpool.

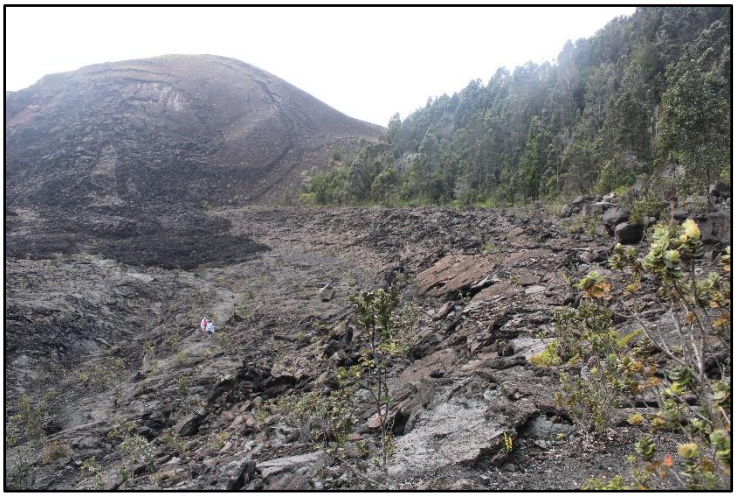


Figure D4-10: Lava subsidence terrace (volcanic bathtub ring) near the western crater floor at the base of the Byron Ledge. Photo credit: A.D. MacTavish (2020).

Stop D4-30-8. Base of cinder cone slump, NPS Marker 8. Data source: NPS Kīlauea Iki Trail Guide.

- **Approximate UTM 263317E, 2148247N.**

Here, the rock (*see* Figure D4-11) looks like jumbled 'a'ā flow; however, it formed when welded spatter, formed during the lava fountaining episodes, broke apart as it slid down the side of the cinder cone during a collapse (slump) on the cone's north flank, which looms over the trail immediately to the south.

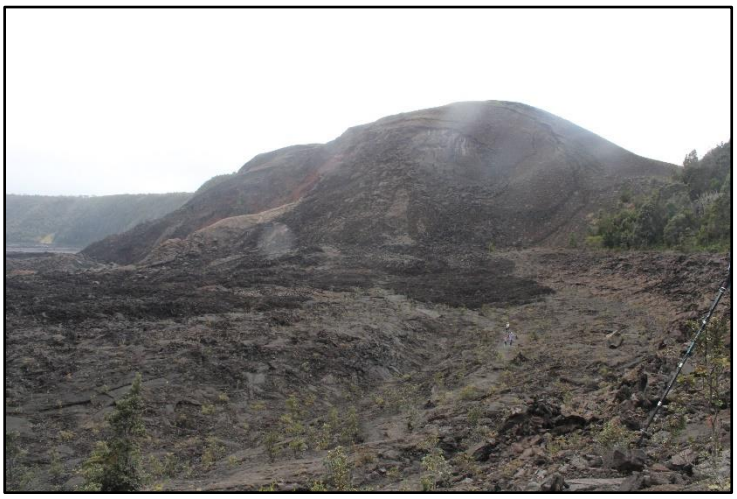


Figure D4-11: Base of cinder cone slump on the floor of the crater marked by the darker lava. Photo credit: A.D. MacTavish (2020). Photo taken during a rain shower (forming water drops on the camera lens) which are common during winter afternoons.

Stop D4-30-9. Western lip of the main 1959 eruptive vent; NPS Marker 9. NPS Kīlauea Iki Trail Guide.

- **Approximate UTM 263485E, 2148193N.**

Here the trail slopes down to the western edge of the main eruptive vent which erupted 17 times during the 26-day eruption. The NPS field guide states that:

"*Each eruptive episode played out differently. Some went on for days, while others only lasted for hours. Molten rock sometimes poured from the vent in a rolling boil. At other times lava burst skyward to form towering fountains in a matter of seconds. Every episode ended with lava draining back into the vent".*

Stop D4-30-10. Buckled lava lake crustal plates, NPS Marker 10. Data: NPS Kīlauea Iki Trail Guide.

- **Approximate UTM 263535E, 2148257N.**

Here, the surface of the crater shows evidence of the ~50ft (15m) collapse of the lava lake's crust after the eruption ceased and the level of the lava lake dropped. As the lake drained back into the vent the lava level dropped and the rigid crust of the lake buckled and cracked creating the uneven rocky ridges observed here (*see* Figure D4-12). The floor of the crater continues to subside at approximately 2cm/year due to ongoing cooling and contraction of the crystallized interior of the >60yr old lava lake.



Figure D4-12: Buckled and uneven crustal plates formed during subsidence of the lava lake after the eruption ended. Photo credit: A.D. MacTavish (2019). Please note that the rain obscuring the crater wall in the distance near the east end of the crater is a common occurrence during the afternoon.

Stop D4-30-11. Raised terraces, NPS Marker 11. Data source: NPS Kīlauea Iki Trail Guide.

- **Approximate UTM 263777E, 2148155N**

Flanking the trail are several raised, 13 to 16ft (4 to 5m) high 'terraces' formed when blocks of the cinder cone slumped into the lava lake and were slowly rafted away as floating cinder islands by the molten lava gushing from the active vent (*see* Figure D4-13). Every time the lake level rose the terraces were covered by lava; however, when the lava drained back into the vent the blocks were again exposed above the surrounding lake surface. Steam is often seen rising from the terraces and cracks in the crater floor due to the heating of rainwater by the still cooling interior of the lava lake.

Safety Note: Be very careful approaching any of the escaping steam since it is extremely hot and dangerous.

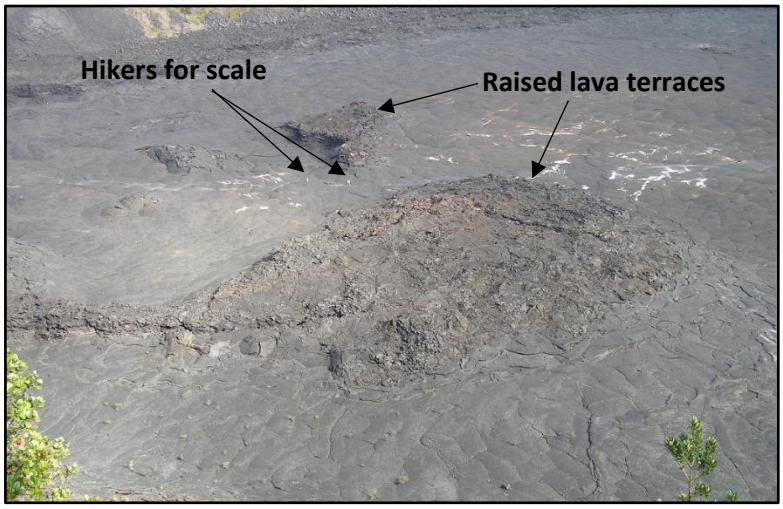


Figure D4-13: Raised terraces formed from slumped blocks of the cinder cone that were rafted away by gushing lava. Photo taken from the south rim of the crater. Photo credit: A.D. MacTavish (2011).

Stop D4-30-12. Crustal overturn plates, NPS Marker 12. Data source: NPS Kīlauea Iki Trail Guide.

- **Approximate UTM 263993E, 2148115N.**

During the eruption a dark solid crust rapidly formed on the surface of the lava lake. This crust readily broke into plates between 10 and 20ft (3 to 6m) across. The cracks between the plates were filled by less dense lava rising from beneath the crust and oozing over and eventually covering the rigid plates and swallowing them back into the lake. This process is referred to as 'crustal overturning' and moved across the entire lake in a matter of minutes and continued for about a week after the eruption ceased. The existing surface at this stop was formed by the final crustal overturn (*see* Figure D4-14).



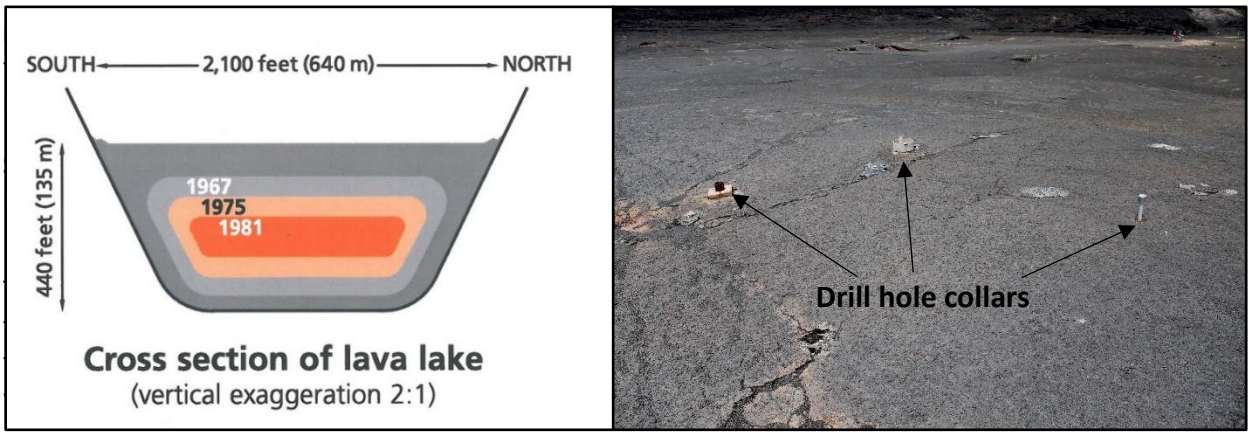
Figure D4-14: The final crustal overturn plates forming the surface of the 1959 lava lake after the eruption was over are shown in these 2 photos. The left photo is a view to the west and shows the cinder cone and Byron ledge in the distance. The right photo looks east with the 2020 field trip participants for scale and the eastern crater wall in the distance. Photo credits: A.D. MacTavish (2019, left; 2020, right).

Stop D4-30-13. Lava lake drill holes; NPS Marker 13. Data source: NPS Kīlauea Iki Trail Guide.

- **Approximate UTM 264080E, 2148095N.**

The lava lake was first drilled in early 1960, 4 months after the eruption ended on December 20, 1959. That hole terminated when it hit molten lava at a depth of 9ft (2.7m).

Later drilling showed that the crust, as one would expect, grew thicker with time (*see* Figure D4-15). The last hole, drilled in 1988, intersected only traces of residual intercumulus melt occurring between 240 and 330ft (73 to 100m) depth. The interior of the lake is now solid, but is still hot. The 1988 hole also showed that the pre-1959 crater floor had dropped during the eruption with the present base of the lake at about 440ft (135m) depth. The visible collars of the drill holes are located between 60 and 175ft (20 to 50m) north of NPS Marker 13.



Please note the ʻōhiʻa trees and other plants that are revegetating the lava. These plants have taken root in cracks where moisture and nutrients have collected. Given enough time the whole of the crater floor will be forested as it was before the 1959 eruption commenced. Also, keep an eye on the sky so that you may be lucky enough to see an ʻio (an endangered Hawaiʻian hawk) soaring on the updrafts above the forested walls of the crater.

The trail ahead switchbacks up the eastern wall of the crater from this point. Once at the top of the crater rim the trail connects with the Thurston Lava Tube (Nāhuku) parking lot. The lava tube was closed during the 2020 field trip, but reopened shortly thereafter. At the northern end of the lava tube parking lot another trail leads to the northwest along the crater rim and ends at the Kilauea Iki trailhead parking lot where the trail began.



Figure D4-16: Eastern 'bathtub ring' and small 'ōhi'a trees. Photo credit: A.D. MacTavish (2019).

Stop D4-31. Pu'u Pua'i Overlook; Devastation Trail Trailhead. Data source: NPS website; Hazlett (2014); Hazlett and Hyndman (2007).

- **UTM 263755E, 2147885N; parking area.**

The Pu'u Pua'i Overlook provides a good view of Kīlauea Iki crater from the southern rim. The old road at the west end of the overlook is buried under the Pu'u Pua'i (Gushing Hill) cinder cone.

The Devastation Trail leaves from the western side of the parking lot for both the overlook and the trail. The trail is an easy 30 minute, approximately 1/2mi (800m) return walk, crossing the eastern flank of Pu'u Pua'i above the southern Kīlauea Iki crater rim. It initially moves northwest towards Pu'u Pua'i and then heads southwest along the eastern edge of the cone and then eventually south through a forest devastation zone caused by the rain of spatter and cinder during the 1959 eruption. Reticulite, cinder, spatter, and ash were blown from the fountains to the southwest by tradewinds into the forest, which was stripped of leaves or buried for about 2.5mi (4km) downwind. The pumice cinders that fell to the surface of the cone close to Kīlauea Iki's fountaining were hot enough to weld themselves together (*see* Figure D4-17, left). Further downwind, the falling material cooled sufficiently to form a blanket of cinders (*see* Figure D4-17, right). The zone of devastation is shown graphically in Figure D4-18. Skeletal tree trunks (Figure D4-17, right) and small tree moulds can be observed in the welded spatter. Few of the skeletal tree trunks remain; however, it can be readily observed in Figure D4-17 (right) that these remnants provide a somewhat stable location for seeds to collect that eventually allowed grasses and then new trees to grow.



Figure D4-17: Welded spatter, eastern flank of the Pu‘u Pua‘i cinder cone (left) and partially revegetated devastation zone (right). Photo credits: A.D. MacTavish (left, 2012; right, 2020)

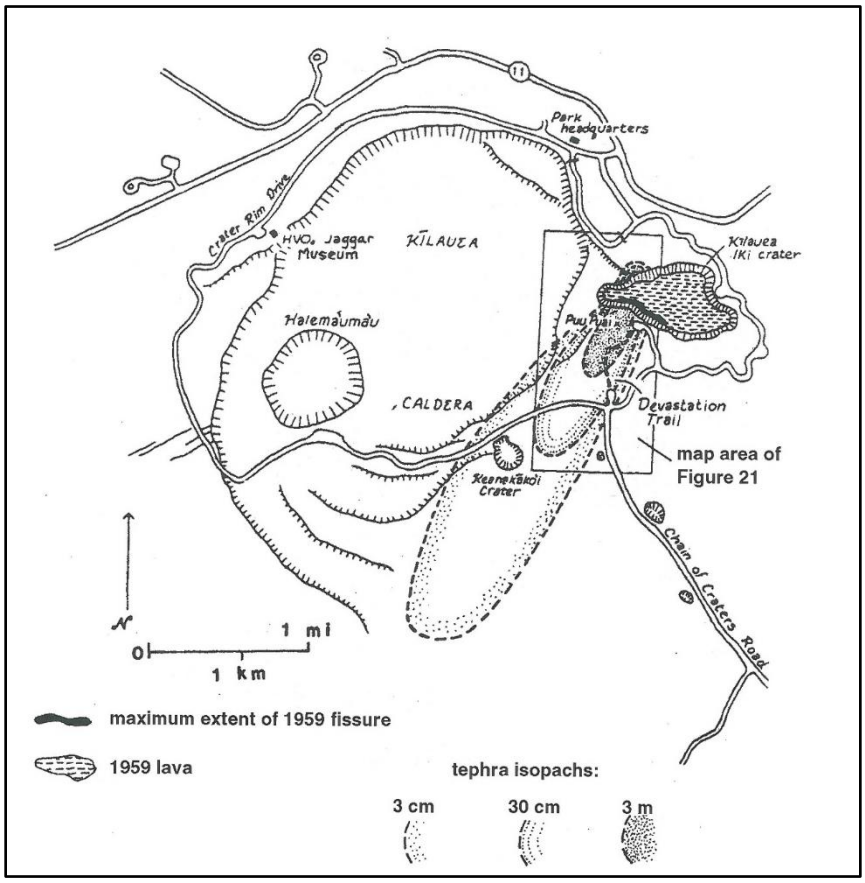


Figure D4-18: Distribution of the tephra blanket that formed the Pu‘u Pua‘i cinder and spatter cone, the downwind forest devastation zone, and lava from Kīlauea Iki during the 1959 eruption. Figure taken from Hazlett (2014, p.71).

Stop D4-32. Keanakāko‘i Crater and Vicinity. Data Source: Hazlett (2014); NPS website.

- **Approximate UTM 263775E, 2147530N; junction between Crater Rim Drive and Pu‘u Pua‘i Overlook Access Road.**

The portion of Crater Rim Drive west of the junction with the Pu ‘u Pua‘i Overlook access road was closed when visited by the 2020 field trip group due to 2018 earthquake damage, and at the time of final writing (February 2023) was still closed. The Park plans to reroute the road, but construction has not yet begun. The 4 sub-stops that comprise Stop D4-32 (shown in Figure D4-19) are accessed on foot along Crater Rim Drive west from where the Pu ‘u Pua‘i Overlook access road joins Crater Rim Drive.

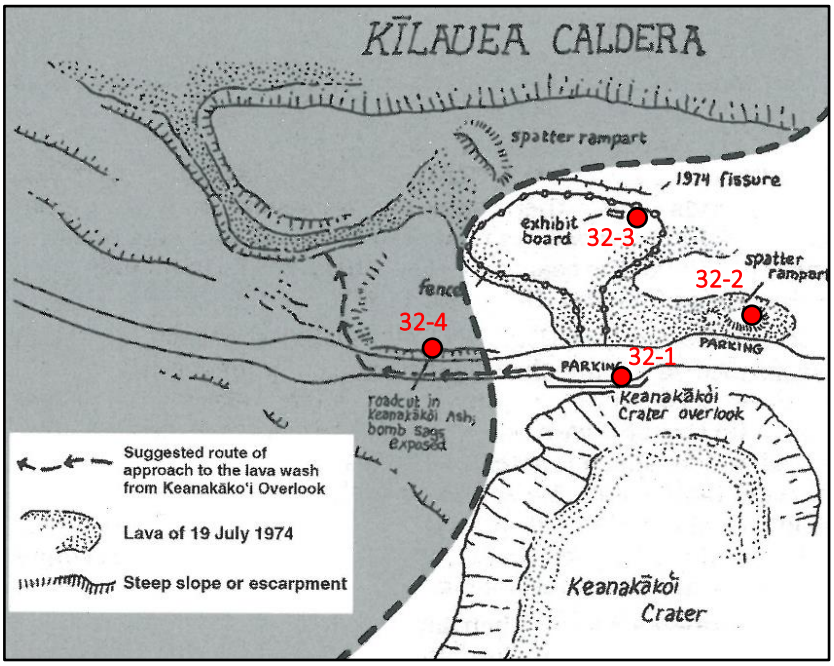


Figure D4-19: Location of field stops in the Keanakāko‘i Crater area. Figure taken from Hazlett (2014, p.73).

Stop D4-32-1. Keanakāko‘i Crater Overlook (south side of Crater Rim Drive). Data sources: Hazlett (2014); Hazlett and Hyndman (2007); Robinson (2012).

- **Approximate UTM 262072E, 2146835N.**

The 115ft (35m) deep, 1500ft (460m) wide Keanakāko‘i Crater (*see* Figure D4-20) is a collapse pit that is the westernmost crater of a crater chain that defines Kīlauea Volcano’s Upper East Rift Zone. It is thought that most of the craters comprising the chain are <1000 years old and that many formed during the great 1790 eruption.

Pit craters like this form by collapse after the underlying magma drains away, which is essentially a smaller version of the caldera collapse observed at Halema‘uma‘u in 2018. If not for lava infill from the eruptions of 1877 and 1974 the crater floor would be funnel-shaped and at least 394ft (120m) deep.

Prior to the 1877 eruption the early Hawai‘ians quarried dense, fine-grained basalt from the crater to make stone tools. The quarry site was buried by lava during the 1877 eruption and was further covered by tephra from the 1959 Kīlauea Iki eruption.

On a clear day, good views of the Mauna Loa summit, to the west, are afforded from this area.



Figure D4-20: Keanakāko‘i Crater from the viewing area. Photo source: Corine Michel Giron on Google Earth.

Stop D4-32-2. Spatter rampart across from Keanakāko‘i Crater Overlook. Data sources: Hazlett (2014); Hazlett and Hyndman (2007); Robinson (2010, 2012).

- **Approximate UTM 262130E, 2146903N.**

North of the Keanakāko‘i Crater overlook parking area on the north side of Crater Rim Drive is a small spatter rampart from which issued a thin pāhoehoe flow that in July 1974 crossed the road and spilled over the Keanakāko‘i crater rim in a cascade onto the floor of the crater.

Stop D4-32-3. Drainage channel. Data sources: Hazlett (2014); Hazlett and Hyndman (2007); Robinson (2010, 2012).

- **Approximate UTM 262060E, 2146935N; the viewing area is accessed via a short trail on the north side of Crater Rim Drive, starting a short distance west of the northern parking area.**

This location allows inspection of another spatter rampart and eruptive fissure formed during the 3-day July 1974 eruption (*see* Figure D4-21). Lava from the fissure flowed down a drainage channel to the west where, as it rounded a bend, it washed up against the channel wall as it flowed towards, and into, the pre-2018 caldera floor.

Stop D4-32-4. Keanakāko‘i Ash deposit. Data sources: Hazlett (2014); MacTavish (2020); White and Houghton (2000).

- **Approximate UTM 261997E, 2146795N.**

This roadcut stop is ~100m southwest of the Keanakāko‘i Crater overlook on the northwest side of the road. It hosts well-bedded, variably sorted, graded, weakly indurated, locally cross-bedded pyroclastic rocks of Keanakāko‘i Ash that accumulated over ~130 years during the 17th and 18th centuries. The unit at this site consists of layers of tuff, lapilli tuff, and localized lapillistone containing variable amounts of ash- and lapilli-size fragments (*see* Figure D4-22, left). The rocks locally contain accretionary lapilli and angular to subangular volcanic bombs (Figure D4-22, right). Accretionary lapilli are spherical aggregates (commonly with a concentric structure) formed by the accretion of moist ash in eruption clouds. They are equivalent to volcanic hailstones. The one observed cross-bedded interval is probably a base surge deposit. The bombs observed are pieces of pre-existing rock blown out of the vent during the eruption.

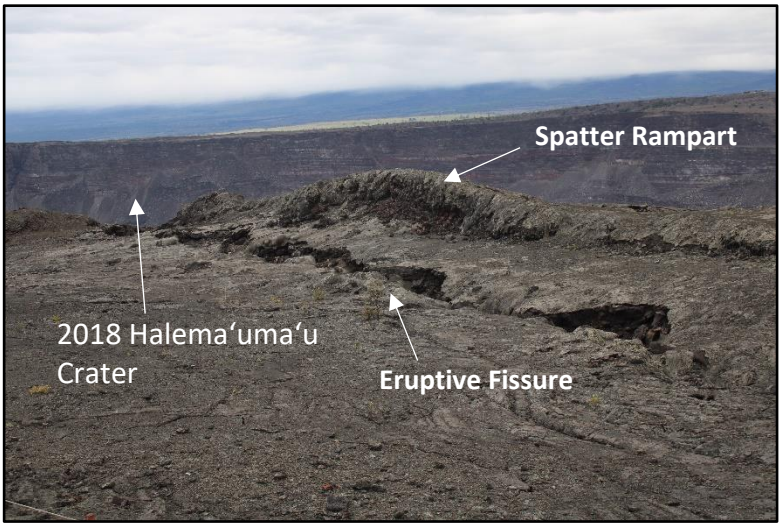


Figure D4-21 Spatter rampart and eruptive fissure formed during a 3-day, July 1974 eruption as viewed from field trip stop D4-28-3. The new 2018 Halemaʻumaʻu Crater is in the background. Photo source: A.D. MacTavish, 2020.



Figure D4-22 Well-bedded Keanakāko'i ash deposits consisting of ash, lapilli, accretionary lapilli, and volcanic bombs. The left photo shows variably-bedded, variably sorted pyroclastic layers with an angular bomb at left centre (pencil magnet for scale in lower centre). The right photo shows a layer containing accretionary lapilli (volcanic hailstones). Photo sources: A.D. MacTavish, 2020.

3.4. Day 4 (Part 2): Koaʻi Fault Zone and Hilina Pali

According to Hazlett (2014) the Hilina Pali Road allows access to the finest examples of faulting on the Hawaiʻian islands and allows examination of the fresh, well-exposed, easily approached escarpments comprising the Koaʻe Fault Zone. Robinson (2010) describes the fault zone as a series of nearly parallel, NE-SW-trending normal faults with a surface length of 9mi (14.5km) and a width of approximately 1.6mi (2.6km). At the end of the road is Hilina Pali which is part of an extensive network of faults that down-drop the southern flank of Kīlauea Volcano (Hazlett, 2014). The road was closed during the 2020 field trip due to road-surface damage by fault down-drop along the Koaʻe Fault Zone during earthquakes associated with the 2018 eruptive events. The damage has since been repaired and the road is now open to vehicular traffic.

The Day 4 (Part 2) Field Trip Stops are (*see* Figure D4-23):

33. Koa'e Fault Zone; can easily view fault scarps on left during drive
34. Kulanaokuaiki Pali (Koa'e Fault Zone);
35. Kulanaokuaiki Campground; rest stop; eastern end of Mauna Iki Trail.
36. Kulanaokuaiki Pali; brown ropey basalts at top of scarp.
37. Tumuli and brown ropey basalts.
38. Hilina Pali (also a rest stop).

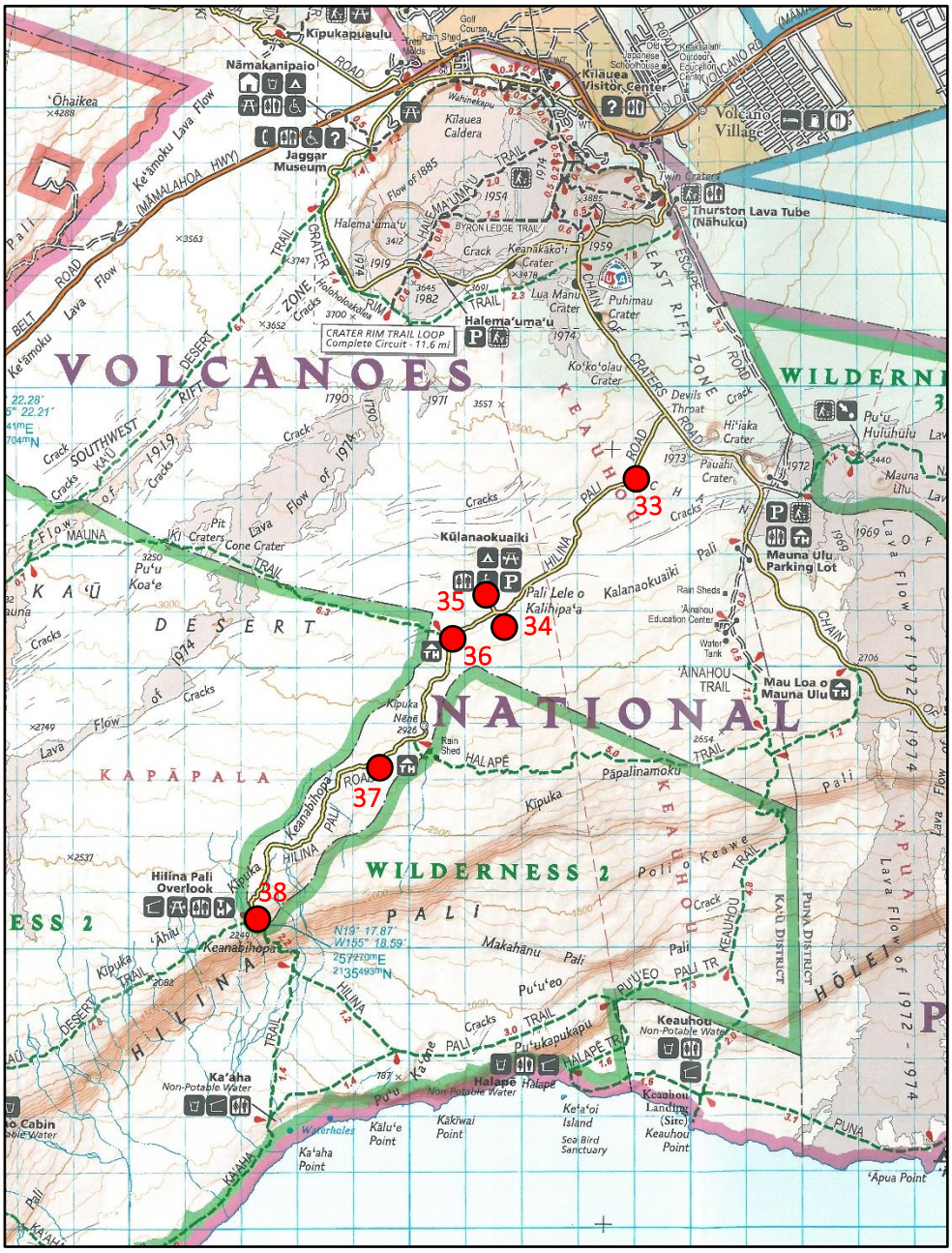


Figure D4-23: Locations of Day 4 (Part 2) field stops. Map taken from National Geographic Hawai'i Volcanoes National Park Illustrated Trails Map (2010).

Stop D4-33. The Koa'e Fault System. Data source: Hazlett (2014).

- **UTM 264210E, 2142940N; small parking area on left with enough room for 1, possibly 2 vehicles.**

A short distance west of Mauna Ulu the Upper East Rift Zone bends sharply to the northwest from a general east-northeast trend (Hazlett, 2014). The Koa'e Fault System is a 9mi (14.5km) long, ~1.2mi (2km) wide segment (extension?) of the East Rift Zone and forms a series of small grabens (*see* Figures D4-24 and D4-1). What is unusual with this fault system is that elsewhere on the south flank of Kīlauea the faults are predominantly south-dipping, whereas within the Koa'e Fault System both north-dipping and south-dipping faults are common, resulting in the formation of grabens.

Easily visible to the south at this stop is an excellent example of a north-facing fault bounding the south-side of one of the grabens. This particular fault trends subparallel the road for the next 0.75mi (1.2km).

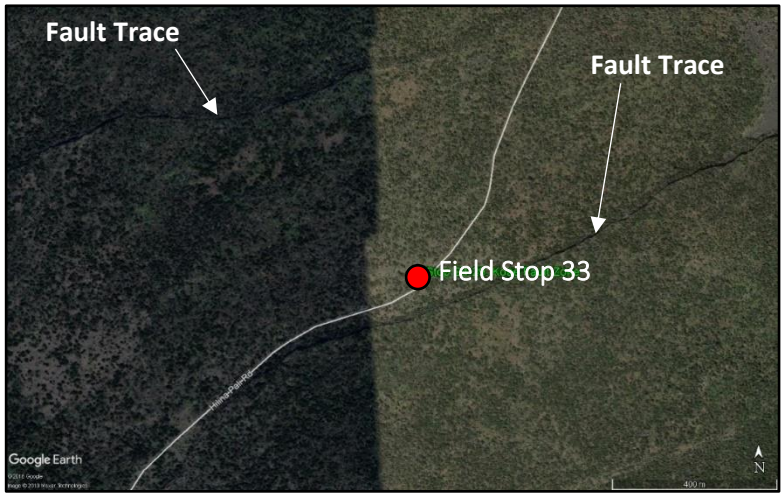


Figure D4-24: Koa'e Fault system on either side of Stop D4-33. Google Earth satellite image.

Stop D4-34. Entrance to Kolanaokuiki Campground.

- **UTM 261190E, 2140295N; park on south side of the road opposite to the campground entrance where the ground is solid enough to take the weight of most vehicles.**

The ~30m high north-facing scarp of Kulanaokuaiki Pali is very visible, easily reachable, and is located ~165ft (50m) south of the campground entrance.

Stop D4-35. Kolanaokuiki Campground.

- **UTM 261125E, 2140430N; parking lot.**

This campground provides a potential rest area with washrooms and picnic tables, if required.

Stop D4-36. Kolanaokuiki Pali. Data source: Hazlett (2014).

- **UTM 260966E, 2140228N; the only parking is on the top of the slope on the south (right) side of the road ~330ft (100m) south of the top of the Pali at UTM 261042E, 2140173N.**
- **The parking lot also services the Mauna Iki Trailhead which is located 165ft (50m) west-northwest of the parking lot at UTM 260995E, 2140190N, about halfway to the pali.**

At this stop the road curves around and up a short slope near the western terminus of the north-dipping Kolanaokuiki Pali normal fault.

This fault marks the southern margin of the Koa'e Fault System in this area, where in December 1965 the road was vertically offset 8.25ft (2.5m) during a major faulting episode (*see* Figure D4-25, left). Hazlett (2014) states that:

'*…along the base of the north-facing scarp the crust of the down-dropped block alternates between monoclinal up-warps and fissured down-warps, referred to as 'rollovers'* (*see* Figure D4-24, right). *The base of some of the monoclinal up-warps show vertical fracturing or thrust buckles, with the up-warps shoved onto the down-dropped blocks. Rollovers are indicators of listric (curved) fault planes and in this case the controlling fault plane may curve northward at depth'*.

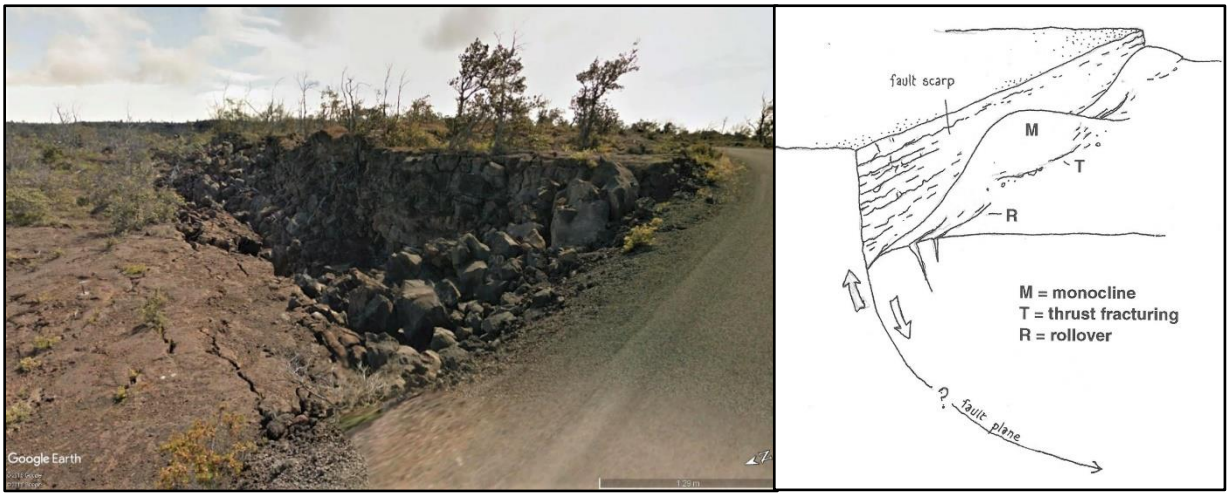


Figure D4-25: The left photo shows Kolanaokuiki Pali, looking east-northeast along one of the north-facing escarpments of the Koa'e Fault system. The diagram on the right explains rollovers, monoclines, and listric normal faulting. Figure taken from Hazlett (2014, p.119). Photo source: Google Earth.

Stop D4-37. Tumuli and ropey pahoehoe flows. Data source: Hazlett (2014); Hazlett and Hyndman (2007); Robinson (2012).

- **UTM 259720E, 2137885N; carefully park along the right (north) side of the road where the road shoulder is slightly wider than elsewhere; be very careful of other road traffic.**

The pāhoehoe flows here were erupted in the 13th or 14th Century from the summit shield of Kīlauea. The area is characterized by good examples of ropey and entrail pāhoehoe flows and well-developed tumuli (*see* Figure D4-26, left). The reddish weathering of the flows indicates age despite the lack of vegetation.

Tumuli is the plural form of tumulus which is described by various authors as (Figure D4-26, right):

- '*a steep mound from a few feet to tens of feet across in a pāhoehoe flow that may form from molten lava heaving up plates of chilled crust or from subsiding flow crust draping over bedrock obstacles*' (Hazlett and Hyndman, 2007).
- '*elliptical, domed structures that form on the surfaces of pāhoehoe flows extruded on flat or gentle slopes. Tumuli form when the upward pressure of slow-moving lava swells or pushes the overlying solidified crust. Sometimes the lava can drain away and leave a hollow shell*' (Robinson, 2012).

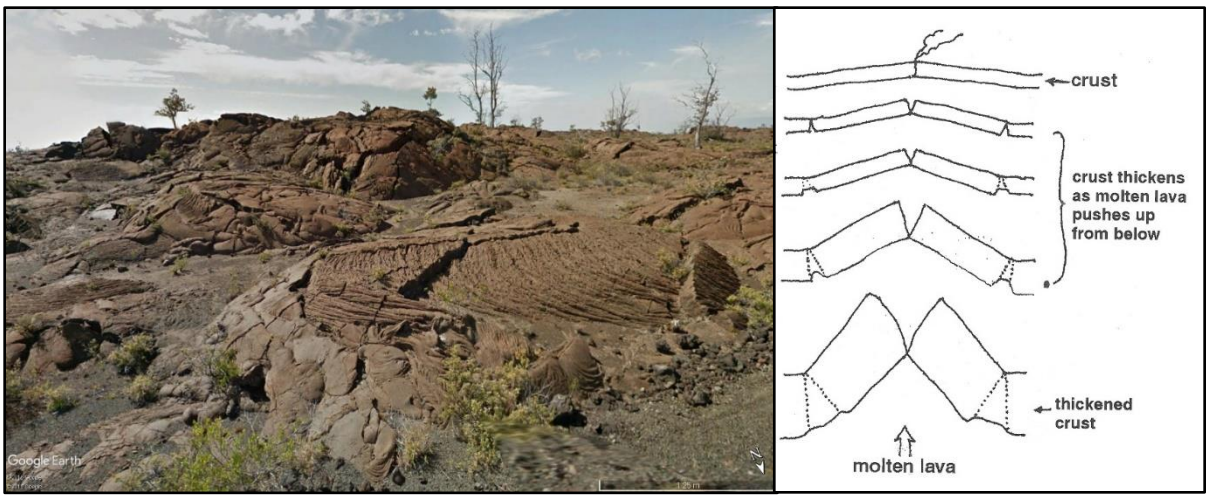


Figure D4-26: Good examples of ropey flows are in the photo foreground with several tumuli in the background. Photo source: Google Earth. The diagram on the right (from Hazlett 2014, p.125) shows tumulus formation by focussed hydrostatic pressure with molten pāhoehoe beneath a cooling, thickening crust.

Stop D4-38. Hilina Pali Overlook. Data source: Hazlett (2014).

- **UTM 257575E, 2135150N; overlook parking lot.**

Walk ~50ft (15m) down the trail from the overlook shelter to a triangulation station and small memorial.

Hazlett (2014) states that: *"Hilina Pali is a part of the extensive network of faults that drop the south flank of Kīlauea seaward in stepwise fashion. The Hilina Fault itself, with a throw of about 1150ft (350m), dips 50-60^{o} to the south, possibly flattening out at depth within the Kīlauea volcanic pile, though this interpretation is controversial. Easton and Garcia (1980) estimated that the fault system has been active for at least 20,000 years".*

Hazlett (2014) also states: *"Look to the east of this location (see* Figure D4-27) *to see the dark, fresh-looking lava flows from the Mauna Ulu eruption cascade over Poliokeawe Pali. On the downthrown fault block, 1600ft (500m) below, meandering stream channels, lava fans, and talus piles are exposed. The lava fans were formed as lava from the Kālu'e eruptions piled up at the base of the pali*.'



Figure D4-27: View looking east from the Hilina Pali Overlook. Photo source: Google Earth.

3.5. Day 5 – Chain of Craters Road, Napaū/Mauna Ulu Trail, Hōlei Pali

The Chain of Craters Road extends for 18.3mi (30km) from Crater Rim Drive to the Puʻu Ōʻō-Kupaianaha lava field. The road follows the northern part of the Upper East Rift Zone, descends the southern flank of Kīlauea Volcano, winds down Hōlei Pali, crosses the southern coastal plain, and then works east along the coast to where it is truncated by the Puʻu Ōʻō-Kupaianaha lava field about ~0.6mi (1km) east of the Hōlei Sea Arch. Numerous volcanic features are present along the route and Field Trip Day 5 will observe or visit many of them. The field stops on the Chain of Craters Road are shown in Figure D5-1 and consist of 10 stops on, or adjacent to, the road as well as various sub-stops associated with the Napaū and the Puʻu Loa Petroglyph trails. The planned stops are:

39. Luamanu Pit Crater and Lava Trees;
40. Pauahi Crater;
41. Mauna Ulu/Napaū (trail);
42. Mau Loa o Mauna Ulu (Alternate;)
43. Muliwai o Pele (Lava River);
44. Kealakomo Overlook;
45. Pāhoehoe transitioning to ʻaʻā;
46. Alanui Kahiko;
47. Puʻu Loa Petroglyphs (trail) (Stops D5-47-a and b);
48. Coastal Sea Arches; and
49. Puʻu Ōʻō-Kupaianaha lava field (mid-1980's).

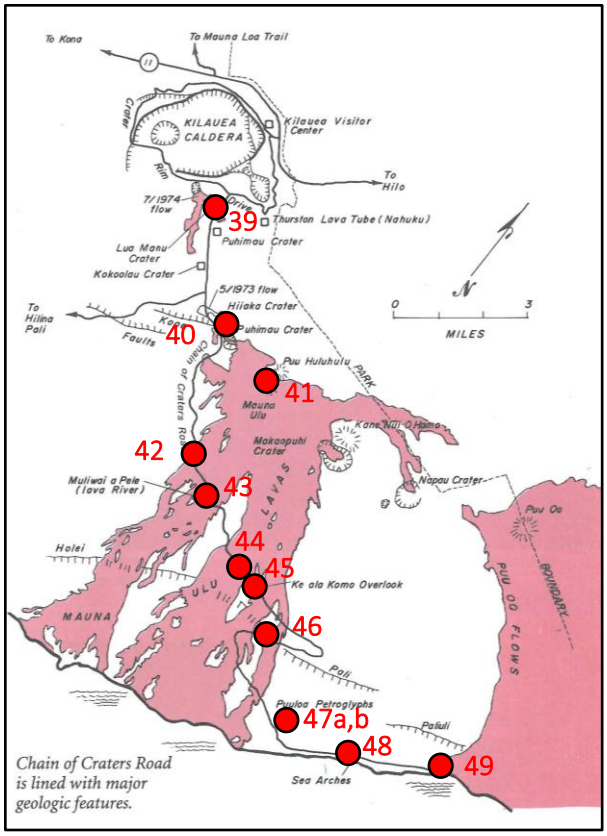


Figure D5-1: Day 5 of the field trip consists of 10 stops along, or near, the Chain of Craters Road. Figure modified from Hazlett and Hyndman (2007, p.80).

3.5.1. The Formation of Mauna Ulu:

This sub-section is summarized from Hazlett (2014, p.88-89).

The 5-year ***Mauna Ulu*** eruption began on May 24, 1969 when a lava curtain erupted along the length of a new, east-northeast-trending fissure extending from south of Pauahi Crater (near the present highway and the start of the Nāpau Trail) through ʻĀloi Crater to the north of ʻAlae Crater. The fountaining soon became focused in the area between ʻĀloi and ʻAlae craters where Mauna Ulu presently stands. Over the next 5 years episodes of sustained fountaining from this vent, sometimes reaching heights of 1770ft (540m), and associated overflows were interspersed with lava lake activity.

By the end of 1970 both ʻĀloi and ʻAlae craters had been completely infilled with molten lava. Flows piling up around the vent formed a low shield that was the beginning of the Mauna Ulu edifice. A lava tube from the top of the shield fed the ʻAlae lava lake which, in turn, fed long-lasting flows that extended down the southern flank of Kīlauea. These flows reached and entered the ocean in June 1969 and September 1970.

Mauna Ulu's central crater extended northeastward in 1971 by merging with a series of small secondary pits on the flank of the shield, forming a trench. Lava continued to be fed to the ʻAlae lava lake and from there down Kīlauea's southern flank. Lava again entered the sea between March 8 and May 25, 1971. In late May 1971 the lava lake within Mauna Ulu began to subside; lava stopped flowing from ʻAlae in July; and lava completely disappeared from view in Mauna Ulu in October 1971.

It was initially thought that the eruption had ended; however, lava returned to the summit crater in February 1973 and the ʻAlae lava tube reactivated soon afterward. After a month the level of the Mauna Ulu lava lake dropped a few metres and new vents opened at Mauna Ulu and ʻAlae. A levéed lava lake formed at ʻAlae and fed numerous overflows which gradually formed the low ʻAlae satellite shield. The ʻAlae flows were active for more than a year with some of the far-travelling flows pouring into and completely filling the western end of Makaopuhi Crater. Other flows eventually formed lava tubes that reached the ocean between August and October 1972 and from February to May 1, 1973.

An M6.2 earthquake on April 26, 1973, centred north of Hilo, may have triggered a drastic change at Mauna Ulu, where, on May 5, 1973 the lava completely drained from both Mauna Ulu and ʻAlae. A few hours later a fissure eruption began at nearby Hiʻiaka and Pauahi craters that lasted less than a day. The Mauna Ulu summit lava lake began to refill 2 days later with lava returning to ʻAlae at the end of May. The last lava to be observed at ʻAlae was on June 7th. Sluggish activity continued at the summit crater until September when a gradual increase began and by early November there was vigorous fountaining accompanied by overflows. On November 10, 1973 the lava lake suddenly drained away at the beginning of another short rift eruption at Pauahi Crater and did not return until a month later.

Strong activity within the lava lake was again present in January 1974 and a steep-sided spatter cone grew within the lava lake. On January 24th a series of vigorous fountaining episodes began with fountains attaining heights of 130ft (40m) and overflows rapidly travelled several miles from the vent. This irregular pattern of fountaining and overflow lasted for 5 months and by June had built the Mauna Ulu shield an additional 100ft (30m) to a height of 390ft (120m).

Activity in the lava lake became sluggish in June 1974. Harmonic tremors and deflation were recorded near the summit of Kīlauea on the morning of July 19th, the Mauna Ulu lava lake level dropped, and a day long fountaining eruption began at Keanakākoʻi Crater within Kīlauea's summit caldera . This marked the end of the Mauna Ulu eruption.

Figure D5-2 shows the lava flows and the year they were erupted from Mauna Ulu and vicinity between May 1969 and June 1974. Figure D5-3 shows the Mauna Ulu area pre-eruption and post-eruption.

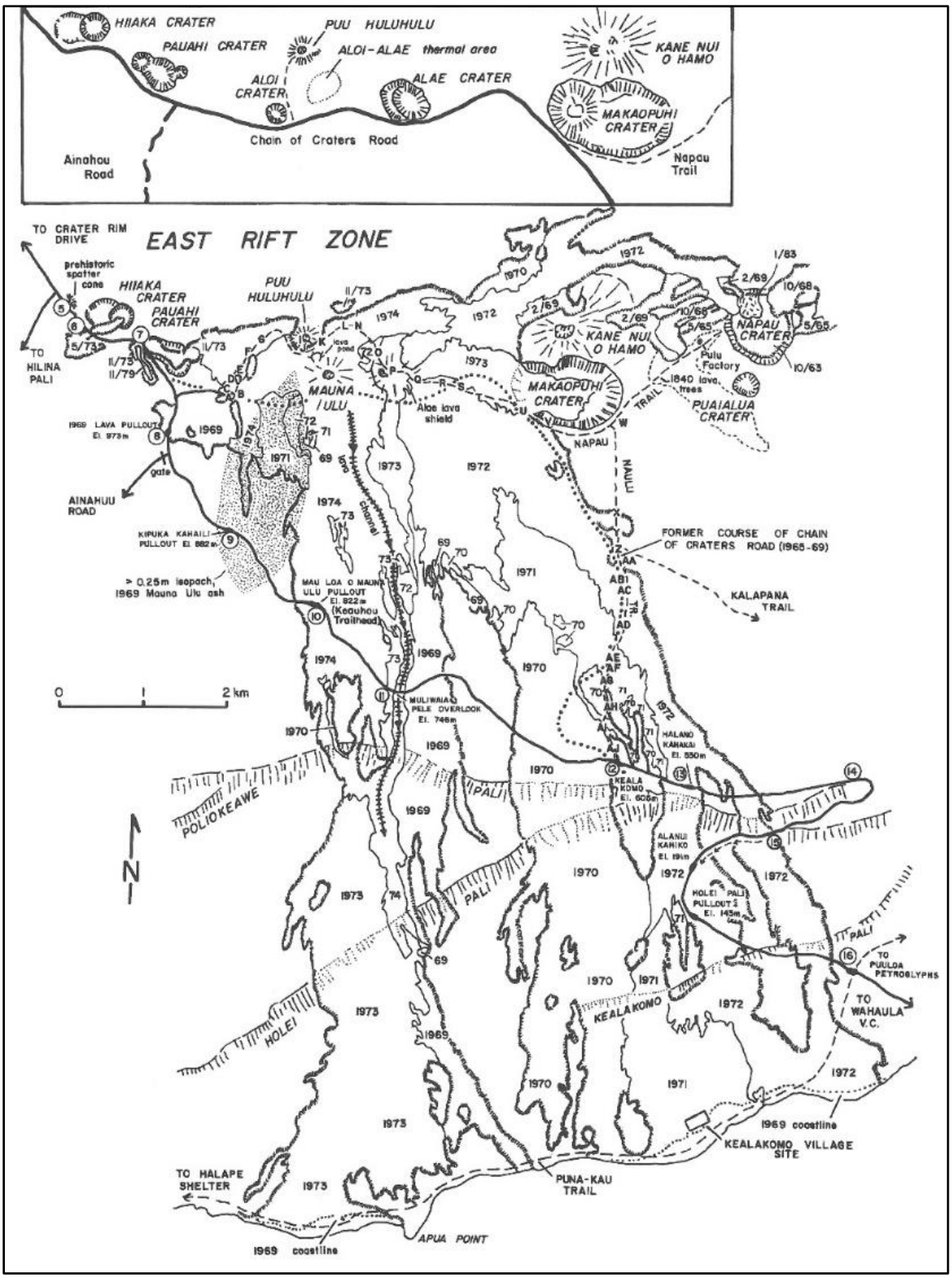


Figure D5-2: Geology associated with the 5-year Mauna Ulu eruption. Figure source: Easton and Easton (1995); the circled numbers are stops from the NVO Chain of Craters Road guide; the letters are stops from the NPS Napaū/Naulu Trail Guide; and the geology is from Holcombe (1976 and 1987).

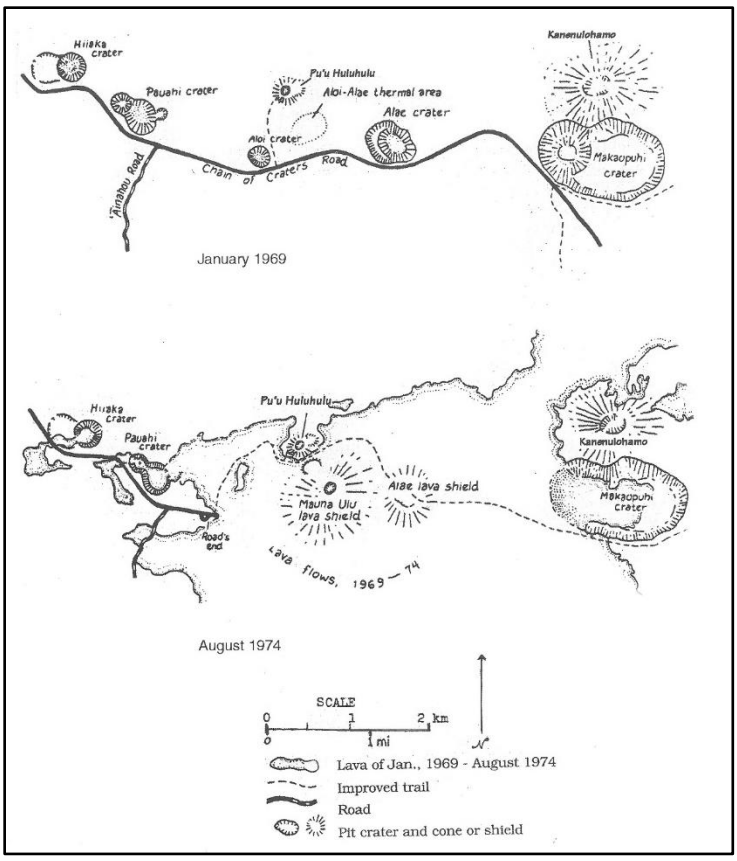


Figure D5-3: The Mauna Ulu area pre-eruption (top half of sketch) in January 1969 and post-eruption (bottom half of sketch) in August 1974. Map from Hazlett (2014, p.94).

Stop D5-39. Lua Manu Pit Crater, Lava Trees. Data Sources: Hazlett (2014); Hazlett and Hyndman (2007), Robinson 2012.

- **UTM 263360E, 2146520N; overlook parking area.**

The small Lua Manu Pit Crater is thought to be the uppermost East Rift Zone crater along the Chain of Craters Road. The 328ft (100m) wide crater was once tree-filled; however, on July 19, 1974 a fissure eruption a short distance north and east of the pit partially infilled the crater to a depth of ~50ft (15m). After the eruption ceased much of the lava drained back into a fissure in the crater's east wall. The high-lava level is easily seen as prominent 'bathtub ring' on the crater walls.

Spatter ramparts marking the locations of the eruptive fissures are visible on both sides of the Chain of Craters Road.

Many fragile lava trees and tree moulds are present on the flows north of the crater. Many of the lava trees have collapsed since the eruption; however, drain-back features and remnant charcoal are preserved on the edges and within some, respectively. Lava quickly chills against the moist, tough ōhi'a hardwood trees as it moves around them. There are numerous preserved, unburned 'ōhi'a trunks that protrude from the lava trees or have toppled onto the surface of the flow.

Safety Warning: Do not attempt to climb or lean against the lava trees since they are fragile and topple easily. Also, the pāhoehoe flow surfaces are brittle and are underlain by large voids, so be very careful where you walk.

Stop D5-40. Pauahi Crater Overlook. Data sources: Hazlett (2014); Robinson (2012).

- **UTM 266230E, 2143410N; large parking area located on the left (east-side) of the highway and reached by 2 short access roads at the north and south ends of the parking lot.**

Pauahi Crater is the largest of the easily reached East Rift Zone pit craters. It is a composite double-pit crater about 1650ft (500m) long and 360ft (110m) deep. A small unnamed pit crater, a short distance east of the main pit can be seen in in the upper left corner of Figure D5-4. Pauahi Crater was the site of 3 eruptions in the 1970's:

1. May 5, 1973: A small amount of lava was extruded onto the crater floor, but ceased when the eruption moved north to nearby Hiiaka Crater.
2. November 10, 1973: A fissure opened on the pit floor near the present overlook a few hours after an active lava lake at Mauna Ulu suddenly drained. Lava fountaining was initially confined to the floor of Pauahi but activity soon moved up the eastern and western crater walls and into the adjacent forest to quickly form a 1.8mi (3km) long west-southwest-striking, en-echelon fissure system. This fissure vented lava from near Pu'u Huluhulu to the east to a short distance west of Pauahi Crater. The bulk of this eruption lasted about 10 hours with lava fountains feeding 2 lava lakes (one in each of the 2 parts of the crater). The individual lakes eventually combined into 1 large lava lake exhibiting huge whirlpools that drained lava out of the lake almost as fast as it was erupted from the fissures. This activity is easily visible from the visitor's platform as dark lines in the far northeast crater wall and just north of the platform. Broken lava trees are found in the lava flow near the entrance to the parking lot showing the high point of the lava flow. Minor eruptive activity continued in the crater until December 9, 1973.
3. November 16, 1979: This less than 24-hour eruption was preceded by an 11-hour earthquake swarm where the earthquakes migrated upward through the crust from ~1.9mi (3km) to ~0.6mi (1km) depth. It is estimated that 915,000yd^3 (700,000m^3) were erupted during an initial fountaining stage followed by flows issuing from fissures west of the crater wall cutting the Chain of Craters Road. Most of the floor of Pauahi is covered by a thin layer of 1979 lava.



Figure D5-4: Pauahi Pit Crater as seen from the viewing platform. Photo credit: A.D. MacTavish (2012).

Figure D5-5 shows the volcanic features in the vicinity of Pauahi Crater and Mauna Ulu as well as the field trip sub-stops along the Napaū Trail. The 13 sub-stops comprising ***Stop D5-41*** are:

1. Napaū trailhead and trail sign.
2. Eastern exposed end of the initial (1969) Mauna Ulu fissure and its associated spatter rampart partially covered by later Mauna Ulu ‘a‘ā flows.
3. Spatter rampart and lava drain-back pits and hornito (?) field.
4. Broken and toppled lava trees.
5. Small-scale pahoehoe lava channel.
6. Old lava rampart with Mauna Ulu lava ‘bathtub ring’.
7. Large lava tree (possibly a hornito?).
8. Ecological Stop.
9. Lower overlook near summit of Pu‘u Huluhulu.
10. Upper Pu‘u Huluhulu Overlook.
11. Perched lava Pond.
12. Well-developed lava channel.
13. Mauna Ulu Summit

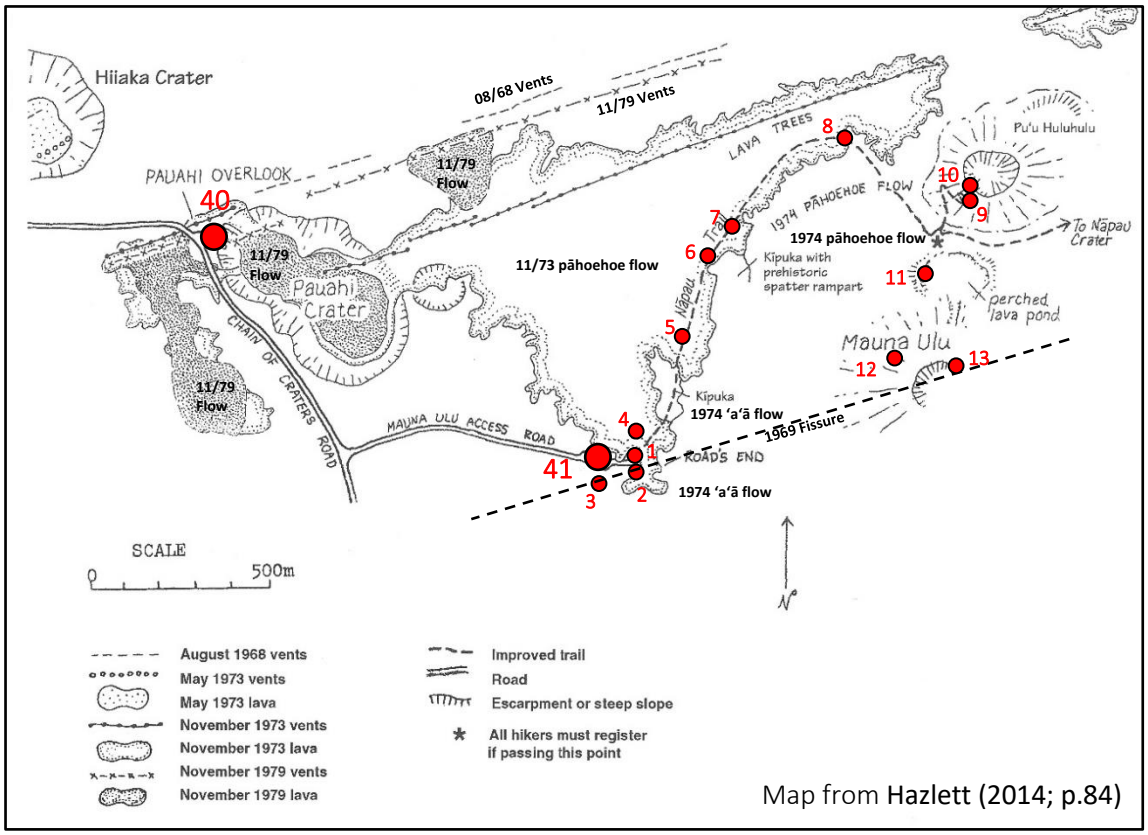


Figure D5-5: Day 5 field trip stops, sub-stops, and volcanic features in the vicinity of Pauahi Crater, Napaū Trail, Pu‘u Huluhulu, and Mauna Ulu.

Stop D5-41. Napaū Trail.

- **UTM 267210E, 2142705N; large parking lot.**

Trail access from the present Chain of Craters Road is via a remnant of the original Chain of Craters Road that was buried by a Mauna Ulu flows in 1973.

Please note: The brown NPS markers with yellow letters scattered along the Napaū Trail do not match the numbers of the field stops within this portion of the guide. The descriptions within the NPS guide tend to be general rather than specific. Where a field stop has an NPS Marker that number is noted.

Stop D5-41-1 (NPS1). Data sources: Hazlett (2014); NPS Mauna Ulu Eruption Guide; Hazlett (2014).

- **UTM 267326E, 2142700N, Napaū Trailhead; NPS Marker 1.**

Walk 330ft (100m) east-southeast along the old highway from the parking lot to the Napaū Trailhead exhibit board located ~15ft (5m) north of the old highway. This trail has 2 segments:

1. A loop that leads east, initially along the old highway, then south to a fissure and spatter rampart, and then west allowing a close-up view of the western end of the fissure that was the beginning of the 1969 Mauna Ulu eruption; and
2. A 2mi (3.25km) round-trip trail that leads northeast to the Pu‘u Huluhulu summit, which is a 400 to 600yr old spatter cone located ~1650ft (500m) north-northwest of the Mauna Ulu lava shield. The trail follows 1973 Pauahi flows and flanking 1974 Mauna Ulu flows for most of its length, passes an old undated spatter rampart, and then through a lava tree forest. The Pu‘u Huluhulu cone is truncated by a 165ft (50m) deep collapse crater, the top of which provides a panoramic view that includes (on a clear day): Mauna Loa; Mauna Kea; Kīlauea summit; the ‘Ailā‘au lava shield; Puhimau and Pauahi Craters; Mauna Ulu; ‘Alae and Kanenuiohamo lava shields; Makaopuhi Crater; and numerous recent flows, fissures, and many vent edifices .

Stop D5-41-2a. Mauna Ulu Spatter Rampart and Eruptive Fissure. Data source: NPS Mauna Ulu Eruption Guide.

- **UTM 267430E, 2142590N**

Walk east-southeast from the trailhead to the end of the paved road. From here a trail leads south (right) to a fissure that opened after a swarm of earthquakes on May 24, 1969 and marked the beginning of the 5-year Mauna Ulu eruption. The fissure first opened at ‘Alae Crater, near where Mauna Ulu now stands, passed through the now infilled Ālo‘i crater, and propagated west-southwest like an opening zipper for over 1mi (1.6km) to near the location of the present Chain of Craters Road.

The eruption at this location lasted less than a single day but during that time it spewed a 100ft (30m) high curtain of lava along the entire length of the fissure. Most of the lava moved south and downslope towards the sea, but what fell on the upslope side formed the present spatter rampart. When the eruption ended at 1100PM that evening most of the nearby lava drained back into the fissure and congealed in place as it poured over the rim. Activity continued at the main Mauna Ulu vent at the eastern end of the fissure between ‘Alae and Ālo‘i craters and by December, 1969 had sustained 12 fountaining episodes where fountains sometimes reached heights of 1770ft (540m). Part of the fissure east of this point is covered by a 1974 Mauna Ulu ‘a‘ā flow (*see* Figure D5-6).

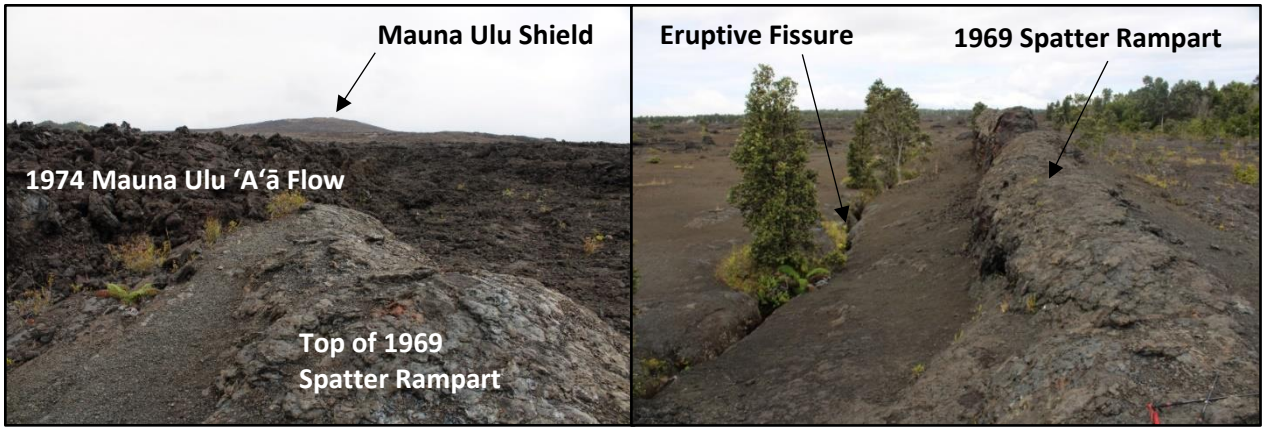


Figure D5-6: The left photo shows the May 24, 1969 spatter rampart truncated by a 1974 Mauna Ulu ‘a‘ā flow with the Mauna Ulu shield in the distance. The right photo shows the 1969 spatter rampart and eruptive fissure, north of where it is truncated by the 1974 Mauna Ulu ‘a‘ā flow. Photo credits: A.D. MacTavish (2019).

As mentioned above, to the left (east-northeast) of the trail the 1969-vintage fissure and spatter rampart are covered by a very irregular, blocky 1974 Mauna Ulu ‘a‘ā flow that covered the fissure and the rampart. This ‘a‘ā flow commonly contains small, green olivine grains.

To get to this stop you walked over relatively smooth, 1973-vintage ropey pāhoehoe lava flows which formed as fluid lava flowing along a relatively flat or gentle slope. This type of flow advances as a series of small lobes and toes that continually expand and break out from the cooling crust along its leading edges. The surface textures of pāhoehoe vary widely; however, the most common is ropey where the numerous folds, wrinkles, and ropes form when the thin partially solidified crust of the flow is slowed or halted. The lava below the crust continues to move forward and drags the malleable crust along.

Notice the extreme difference between the 2 types of flow even though they have essentially the same composition. An ‘a‘ā flow forms due to factors such as: lower temperature; gas loss; onset of crystallization; a loss of elasticity, such that it fractures instead of stretches; being forced to move faster, such as being pushed from behind by an upslope surge; or if it has to move down a steeper slope.

Stop D5-41-2b. Spatter mound field. Data source: A.D. MacTavish (2020); AGI Glossary of Geology, 4th Edition (1997).

- **UTM 267370E, 2142546N.**

Directly adjacent to the spatter rampart and eruptive fissure described immediately above at Stop D5-41-2a is a small spatter mound field. This field was initially incorrectly identified by AM as a hornito field. The AGI Glossary of Geology, 4th Edition (1997) defines a hornito as ‘*a small mound of spatter built on the back of a lava flow (generally pahoehoe), formed by the gradual accumulation of clots of lava ejected through an opening in the roof of an underlying lava tube*’. After close examination the hornito interpretation was discarded in favour of spatter mounds that did not build vertically enough to become hornitos. At this location several good examples, up to ~8.2ft (2.5m) in height, are readily observable. The shape of these formations, particularly the one shown in the right photo of Figure D5-7, are reminiscent of mushrooms, or flowerpot structures formed by tidal action in the Bay of Fundy in New Brunswick, where the flare at the top of the flowerpot shows the maximum water level at high tide. In a similar way the flaring at the top of these features defines the maximum height of the host lava flow, upon which the spatter mound was building, before the volume of lava within the tube decreased and the upper surface of the lava flow dropped as eruption volume waned.



Figure D5-7: The left photo shows the spatter mound field at Stop D5-37-2b. On the right is a 2.5m tall, mushroom-shaped mound showing the characteristic shape formed when the host lava flow surface deflates as the volume of lava in the underlying flow decreases. Steve Fox for scale. Photo credits: A.D. MacTavish (2020).

Stop D5-41-3. Drain-back pits. Data source: NPS Mauna Ulu Eruption Guide.

- **UTM 26720E, 2142530N.**

Walk west along the southern edge of the fissure until you reach a series of small pits that occur along the fissure for about 200ft (60m). These are where lava drained back into the fissure and then solidified when lava fountaining ended. On the inner walls of these pits iron-rich minerals within the lava quickly oxidized in the residual stream of the lava and turned bright red and yellow. The fissure can be traced intermittently west of these pits for about another 825ft (250m). Good photos of the drain-back pits can be obtained from the top of the adjacent spatter rampart located a short distance north of the pits (*see* Figure D5-8, left). Also at this location is a good example of a welded spatter mound sitting on top of the spatter rampart (*see* Figure D5-8, right).

Walking west from Stop D5-41-3 there may be solidified ejecta (or tephra) of several forms along the side of the trail such as: lapilli-sized pumice (cinders with a profusion of gas bubbles) are the most common; Pele's Tears (black, teardrop- or sphere-shaped droplets of obsidian) are less common; reticulite, which is a delicate lava foam version of pumice is uncommon; and thin, very fragile and delicate threads of, often golden-coloured Pele's Hair are rare.

There are also some good examples of lava trees (and tree moulds) that can usually be identified as narrow structures projecting above the top of the lava flows.

From this stop cross to the northern side of the spatter rampart and follow the trail to the east along the fissure and through the forest back to the northern trailhead, then walk northeast along the trail to the next stop (D5-41-4).



Figure D5-8: A drain-back pit within the May 24, 1969 fissure is shown in the left photo with Dr. Juk Bhattacharyya for scale. The welded spatter mound on the top of the spatter rampart adjacent to the north of the drain-back pits is shown on the right. Photo credits: A.D. MacTavish (2019).

Stop D5-41-4. Lava trees and Mauna Ulu and ʻĀloʻi Shields in the distance. Data source: NPS Mauna Ulu Eruption Guide.

- **UTM 267358E, 2142763N; Lava Trees located 100ft (30m) west-northwest (left) of the trail.**

There are numerous, usually toppled or broken lava trees northwest (left) of the trail at this location. The lava trees in this area are sometimes associated with pieces of the original ōhiʻa trees that formed the mould. Looking east from this point, across the 1973 Pauahi flows and the ʻaʻā flow in the middle distance, you can readily see the summits of Puʻu Huluhulu (tree-covered) and Mauna Ulu, and, to the right of Mauna Ulu the dimpled lava mound of the ʻĀloʻi Shield. The ʻĀloʻi Shield, which grew above the pre-1970 ʻĀloʻi Crater, and the ʻAlae Crater to the south were completely infilled as lava overflowed the growing Mauna Ulu shield. As lava flowed over the rim of the crater it formed several approximately 80ft (24m) high lava falls. The resulting lava lakes overflowed both craters with each new lava surge from Mauna Ulu. This process added layers and elevation to the surrounding terrain and eventually produce a low, dimpled, readily visible lava mound that grew above the older crater. Figure D5-9 (taken from the NPS Mauna Ulu Eruption Guide) diagrammatically illustrates the formation of the Mauna Ulu and the ʻĀloʻi Shields.

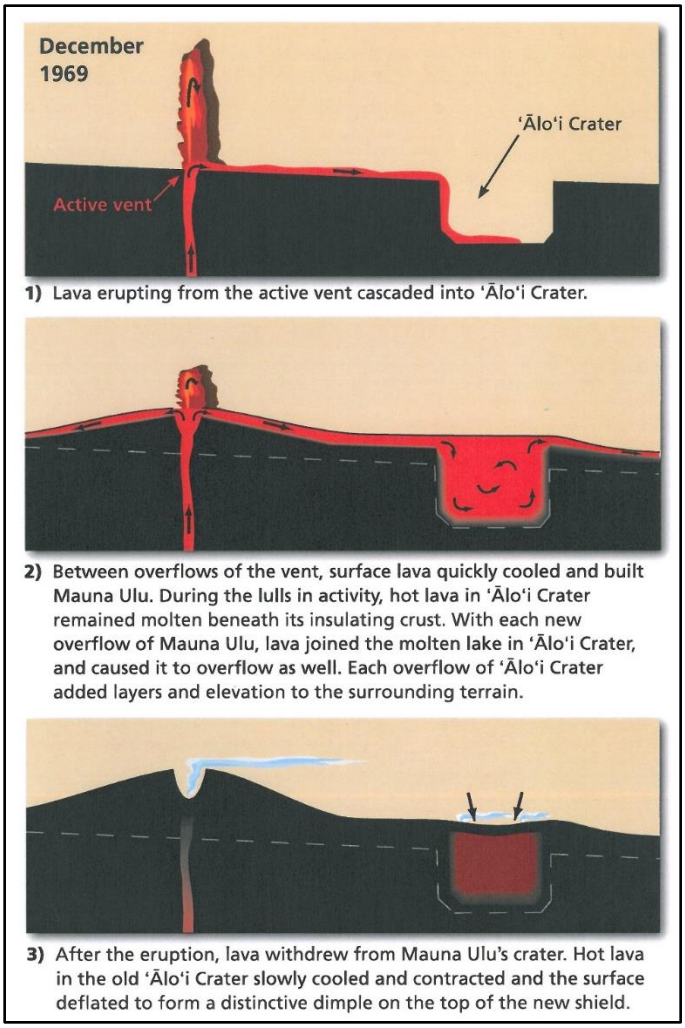


Figure D5-9: This illustration, taken from the NPS Mauna Ulu Eruption Guide, diagrammatically illustrates the formation of the Mauna Ulu and the ʻĀloʻi Shields.

Stop D5-41-5. Small-scale lava channel, lava trees, and tree moulds. Data sources: MacTavish (2019); NPS Mauna Ulu Eruption Guide.

- **UTM 267554E, 2143030N**

The trail here follows a small-scale lava channel preserved on the surface of a pāhoehoe flow from the 1973 Pauahi eruption (see Figure D5-10).

Look for evidence of flowage around the lava trees with a lava crust on the north side of the trees and the flowage of lava ropes around the trees. In some instances, tree moulds and lava trees can be used as flow direction indicators with an obvious asymmetry where the upstream edge of the tree is rounded and the downstream portion is roughly pointed (see Figure D5-11).



Figure D5-10: Small-scale pāhoehoe lava channel flowing down the slope. The trail follows the channel in this location. Photo credit: A.D. MacTavish (2019).

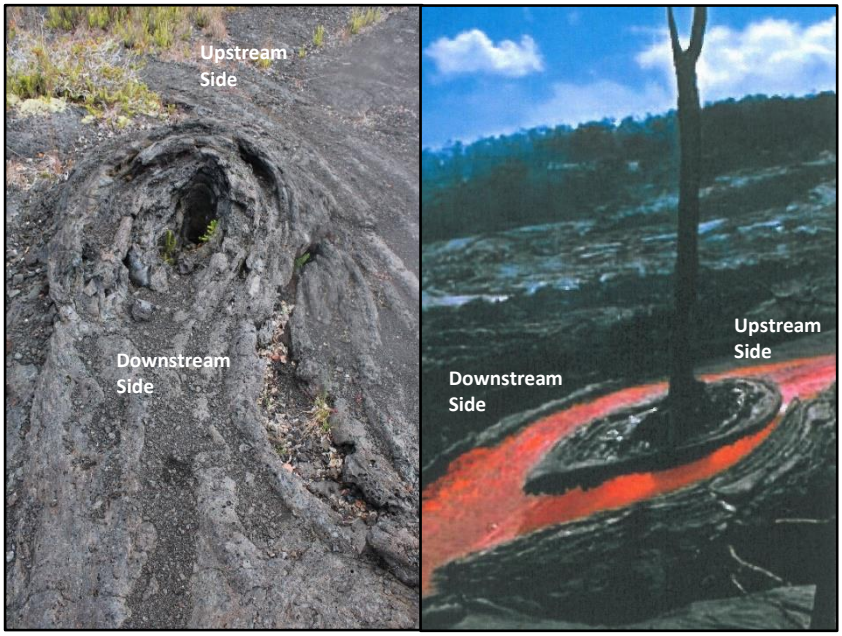


Figure D5-11: The right photo dramatically illustrates a lava tree/tree mould in the process of formation with a rounded upstream portion and a pointed downstream portion. These features are preserved in the tree mould in the left photo at Stop D5-41-5. Photo credits: A.D. MacTavish (left, 2019); NPS Mauna Ulu Eruption Guide (right).

Stop D5-41-6 (NPS-8). 500yr old spatter rampart. Data source: NPS Mauna Ulu Eruption Guide.

- **UTM 267632E, 2143270N.**

In the distance in the northeast (well left of the trail) along the forest edge are the spatter ramparts from the 1973 eruptive vents that formed the lava flow presently under foot.

The low, vegetated hill to the right of the trail southeast of the NPS #8 marker is an approximately 500yr old spatter rampart that was encroached upon by 1973 Pauahi Crater eruption flows. These 1973 flows built up and inflated against this side of the rampart and were deflected to the southwest along the present path of the trail. When the <1-day long eruption ended the lava drained away and left a black, bathtub ring-like, high lava mark against the rampart (3 to 5ft or 1 to 1.5m, above the present flows).

Stop D5-41-7. Large well-developed lava trees. Data sources: NPS Mauna Ulu Eruption Guide; MacTavish (2019).

- **UTM approximately 267869E, 2143482N.**

About 25m south of the trail are several very well-developed lava trees (*see* Figure D5-12). A single larger formation (Figure D5-13), initially thought by AM to be a hornito, was determined by closer inspection to be a large, very well-developed, composite lava tree composed of multiple, closely-spaced lava tree impressions. The interior of this formation exhibits lava drips.



Figure D5-12: The left photo shows a large lava tree and the right photo shows a tree mould along the edge of another lava tree. Photo credits: A.D. MacTavish (2019).



Figure D5-13: On the left is a large, complex, well-developed, composite lava tree looking a lot like a hornito, that is composed of multiple, closely-spaced lava trees. The interior of this formation (right photo) exhibits lava drips. Small, silver jackknife for scale. Photo credits: A.D. MacTavish (2019).

Stop D5-41-8 (NPS16). Plants and animals of recent lava flows in Hawai‘i. Data sources: Tom Callus, Hawaii Tribune Herald (March 25, 2019); Howarth (1979); NPS Mauna Ulu Eruption Guide; nature.Berkeley.edu.

- **UTM 268115E, 2143565N; NPS Marker 16.**

Several animals arrive to inhabit Hawai‘ian lava flows within a few months of their formation. The first two are a wingless, soundless cricket (*Caconemobius fori,* or *‘ūhini nēnē pele* in Hawai‘ian; *see* Figure D5-14, left) and a large wolf spider (*Lycosa sp.*) that feeds on the crickets (Figure D5-14, right).

Hawai‘an lava crickets are the first to arrive on new lava flows, are found nowhere else in the world, and eat decaying plants swept in by the wind. They were not documented in scientific literature until 1978, four years after scientists from the Bishop Museum in Honolulu discovered them on new Kīlauea lava fields. They abandon the flows once they are covered by vegetation and move on to younger flows, or they will die out. Soon after the crickets and spiders arrive come the algae, ‘ōhi‘a trees, lichens, and mosses – in that order. Within 15 years small shrubs are growing in cracks and the original plants are joined by pūkiawe, ‘a‘ali‘i, kūpaoa, and ‘ōhelo. Some species, like pāwale, only grow on the active volcanoes of the island of Hawai‘i and they disappear as other plants crowd them out.



Figure D5-14: On the left is *Caconemobius fori,* a wingless, soundless cricket which is the first animal to colonize fresh Hawai‘ian lava flows. On the right is *Lycosa sp*., a large wolf spider that eats the crickets and is the second animal to colonize fresh Hawai‘ian lava flows. Photo credits: nature.berkeley.edu.

Stop D5-41-9. Lower Pu‘u Huluhulu Overlook. Data source: NPS Mauna Ulu Eruption Guide.

- **UTM 268364E, 2143353N.**

This spot provides a good unobstructed view of Mauna Ulu and a perched lava pond located on the northern flank of the shield mid-way between Pu‘u Huluhulu and Mauna Ulu and partway up the northern slope of the shield (*see* Figure D5-15).

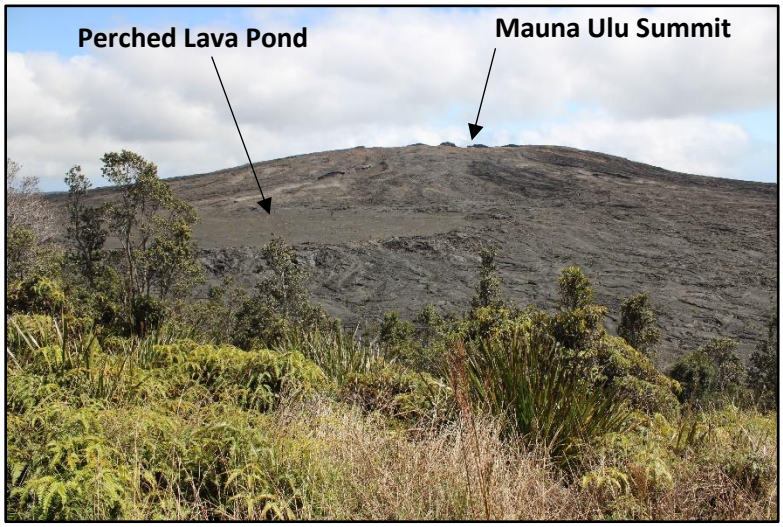


Figure D5-15: Photo of Mauna Ulu and the perched lava pond from the lower Pu‘u Huluhulu viewpoint. Photo credit: A.D. MacTavish (2019).

Stop D5-41-10 (NPS 14). Pu‘u Huluhulu Overlook. Data source: NPS Mauna Ulu Eruption Guide.

- **UTM 268382E, 2143376N; NPS Marker 14.**

Before the Mauna Ulu eruption the overlook provided a view of the forest that surrounded Pu‘u Huluhulu on all sides with the southern horizon view unobstructed down to the Pacific Ocean (*see* Figure D5-16, right). The overlook was constructed in 1934 at an elevation that was about 300ft (94m) above the surrounding land surface.

When the eruption ended in 1974 the unobstructed view was blocked by the Mauna Ulu shield (Figure D5-16, left). During the eruption the overlook was the primary viewing platform for HVO scientists.

The Mauna Ulu summit crater is >100ft (30m) deep.

On a botanical note: The Pu‘u Huluhulu Crater protects rare native plants, like the ‘ōhā (*see* Figure D5-17) which is rare outside the crater, from feral pigs that roam the nearby forests.

The other end of the platform provides a view of the summits of Mauna Loa and Mauna Kea in the far distance and in the middle distance is the caldera at the summit of Kīlauea. The brass plaque located at the northwest corner of the overlook was installed in 1934 and points to the volcanic features visible at that time such as ‘Alae and ‘Āloi craters, which no longer exist, but does not point to Mauna Ulu, which did not then exist.

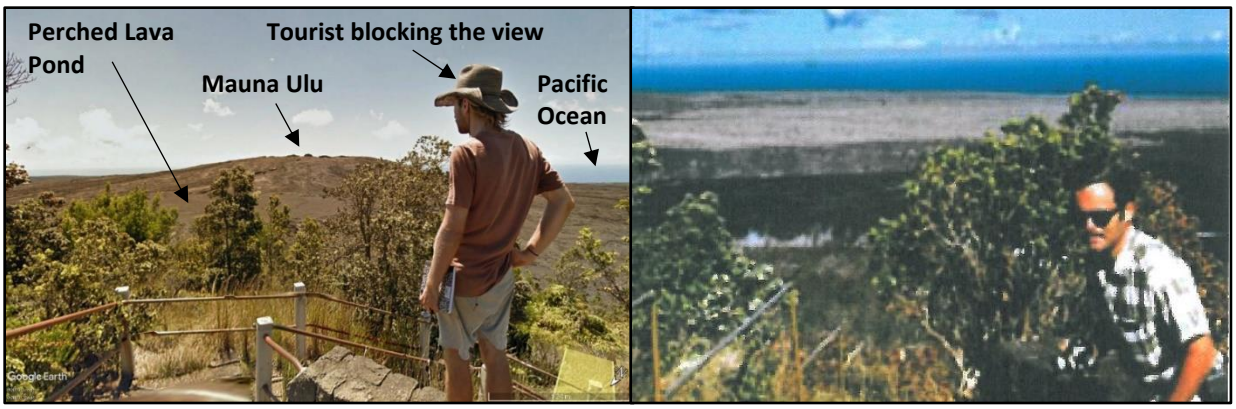


Figure D5-16: The left photo shows a modern Google Earth image of the view south of the viewpoint at the summit of Pu‘u Huluhulu. The right photo is a 1969 image that provides a similar view as the modern photo on the left. Please note the steam rising from fissures near left centre and no Mauna Ulu shield, or tourists, blocking the view. Right photo credit: NPS Mauna Ulu Eruption Guide.



Figure D5-17: Photo of a rare ‘ōhā wai nui or Clermontia Hawaiiensis which grow within the Pu‘u Huluhulu crater and are therefore protected from the feral pigs roaming the surrounding forests. Photo credit: Google Earth.

Stop D5-41-11 (NPS 13). Perched lava pond. Data source: NPS Mauna Ulu Eruption Guide; Easton and Easton (1995).

- **UTM 268499E, 2143189N; breach in southwestern perched lava pond wall.**

After climbing back down the trail from the top of Pu‘u Huluhulu to the trail junction turn left and walk about 720ft (220m) to the east along the Makaopuhi Trail. This will take you out into the flow field to examine the well-developed perched lava pond located mid-way up the northern flank of Mauna Ulu (Figure D5-15). The pond formed when lava pooled behind self-constructed levées that contained the lava surface and became perched when those levées (*see* Figure D5-18, left) kept the surface of the lava higher than the surrounding terrain. Breaches in the levée are visible locally (*see* Figure D5-18, right).

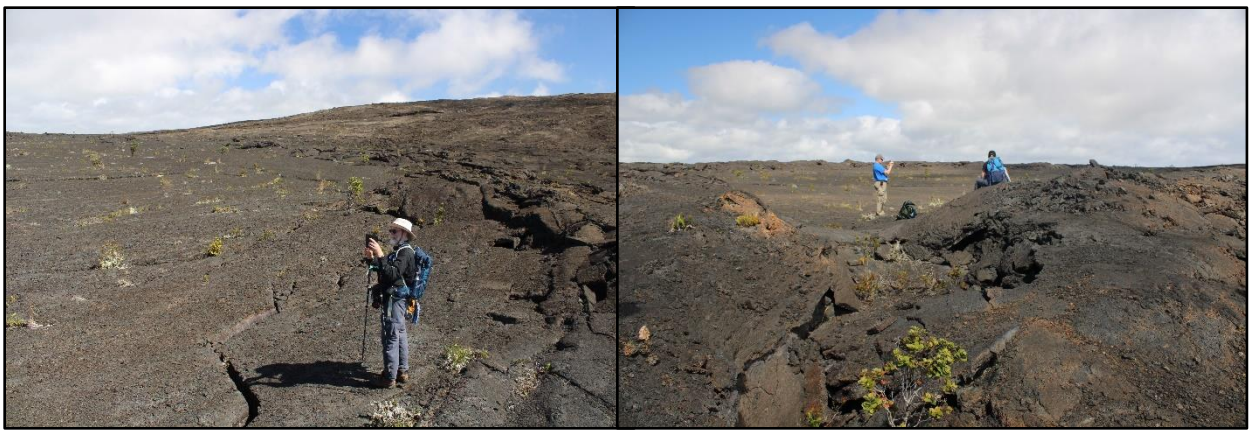


Figure D5-18: The left photo shows the Southern levée of the Mauna Ulu perched lava pond with Tom Erikson for scale. The right photo shows one of many visible breaches in the levée wall (this is the southwestern breach) that allowed lava to escape the perched lava pond and flow downslope (Peter Hinz and Lindsay Smith for scale). Photo credits: A.D. MacTavish (2020).

Stop D5-41-12. Lava channel, western flank of Mauna Ulu. Data Source: MacTavish (2020).

- **UTM 268555E, 2143020N.**

Numerous lava rivers once cascaded down the flanks of Mauna Ulu. The empty remnants of those lava channels now form a pattern somewhat reminiscent of curved spokes on a bicycle wheel. The example at this sub-stop (*see* Figure D5-19) is one of the better examples (Peter Hinz for scale) and exhibits quite high, well-defined marginal levées with well-defined drain-back lines, which are readily visible in the lower right corner of Figure D5-19.



Figure D5-19: This photo shows one of the numerous lava channels that radiate out from the summit of Mauna Ulu (Peter Hinz for scale). Photo credit: A.D. MacTavish (2020).

Stop D5-41-13. Mauna Ulu Summit. Data sources: NPS Mauna Ulu Eruption Guide; MacTavish (2020).

- **UTM 268747E, 2142870N; southern rim of crater.**

Walk upslope along the south side of the lava channel viewed at Stop D5-41-12 for about 500ft (150m) until reaching the summit crater of Mauna Ulu. The summit crater (*see* Figure D5-20, left) is over 100ft (33m) deep and often exhibits rising steam due to the still hot rock present in the interior of the shield. The rocks exposed at the summit, particularly arcing around the northwestern side, show considerable evidence of reddish to reddish-brown hydrothermal alteration due to the passage of superheated steam through the rock along fractures. This can be seen particularly well in the southwest adjacent to several small collapse pits. The pit shown in the right-hand photo of Figure D5-20 has a faint, but readily visible wisp of steam rising from it. The HVO constantly monitors Mauna Ulu. The instrument package is visible near the eastern rim of the crater.

Warning: The entire crater rim is very unstable and prone to collapse. Do not approach too closely.

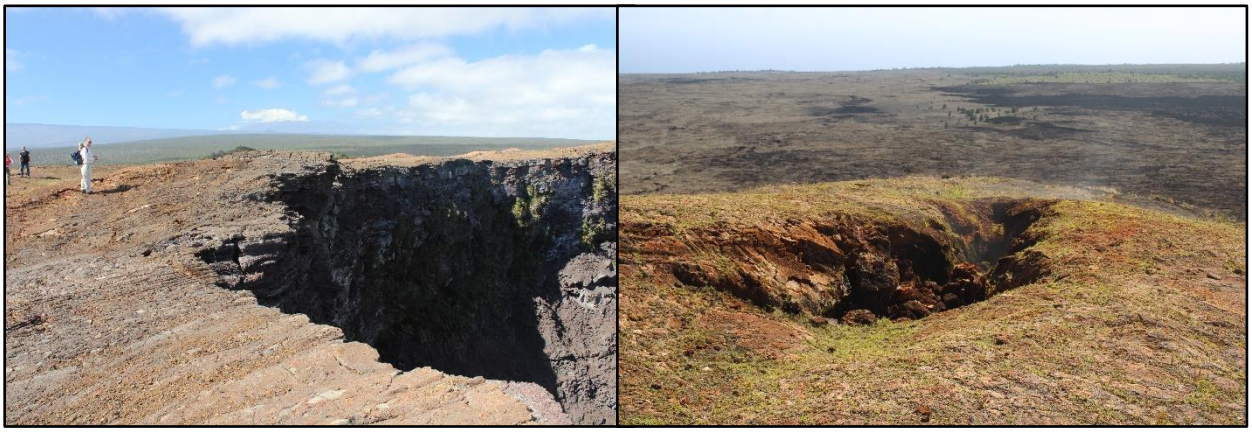


Figure D5-20: The left photo shows the western rim of the central Mauna Ulu crater with 2020 field trip participants for scale. The right photo shows a collapse pit with wisps of visible steam rising from it. Note the clearly visible reddish-brown alteration of the rock surrounding the pit. Photo credits: A.D. MacTavish (2020).



Figure D5-21: The reddish hydrothermal alteration and lizard skin-like weathering pattern characteristic of the summit of Mauna Ulu is easily visible in this photo. Trekking poles for scale. Photo credit: A.D. MacTavish (2020).

3.5. Day 5 (Part 2) – Chain of Craters Road

Stop D5-42. Mau Loa o Mauna Ulu; alternate stop. Data source: Hazlett (2014).

- **UTM 268450E, 2139575N; parking area.**

This stop is on the western border of the 1969 to 1974 Mauna Ulu flow field and is also the trailhead for the Keauhou Trail. This flow field is composed of approximately 440 million cubic yards (340 million m^3) of lava covering 10.5mi^2 (45km^2) of the southern flank of Kīlauea to depths ranging from 3.3ft (1m) to >330ft (100m). The flow field buried 12.5mi (20km) of the original Chain of Craters Road. The longest flows reached the ocean, a distance of 7.5mi (12km) from Mauna Ulu. Most of the surrounding sea of pāhoehoe at this location erupted from the Mauna Ulu vent in 1974. The flows in this area are quite thin and average only a few metres in thickness.

Safety and Endangered Species Note: Nēnē, the endangered Hawai'ian geese, frequently graze along the shoulders of Chain of Craters Road between this parking lot and Muliwai a Pele and also between Maulu and Hōlei arches at the end of the road below on the coastal plain. Take care accordingly since most of the nēnē killed in the park has been along these 2 stretches of highway.

Stop D5-43. Muliwai a Pele. Data source: Hazlett (2014).

- **UTM 269630E, 2138540N; parking area.**

A short 160ft (50m) walk south of the parking area leads to a viewing platform that overlooks a well-developed 'a'ā lava channel with accretionary lava balls deposited on its levée (*see* Figure D5-22, left). It is possible that several portions of this channel were in the preliminary stages of transitioning into a lava tube. This channel formed in 1974 during one of the many Mauna Ulu lava overflows and travelled about 5mi (8km) from the vent to the base of Poliokeawe Pali located ~2135ft (650m) to the south. Mauna Ulu is easily visible to the north on a clear day (*see* Figure D5-22, right).

The walk from the parking lot is over one of many pāhoehoe overflows from the channel. Close inspection of the edge of this flow away from the channel shows that the original underlying flows were all 'a'ā. The parking lot roadcut shows that the channel levées are built of several pāhoehoe overflows. Flows that start from the vent as 'a'ā, with 'a'ā flowing in a channel, are commonly overlain by later pāhoehoe within the channel.

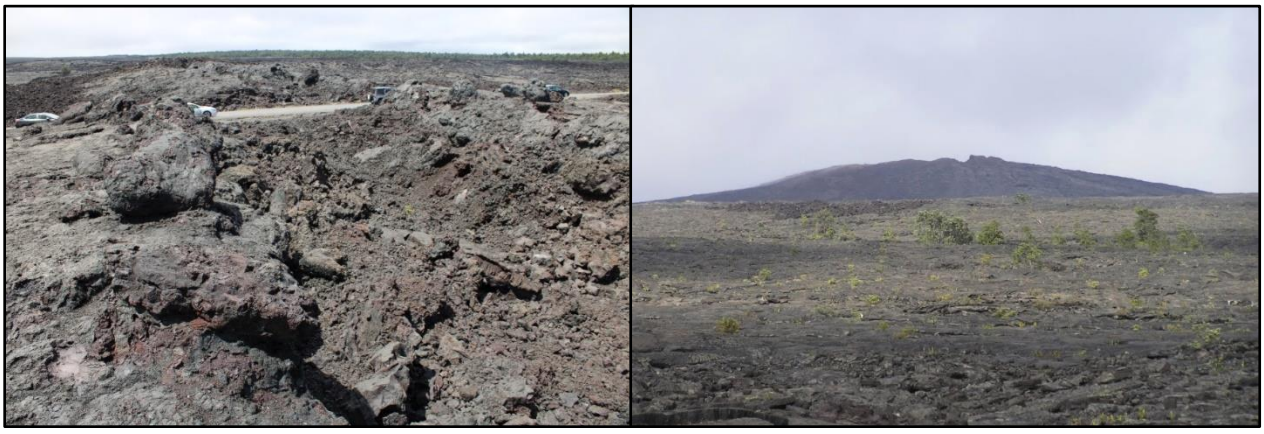


Figure D5-22: The left photo shows a channelized 'a'ā flow with accretionary lava balls on the top of well-developed channel levées. The photo view is north-northeast. The right photo shows Mauna Ulu located ~2.75mi (4.4km) north of this stop. Photo credits: A.D. MacTavish (left 2019; right 2008).

Stop D5-44. Pāhoehoe transitioning to ʻaʻā flows. Data source: MacTavish (2019).

- **UTM 272305E, 2137347N; narrow roadside parking area on right of the highway.**

Here can be seen what may be a pāhoehoe flow transitioning into an ʻaʻā flow north of the highway. Another explanation is that an underlying ʻaʻā flow is being covered by thin pāhoehoe flows.

This stop also affords a good view of the coastal plain (*see* Figure D5-23). Look below and to the right to see the dark ʻaʻā flow in the distance. This may be the flow that was viewed at the last stop (D5-39).

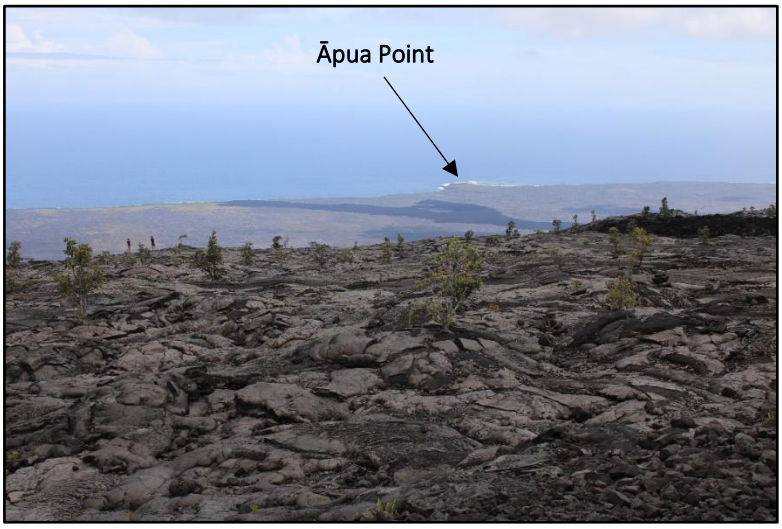


Figure D5-23: The view looking southwest from the Kealakoma viewpoint. The distant, dark ʻaʻā flow is possibly the flow we viewed at the last stop. To the right of the flow, you can see Āpua Point. Photo credit: A.D. MacTavish (2019).

Stop D5-45. Kealakomo Overlook. Data source: Hazlett (2014).

- **UTM 272825E, 2137340N; parking area.**

This overlook is in a kīpuka surrounded by Mauna Ulu flows and looks south over Hōlei Pali with a good view of the pali slope and the coastal plain. Mauna Ulu-era lava flows are very easy to distinguish from the older, originally grassy terrain with the dark gray areas representing ʻaʻā flows and the light gray areas representing pāhoehoe flows.

The prominent point of land to the south-southwest is Āpua Point and is the site of a village destroyed during a tsunami and coastal subsidence associated with the 1868 earthquake. Also destroyed during these episodes were the coastal villages of Keauhu Landing, at Keauhu Point located to the west-southwest, and Kealakomo located to the south-southeast. Petroglyphs and house sites at Kealakomo were again destroyed by Mauna Ulu flows in 1971. Additional archeological sites at Āpua Point were drowned by subsidence during the November 29, 1975 earthquake.

Stop D5-46. Alanui Kahiko Pullout; Hōlei Pali flows. Data source: Hazlett (2014).

- **UTM 273780E, 2135810N; pull-out on left side of highway.**

This narrow pullout affords a good view of the Hōlei Pali, from below, with 1972 Ālae Shield/Mauna Ulu pāhoehoe and ʻaʻā flows cascading down the steep slope of the pali (*see* Figure D5-24, left). It is easy to see in this location that most of the ʻaʻā flows overlie the pāhoehoe flows. About 100ft (30m) southeast of the upslope half of the parking area are 2 small remnants of the pre-Mauna Ulu Chain of Craters Road that occur as uncovered windows within the pāhoehoe flows (*see* Figure D5-24, right).



Figure D5-24: The photo on the left shows Hōlei Pali with 1972 (Ālae Shield) Mauna Ulu pāhoehoe and ʻaʻā flows cascading down the steep slope. The photo on the right shows 2 windows through Mauna Ulu pāhoehoe flows revealing a remnant of pavement from the pre-1972 Chain of Craters Road. Photo credits: A.D. MacTavish (2008).

Stop D5-47a. Puʻu Loa Petroglyphs Trailhead. Data source: Hazlett (2014); MacTavish (2019).

- **UTM 276170E, 2134160N; parking area.**

The 1.4mi (2.25km) long trail exiting this parking area leads to the Puʻu Loa archeological site where early Hawaiʻians carved at least 23,000 petroglyphs as figures, shapes, and forms into the pāhoehoe surface. There are no formal field trip stops on the trail until you reach the archeological site; however, several large tumuli and pressure ridges (which we have seen on other trails previously) occur along the path that may provide some informal stops (*see* Figure D5-25).



Figure D5-25: This photo shows an excellent example of the turtle shell-like surface of a wind-polished pāhoehoe flow adjacent to the Puʻu Loa Petroglyphs Trail near the trailhead. Photo credit: A.D. MacTavish (2019).

Stop D5-47b. Pu‘u Loa Petroglyphs Site. Data sources: Robinson (2012); Hazlett (2014).

- **UTM 276175E, 2134180N; entrance to boardwalk at petroglyphs site.**

This site hosts the largest collection of petroglyphs (rock carvings) in Hawai‘i with most inscribed centuries before the arrival of westerners. Petroglyphs can be seen on both sides of the wooden walkway.

Hawai‘ian fathers would places pieces of their children’s umbilical cords within small holes often surrounded by concentric circles (*see* left photo in Figure D5-26). There are ~16,000 of these holes at the site. The stick-like figure, also seen in Figure D5-26, was carved before the arrival of Westerners. After that arrival carved figures became more detailed and less stick-like (*see* right photo in Figure D5-26).

Do not leave the walkway once you arrive at the site and please do not attempt to make any tracings of the petroglyphs.



Figure D5-26: The photo on the left shows a stick human figure that was carved before the arrival of Europeans in the islands. The human figures in the photo on the right were carved after the arrival of Europeans and are less stick-like and more human-shaped. Photo Credits: A.D. MacTavish (2019).

Stop D5-48. Hōlei coastal sea arches. Data source: MacTavish (2019).

- **UTM 279425E, 2134790N, parking area.**

Walk south (toward the ocean) from the parking lot to the viewing area located at the coastal cliff. The cliffs here are ~100ft (30m) high with vertical to locally undercut walls and sea arches are common (*see* Figure D5-27). A stone guard-wall is only present at the end of the trail. Arches are visible in both directions from the viewpoint.

The east-facing photo in Figure D5-27 (right) was taken in late December 2008 when flows originating at the Pu‘u Ō‘ō vent were entering the ocean via a long-active lava tube. The lava entry point is the grey plume at the horizon in the distance.

Warning: Do not venture along the cliffs past where the guard walls end since these cliffs can be very unstable. Also, beware of large waves which can break over the top of the cliffs. The 2020 field trip group were inundated by one such wave. Luckily no cameras we destroyed by the sea water. Over the years AM has had 2 cameras destroyed by seawater from breaking Hawai‘ian waves and almost lost a third at this viewpoint.



Figure D5-27: The left photo shows the Hōlei Sea Arch located west of the viewing platform. The right photo shows another sea arch located east of the platform. In the distance is a volcanic haze ('vaze') plume produced in late December 2008 by lava entering the sea from a lava tube originating at Pu'u Ō'ō. Photo credits: A.D. MacTavish (2008).

Stop D5-49. End of Road (Alternate stop due to long walk). Data source: MacTavish (2008).

- **UTM 280390E, 2135255N; end of road past gate.**

The road was gated past the buildings and restrooms in 2020. The end of the road pre-2014, was a 2950ft (900m) walk to the east past the gate; however, in 2014 a non-paved extension of the Chain of Craters Road was completed that connected with the road on the far side of the flow field. Vehicle access past the gate is not allowed, unless under special permission. This road extension was again cut by Pu'u 'Ō'ō flows in 2016. Figure D5-28 shows a very appropriate road sign almost covered by 1980's-vintage basalt flows.



Figure D5-28: This photo shows one of the incongruities of Hawai'i – a Road Closed sign in the middle of an almost unending field of Kīlauea basalt. The photo was taken in 2008 several hundred metres east of Road's End. The vase plume from the 2008 lava sea entry is visible in the centre background. Photo credit: A.D. MacTavish (2008).

3.6. Day 5 (Part 1): Helicopter Flight over Kīlauea (Morning)

During the morning of Day 6 the 2020 field trip participants partook in a 75-minute helicopter flight over Kīlauea and its East Rift Zone. Dr. Jack Lockwood (retired HVO volcanologist) and AM acted as aerial tour guides. Some of the features observed are shown in Figures D6-2, -3, and -4. The very approximate flight path is shown on Figure D6-1. The features observed during the flight were:

- **A.** The Kīlauea Caldera, including the new, larger, and deeper Halemaʻumaʻu crater;
- **B.** The Kīlauea Southwest Rift Zone and the Koaʻe Fault system;
- **C.** The Mauna Ulu Shield (1969 to 1974 upper East Rift Zone eruption) and its associated flow field and various pit craters;
- **D.** The Puʻu ʻŌʻō Shield (primary vent for much of the 1983 to April 2018 eruption) on the Central East Rift Zone;
- **E.** The southern coastal plain covered by 1983 to 2018 Puʻu ʻŌʻō flows;
- **F.** Kīlauea surface flows near the base of Hōlei Pali; flows from the 1983 to 2018 eruption and a landing on the flows (Stop D6-50**)**; and
- **G.** The Lower East Rift Zone and features of the May to August 2018 eruption.

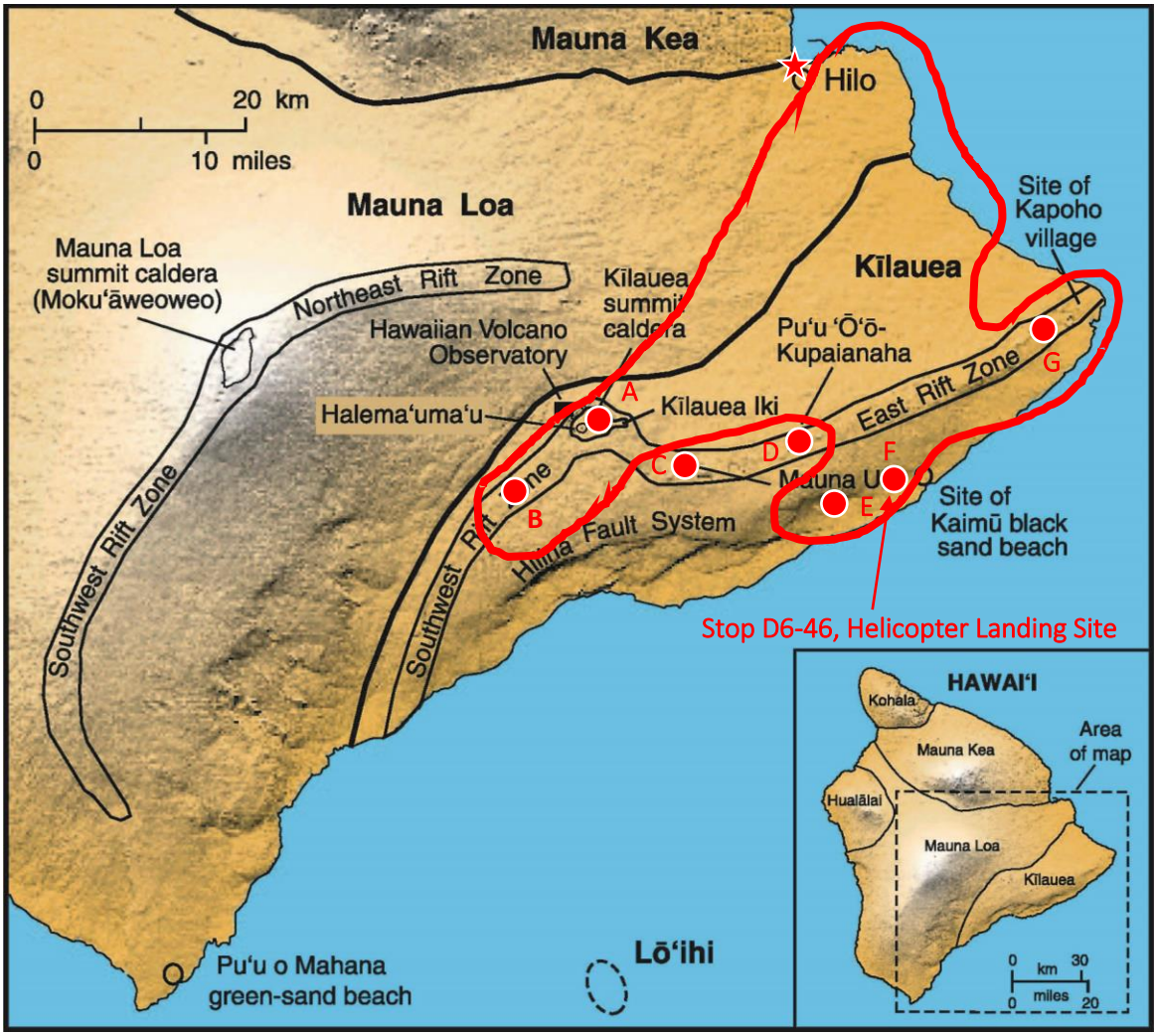


Figure D6-1: Map showing approximate 2020 helicopter flightpath over various portions of Kīlauea Volcano starting from Hilo Airport. Map is modified from USGS General Information Product 117 (2010), p.3.



Figure D6-2: The Puʻu Ōʻō Cone located in Kīlauea's Central East Rift Zone. This cone, which was in the process of transitioning into a shield, was the focus of most of the magmatism and lava flow activity during Kīlauea's 1983 to 2018 eruption. Photo credits: A.D. MacTavish (2019, left; 2020 right).

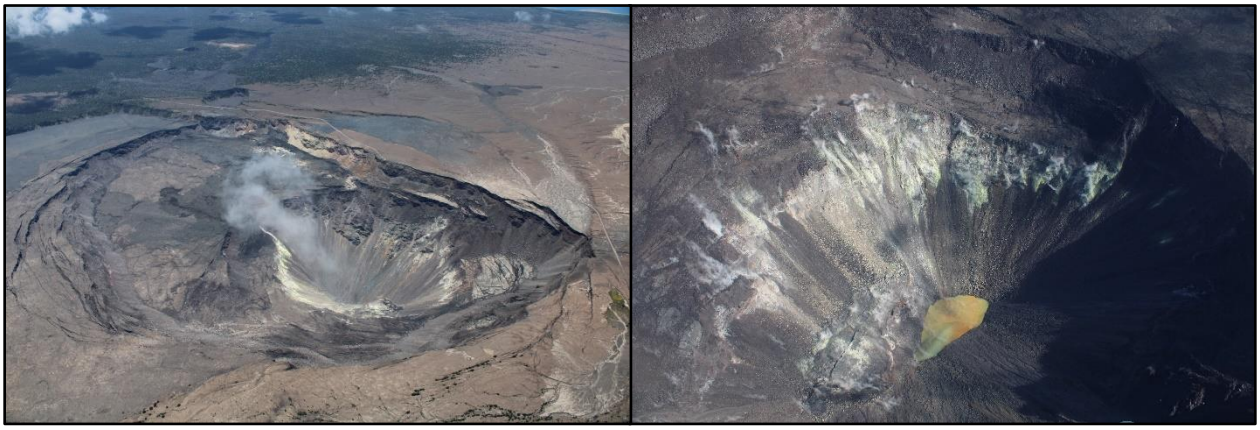


Figure D6-3: The new crater located within Kīlauea's summit caldera that formed after the lava lake within the original Halemaʻumaʻu Crater drained away in May 2018. A water lake was forming at the bottom of the pit in the right photo during the 2020 overflight. Photo credits: A.D. MacTavish (2019, left; 2020, right).

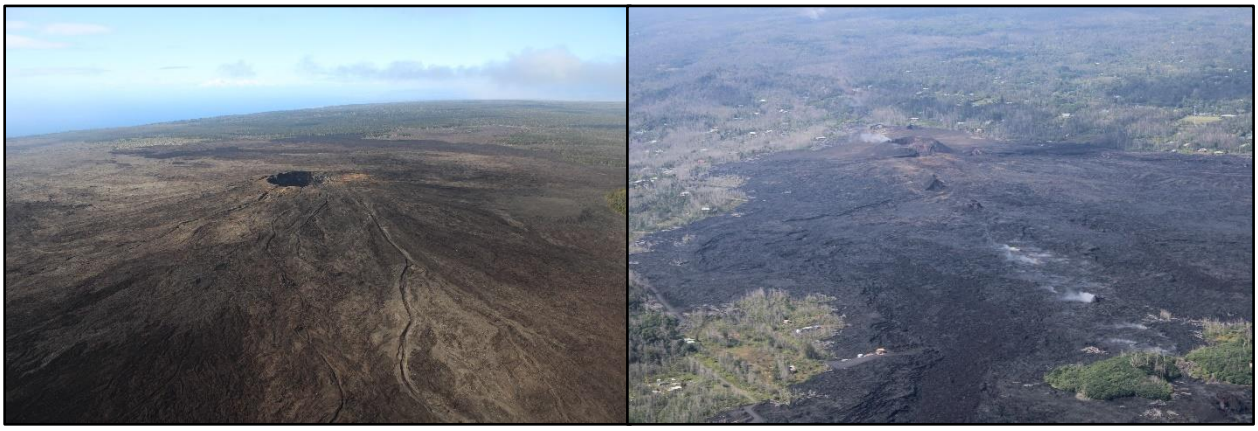


Figure D6-4: The left photo is an aerial view of the Mauna Ulu Shield taken from the east. Note the lava channel on the east-facing slope. The right photo is of the Fissure 8 area of the Lower East Rift Zone, formed during the 2018 eruption and taken from the east in August 2019. Note the steam still issuing from the rift zone and the various cinder cones located along it. Photo credits: A.D. MacTavish (2019).

Stop D6-50. Helicopter landing site. Data source: MacTavish (2019, 2020).

- **UTM 289790E, 2140860N (approximate).**

This site (*see* Figure D6-3 for location) is owned by volcanologist Dr. Jack Lockwood (HVO retired) and is located on the coastal plain ~1.5mi (2.3km) west of the destroyed town of Kalapana and ~2.2mi (3.5km) west-southwest of the present Village of Kaimu. The pre-1983 forest floor at this location was completely covered in 1990 and 1992 by the extensive Pu‘u ‘Ō‘ō flow field to a depth of at least 80ft (25m) by basalt flows (J. Lockwood, personal communication, 2019). This stop (*see* Figures D6-5 and D6-6) allowed the 2020 field trip participants to view many pāhoehoe flow forms with a well-respected and exceptionally experienced volcanologist available to point out and explain the features observed.



Figure D6-5: Helicopters (left photo) parked on the uneven, 1990 and 1992-vintage, Pu‘u ‘Ō‘ō pāhoehoe flows overlying property owned by retired HVO volcanologist Dr. Jack Lockwood (shown in the right photo). Photo credits: A.D. MacTavish (2020).



Figure D6-6: The left photo shows and earlier pāhoehoe flow (1990 flow?) with a crack partially infilled by a later elongate rope of pahoehoe (Tom Erikson for scale). The right photo shows the complex irregularity of the flows. Photo credits: A.D. MacTavish (2020).

3.6. Day 6 (Part 2): Kīlauea Lower East Rift Zone (afternoon)

The field trip stops visited on the Lower East Rift Zone during the afternoon of Day 6 (*see* Figure D6-7):

51. Pāhoa Flows (2014 June 27th Flow that issued from the Pu'u 'Ō'ō shield);
52. 'A'ā flow, 1955 eruption; 2 large spatter and cinder cones to west (alternate stop);
53. 1989 Pu'u Ō'ō-Kupaianaha pāhoehoe flows (49a) and the New Kaimu Black Sand Beach (49b);
54. Palagonatized ash beds erupted approximately 1745AD;
55. MacKenzie State Park; 'a'ā flows and rest stop;
56. Eruption-truncated Leilani Street within Leilani Estates subdivision;
57. Fissure 9, located a short distance east of Moku Street, Leilani Estates; and
58. 13-3574 Makamae St., Leilani Estates; home is located a short distance south of Fissure #8 which formed during 2018 Lower East Rift Zone eruption; provides access to Fissure 8 cone.

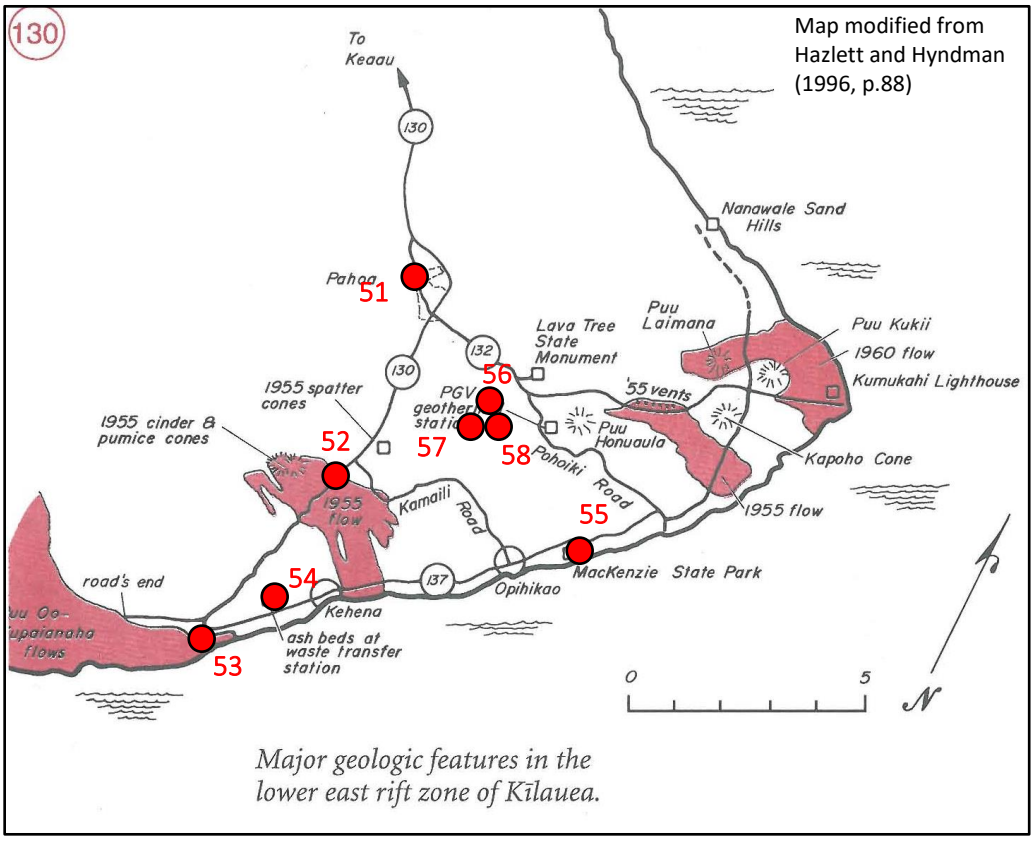


Figure D6-7: Location of field stops during the afternoon of Day 6.

The map shown in Figure D6-8, below, shows the extent of the flows (salmon coloured region on the map) erupted from the Lower East Rift Zone between May 3 and August 14, 2018. The map also shows a closer view of 3 field trip stops made at the western end of the area affected by the eruption.

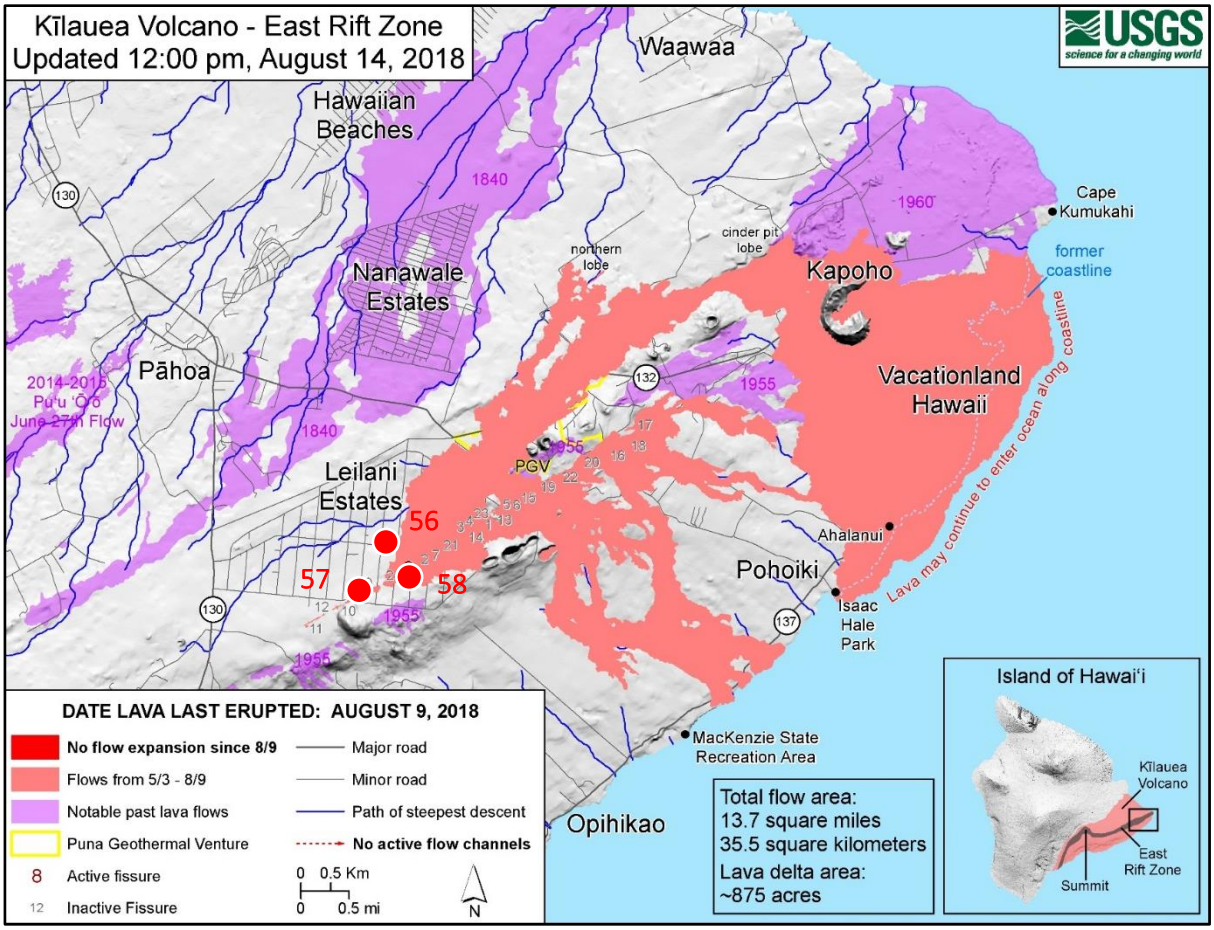


Figure D6-8: Map showing the locations of field stops, fissures, and flows that issued from the fissures during the May 3 to August 9, 2018 eruption from Kīlauea's Lower East Rift Zone. The salmon-coloured region represents the 2018 flows. Map modified from the USGS HVO website.

Stop D6-51. June 27th Flow, Pāhoa, Lower East Rift Zone. Data Sources: USGS HVO Website; MacTavish (2019).

- **UTM 294350E, 2156355N; Pāhoa Transfer Station (Recycling Depot) Parking Area.**

Between 2014 and 2016 a series of flows issued from the north flank of Pu'u Ō'ō that eventually approached the town of Pāhoa, which straddles Highway 130, ~12mi (19.5km) northeast of the Pu'u Ō'ō vent. Two lobes of the 'June 27th Flow' threatened Pāhoa in 2014. The northern tongue of this particular flow-lobe (*see* Figure D6-9) threatened the town's Transfer Station (recycling depot) and came within a few metres of destroying the station. The southern part of the Transfer Station fence and road were damaged. The fence acted as a partial barrier to the flow, which inflated against it until small breakouts at the base of the flow punched their way through the fence into the station after melting the fence steel (*see* Figures D6-10 and D6-11). The flow destroyed several outbuildings at a farm directly across Apa'a St. to the east from the station and part of a Japanese cemetery located midway between the station and the town. The southern tongue of the flow extended to within 625ft (190m) of the Town of Pāhoa before it permanently stalled.

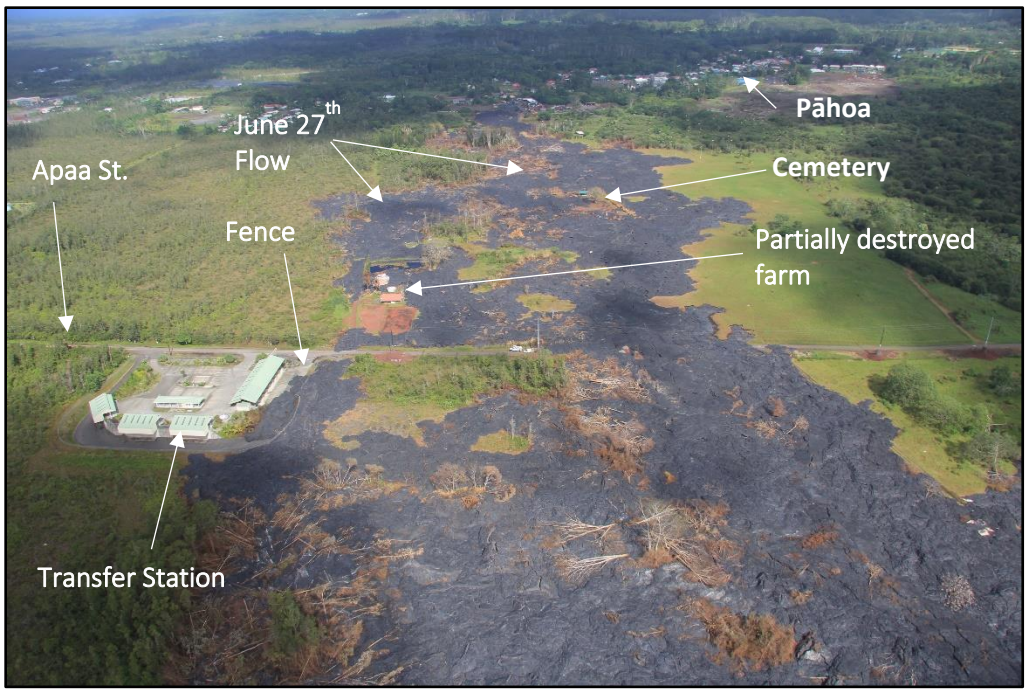


Figure D6-9: Aerial view, looking northeast toward the Town of Pahoa. The location of the June 27th flow is readily visible and the various features of interest are labelled. Photo credit: USGS HVO Website.



Figure D6-10: The left photo shows a lobe of the June 27th Flow encroaching upon the Pahoa Transfer Station (photo taken on November 13, 2014). The right photo shows the same flow inflated against the barrier of the Transfer Station fence and the small flow lobes that oozed through the fence and onto the road of the station (photo taken on November 16, 2014). Photo credits: USGS HVO Website.



Figure D6-11: These close-up photos were taken on August 4, 2019. The left photo shows the flow against the Pahoa Transfer Station fence after the station roadway has been repaired. The photo on the right shows the partially destroyed fence with the inflated flow abutting against it. Photo credits: A.D. MacTavish (2019).

Stop D6-52: The 1955 ʻaʻā flow, Lower East Rift Zone (Alternate Stop). Data source: Hyndman and Hazlett (1996).

- **UTM 294308E, 2148815N; pull-over on right side shoulder of Highway 130 a short distance past the outcrop.**

This stop is located at the southern edge of a huge ʻaʻā flow erupted from the Lower East Rift Zone in 1955. These flows erupted from a pair of large spatter and cinder cones located on the horizon west of the highway. The flows contain large numbers of glassy green olivine crystals and are well exposed in the rock cuts located immediately northeast of the parking area. Because of the wetter climate in this area these flows are well-vegetated compared to what is visible farther to the west.

Stop D6-53a. New Kaimu Black Sand Beach. Data sources: MacTavish (2019, 2020).

- **UTM 293050E, 2141970N. Parking area at Kalapana Village Café and Kaimu Korner Store.**

The beach and **Stop D6-53b** are located at **UTM 293270E, 2141490N** at the end of a 1800ft (550m) long jeep trail leading to the south-southeast from the parking lot. Vehicle traffic along this trail is restricted.

The road to Kaimu and the edge of the vegetation to the north roughly mark the pre-1989 shoreline in this area. The former, famous Kaimu Black Sand beach used to lie immediately opposite this parking lot (*see* Figure D6-12). The Puʻu ʻŌʻō-Kalapana flow field in this area developed between 1989 ad 1993. After completely destroying and covering the former site of the Kalapana village the flows were channelized by the low-tide shelf, and the former coastline beach, leaving the road and buildings at this site intact.

- **Trail to Stop D6-49b**

The 4x4 trail to the new Kaimu black sand beach passes through an area that is under active, guided, and tended revegetation by native Hawaiʻians. Identified species that have been planted and tended here include, but are not restricted to, coconut palm, papaya, and breadfruit (*see* Figure D6-13). Also, there are numerous pieces of recent indigenous art and shrines flanking the trail (Figure D6-13). Please be respectful of the indigenous culture since it is immediately apparent from the efforts made that this place is important to the native Hawaiʻians.

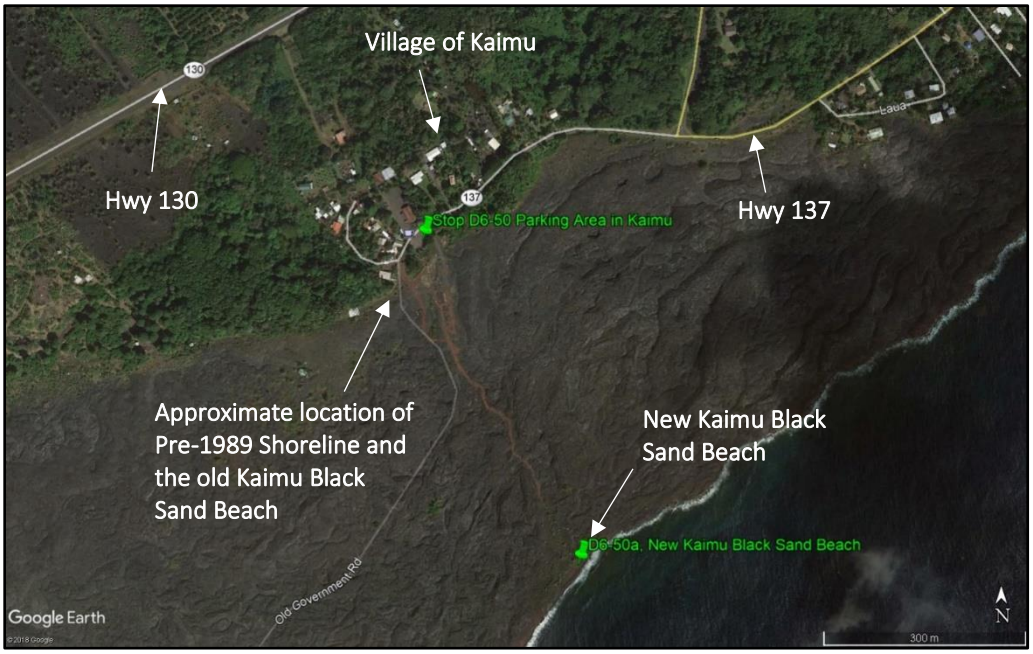


Figure D6-12: Google Earth satellite image of the New Kaimu Black Sand Beach area.



Figure D6-13: Planted and tended plants along the trail to the New Kaimu Black Sand Beach (left photo). Indigenous art along the trail to beach (right photo) Photo credits: A.D. MacTavish (2019).

Stop D6-53b. New Kaimu Black Sand Beach. Data source: MacTavish (2019).

- **UTM 293260E, 2141485N; end of trail above new beach.**

The natural construction of the New Kaimu Black Sand Beach began immediately after the flows reached the ocean and formed fine hyaloclastites upon contact with sea water that were further broken down to sand-sized particles due to intense wave erosion at the shoreline.

The beach is narrow and at high-tide. When there is a high on-shore wind, the beach is underwater and essentially inaccessible and invisible. The walk to the beach is well worth the effort, even if the beach is under water, just to view the revegetation efforts and the examples of indigenous art on the some of the adjacent flows.

Stop D6-54. Palagonitized ash beds at Waste Transfer Station. Data sources: Easton and Easton (1995); Hazlett and Hyndman (2007).

- **UTM 294640E, 2142975N; parking on right (south) highway shoulder.**

At this location beds of palagonitized and limonitized ash and lapilli (*see* FigureD6-14), most probably erupted during littoral steam explosions along the ancient coastline, underlie a weathered ʻaʻā flow immediately overlain by soil. The overlying flow has been dated using ^{14}C methods (Carbon 14) at 2360±90 years Before Present (BP). The exposures of the ash are on the west side of the Waste Transfer Station near the base of an east-facing scarp and can be readily observed from the highway if the gates of the station are closed.

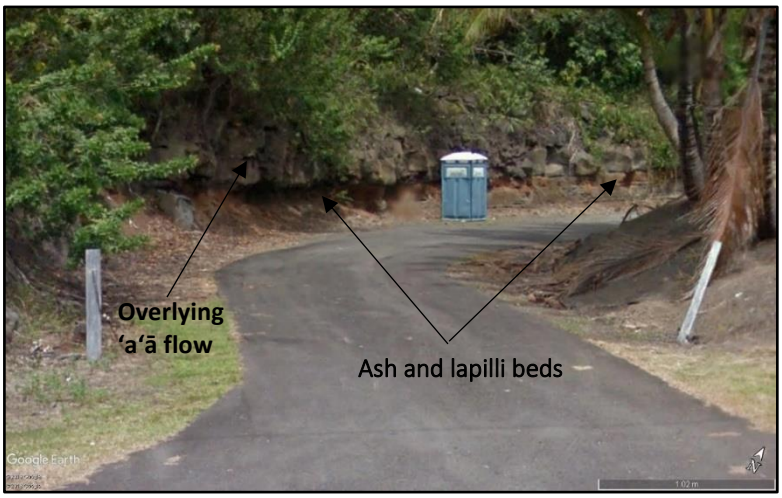


Figure D6-14: Ash and lapilli beds overlain by 2360yr old ʻaʻā flow. Photo credit: A.D. MacTavish (2019).

Stop D6-55. MacKenzie State Park, Rest Area (Alternate).

- **UTM 304225E, 2150530N; park entrance.**

The park is a good afternoon rest stop, if not too busy or overcrowded. The park provides an excellent place to watch surf pound the resistant ʻaʻā flows exposed in a shoreline cliff into rubble.

Stop D6-56. Leilani Street truncated by 2018 Eruption. Data source: MacTavish (2019).

- **UTM 299335E, 2153310N; eastern end of Leilani Street, where truncated by 2018 flows; park along the side of the street, where it is wide enough**.

From this point you can readily see the spatter rampart formed along Fissure 24 and the southwestern slope of the Fissure 8 Cone (*see* Figure D6-15, left) formed during the 2018 Lower East Rift Zone eruption (LERZ). Figure D6-15 (right) provides a closer view of the Fissure 24 spatter rampart.



Figure D6-15: These photos show Leilani Street, within Leilani Estates, truncated by flows and edifices from the 2018 LERZ eruption. In the left photo the Fissure 12 spatter rampart is in the distance beyond the road and the southwestern side of the Fissure 8 Cone is at the right, partially obscured by dead trees. The photo on the right provides a closer view of the irregular Fissure 12 spatter rampart. Photo credits: A.D. MacTavish (2019).

Stop D6-57. Fissure 9 spatter rampart (2018 eruption). Data source: MacTavish (2019).

- **UTM 298740E, 2152523N; stop and park along the west side of Moku Street.**

At this location in 2020 the 2018 LERZ Fissure 9 was still issuing sulphurous gas and steam, as it was when the Figure D6-16 photos were taken on August 4, 2019. The opening of this fissure destroyed the house that was at the end of the truncated driveway at the lower left of the photo in Figure D6-16. Also, the neighbour on the right was lucky to escape destruction as the spatter rampart was built around the fissure. A close-up of steaming Fissure 9 and its associated hydrothermally steam-altered spatter rampart is shown in Figure D6-16 (right). The red pile to the right of the fissure are the remains of the roof of the house that once stood where the fissure is now located.



Figure D6-16: These 2 photos show Fissure 9 and it's accompanying spatter rampart located a short distance east of Moku Street, Leilani Estates. The house on the right in the left photo had a narrow escape from the destruction visited upon the house located where the fissure now sits. A close-up of Fissure 9 is shown on the right with the hydrothermally-altered spatter rampart readily visible. The red pile located a short distance right (south) of the fissure are the remnants of the roof of the home that once stood where Fissure 9 now gapes. Photo credits: A.D. MacTavish (2019).

Stop D6-58. Lower East Rift Zone, Fissure 8 Area (2018 eruption). Data source: MacTavish (2019).

- **UTM 299760E, 2152625N, stop is at 13-3574 Makamae St., Leilani Estates.**

The winter home here is owned by Mark Bishop, from Minnesota, and he graciously allowed the 2020 field trip property access (**one time access only; will not apply to anyone else using this guide**), which provided an excellent view of the Fissure 8 cone and the edge of the 2018 LERZ eruption flow field. He also obtained permission from other landowners and led the group to the top of the Fissure 8 Cone All land underlying the flow field is privately owned and access permission is required from those landowners. Please do not walk onto the flow field without permission.

Figure D6-17 shows the May 29, 2018 Fissure 8 fountaining episode, as viewed by helicopter from the north. The upper left edge of the photo is near the edge of Mr. Bishop's property. The left photo in Figure D6-18 shows a close-up of Fissure 8 fountaining on June 2, 2018 and the right photo of the same figure shows the breached Fissure 8 cone on September 2, 2018 after the eruption had ended.



Figure D6-17: Fountaining at Fissure 8 on May 29, 2018. Photo credit: USGS HVO website.



Figure D6-18: The left photo shows a Fissure 8 fountaining episode on June 2, 2018 that fed a perched and channelized flow. The photo on the right shows the inactive Fissure 8 vent and breached spatter and cinder cone on September 2, 2018. Photo credits: USGS HVO website.

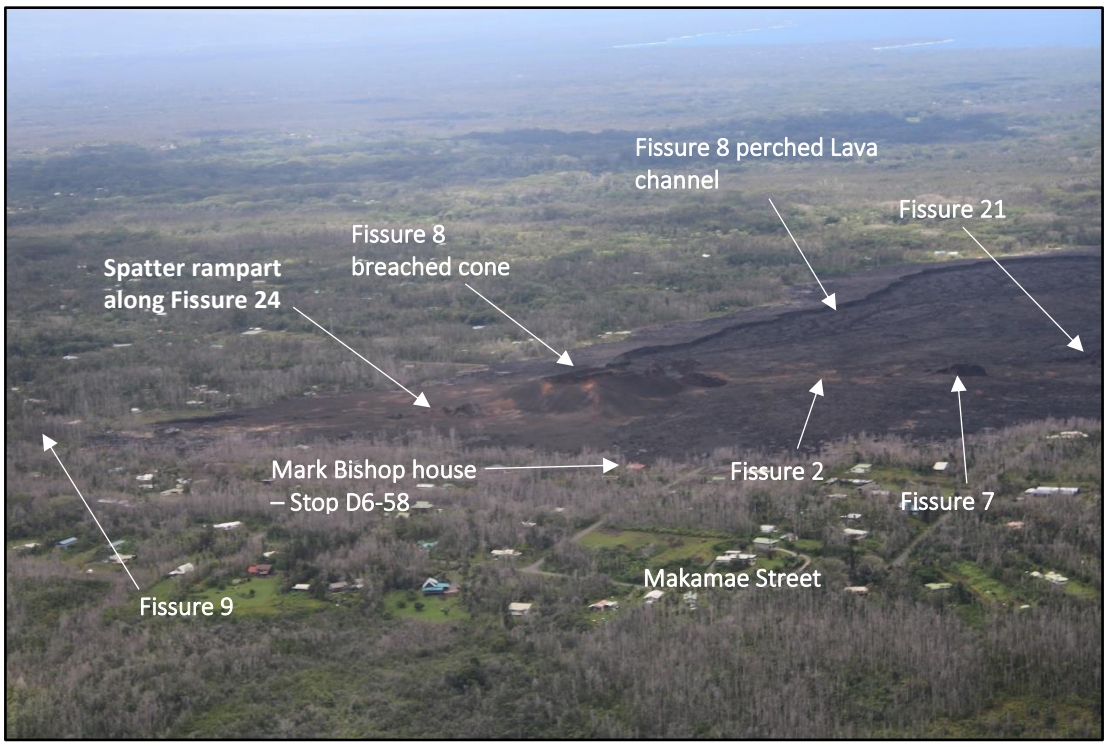


Figure D6-19: Aerial view of the Fissure 8 Cone area and it's associated perched perched lava channel from the 2018 LERZ eruption (August 4, 2019 photo). Also shown are the house at Stop D6-58 and Fissures 2, 7, 9, 21, and 24. Photo credit: A.D. MacTavish (2019).

Figure D6- 19 (above), taken from a helicopter late in the morning of August 4, 2019, shows the Fissure 8 cone and resulting perched lava channel as well as adjacent fissures that were active for a short time at some point during the eruption by issuing spatter, gas, or short-lived flows. Fissure 8 was the longest acting fissure and erupted by far the largest volume of lava during the 3-month eruption.

The 2 photos in Figure D6-20 (below) were taken on August 4, 2019, almost a full year after the 2018 Lower East Rift Zone eruption ended, from the edge of the 2018 flow-field just past the present end of Makamae St. and adjacent to the home owned by Mark Bishop.



Figure D6-20: The left photo shows 3 well-developed lava trees formed on the Fissure 8 flow field. The photo on the right shows the Fissure 8 cinder and spatter cone seen from Makamae Street. The. Photo credits: A.D. MacTavish (2019).

3.7. Day 7 (Mauna Loa) and Day 8 (Mauna Kea)

The various field trip stops for Day 7 and Day 8 are as follows (*see* Figure D7-1):

Hilo Area:

59. Hilo Waterfront (Coconut Island Park)
60. Rainbow Falls
61. Kaūmana Cave

Mauna Loa:

62. Pu‘u Huluhulu (summit of Saddle);
63. Rough lava channel with high levées
64. Road junction with Mauna Kea view
65. Multicoloured flows
66. 2022 Mauna Loa Fissure 4 Flow
67. Mauna Loa Observatory
68. Lava Flow diversion barriers

Mauna Kea Summit Road:

69. Breached Pu‘u Kalepeamoa cinder cone
70. Mauna Kea Visitors Centre at Halepōhaku
71. Ellison B. Onizuka Astronomical Complex
72. Lake Waiau Trailhead
73. Top of pass on Lake Waiau Trail
74. Lake Waiau
75. Mauna Kea Observatory Complex, summit cinder cones, glacial features

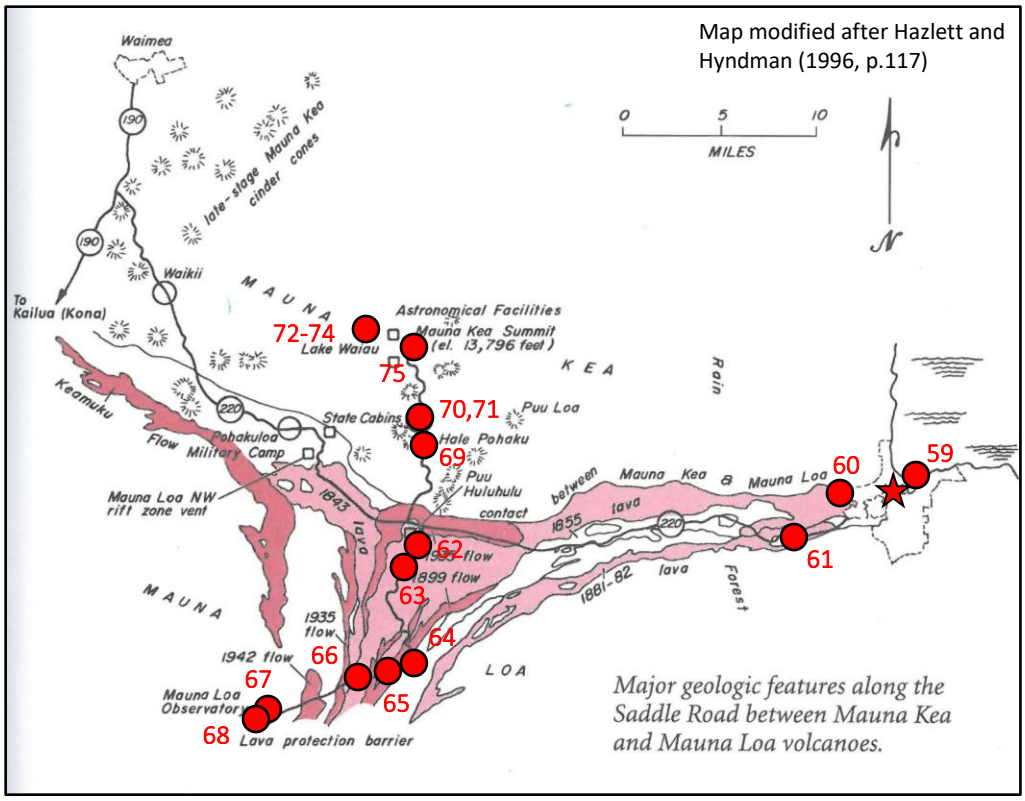


Figure D7-01: Location map of field trip stops on Day 7 and Day 8.

3.7. Day 7 (Part 1) – Hilo Area

Day 7 consists of 4 stops in the Hilo area (Part 1) and a drive up the Saddle Road and the Mauna Loa Weather Observatory Road, with several stops on the way up the mountain (Part 2). There is little walking on this portion of the field trip. The stops in the Hilo Area are listed below and shown on Figure D7-2, below:

59. Hilo Waterfront
- **a.** Coconut Island Park
- **b.** Tsunami Park (Alternate Stop if cannot get into Coconut Island Park)

60. Rainbow Falls, Wailuku Valley

61. Kaūmana Cave (Lava Tube)

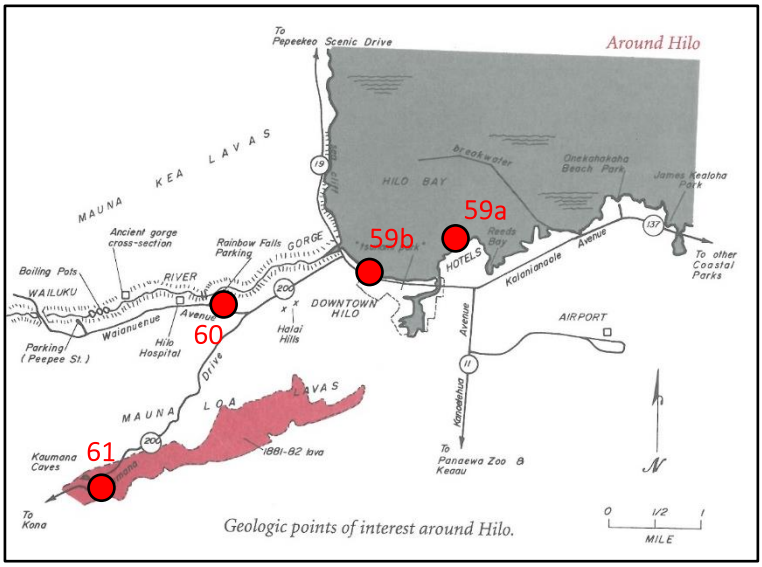


Figure D7-2: Hilo Area Day 7 field stops. Map modified after Hazlett and Hyndman (2007, p.57).

Stop D7-59a: Hilo Waterfront. Coconut Island Park; alternate Stop if a clear day to view the volcano summits. Data sources: Hazlett and Hyndman (2007); Easton and Easton (1995).

- **UTM 283145E, 2182600N; parking area.**

This location provides a good view of Hilo Bay and, on a clear day looming in the background, the summits of Mauna Kea and Mauna Loa, and Hilo to the southwest along the bay coastline.

Hazlett and Hyndman (2007) state that Hilo Bay is a notorious tsunami trap, most of which originate from Pacific Rim megathrust earthquakes. The funnel shape of the bay, its location on the northeast side of the island, and the steep offshore slope off the harbour causes tsunami waves to build quickly. Once inside the bay the waves reflect off the coastlines which causes positive wave interference where the wave crests combine to form waves with extraordinarily high crests. This positive reinforcement has produced numerous tsunami waves that have killed many people and have caused a lot of damage to the city. Tsunamis have killed more people in Hawai‘i than all other natural disasters put together (www.darktourism.com). The 2 most damaging tsunamis in modern history took place in 1946 and 1960.

Stop D7-59b. Tsunami Park (Alternate Stop). Data source: Hazlett and Hyndman (2007).

- **UTM 281880E, 2182227N, parking area.**

The April 1, 1946 and May 22, 1960 tsunamis killed a combined total of 141 people in the Hilo area. After the 1946 tsunami residents of Hilo rebuilt in the devastated area like they had always done in the past. However, after the 1960 tsunami rubble was cleared away, it seems that a lesson was learned and residents now prefer to build their homes on higher ground, away from the waterfront. The area cleared in 1960 remains as a wide grassy strip containing only a few structures that the locals now call Tsunami Park. Still, those parts of Hilo close to the sea remain vulnerable. Evacuation routes are mapped out and available online and are printed in every telephone directory and on signs throughout the city. An early-warning system is in place which includes sirens that sound if a tsunami is detected out to sea.

Stop D7-60. Rainbow Falls. Data source: Hazlett and Hyndman (2007).

- **UTM 279015E, 2181735N, parking area.**

Rainbow Falls (*see* Figures D7-3 and D7-4) is on the Wailuku River at the western edge of Hilo. Hazlett and Hyndman (2007) state that the plunge pool at the base of the falls undercuts the thick ledge of an ʻaʻā basalt flow. In the proper light the curving base of this flow can be seen to follow the outline of an older river bed that was infilled by an earlier eruption. The river occupies a low area between the volcanoes and cannot erode deeper because Mauna Loa flows commonly flow along it and displace the stream. This gorge contains excellent evidence of this happening repeatedly. How the channels formed is illustrated in the upper portion of Figure D7-3. An excellent palisade of columns within two thick Mauna Kea ʻaʻā flows is visible in the walls of the gorge below the falls (above the infilled channel). How the palisades formed is illustrated in the lower portion of Figure D7-3.

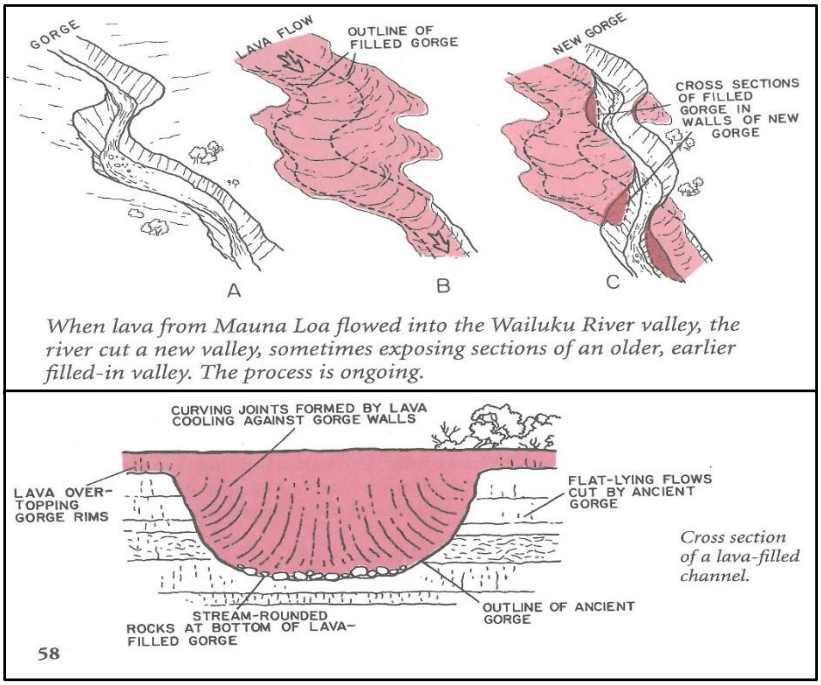


Figure D7-3: The upper panel illustrates the repeated infilling and cutting of the gorge by the river with no overall deepening of the resulting gorge. The lower panel illustrates the formation of joints produced when the flow infilling the lava channel cools to produce the palisades. Diagrams from Hazlett and Hyndman (2007, p.58).



Figure D7-4: Rainbow Falls. Photo credit: A.D. MacTavish (2020).

Stop D7-61. Kaūmana Cave (Lava Tube). Data source: Hazlett and Hyndman (2007).

- **UTM 276605E, 2178200N, a large parking lot on the west side of the highway.**

Be very careful crossing the highway to access the cave entrance due to vehicle traffic along the busy highway.

At this small private park, a collapsed skylight opens into a large, easy-access lava tube with a 20 to 25ft (6 to 8m) high ceiling (*see* Figure D7-5). It is possible to walk or crawl downslope within the tube for almost 3000ft (915m). This tube was the main lava conduit during the 1880 to 1881 Mauna Loa eruption. The tube allowed lava to reach to within 2km of Hilo Harbour, which is 5km east of this point. The walls of the tube expose the internal structure of a pāhoehoe flow. The layering visible in the upper wall formed due to multiple lava spillovers over the levées of a channelized flow before it roofed over to form the lava tube. Fast flowing lava filled the tube when it first formed; however, later on when the lava level dropped the lava sometimes slopped from side to side building the smooth shelves visible near the tube entrance. When the lava finally drained away an empty channel was left between the shelves. Occasionally blocks of the roof fell into the flowing lava becoming partially embedded within, and coated by, lava. Visible on the upper walls and ceiling are numerous small stalactites and lava drip tracks. The cave is also home to a host of underground animals, the largest being insects and spiders.

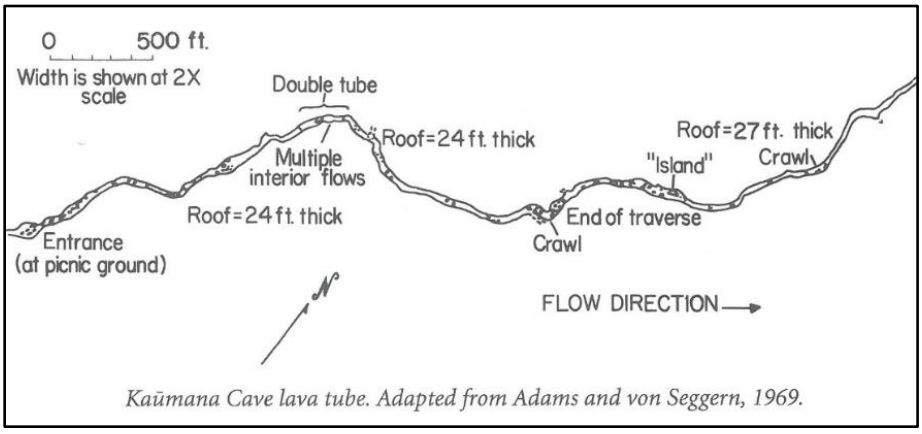


Figure D7-5: This figure is a map of the lava tube. Diagram was taken from Hazlett and Hyndman (2007, p.60).

3.7. Day 7 (Part 2): Saddle Road (Highway 220) and Mauna Loa Observatory Road

The Saddle Road (Highway 220) crosses the mainly unpopulated central plateau of the island and passes through the gap between Mauna Loa and Mauna Kea volcanoes known as the Humuʻula Saddle. The top of the saddle is at an elevation of 6500ft (1980m) ASL.

The Saddle Road was built in 1942 shortly after the Japanese attack on Pearl Harbour to access the U.S. Army's Pohakuloa Training Area and Bradshaw Army Airfield. In 1945 the road was transferred to the Territory of Hawaiʻi and designated Route 20; however, no maintenance funds were available for a road that was never designed for civilian travel. In 1959 the new State of Hawaiʻi gave the road to the County of Hawaiʻi, but, again, there were no funds for road maintenance. Finally, in 2004 Federal funds allowed for road re-alignment and upgrading to the present modern, paved, and well-maintained Highway 220.

The Saddle Road starts at the Hilo Waterfront, as Waiānuenue Ave., and ends at Highway 190, a short distance southwest of the Town of Waimea. For much of the distance between Hilo and Puʻu Huluhulu the road follows the 1935 and 1936 Mauna Loa flow which mostly covers the Humuʻula Saddle plain. On approach Puʻu Huluhulu the flow changes from ʻaʻā to pāhoehoe.

Stop D7-62: Puʻu Huluhulu (Hairy Hill). Data sources: Hazlett and Hyndman (2007); Robinson (2010).

- **UTM 241390E, 2178890N; parking lot (if open). In August 2019 access to the cone was not possible due to roadblocks erected by political and religious protestors. The site was opened in February 2020 and was apparently still open as of December 2022.**

Puʻu Huluhulu is a small, wooded, alkalic Mauna Kea cinder cone (>10,000 years old) located adjacent to the highway about 100m south of the junction with the Mauna Kea access road and 400m west the junction with the Hilo-Kona Road (*see* Figure D7-5).

The cone is part of the alkalic Laupāhoehoe formation, is now a kīpuka surrounded by younger Mauna Loa flows, and is at the transition between the montane and sub-alpine vegetation zones.

Near the northwest base of the cone is a partially buried stone wall constructed in 1935 in an attempt to deflect the 1935 Mauna Loa flow (*see* Figures D7-5 and D7-6). Hazlett and Hyndman (2007) state that:

ʻ[A]*fter the lava pooled in the saddle and a hard crust formed on the surface, molten lava pouring down the long slope of Mauna Loa continued to feed the flow beneath the crust, lifting and splitting the crust as though it were rising bread dough* [inflation]. *You can judge the amount of the rise as you walk along the wall. In a few places the lava buried the wall, but in most places the flow was too thin and the crust too stiff to shift across the top of the wall*ʼ.

The cone's interior structure is exposed by an old quarry in its western flank (Figure D7-5). Clearly visible are basaltic dykes that intruded into the cone. The lava confined beneath the surface of the Mauna Loa flows was under pressure and was able to push sheets of molten lava into the unconsolidated debris of the cinder cone.

A road leads from the quarry to the summit of the cone. From the summit the stone wall to the west is readily visible, as are numerous other alkalic Mauna Kea cinder cones formed during late-stage activity on the South Rift Zone. A group of cones located near the towers of the National Radio Astronomy Observatory, a few miles north of Puʻu Huluhulu, are between 20,000 and 40,000 years old. Younger cinder cones, ~4500 years old, are located further upslope. The ash and cinder from these vents covered a wide area to a depth of ~1ft (30cm). This ash can be observed in a gully that is crossed by the Highway. This ash (now a soil) contains bits of charcoal from wood that is thought to have been burned during the eruption.

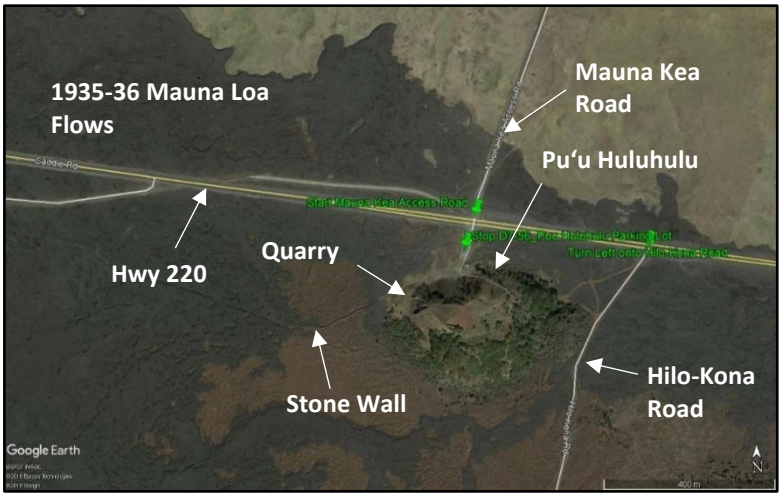


Figure D7-5: Google Earth satellite image of the Pu'u Huluhulu area showing various points of interest.



Figure D7-6: The partially buried stone wall located west of Pu'u Huluhulu. The wall was built in an attempt to stop or deflect a Mauna Loa flow during the 1935 to 1936 eruption. Photo credit: Hazlett and Hyndman (2007, p.120).

3.7.1. Mauna Loa Observatory Road:

The November 28 to December 10, 2022 Mauna Loa summit and Northeast Rift Zone eruption truncated road access and the final 2 of the planned stops for the field trip Day 7 and are no longer accessible. We cannot yet properly describe the flows and other volcanogenic features formed by the new eruption so we recommend that users of this guide examine the accessible portions of the flows at their leisure.

Before the eruption the 17.4mi (28km) long, steep, and narrow Mauna Loa Observatory Road wound up the northern flank of the mountain to the Mauna Loa Weather Observatory operated by the National Oceanic and Atmospheric Administration (NOAA) situated at 11,000ft (3353m) ASL. The road passed through multiple climactic zones ranging from moist subtropical to alpine and provided a feel for the enormous size of the volcano. The road also passed over numerous, well-exposed lava flows of widely differing ages that due to sparse vegetation and slow weathering are almost indistinguishable from one another.

All the originally planned stops have been left in place with the addition of one field stop where the flow now blocks the road. The road will eventually be rebuilt and the final 2 stops will again be accessible.

Stop D7-63: Rough lava channel (Alternate). Data source: Hazlett and Hyndman (2007).

- **UTM 240950E, 2175580N, parking area is widened road within channel.**

The road passes through an extremely rough 1935-1936 ʻaʻā lava channel with high levées. The huge blocks scattered downslope on the flow from the parking area originated when the levée walls of this flow channel collapsed into the lava stream and were carried downslope.

The lava channel is very difficult to identify while driving so keep a close look at the GPS to be able to identify the right location.

Stop D7-64. Road Junction at ~13.8km. Data source: Hazlett and Hyndman (2007).

- **UTM 242570E, 2167240N, park to the left near the microwave dishes.**

When the sky is clear this road junction provides a superb view of the Saddle Road and Mauna Kea in the distance (*see* Figure D7-7).

This is also a good location for a short ½ to 1 hour break (possibly lunch) to partially acclimatize to the high altitude before climbing any higher.



Figure D7-7: Spectacular view of Mauna Kea located to the north of Stop D7-60. Photo credit: Google Earth.

Stop D7-65. Multicoloured flows. Data source: MacTavish (2019).

- **Approximate UTM 241400E, 2166690N; park to side of road where it is wide enough.**

Upslope, to the south, are multiple pāhoehoe and ʻaʻā flows, the oldest with some vegetation. The flows exhibit multiple colours due to age and weathering (*see* Figure D7-8) with the oldest rocks comprising the red, partially vegetated pāhoehoe (left centre of the photo), the youngest are the dark brown ʻaʻā, and in between are grey pāhoehoe flows (right centre of the photo).

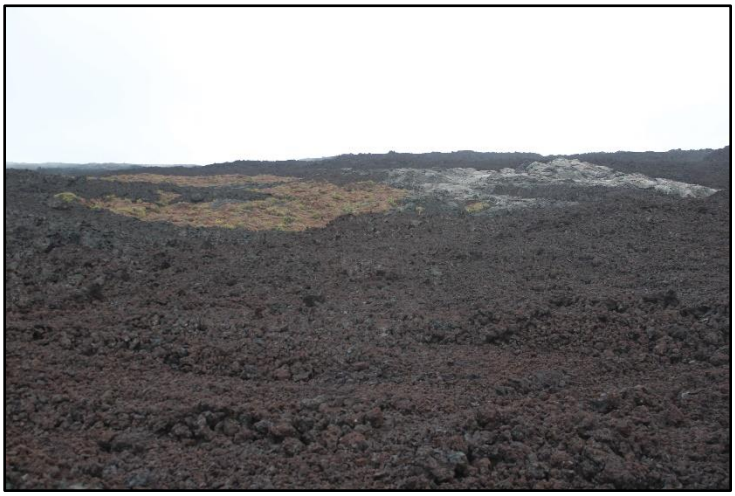


Figure D7-8: Multi-coloured flows of differing ages on the north flank of Mauna Loa at Stop D7-61. Photo credit: A.D. MacTavish (2019).

Stop D7-66. 2022 Mauna Loa Fissure 4 Flow Blocking Mauna Loa Observatory Road. Data Sources USGS HVO website; Google Earth.

- **UTM 239365E, 2166345N (approximate location derived from Google Earth). Until road is re-established travel by road past this point will be impossible. As of June 6, 2023 the lates Google Earth image shows that the road is still blocked.**

The ~1000ft (300m) wide 2022 Mauna Loa flow truncating the road here issued upslope from Fissure 4 (F4) on the northeast rift zone. It did not advance much past this point (600m) because lava ceased issuing from F4 shortly after the road was cut. It may be possible to walk around the north end of this flow and then walk further to the west to where the F3 flow field crosscuts the road; however, the older flow located west of the new flow is an ʻaʻā flow and walking across it would be extremely dangerous. Figure D7-9 shows an aerial view of the F3 flow field crosscutting the road in multiple places.

Safety Note: If the new flow is pāhoehoe please be very careful walking across it since these flows are brittle and there will be a large number of hidden voids. If this is an ʻaʻā flow then do not attempt to cross it under any circumstances. ʻAʻā flows, particularly young ones, are very rough, very unstable, and all surfaces consist of razor-sharp edges that easily slice flesh and destroy footwear, even sturdy footwear. They are extremely dangerous to walk upon. The authors do not know how far the walk is around the toe of this flow. Only attempt it if the distance is relatively short and the underlying older flows are not ʻaʻā flows.

The location of this and other flows, the F3 and F4 vents, and the Mauna Loa Observatory Road are shown in Figure 13, above.

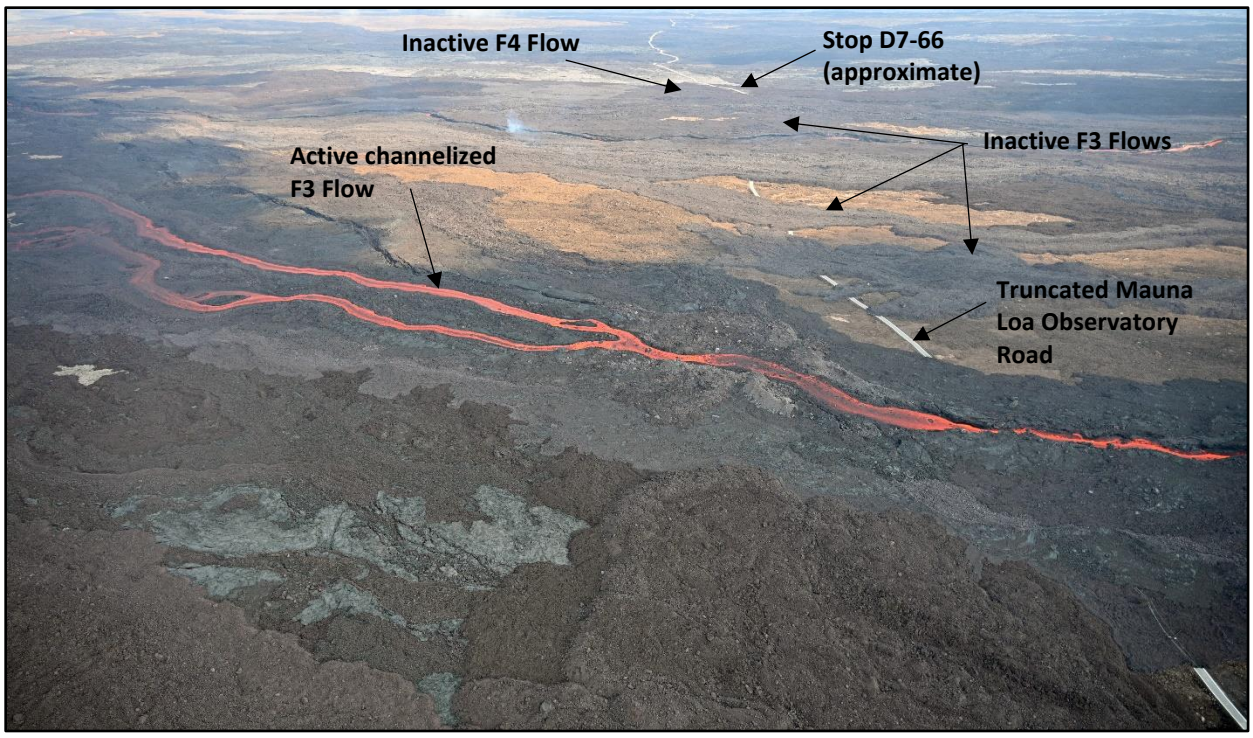


Figure D7-9: Aerial view of the active F3 flow field crosscutting the Mauna Loa Observatory Road on December 5, 2022. The inactive F4 flow field is identifiable to the east at the top pf the photo. This view is looking roughly east-southeast on the north flank of Mauna Loa toward Stop D7-66. Photo credit: USGS HVO website (2022).

Stop D7-67. Mauna Loa Weather Observatory (~11,000ft, 3355m ASL). Data source: Hazlett and Hyndman (2007).

- **UTM 229765E, 2162390N, parking area just before the gate to the observatory. Travel by vehicle, except for authorized NPS vehicles, past this point is restricted. Only foot travel is allowed. The road past this point ends at the summit of Mauna Loa.**

On clear days this location provides a spectacular, panoramic view of 3 of the other volcanoes on the island with Mauna Kea to the north, Kohala to the north-northwest, and Hualālai to the west. Barely visible in the distance in this photo, between Kohala and Hualālai, and above a narrow line of cloud is the summit of Haleakalā volcano located on the Island of Maui (*see* Figure D7-10). The Mauna Loa Observatory is a facility for studying the earth's atmosphere, particularly atmospheric CO_2 and ozone loss and is operated by the American National Oceanic and Atmospheric Administration.

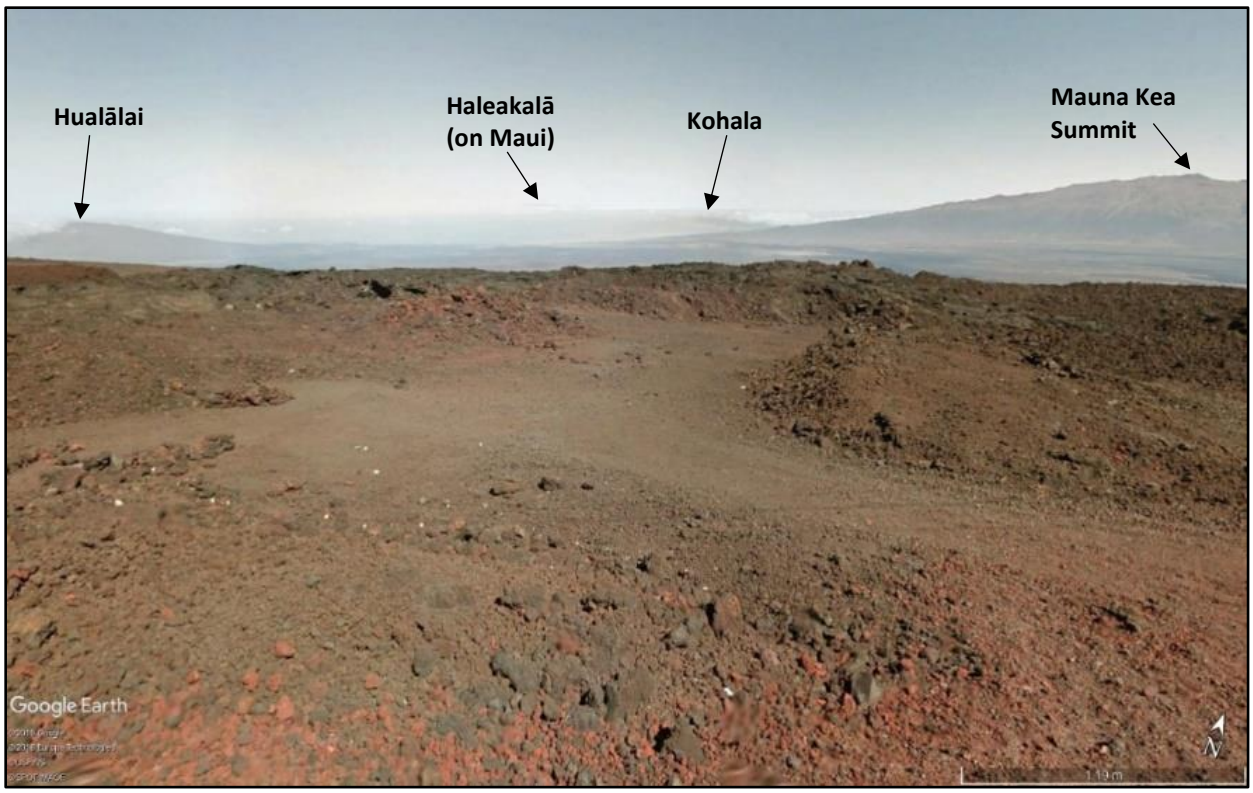


Figure D7-10: Panoramic view from Stop D7-62 and the Mauna Loa Weather Observatory parking area. Photo credit: Google Earth.

Stop D7-68. Lava flow diversion barriers. Data source: Hazlett and Hyndman (2007).

- **UTM 229550E, 2162165N; 160m south of the Mauna Loa Summit Trail a short distance past the gated road leading to the Mauna Loa Observatory.**

To get to this location either go through the observatory grounds (permission will be required) or walk along the summit road for a distance of 850ft (260m) until a window of the underlying pāhoehoe is exposed, then walk slightly east of south for 525ft (160m) until you see the end of the western diversion barrier. This diversion barrier was designed by Dr. Jack Lockwood of the HVO, retired (personal communication, 2019).

These diversion barriers (*see* Figure D7-11) protect the observatory from Mauna Loa lava flows and were the first such structures constructed in the USA. Note how the 2 barriers form an acute angle into the direction of downslope flow. This shape and orientation are designed specifically to deflect, rather than stop, any flows striking the barriers. Barriers erected across the direction of flow will eventually be engulfed and overridden after the flows inflate at the barrier, as was seen at the wall observed at field trip Stop D7-58.

If it is raining, please do not attempt to walk to the diversion barriers from the road since walking on the ‘a‘ā flows located between the road and the western diversion barrier is very dangerous.

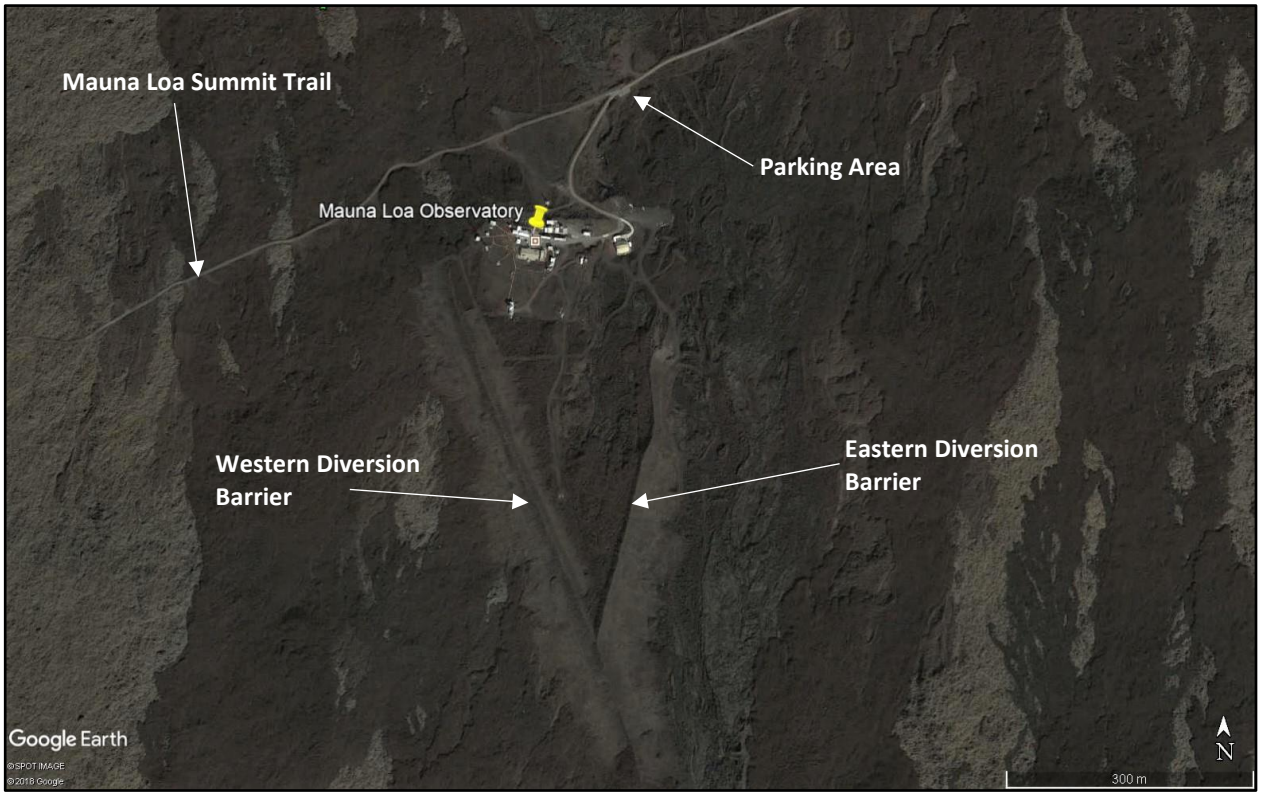


Figure D7-11: Google Earth satellite image of the area of the Mauna Loa Weather Observatory with the location of the lava flow diversion barriers shown by the labels and arrows.

3.8. Day 8 – Mauna Kea Summit Road

Stop D8-69: Pu‘u Kalepeamoa Crater. Data source: Hazlett and Hyndman (2007).

- **UTM 242600E, 2186430N; gated entrance to tower access road.**

Having just passed through the breached crater wall, this stop is on the northern edge of the horseshoe-shaped Pu‘u Kalepeamoa Crater The ridge west of the road is the crater rim where trade winds piled cinder high to one side. The cinder of this cone contains many fragments of older rock, including gabbro and green dunite.

Stop D8-70: Mauna Kea Visitors Centre at Hale Pōhaku. Data sources: Hazlett and Hyndman (2007); Robinson (2010).

- **UTM 242640E, 2186710N; Visitors Centre parking lot.**

This is a rest stop because there are no public facilities at the summit. The store within the centre should be open and will be able to tell you whether travel is permitted higher, particularly if there is snow cover from a recent snowfall. The center sits on fresh-looking ash and cinder.

All visitors planning on driving to the top of the mountain are required to stop here at an elevation of 9200ft (2804m) for at least an hour to acclimatize to the altitude before moving higher on the mountain. At the summit the atmospheric pressure is 40% of that at sea level and acute altitude sickness is common. Symptoms are: headaches, drowsiness, nausea, shortness of breath, and poor judgement (*see* Figure D8-5, left photo, taken at the summit of Mauna Kea, for a possible illustration of poor judgement). The optional 1 hour stay at this altitude will help reduce the symptoms. The high elevation

also requires sunscreen and sunglasses. Appropriate clothing should be used as protection against the higher levels of UV radiation. It will be cold (usually below freezing) and windy at the summit and warm clothing will be necessary and should consist of gloves or mitts, warm jacket, hats with ear protection, and sunglasses.

There is a short trail that heads to the summit of the nearby cinder cone west of the Visitor's Center. This cone contains numerous cored spindle bombs formed around large, mainly gabbroic xenoliths.

Stop D8-71. Ellison B. Onizuka center for International Astronomy; Astronomer's Mid-Level Facility.

- **UTM 242630E, 2186970N, parking lot.**

The Ellison B. Onizuka Center for Astronomy is where astronomers live and work rather than having to physically be at the telescopes at the summit. This cuts down on the number of adverse altitude effects that would be suffered if astronomers had to physically be at the telescopes on the summit.

The map in Figure D8-4, below, shows the geological features at the summit of Mauna Kea and the location of the astronomical observatories (black dots).

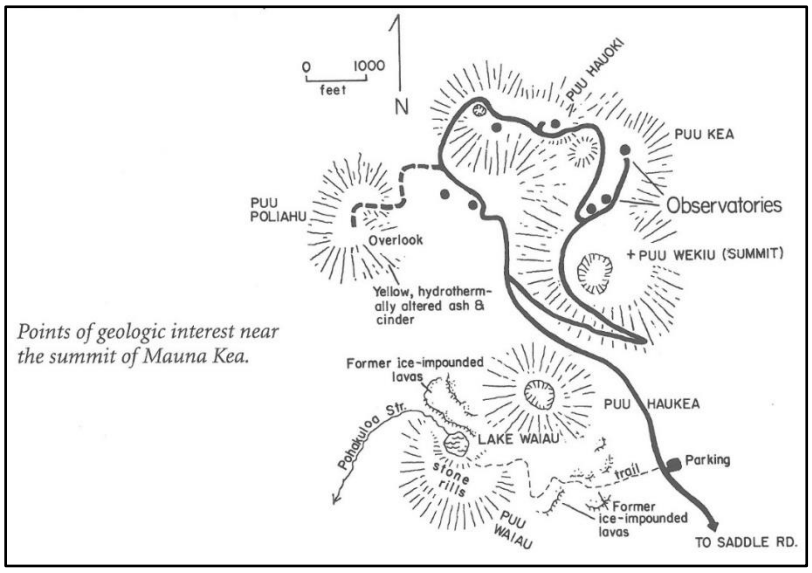


Figure D8-4: Map of the summit of Mauna Kea showing geological features and the location of the various telescopes. From Hazlett and Hyndman (2007, p.125).

Stop D8-72. Lake Wai'au Trailhead. Data sources: Hazlett and Hyndman (2007); Meguerian and Okulewicz (2007).

- **UTM 241495E, 2192385N; parking lot (mile 12.5) on right (east) side of road.**
- **UTM 241471E, 2192349N; Lake Wai'au Trailhead; west side of the highway a short distance south of the parking area.**

The light-coloured patches visible on the flanks of the Pu'u Wai'au cone, located due west of the parking area, are due to hydrothermal alteration produced when steam and hot water percolated through the cone near the end of its eruption. The clay within the alteration products decreased the permeability of the cinder and resulted in increased runoff from rain and melting snow producing more erosional gullies than is evident on the flanks of unaltered cones.

The trail leads upslope past the steep lobate edge of a flow erupted from Pu'u Hau Kea ~40,000 years ago. The fracture patterns along the edge of the flow suggest the lava cooled while banked against ice.

Stop D8-73. Top of pass, 230ft (70m) northwest of trail junction. Data sources: Hazlett and Hyndman (2007); Meguerian and Okulewicz (2007).

- **UTM 240690E, 2192472N.**

This point is the top of the pass between Pu‘u Wai‘au to the south and west and the taller Pu‘u Hau Kea to the north (*see* Figure D8-5). Lake Wai‘au should be just visible several hundred metres downslope to the right within a blasthole located at the north end of the crater floor.

Stop D8-74. Lake Wai‘au. Data source: Hazlett and Hyndman (2007).

- **UTM 240690E, 2192472N.**

Tiny Lake Wai’au is one of the few natural bodies of water found within the State of Hawai‘i and is the highest lake in the state at 13,160ft (4011m). It persists rather than draining away due to impermeable clay weathered from ~3300-year-old Mauna Kea ash and the clay-rich hydrothermally altered cinder that comprises the cone. The lake occasionally overflows through a notch in the northwest rim of the crater.

On the floor of the crater south of the lake is the remains of a rock glacier composed of a mixture of rock and ice that once flowed toward the lake. It is now a mass of hummocky light grey debris (Figure D8-5).

The rough lava embankment along the north side of the lake is part of the 40,000yr old flow that was walked past downslope toward the road. The cavernous voids, mosaic fractures, and lava pillows suggests that this flow stopped against ice. There are many inclusions of coarsely granular gabbro and green dunite within the flow.

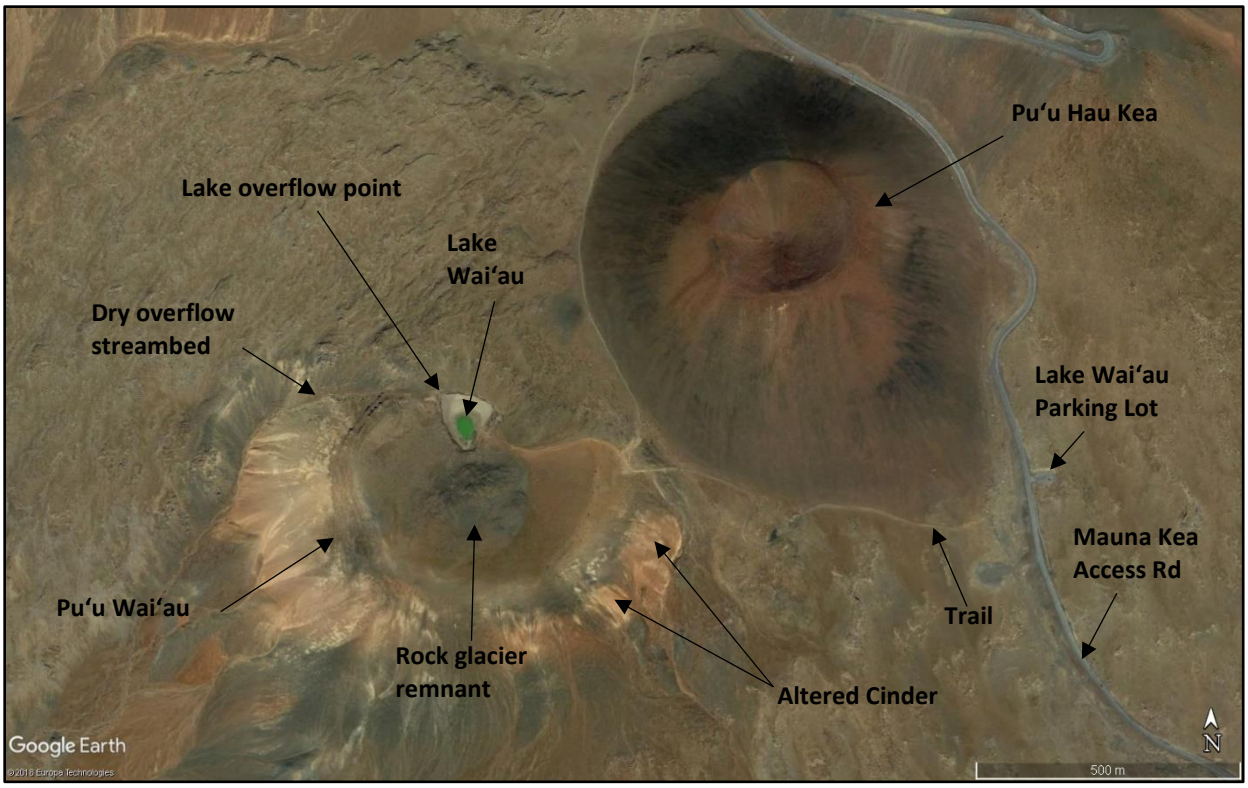


Figure D8-5: Google Earth Satellite image of the Lake Wai’au area and the various geological features.

Stop D8-75a. Mauna Kea Summit Trailhead. Data source: Hazlett and Hyndman (2007).

- **UTM 241195E, 2193670N, Trail and Summit Parking Lot.**

The 1970ft (600m) long Mauna Kea Summit Trail begins on the other side of the road from the north end of the parking area located a short distance southwest from the Gemini Telescope.

Stop D8-75b. Mauna Kea Summit. Data source: Hazlett and Hyndman (2007).

- **UTM 241474E, 2193526N (top of Puʻu Wēkiu Cinder Cone).**

Mauna Kea's summit (*see* Figure D8-6, left) is at the top of Puʻu Wēkiu Cinder Cone at 13,796ft (4205m). On a clear day Mauna Loa is south; Hualālai is southwest; Kohala is north; and in the distance past Kohala is Haleakalā, on Maui. To the north and northwest are the domes of the summit telescope complex. The westernmost 4 telescopes are shown in Figure D8-6 (right). Figure D8-7 (left) shows a happy guy, possibly feeling the effects of altitude sickness (although this may his normal). Nonetheless, he was entertaining and did act relatively normal, except for the lack of clothing at an ambient temperature of <0°C (<32°F). His warmly dressed girlfriend consented to take a photo of the seven summiteers from the 2020 field trip (D8-7, right). The field trip participants missing from the photograph did not make the climb due the altitude (that is their story, and they are sticking with it).



Figure D8-6: On the left is the snow-covered cinder cone comprising Mauna Kea's summit. 4 of the mountain's astronomical observatories, as seen from the summit, are on the right. Photo credits: A.D. MacTavish (2020).



Figure D8-7: The left photo may illustrate the effects of high-altitude judgement loss on an unidentified gentleman at Mauna Kea's summit (<0°C). The gentle slopes of Mauna Loa are in the right background. The right photo shows the seven 2020 Field Trip summiteers. Photo credits: A.D. MacTavish (2020).

3.9. Day 9: Mamaloa Highway (Hawai‘i Belt Road; Hāmākua Coast)

Between the northern end of Hilo Bay and the town of Honoka‘a, Highway 19 crosses the slopes of Mauna Kea’s extinct shield stage. These rocks are mostly Hāmākua Formation basalt flows overlain by up to 15ft (4.5m) of Laupāhoehoe Formation ash deposits erupted from vents near the summit of the volcano. This area once supported vast sugar cane fields which thrived on the chemically-weathered, red, volcanic ash soil and the high rainfall experienced on the windward side of the island.

Geologically young gulches, some quite large and deep, have eroded down through the ash into the shield-stage flows. Three major gulches are crossed by this stretch of highway.

Between Honoka‘a and Waimea the highway passes into a scenically beautiful saddle located between Mauna Kea and Kohala where there are remarkable changes in vegetation as you pass from the wet east side to the dry west side of the island. The Highway follows along the mostly alluvium-buried contact between the 2 volcanoes. Dozens of eroded and vegetated Laupāhoehoe alkalic cinder cones, erupted over the last 65,000 years, can be seen scattered over the slopes of Mauna Kea

The forested Kohala East Rift Zone lies along the horizon to the north; Mauna Kea dominates the south.

Day 9 Field trip stops on the Hāmākua Coast, Mauna Kea (*see* Figure D9-1) are:

76. Hawai‘i Tropical Botanical Gardens; accessed via the Old Mamaloa Highway, which diverts right from Highway 19 at the village of Papaikou; the diversion rejoins Highway 19 at the town of Papeeko via a left turn on Kuliamano Road and a right tun onto the highway;
77. ‘Akaka (442ft or 135m) and Hakūnā Falls (400ft or 122m);
78. Laupāhoehoe basalts;
79. Waipi’o Valley Overlook;
80. Waipi’o Valley Road and valley floor;
81. Scenic saddle between Kohala and Mauna Kea; dozens of alkalic Laupāhoehoe cinder cones.

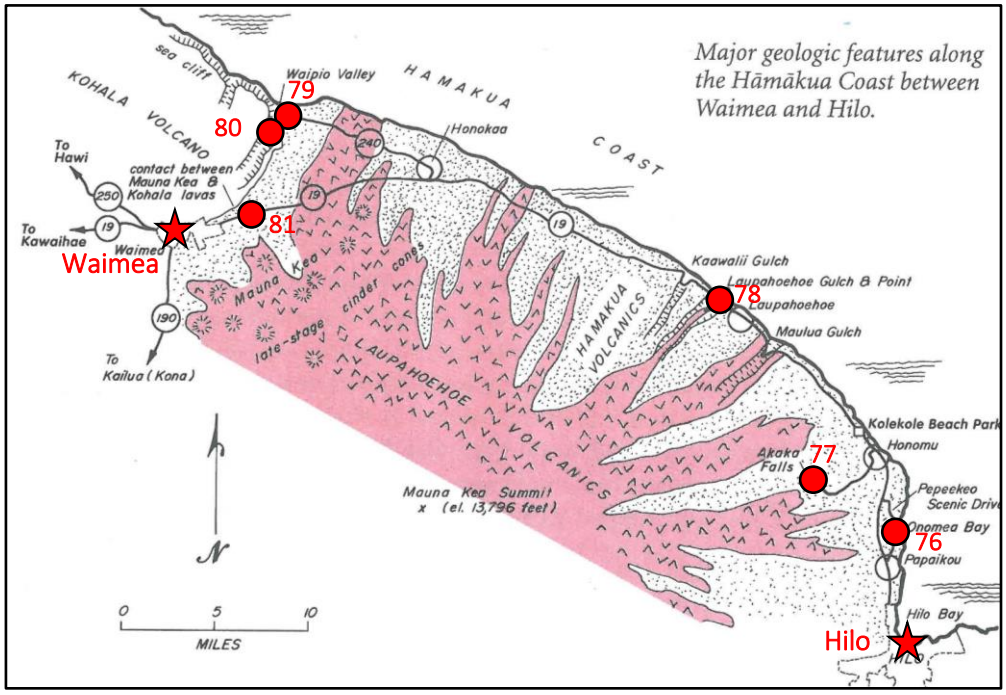


Figure D9-1: Day 9 field trip stops on Mauna Kea’s Hāmākua Coast. Figure modified after Hazlett and Hyndman (2007, p.114).

Stop D9-76. Hawaii Tropical Botanical Garden. Data source: Hawai'i Tropical Botanical Garden website (2019).

- **UTM 280430E, 2191905N; large parking lot on right (east) side of the Old Mamaloa Highway with access to the gardens; visitors must pay at the building opposite the parking lot for entry.**

The Hawaii Tropical Botanical Garden website states that the garden '*is a museum of living plants that attracts photographers, gardeners, botanists, scientists, and nature lovers from around the world'.* The garden contains over 2,000 species of tropical plants (*see* Figures D9-2 and D9-4, right) representing more than 125 families, and 750 genera. Two varieties of the orchids growing in the garden are shown in Figure D9-2. The 40-acre valley hosts a true tropical rainforest and is a natural greenhouse with fertile volcanic soil that is protected from the strong trade winds. Nature trails meander throughout the valley and provide beautiful views of waterfalls (*see* Figure D9-3) and the rugged coastline (Figure D9-4, left).



Figure D9-2: Two of the many varieties of orchids in the Hawai'i Tropical Botanical Garden. Photo credit: A.D. MacTavish (2012).



Figure D9-3: Onomea Falls, Hawai'i Tropical Botanical Garden. Photo credit: A.D. MacTavish (2012).



Figure D9-4: Twin Rocks, Onomea Bay (left photo); Giant Spider Lily (Amaryllidaceae) (right photo); Hawai'i Tropical Botanical Garden. Photo credits: A.D. MacTavish (2012).

Stop D9-77. 'Akaka Falls and Hakūnā Falls (alternate). Data sources: Hazlett and Hyndman (2007); Robinson (2010).

- **UTM 274620E, 2196745N; parking lot.**

The trail to the falls (*see* Figure D9-5) is on the southwest side of the parking lot. This is a very popular and busy spot; if there is nowhere to park along the access road within a reasonable walking distance then this stop can be skipped.

The walking roundtrip to both waterfalls takes about 30 minutes (not including the oohs and aahs). 'Akaka Falls on Kolekole Stream is the tallest single waterfall in the state of Hawai'i at 442ft (135m). Hakūnā Falls, located about 1800ft (550)m south of 'Akaka Falls, is 400ft (122m) high, but was formed on a tributary flowing into Kolekole Gulch. Both formed as water flowed over resistant Hāmākua lava flows at the head of Kolekole Gulch. The view of Hakūnā Falls from the trail is disappointing due to tree growth and can be easily skipped.

A careful look at the walls of the gorge after a rainfall will reveal a network of small falls resembling delicate shreds of lace on the cliffs.



Figure D9-5: 'Akaka Falls. Photo credit: Will Seaborn (2016), willseaborn.com website.

Stop D9-78. Laupāhoehoe Point. Hazlett and Hyndman (2007); Robinson (2010); AGI Glossary of Geology, 4th Edition (1997).

- **UTM 265625E, 2212210N; parking area; good, if somewhat windy, lunch stop**

At Laupāhoehoe Point (*see* Figure D9-6) is a late-stage Mauna Kea ʻaʻā flow of hawaiite that erupted from a vent well upslope that flowed into Laupāhoehoe Gulch and then into the sea. Hawaiite is a post-shield stage, alkaline olivine basalt midway in composition between alkali olivine basalt and mugearite and is gradational into both (AGI Glossary of Geology, 4th Edition, 1997).

This area was devastated on April 1, 1946 by a series of 6 tsunami waves, between 30 and 37ft (9 and 11m) high, that originated in the Aleutian Islands after a large megathrust earthquake. These waves destroyed a school and killed 21 students and 3 teachers. This same tsunami also struck Hilo and killed 159 people and destroyed more than 1300 homes and businesses (Tsunami Park).



Figure D9-6: Laupāhoehoe Point from the 656 to 985ft (200-300m) high cliffs located to the south (left photo). Wave-washed Laupāhoehoe hawaiite ʻaʻā flow with the cliffs of the northeastern coastline in the background (right photo). Photo credits: A.D. MacTavish (2019).

Stop D9-79. Waipiʻo Valley Overlook. Data sources: Hazlett and Hyndman (2007); Robinson (2010); Easton and Easton (1995).

- **UTM 229878E, 2226615N; parking area for viewpoint.**

The almost 1mi (1.6km) wide, ~6mi (9.6km) long Waipiʻo Valley (*see* Figure D9-7) is the largest and southernmost of 7 similar valleys that wrap around the eastern side of the extinct Kohala volcano. This valley was once 300 to 400ft (100 to 130m) deeper and was cut during the Pleistocene to a point about 360ft (110m) below present sea level (the Lualualei Stand). As continental glaciers receded on the northern continents the valley was gradually flooded by rising sea levels and is now gradually being infilled by sediment from Lālākea and Waipiʻo streams, which have created a broad valley floor with a very fertile floodplain that was once an important old Hawaiʻi population centre.

This lookout provides a spectacular view of the valley, its 1500 to 2000ft (460-610m) high northern wall, and the dark grey sandy beach. The exposed valley walls are composed of the slightly alkaline basalts of the 400,000 to 150,000yr old upper Pololū Formation which comprised the last eruptive activity of Kohala volcano.

Steep sea cliffs and deep amphitheater-headed valleys are typical of the windward coasts of the Hawaiʻian Islands.

There are several signboards near the lookout wall that provide information on the valley.



Figure D9-7: Head of the Waipiʻo Valley and beach, from the overlook to the south, with the 1500 to 2000ft (460 to 610m) high sea cliffs in the back ground. Photo credit: A.D. MacTavish (2020).

Stop D9-80. Waipiʻo Valley Road and Beach, Alternate (no formal stops). Data sources: Hazlett and Hyndman (2007); Robinson (2010).

- **UTM 228915E, 2226815N; road junction on valley floor.**

No formal stops are set for this road since there is little in the various guidebooks and the authors have not walked the road. Hazlett and Hyndman (2007) state that a walk along the road to the valley floor reveals several flows containing large, white, weathered, soft and crumbly plagioclase crystals up to 1in (2.5cm) in length (phenocrysts). Such a concentration of large crystals suggests that they accumulated near the top of a stagnant magma chamber after the main phase of shield activity had ceased.

Lālākea Stream enters the valley over 2, narrow, 300 ft (90m) high waterfalls which can be easily seen from where the road reaches the valley floor. The cobbles in the stream bed contain many large phenocrysts of black pyroxene and green olivine. The mouth of the valley acts as a tsunami funnel which raises the waves to towering heights. The 1946 tsunami that devastated Hilo and the Laupāhoehoe school was about 40ft (12m) high at the beach and swept inland over ½ a mile (800m). The right fork in the road at the valley floor leads east to Waipiʻo Valley Beach.

Stop D9-81. Saddle between Kohala and Mauna Kea Volcanoes. Data sources: Hazlett and Hyndman (2007); Robinson (2010); MacTavish (2019).

- **There are no formal stops on this stretch of highway due to a lack of safe parking areas.**

Between Honokaʻa and Waimea the Highway follows the elevated saddle and contact between the flows from Kohala and Mauna Kea. This contact is mostly buried beneath recent alluvium. Due to the funneling effect between the 2 volcanoes the velocity of the westward-blowing trade winds increases as it flows toward Waimea (known as the Venturi Effect). During the traverse from east to west the vegetation cover will change dramatically as the highway transitions from the often thickly forested (eucalyptus, swamp mahogany, cypress, iron wood pine, etc.) windward (wet) side of the island to the less-forested undulating grasslands characteristic of the leeward (dry) side of the island. Little rock is exposed along the Highway but there are some deeply-weather road cuts. As Waimea is approached the weathered and vegetated remnants of small cinder cones can sometimes be identified along both sides of the highway and on a clear day there are good views of Mauna Kea's summit.

3.10. Day 10 – Kohala Volcano – Waimea to Hāwī

Day 10 examines Kohala Volcano, which, as described previously, is an extinct volcano forming the large, ridge-shaped northern peninsula of Hawai'i. It is the oldest volcano on the island and last erupted ~100,000 years ago. Kohala was higher in the past; however, after >100,000 years of subsidence and erosion it is now 5480ft (1670m) high. It is mainly covered by Hāwī Formation alkalic cinder cones and lava flows which overlie the older, late shield stage, ~400,000yr old Pololū Formation flows.

Much of the northeastern flank of Kohala slid into the ocean somewhere between 400,000 and 150,000 years ago producing the >1500ft (460m) high cliffs that characterize the volcano's northeastern shoreline (Hazlett and Hyndman. 2007). There are innumerable streams that have yet to erode the cliffs down to sea level producing a large number of waterfalls, particularly after heavy rain.

The 10 stops planned for Day 10 examine the geological, archeological, and cultural aspects of the Kohala volcano (*see* Figure D10-1):

82. Pu'u Kawaiwai cinder cone (lava of alkalic Hawaiite composition), southern Northwest Rift Zone;
83. Scenic Overlook, Northwest Rift Zone axis, benmoreite exposure;
84. Cinder cones on the north-northwest oriented axis of the Northwest Rift Zone; driving stop;
85. View of Cinder Cones as well as Haleakala Volcano located on the Island of Maui;
86. Pololu Valley Lookout;
87. Residual coastal boulders;
88. Mo'okini Luakini Heiau and Kapakai Kokoiki (King Kamehameha birthplace);
89. Lapakahi State Park, ruins;
90. Mugearite flow, Hawi Volcanics; pseudodykes in colluvium

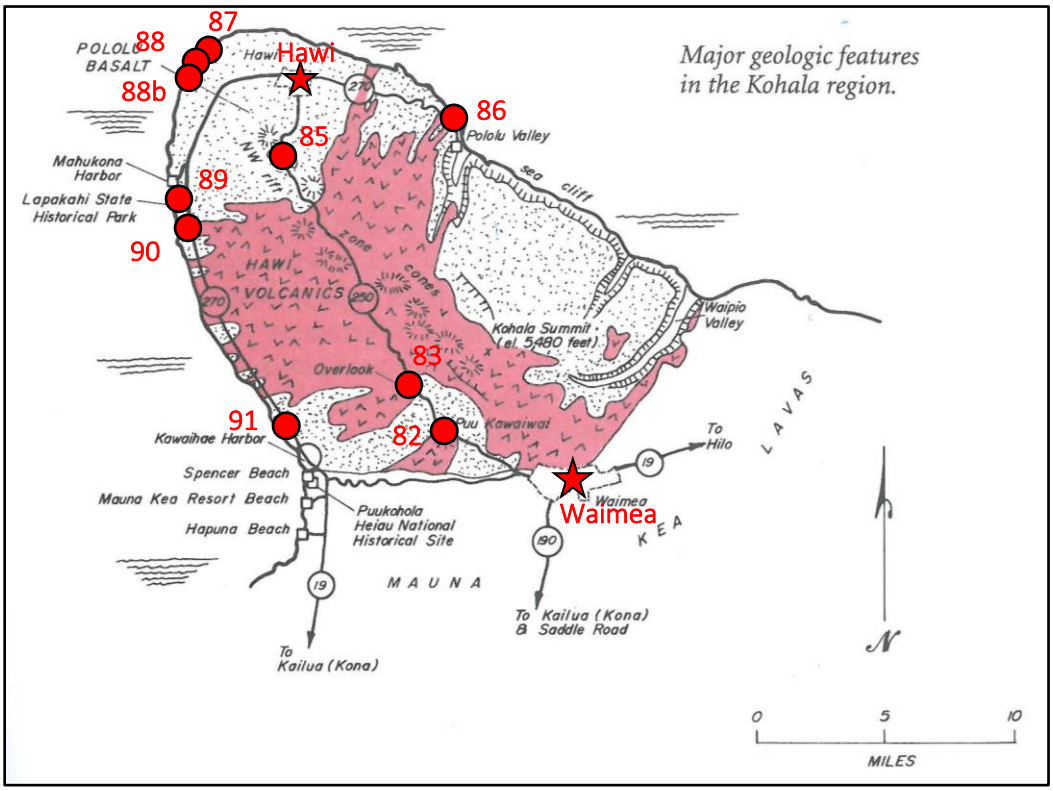


Figure D10-1: Day 10 field stops on Kohala Volcano. Figure modified after Hazlett and Hyndman (2007, p.111).

Stop D9-82. Pu‘u Kawaiwai Cinder Cone. Data source: Hazlett and Hyndman (2007).

- **UTM 214165E, 2218875N; parking area is a pull-out on the left (west) side of Highway.**

A gated road leads into the Pu‘u Kawaiwai hawaiite cinder cone (*see* Figure 10-2); if the owners are not present the walk can be made into the quarry, otherwise it can easily be viewed from a distance.

In the quarry wall nearest the road (Figure 10-2, right) the structure of the cone as it grew is visible with crossbedding, erosional unconformities, and large blocks scattered throughout. The cone’s crater was filled with spatter and cinder when the eruption shifted to 3 other vents further downslope.

Good views of Mauna Kea (*see* Figure 10-3), Mauna Loa, and the Kona coast of Hualālai are possible from the scenic lookout on a clear day.



Figure D10-2: The left photo shows Pu‘u Kawaiwai Cinder Cone from Highway 19. The right photo is a close-up of the quarry excavated into the northeastern flank of the cinder cone. Photo credits: A.D. MacTavish (2019)



Figure D10-3: The northern flank of Mauna Kea seen from the Stop D9-77 parking area located on the southwestern flank of Kohala. Photo credit: A.D. MacTavish (2019).

Stop D9-83. Scenic Lookout, Benmoreite Lava. Data sources: Hazlett and Hyndman (2007); AGI Glossary of Geology (1997).

- **UTM 211338E, 2221675N; overlook parking area.**

Medium-grey benmoreite of the Hawi Volcanics (*see* Figure 10-4) comprise the rock-cuts across from, and to the north of the parking area. These rocks were erupted upslope from near the Puʻu Loa Cinder Cone about 140,000 years ago. The hillsides around this location host numerous clusters of cacti.

Benmoreite is a rare, unusual alkalic rock which at this locality consists of black plagioclase- and amphibole-porphyritic flows and chaotic mass-flow deposits, possibly lahars (Figure 10-4). Amphibole phenocrysts are rarely observed within Hawaiʻian lava and the ones here exhibit brown haloes. The AGI Glossary of Geology (1997) describes benmoreite as a silica-saturated to silica-undersaturated igneous rock intermediate between mugearite and trachyte in composition with a differentiation index of between 65 and 75 and with K_2O:Na_2O <1:2.



Figure D10-4: Closeup of the benmoreite mass flow deposit (lahar?) located north of the field stop parking area. Photo credit: A.D. MacTavish (2019).

Stop D9-84. Cinder cones along the Highway. Data source: MacTavish (2019).

- **UTM 207115E, 2229755N; no suitable road stops available, view from vehicle**

Along this stretch of highway south of the town of Hawi, where there are fewer trees bordering the road, can be seen a series of vegetated cinder cones that erupted along a north-northwest-oriented Kohala Northwest Rift Zone axis.

Stop D10-85. Cinder cones and Hāleakala Volcano. Data source: MacTavish (2019).

- **UTM 204798E, 2233056N; park on widened area on right (east) side of highway.**

This is one of few the places along this highway where vehicles can safely stop to view old Kohala cinder cones located to the south (*see* Figure D10-5, left). On a clear day this is also a good location to view Hāleakala Volcano on the Island of Maui which is located to the northwest (*see* Figure D10-5, right). This stop can be skipped if the weather is not clear enough to view Hāleakala on Maui.



Figure D10-5: The left photo shows a vegetated Kohala cinder cone. Hāleakala Volcano on the Island of Maui can be seen in the distance in the right photo. Photo credits: A.D. MacTavish (2019).

Stop D10-86. Pololū Valley Scenic Lookout and trail. Data source: Hazlett and Hyndman (2007); Love Big Island website; Big Island Hikes website.

- **UTM 214210E, 2236565N; parking area and trailhead.**

This busy spot provides a good view of the scenic Pololū Valley and the associated coastline (*see* Figure D10-6). This valley is the northernmost of 7 large erosional valleys (gulches) located along the eastern coastline of Kohala. It is a large, flat-floored, amphitheatre-headed valley, like Waipi'o Valley, and during the last ice age it was much deeper. The valley head, ~4mi (6.4km) inland (*see* Figure D10-6, right), is filled with a mugearite flow that flowed over fault scarps ~140,000 years ago. This spot provides good views of Kohala's northeastern coastal cliffs (Figure D10-6, left), which are the headwall of a massive slide that carried debris into the Hawaiian Deep located 75mi (120km) away. In April 1946 a tsunami devastated the valley. The initial wave was 55ft (16.7m) high at the beach when it hit.

The short, but steep, slippery when wet, 0.5mi (1km) long Pololū Trail (or Āwini Trail) switchbacks from the overlook down to the valley floor and a black sand beach. There is an elevation change of 490ft (150m) and the hike takes ~20-25min. The boulder strewn black sand beach is backed by lush tropical forest and is flanked by ~500ft (150m) cliffs. This segment of the Pololū Trail is apparently the first part of an extended trail that leads southeast to the Honokane Nui valley, but there is little information available on the extension. Only the beach is public land, the rest of the valley is privately-owned



Figure D10-6: On the left is the northeastern coastline of Kohala near the Pololū Valley Scenic Lookout. On the right is the head of the Pololū Valley located south of the Scenic Lookout. Photo credits: A.D. MacTavish (2019).

Stop D9-87. Residual Boulders. Data source: MacTavish (2019).

- **UTM 200345E, 2243410N, parking a short distance upslope from exposure.**

At this location are a large number of alkali basalt boulders resting on the surface of a highly-weathered alkalic basalt. These boulders were not formed by beach wave action and are certainly not erratic glacial boulders (*see* Figure D10-7). By looking closely, it can be easily seen that these are residual boulders remaining after fracture surfaces within the original flows were deeply weathered in the moist tropical Hawai‘ian environment. This produced a saprolite that was then eroded away (*see* Figure D10-8). At this location the saprolite process is incomplete with the softer saprolitized rock weathering away to leave the relatively less-altered rock core intact. The weathering here consisted of a combination of rainwater, wind, and possibly the occasional high wave. What remains are many rounded surface boulders and numerous partially exposed boulders within variably-weathered saprolite.



Figure D10-7: Coastline residual boulders at field trip Stop D9-87 located at the northern tip of the island. Photo credit: A.D. MacTavish (2019).



Figure D10-8: Residual boulders eroded out of saprolitized alkalic basalt flows. Note that many of the boulders remain imbedded within the strongly weathered flow in the photo on the right. Photo credits: A.D. MacTavish (2019).

Stop D10-88a. Mo‘okini Luakini Heiau, Kohala Historic Sites Monument. Data source: NPS Website.

- **UTM 199455E, 2242575N; drive east from Stop D10-87; park and walk to site if road too wet.**

Mo‘okini Luakini Heiau (*see* Figure D10-9, left) is one of the oldest and most sacred ‘*heiau’* (places of worship) in the Hawai‘ian Islands and is considered a living spiritual temple. The ancient Hawai‘ians had many types of *heiau*, each with their own distinct function and use. *Heiau* ranged in size from single upright stones to massive, complex structures. Larger *heiau* were built by *ali'i* (chiefs), but the largest and most complex *luakini heiau* (sacrificial temples), could only be constructed and dedicated by an *ali'i 'ai moku*. *Luakini heiau* were reserved for human or animal sacrifice rituals and were usually dedicated to the war god *Ku*. Rituals performed at these sites highlighted the *ali'i 'ai moku's* spiritual, economic, political, and social control over his lands and his authority over the life and death of his people.

Mo'okini Heiau was a *luakini heiau* built in the shape of a parallelogram: the west wall is 267ft (81.3m) long, the east wall 250ft (76.2m), the north wall 135ft (41.1m), and the south wall 112ft (34.1m). Tapered, dry-stacked, mortarless stone walls that are 10ft (3m) wide at their base and between 7 and 14ft (2.1-4.3m) high enclose the *heiau*. Oral tradition says the rocks forming the walls were passed hand to hand along a line of thousands of men from the Niuli'i area 10mi (16km) to the east. Inside the northern end of the *heiau* is a large stone platform with smaller platforms scattered throughout the site that once supported thatched temple buildings. Outside, on the north side, is *Papa-nui-o-leka*, a stone on which human flesh was separated from bones after ritual sacrifice (*see* Figure 10-9, right). According to tradition, Mo'okini Heiau was the primary place of worship of the northern part of the Island. The site was active through the early part of the 19th century and was the war temple of King Kamehameha I, housing the war god of his family, ‘*Ku-ka-'ili-moku*’, before the transfer of the god to Kamehameha's new war temple, ‘Pu'ukohola Heiau’, located 21mi (33km) south near Kawaihae. Kamehameha’s son and heir Liholiho also used Mo'okini Heiau. In 1819, after his father's death, Liholiho ended kapu and abolished that part of the Hawaiian religion that depended on *heiau*. In spite of royal orders that they be destroyed, Mo'okini and several other large *heiau* were spared.

In 1978, ‘*Kahuna Nui*’ (High Priestess) Leimomi Mo‘okini Lum lifted the *kapu* (taboo) forbidding anyone but *ali'i* and *kahuna* from entering Mo'okini Heiau and also rededicated the *heiau* to the children of the land. In 1994, she again rededicated the *heiau*, this time to the children of the world. Visitors to the site often bring a flower or a *lei* to leave at the *heiau* as an offering of respect.



Figure D10-9: The left photo shows the ruins of Mo‘okini Luakini Heiau from the east. The flat-topped stone, shown in the right photo, is thought to be a where humans were ceremonially sacrificed and then skinned. Photo credits: A.D. MacTavish (2020).

Stop D10-88b. Kapakai Kokoiki, King Kamehameha I Birthplace. Data source: NPS Website.

- **UTM 198805E, 2242410N; alternate stop.**

Approximately 2,000ft (610m) south of Mo'okini Heiau, is Kapakai Kokoiki (Royal Housing Complex) and the birthplace of King Kamehameha I (*see* Figure D10-10). It was typical for the housing complex of an *ali'i 'ai moku* to be near, and associated with, a *luakini heiau*. This is one of the few places in the Hawai‘ian Islands where historians know the exact location of a housing complex and its associated *heiau*. Over the centuries Kapakai served as the residence of *ali'i 'ai moku* when ceremonies were conducted in Mo'okini Heiau. Religious ceremonies lasted several days and nights and during this time, *ali'i 'ai moku* and high priests would leave the *heiau* for short periods to return to Kapakai. Kamehameha I was born in the Kapakai Royal Housing Complex and later stayed there while conducting ceremonies in Mo'okini Heiau.



Figure D10-10: Western wall of Kapakai Kokoiki. Photo credit: Donnie B. MacGowan, lovebigIsland.com website

Stop D10-89. Lapakahi State Park (Old Hawaiian Village Ruins). Data source: bigislandhikes.com.

- **UTM 197345E, 2233475N; park entrance; turn right (west) from Highway 270 to access road.**
- **UTM 187140E, 2233525N; small parking area in front of small park building and picnic area.**

Lapakahi State Historical Park is a large area of ruins from an ancient Hawaiian village (*see* Figures D10-11 and -12). The area offshore from the ruins is now a Marine Life Conservation District.

Lapa kahi means "single ridge" and refers to the ancient ahupua'a (land subdivision) that existed here some 600yrs ago. The village was a place of maka‘āinana where fisherman and farmers lived and worked together. The farmers grew kalo (taro) and ‘uala (sweet potato).

There are many kinds of ancient structures and artifacts to be viewed along the short, easy 1mi (1.6km) hike, including individual houses, large residential complexes, canoe storage houses, salt-making pans, kukui nut lampstands, and even a few kōnane games. Walk the trail through the village in a clockwise direction after taking a guide pamphlet from the building at the edge of the parking lot. The guide will describe what you are seeing at the various numbered stops. This trail takes 45-60min to complete.



Figure D10-11: The left photo shows the southwestern portion of the ancient village. The right photo looks north along the northwestern coastline of the island from the southwestern end of the village. Photo credits: A.D. MacTavish (2019).



Figure D10-12: The NPS Marker 8 in the left photo denotes a hollow stone used to make salt from sea water. The white stones are bleached coral. The right photo shows a stone 'board' used to play the game of Kōnane, which is similar to checkers. Photo credits: A.D. MacTavish (2019).

Stop D10-90. Mugearite Flow, Hawi Volcanics. Data sources: Hazlett and Hyndman (2007); AGI Glossary of Geology (1997); MacTavish (2019).

- **UTM 197488E, 2232149; park on gravel road on right side of highway about 260ft (80m) north of field stop.**
- **UTM 197520E, 2232065N; field stop, on east side of highway.**

This low outcrop is composed of vesicular, plagioclase feldspar-porphyritic mugearite which also seems to contain reddish to greenish grains which could be olivine partially altered to iddingsite.

The AGI Glossary of Geology (1997) describes mugearite as an extrusive or hypabyssal alkaline igneous rock consisting of oligoclase with subordinate alkali feldspar and mafic minerals, often with olivine more abundant that clinopyroxene. Although generally nepheline-normative the rock may contain normative hypersthene, or even quartz and will exhibit a 45-65 differentiation index with normative plagioclase more sodic than An_{30}.

Stop D10-91: Pseudodykes in colluvium (alternate). Data source: Easton and Easton (1995); AGI Glossary of Geology (1997).

- **UTM 202825E, 2219965N; parking on gravel road, right (west) side of highway, ~395ft (120m) north of outcrop.**
- **UTM 202890E, 2219855N; outcrop.**

This large highway road cut provides a good view of an outcrop consisting mainly of colluvium overlain by an ʻaʻā flow. Colluvium is defined by the AGI Glossary as any loose, heterogeneous, and incoherent mass of soil and/or rock fragments deposited by rain-wash, sheetwash or slow, continuous downslope creep at or near the base of slopes or hills. What makes this outcrop interesting are the at least 5 pseudodykes developed in the colluvium on the seaward (west) side of the highway (*see* Figure D10-13).

The authors have been unable to find a satisfactory or consistent definition in the literature of the Easton and Easton (1995) 'pseudo-dykes'. Most suggest that the 'pseudodykes' are not intrusive, but are similar to clastic dykes seen in purely sedimentary environments. What do you think?

Safety Warning: This is a very busy highway. Stay well to the right while walking south along the paved shoulder from the vehicles and while viewing the pseudodykes at the field stop. It is preferrable to view the pseudodykes from across the highway from the road cut that hosts them, so take considerable care when crossing the road.



Figure D10-13: Colluvium outcrop with 3 of the 5 pseudodykes highlighted. Photo credit: Google Earth.

3.11. Day 11 – Waimea to Kailua-Kona

Most of Day 11 (the final day of the field trip) will be examining the rocks of Hualālai Volcano.

The stops planned for Day 11 are (*see* Figure D11-2):

92. Mauna Kea western rift zone cinder cone field
93. Hāpuna beach; basaltic ankaramite lava with pyroxene and olivine phenocrysts
94. Hualālai and 1859 Mauna Loa flows contact
95. Hualālai trachyte flows with large Puʻu Waʻawaʻa trachytic cinder/pumice cone to the southeast; and
96. Scenic Lookout; Kaʻūpūlehu Flow, Hualālai Northwest Rift Zone; alkalic basalt (1801-1802, from last known eruption), mafic/ultramafic intrusive xenoliths; cinder cones along rift to summit.

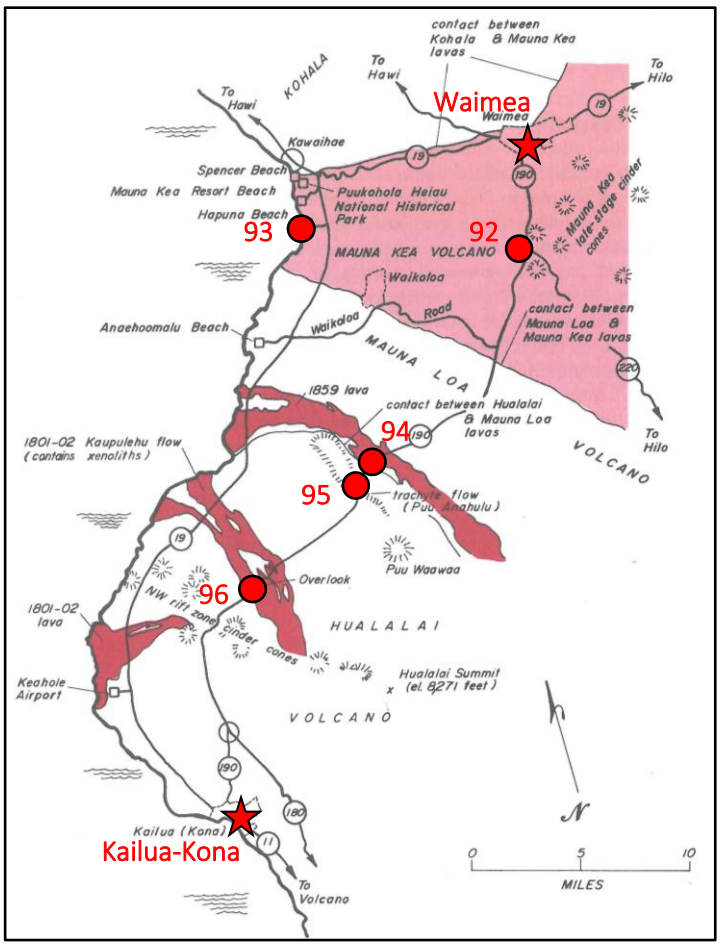


Figure D11-2: Location of Day 11 field trip stops. Figure modified from Hazlett and Hyndman (2007, p.106).

Stop D11-92. Mauna Kea Western Rift Zone cinder cone field. Data source: MacTavish (2019).

- **UTM 218840E, 2206290; widened gravel shoulder on right side of Highway 200, about 1300ft (400m) past the junction with Highway 190.**

This location provides a good view of a large, vegetated, breached cinder cone (*see* Figure D11-3) and other, generally smaller cones associated with the Mauna Kea Western Rift Zone Cinder Cone Field.

The only turn-around spot about is ~4600ft (1400m) southeast along Highway 200 on the right where a gated road leads into the large cinder cone. After turning around drive back to Highway 190 and turn right. Drive to the junction with Highway 19 in Waimea and turn west on Highway 19 and drive to the Hapuna Beach access road near the western coastline of the island.



Figure D11-3: Breached and vegetated cinder cone associated with the Mauna Kea Western Rift Zone Cinder Cone Field. Photo credit: A.D. MacTavish (2019).

Stop D11-93. Ankaramite Lava, Hapuna Beach State Park. Data source: Hazlett and Hyndman (2007); AGI Glossary of Geology (1997); MacTavish (2019).

- **UTM 204450E, 2212930N; parking lot.**
- **UTM 204310E, 2213195N; take access walkway from parking lot to beach then walk north along beach to the outcrop on the east side of the beach at this location.**

Near the north end of the beach, just before it passes into the resort area to the north, are rock ledges composed of the rare basaltic lava ankaramite (*see* Figure D11-4). The AGI Glossary of Geology (1997) describes ankaramite as an olivine-bearing basanite containing numerous olivine and pyroxene phenocrysts.

At this location the flow forms an irregular steep-sided ledge composed of a dark grey, thick, variably vesicular massive flow overlain by a well-developed and defined blocky ʻaʻā flowtop. A close look at the base of the flow top shows blocks that are still partially connected to the underlying mass of the flow. A closer look shows that the flow contains numerous green, to yellowish-green olivine crystals and glomerocrysts and fewer black pyroxene grains, which are often associated with the olivine grains.



Figure D11-4: The left photo shows the ankaramite outcrop at Hapuna Beach. The right photo is a closeup of the flow-top breccia at the top of the massive ankaramite flow. Photo credits: A.D. MacTavish (2019).

Stop D11-94. 1859 Mauna Loa ʻaʻā flow. Data source: Hazlett and Hyndman (2007).

- **UTM 204505E, 2104910N; parking in gravel lot on right side of highway.**

This partially vegetated 1859 Mauna Loa ʻaʻā flow (*see* Figure D11-5) is the youngest Mauna Loa flow on this side of the island and it overlies older Hualālai flows.



Figure D11-5: Partially vegetated 1859 Mauna Loa ʻaʻā flow. Photo credit: A.D. MacTavish (2019).

Stop D11-95. Puʻu Waʻawaʻa Cinder Cone State Park. Data source: Puʻu Waʻawaʻa Ahupuaʻaʻ Ōhiʻa Cone Trail System Visitor Guide; AllTrails website.

- **UTM 202159E, 2192490N; automatic entrance gate; drive through gate and along road to the left to an information kiosk.**

Stop D11-95a. Information Kiosk.

- **UTM 202255E, 2192375N; information kiosk with parking.**

Puʻu Waʻawaʻa Cinder Cone (*see* Figure D11-6) is a large trachyte cinder and pumice cone that erupted from Hualālai about 100,000 years ago producing a set of thick trachyte flows. It is considered the largest cinder cone on the island and the oldest feature on Hualālai Volcano. Cone Trail guides and maps are available at the kiosk.

The sharp curve on the highway just before the turnoff to the cone curves around exposed expressions of the trachyte flows and underlies most of the town of Puʻuanahulu and the golf course at the Big Island Country Club.

Stop D11-95b, Puʻu Waʻawaʻa Cinder Cone Trail (Alternate).

- **UTM 202965E, 2188455N, Summit**

The popular, moderate difficulty, 6.5mi (10.5km) long Puʻu Waʻawaʻa Cinder Cone Trail takes ~4hrs to complete and leads to the summit of Puʻu Waʻawaʻa at 3967ft (1209m). The summit peak provides an excellent view of the surrounding area to the sea and along the coast. Along the hike there is also a chance to see the native Hawaiʻian owl known as pueo and the native hawk known as ʻio. The cone once hosted an obsidian mine and is still part of a working ranch.



Figure D11-6: Puʻu Waʻawaʻa Cinder and Pumice Cone. Photo credit: A.D. MacTavish (2019).

Stop D11-96. Kaʻūpūlehu Flow, Hualālai 1801 to 1802 Alkalic Lava Flow. Data source: Hazlett and Hyndman (2007).

- **UTM 192870E, 2188715E; scenic lookout at widened highway shoulder just before the bridge that spans part of the flow. Please be very careful of traffic on the highway at this stop.**

This stop overlooks the partially vegetated alkalic Kaʻūpūlehu Flow field from the last known Hualālai eruption that took place in 1801 and 1802 (*see* Figure D11-7, left). These flows emanated from the Northwest Rift Zone located upslope to the southeast and contain a large number of dunite, gabbro, and peridotite xenoliths which will look like angular dark to light green chunks within the dark grey lava.

This ~0.9mi (1.5km) wide flow field consists of both pahoehoe and ʻaʻā flows, several well-developed surface flow channels, and some partially collapsed lava tubes (*see* Figure D11-7, right)



Figure D11-7: The left photo shows the partially vegetated 1800 to 1801 Hualālai Kaʻūpūlehu alkaline lava flow field that heads downslope to the sea. The right photo shows a partially collapsed lava tube (skylight?) in the 1800-1801 flow field. Photo credits: A.D. MacTavish (2019).

Safety Note: This a narrow pull-out along a very busy road, so be very careful of highway traffic.

THIS IS THE FINAL STOP OF THE FIELD TRIP.

4. Glossary of Volcanic Terms; (© G. J. Hudak, NRRI University of Minnesota, 2020)

'A'ā lava: A Hawaiian term for lava that has a rough, jagged, spiny, and often clinkery surface. In thick aa flows, the surface comprises rubble composed of loose, rough lapilli and blocks that generally hides a thick, more massive flow interior (Tilling et al., 1987). The thickness of the surface crust of aa lavas is controlled by cooling (Kilburn, 2000, p. 291).

Active volcano: A volcano that is currently erupting, one that has erupted during recorded history, or one that has erupted during recorded history and is likely to erupt again (Foxworthy and Hill, 1982).

Accessory fragment: A lithic fragment composed of country rock that has been explosively ejected during an eruption (Cas and Wright, 1987, p. 54). Accessory fragments within pyroclastic deposits may be difficult to distinguish from accidental fragments. In general terms, referred to as a xenolith.

Accidental fragment: A clast picked up locally by pyroclastic flows and surges (Cas and Wright, 1987, p. 54). Accidental fragments may be difficult to distinguish from accessory fragments. In general terms, referred to as a xenolith.

Accretionary lapilli: Spherical aggregates (commonly with a concentric structure) formed by the accretion of moist ash in eruption clouds (White and Houghton, 2000, p. 495). Also used for all ash aggregates, including mud lumps (Houghton et al., 2000, p. 513).

Achnelith: A type of juvenile fragment characterized by smooth, glassy moulded surfaces formed from lava spray from extremely fluid mafic eruptions (Walker and Croasdale, 1972).

Agglomerate: A course, pyroclastic deposit composed of a large proportion of *fluidal-shaped volcanic bombs* that are formed, in the strictest sense, by a fall deposit in the immediate vicinity of a volcanic vent. It is best applied to describe bomb and scoria deposits that build strombolian cones, and should never be used as a non-generic term for a "volcanic breccia" (Cas and Wright, 1987, p. 359). A key component of identifying an agglomerate is that many bombs will plastically deform and will become agglutinated.

Agglutinated: Melted together to form a single solid mass upon cooling (Hazlett and Hyndman, 1996).

Aerosol: Fine liquid or solid particles suspended in the atmosphere. Aerosols composed of tiny droplets of sulfuric acid are commonly formed during explosive volcanic eruptions.

Airfall: Volcanic ash that has fallen through the air from an eruption cloud. Airfall deposits are characteristically well-sorted and well-layered, and typically exhibit mantle bedding (Foxworthy and Hill, 1982; Cas and Wright, 1987).

Alkalis: The elements potassium and sodium (Hazlett and Hyndman, 1996).

Alkalic Basalt: Basalt-like rock compositions that are enriched in the alkali element sodium. Examples include nephelinites, hawaiites, and ankaramites (Hazlet and Hyndman, 1996).

Alteration (see Hydrothermal Alteration).

Alteration mineral assemblages: Mineral assemblages found in rocks that result from chemical reactions between the original rock and an agent of alteration (for example, hot volcanic vapors or hydrothermal fluids).

Amygdaloidal: A volcanic texture comprising vesicles (rounded holes resulting when magma cools around gas bubbles) which have been subsequently filled by secondary minerals.

Amygdule: An individual vesicle which has been subsequently filled-in by secondary minerals.

Andesite: A grey to grey-green colored volcanic rock containing 53% to 63% silica (compositionally between basalt and dacite). Minerals commonly found in andesite include intermediate composition plagioclase and hornblende.

Andesite magma: A magma with a chemical composition ranging from 53% to 63% which, upon crystallization, forms an andesite.

Ankaramite: An alkalic basalt containing many large, black pyroxene crystals and a lesser number of green olivine crystals (Hazlett and Hyndman, 1996).

Armoured lapilli: A type of accretionary lapilli composed of a crystal, pumice, or lithic fragment core which is surrounded by a rim of fine to coarse ash (McPhie et al., 1993, p. 29).

Ash: A textural term for volcanic fragments less than 2mm in diameter (Fisher, 1966; Schmid, 1981). Ash is a common product of explosive volcanic eruptions.

Ash cloud: A cloud of ash produced during pyroclastic eruptions (Miller, 1989). These clouds can result from rapid rising of the hot, buoyant ash-rich eruptive plume, or can be derived by elutriation at the top of a pyroclastic flow (Cas and Wright, 1987).

Ash Cone: A low, broad volcanic cone enclosing a wide, shallow crater (Hazlett and Hyndman, 1996).

Ash flow: A type of pyroclastic flow comprising dominantly ash-sized particles. Hot ash flows may be called "glowing avalanches" or "nuee ardentes", and if their volume is large enough, may eventually form deposits known as welded tuffs. These types of flows are extremely dangerous and historically have killed hundreds of thousands of people.

Asthenosphere: A zone of soft, nearly molten rock within the earth's upper mantle. The tectonic plates of the earth ride on top of the asthenosphere (Hazlett and Hyndman, 1996).

Atmospheric shock wave: A strong compressional shock wave caused by a combination of volcanic ejecta and sonic waves.

Avalanche: A large mass of material or mixtures of materials (e.g., snow, ice, rock, soil, etc.) that is falling or sliding rapidly due to the force of gravity. Debris avalanches are avalanches composed of a mixture of earth materials (Foxworthy and Hill, 1982).

Ballistic fragment: An explosively ejected rock fragment that follows a ballistic (arced) trajectory.

Basalt: A dark colored (usually dark grey, dark green, or black), low silica content (45% to 53% SiO_2) volcanic rock. Minerals commonly found in basalt include intermediate to calcium-rich plagioclase, pyroxene, and commonly olivine. Accessory minerals commonly include ilmenite and magnetite.

Basaltic magma: A low viscosity, low silica (45% to 53% silica) magma that, upon crystallization, forms the volcanic rock basalt.

Basanite: A variety of basalt that contains small crystals of plagioclase and pale gray nepheline (Hazlett and Hyndman, 1996).

Base surge: A turbulent, low-density cloud of rock debris, water, and/or steam that moves over the ground surface at extremely high speeds. Base surges are commonly the result of directed volcanic explosions. Base surge deposits are commonly composed of cross-bedded deposits comprising ash and lapilli.

Bimodal: A term used to describe a material composed of two distinctly compositionally and/or texturally different components. Commonly used to describe volcanic terrains that have nearly equal proportions of felsic and mafic volcanic rocks.

Blocks: Fragments of solid rock greater than 64 millimeters in diameter that are ejected during volcanic eruptions. Blocks are commonly composed of accessory fragments made up of crystallized magma associated with the eruption (e.g., pieces of a lava dome).

Blocky lava: Lava flows that are characterized by highly fractured surfaces which contain fragments of debris (usually flow fragments) up to several meters in diameter. The size of the surface fragments in blocky lavas is controlled by the rheology of the lava in the interior of the flow (Kilburn, 2000, p. 291).

Boiling lake: A lake which has a temperature of nearly 100°C. Examples include the "Boiling Lake" on Dominica and a lake of mud on Saint Lucia (Bardintzeff and McBirney, 2000, p. 159).

Bombs: Juvenile fragments of semi-solid or plastic magma ejected during a volcanic eruption. Based on their shapes after they hit the ground and cool, bombs are given various textural names including breadcrust bombs, cow-dung (cow pie) bombs, spindle bombs (fusiform bombs) and ribbon bombs.

Bomb Sag: A depression in an ash layer made by the impact from a fragment deposited in the ash (Hazlett and Hyndman, 1996)

Caldera: Large, circular to elongate, volcanic collapse depressions that form from the rapid extrusion of magma form a shallow subterranean magma chamber. In general, the diameter of a caldera is much greater than any of its individual volcanic vents (Williams and McBirney, 1979, p. 207).

Caldera cycle: A commonly observed evolutionary sequence recognized in many caldera complexes. From oldest to youngest, the seven stages of the caldera cycle are: 1) regional tumescence and generation of ring fractures; 2) ignimbrite (pyroclastic) eruption(s); 3) caldera collapse; 4) pre-resurgent volcanism and intra-caldera sedimentation; 5) resurgent doming; 6) major ring fracture volcanism; and 7) terminal fumarolic and/or hot spring activity.

Cinders: A term to describe generally highly vesicular, mafic lava lapilli.

Cinder cone: A small, generally conical-shaped volcano formed by accumulation of ejected cinders and other volcanic debris that falls back to the earth close (proximal) to the location of the volcanic vent (Gardner et al., 1995).

Clay (minerals): A group of aluminum-bearing hydrous phyllosilicate minerals (for example, kaolinite).

Clay (textural): A sedimentary grain size classification for particles less than 1/256 mm in diameter, regardless of mineralogy.

Cognate lithic fragment: Non-vesiculated juvenile magmatic fragments that have silicified from the erupting magma (Cas and Wright, 1987, p. 54).

Columnar jointing: A type of fracture pattern resulting from the thermal contraction of hot volcanic rocks after their crystallization which commonly is expressed in elongate, pentagonal or hexagonal columns oriented perpendicular to the cooling surface. Columnar jointing is common in all compositions of lava flows, although it is generally best developed in mafic (basalt) lava flows and in felsic welded tuffs.

Composite volcano: A generally steep sided volcano composed of a mixture of lava flows, pyroclastic deposits, and volcaniclastic sedimentary deposits. Composite volcanoes commonly have increasing slopes toward their summits since they generally have mainly lava flows and sedimentary deposits near their base and pyroclastic (tephra) deposits near their summits.

Conduit: The underground passage or passages through which magma makes it way to the earth's surface.

Cooling unit: A group of hot pyroclastic deposits (ignimbrites) that cools at more or less the same time. A deposit from a single eruption that shows simple variations in the degree of welding is known as a *simple cooling unit*. When many ignimbrites occur over an extremely short period of time, each individual ignimbrite may be deposited, and start to weld over a previous deposit or group of deposits that are cooling and undergoing welding. The resulting deposits have several zones of partial and dense welding, and since they more or less cool together, are known as *compound cooling units* (Cas and Wright, 1987, p. 253-255).

Coulée: A type of rhyolite lava flow that forms when lava issues from one side of a volcanic vent and produces a lava flow which is elongate in plan-view (Cas and Wright, 1987, p. 81).

Crater: A steep sided, usually bowl or funnel shaped depression that commonly occurs at the top of a volcanic cone, and is often a vent for eruptions (Lipman, 2000, p. 643). Volcanic craters may be formed by either explosion or collapse in the vicinity of the volcanic vent.

Crossbeds: Layers within sedimentary and/or volcaniclastic rocks that are inclined relative to the major bedding structures within the unit.

Curie point: The temperature at which a body loses (by heating) or preserves (by cooling) its permanent magnetization. As rocks cool, the electromagnetic field aligns magnetic minerals in the magma, and their orientation is preserved as the rocks cool below the Curie point.

Dacite: A generally light-colored, relatively silica rich (65% to 68 % SiO_2) volcanic rock (extrusive equivalent of a quartz diorite or a tonalite). Dacitic magmas have a relatively high viscosity, and their associated volcanic eruptions may produce thick, muffin-shaped lava flows (lava domes) or, commonly, may be explosive and produce abundant tephra resulting in ash falls, ash flows, and surges. Dacites typically contain intermediate plagioclase (andesine or oligoclase) and quartz (>10%) with pyroxene and/or hornblende with minor biotite and/or sanidine (volcanic K-feldspar).

Debris flow: A type of mass flow comprising a dense, cohesive, flowing mixture of sediment (mud through boulder sized materials, generally >50% by volume), water, and commonly, organic debris. Debris flows generally move downslope in laminar fashion due to the force of gravity (Vallance, 2000, p. 601; Carey, 2000, p. 627). Debris flows generated at volcanoes are commonly referred to as *lahars*.

Decompressive melting: Melting that occurs when rocks undergo a decrease in pressure. This commonly occurs in the vicinity of hot spots as mantle rocks rise to shallower levels in the earth due to convective rise and upwelling (Sigurdsson, 2000, p. 15). Melting occurs as a result of decreasing pressure, not increasing temperature.

Deposit: Earth materials that have accumulated by some natural process (Gardner et al., 1995). Deposits may be the result of volcanic (e.g., lavas or pyroclastic), sedimentary (either clastic or chemical), or hydrothermal (precipitation) processes.

Devitrification: The solid-state transformation of volcanic glass into crystalline materials (AGI, 1976, p. 117). Devitrification tends to be more prevalent in densely-welded tuffs, but may also occur in less densely-welded or unwelded pyroclastic and/or volcaniclastic deposits. The main products of devitrification are cristobalite (SiO_2) and alkali feldspar ($KAlSi_3O_8$) (Cas and Wright, 1987, p. 258).

Diatreme: A funnel-shaped, pipe-like volcanic conduit, usually filled with volcaniclastic debris, emplaced by the explosive energy of gas-charged magmas. Diatremes are believed to result from hydrovolcanic fragmentation and subsequent wall rock collapse (Vespermann and Schminke, 2000, p. 683), and may reach depths up to 2500 meters. Diamond-bearing diatremes are economically important and are referred to as kimberlite pipes.

Dike: A discordant, sheet-like body igneous body formed from the injection of magma into a fracture within the brittle crust of the earth (Carrigan, 2000, p. 219: Marsh, 2000, p. 191). Generally, a tabular igneous body which cross-cuts the planar structures in the adjacent rocks.

Directed blast: A hot, low-density mixture of gas, rock debris, and ash that is propelled by a volcanic eruption and generally moves along the ground at high speeds (Miller, 1989).

Dome (aka Lava Dome): A steep-sided mass of lava that is generally formed immediately above the volcanic vent from which it was extruded. Domes are generally circular in plan and have a relatively small surface area relative to other types of lava flows. Domes may be spiny, rounded, or flat on top, and often have rough, blocky surfaces formed by the fragmentation of the dome's crust during intrusion. Domes may grow by extrusion of lava onto the outer surface of a previously formed dome (exogenous dome) or may be formed by inflation of a pre-existing dome (endogenous dome). Domes are most commonly the result of extrusion of viscous lava (primarily of the composition of rhyolite and dacite, but andesite may occur as well).

Dormant volcano: A volcano that is not currently erupting, but is thought to be likely to erupt in the future.

Downsag caldera: A type of caldera characterized by inward sloping topography, inward tilted wall rocks, and an apparent absence of large displacement caldera bounding faults (Lipman, 1997). Down-sag calderas are believed to result from small volume eruption from a deep-seated subvolcanic intrusion.

Dunite: A plutonic rock composed primarily of olivine. More specifically "A dunite is an ultrabasic igneous rock dominated by essential olivine (>90% volume), often with accessory clinopyroxene, orthopyroxene, spinel, ilmenite, and magnetite. Dunite is usually coarse- to medium grained and is a peridotite." (http://www.alexstrekeisen.it/english/pluto/dunite.php).

Epithermal mineralization: A mineral deposit formed from relatively low temperature (generally <350° C) hydrothermal solutions at shallow levels (<2km) in the earth's crust. Epithermal mineralization is a common feature on many volcanoes.

Eruption: The expulsion of volcanic materials (magma, volcanic gases) from a vent or fissure at the earth's surface. In a general sense, eruptions are considered to be relatively large explosions which result in the expulsion of volcanic materials at or onto the earth's surface.

Extinct volcano: A volcano that is not presently erupting and is unlikely to do so in the future (Foxworthy and Hill, 1982).

Extrusion: The eruption of molten rock (Hazlett and Hyndman, 1996).

Facies: A part of a rock body that can be differentiated from another part of a related rock body by textural or compositional variations. The general appearance or composition of one part of a rock body as contrasted with other parts (AGI, 1976, p. 155).

Facies changes: The textural and compositional changes that occur laterally and/or vertically within related rock bodies.

Fire fountain: A spray of lava emitted from a vent or a fissure composed of a highly fluid mixture of basaltic magma and gas (Vespermann and Schminke, 2000, p. 683: Spudis, 2000, p. 697). Deposits from fire fountains produce mantling deposits composed of dense, plastic juvenile fragments and ash known as "agglomerates".

Fissure: A fracture or crack in the earth with an open separation.

Flow banding: A foliation commonly observed in intermediate and felsic lavas, that results from shearing of the lava during laminar flow (Cas and Wright, 1987, p. 78). In rhyolite flows, flow banding is commonly exhibited by alternating bands comprising volcanic glass and spherulites (small, radiating bodies of devitrified glass).

Fuel-coolant interaction: The interaction of magma (fuel) with external water (coolant) that may result in thermal explosions (Vespermann and Schminke, 2000, p. 683).

Fumarole: A vent which releases volcanic gases. These include steam (H_2O), carbon dioxide (CO_2), sulfur dioxide (SO_2), hydrogen sulfide (H_2S), as well as other volatile gases emitted from subterranean magmas.

Fumarolic activity: Volcanic gas emissions, with or without an accompanying change in the temperature or compositions of the gasses/fluids emitted (USGS Glossary of Volcano and Related Terminology).

Gabbro: A phaneritic mafic igneous rock that is chemically equivalent to basalt. In detail, "Gabbros can contain: 25-50% of mafic minerals (Augite, Hypersthene, Olivine, Hornblende) and 45-70% of plagioclase (Labradorite or bytownite). If the plagioclase is less calcic than labradorite, the rock belongs in the Diorite family. Some low silica, dark-colored rocks containing olivine and plagioclase of the andesine range are by some petrologist included as gabbros." (http://www.alexstrekeisen.it/english/pluto/quartzgabbro.php).

Geyser: A special type of hot spring characterized by intermittent discharged of water and volcanic gases brought about by expansion of a vapor phase (generally steam) in the subsurface.

Graben: An elongate crustal block that has moved downward relative to bounding fault systems (Foxworthy and Hill, 1982).

Hawaiite: A type of alkalic basalt (Hazlett and Hyndman, 1996).

Heterolithic: A clastic (volcaniclastic) deposit containing of a variety of different types of rock fragments.

Hot spot: An area, generally located in the middle of a lithospheric plate, characterized by anomalous heat flow. Mantle material rises toward the earth's surface and undergoes decompressive melting at hot spots which may form volcanoes (as in Hawaii) or cause partial melting of the overlying crust which leads to the formation of volcanoes (e.g., Yellowstone region).

Hot spring: A thermal spring containing water at a higher temperature than the human body (98°F/37°C)

Hydrothermal: Pertains to hot water or the action of hot water which has been heated by or in association with magma (Gardner et al., 1995).

Hydrothermal alteration: Changes in rocks or minerals brought about by metasomatism with hydrothermal fluids (generally hot water).

Hydrothermally altered: Minerals or rocks that have undergone hydrothermal alteration.

Hydrothermal system: The system comprising the rocks, fluids, vapors, and conduits associated with hydrothermal activity. In general, hydrothermal systems have the following components: 1) a shallow magma chamber or cooling intrusion (provides the heat for the system); 2) fluids which can be of magmatic, meteoric, or connate origin, that are heated by the intrusion and flow through the rocks adjacent to (or sometimes within) the heat source; 3) fractures or high permeability zones which allow transfer of fluids from one part of the system to another part of the system. In most cases, this transfer

is believed to be the result of buoyancy contrasts between the colder and warmer fluids within the system.

Hydrovolcanic eruptions: A general term for eruptions caused by the mixing of magma with water (Vespermann and Schminke, 2000, p. 683). Encompasses hydroclastic, hydromagmatic, and phreatomagmatic eruptions.

Hyaloclastite: A deposit comprising small, angular glass fragments formed by nonexplosive shattering of lava or magma flowing into water, ice, or water-saturated sediment (Batiza and White, 2000, p. 361: Schmidt and Schmincke, 2000, p. 383).

Igneous: Refers to the processes associated with magma, or the rocks formed via the solidification of magma.

Igneous rock: A variety of rock formed via crystallization from a magma. The two major classes of igneous rocks are volcanic (crystallized at or near the earth's surface, for example, basalt) and plutonic (crystallized at depth within the earth, for example, gabbro).

Ignimbrite: A term used for pyroclastic flow deposits, that is synonymous with "ash tuff" (Lipman, 2000, p. 643). According to Cas and Wright (1987, p. 98), the term should only be used to describe pumiceous pyroclastic flow deposits.

Island arc: A curved chain of islands, generally convex towards the open ocean, which is bounded on its convex side by a deep oceanic trench (typically a subduction zone) and generally a deep-sea basin (AGI, 1976, p. 234).

Jokulhlaup: The Icelandic term for "glacial outburst floods" which are commonly caused by subglacial volcanic eruptions.

Juvenile fragment: Glassy or partially crystallized fragments which represent samples of an erupting magma. These include fragments such as pumice, scoria, reticulate, achneliths (Pele's tears, Pele's hair), and various types of volcanic bombs (Cas and Wright, 1987, p. 47-53).

Kipuka: An area of older land surrounded by younger lava flows (Hazlett and Hyndman, 1996).

Lahar: The Indonesian term for a debris flow or a mudflow originating on a volcano (Harris, 2000, p. 1301). Lahars are generally composed of volcanic materials, but can contain significant amounts of non-volcanic materials derived from erosion during flow. Most volcanologists prefer this term to be used for the process and not the sedimentary deposits that it forms, but unfortunately, this distinction has been largely ignored in the geological literature. Many lahars are composed of sand and coarser materials, and thus, can be distinguished from "mudflows" which predominantly contain silt- or clay-sized grains (Rodolfo, 2000, p. 973).

Landslide: A general term for relatively dry, gravity-induced movements of rock, sediment and/or soils (commonly with associated organic debris and/or human-made construction materials (e.g., houses, buildings, roads, etc.)) that are perceptible to the human eye.

Lapilli: A textural term for fragments in volcanic rocks and volcanic deposits that range from 2mm to 64mm in diameter (Fisher, 1966; Schmid, 1981).

Lateral blast: A volcanic eruption which is directed horizontally instead of vertically. Lateral blasts may be caused by sudden decompression of a shallow magma chamber residing within the flanks of a volcano (for example, the 1980 eruption of Mt. St. Helens), or along the base or side of a lava dome (for example, the 1902 eruption of Mt. Pelée in Martinique) (Nakada, 2000, p. 945).

Laterite: A type of soil that forms in regions with warm, moist climates. Lateritic soils are commonly composed of kaolin clay, aluminum oxide, and iron oxide. Lateritic soils are commonly red in color (Hazlett and Hyndman, 1996).

Lava: The term used for magma that has been erupted on to a planet's surface.

Lava flow: An outpouring of lava from a vent or fissure that spreads along the ground surface, as well as the crystallized rock resulting from solidification of the outpouring (Peterson and Tilling, 2000, p. 957).

Lava lake: A region typically within the summit of a shield volcano which contains partially crystallized or molten lava which lies immediately above a volcanic conduit which joins the lava lake to the magma chamber. Strong magma convection within volcanic conduits sustains lava lakes within their respective volcanic vents (Walker, 2000, p. 285).

Lava tube: A hollow region, commonly found within crystallized pahoehoe lava flows, which was filled with hot, flowing lava during a volcanic eruption. Lava tubes are formed when the top surface of a channelized lava flow crystallizes, and the magma flowing in the interior of the lava flow drains during and/or immediately following a volcanic eruption.

Levées: Walls of lava that form at the margins of a lava flow.

Lherzolite: "A lherzolite is an ultrabasic igneous rock dominated by essential Olivine and clinopyroxene and orthopyroxene in equal proportions. Accessory minerals include plagioclase, spinel, garnet, ilmenite, chromite and magnetite. Lherzolites are a peridotite and the main component of the upper mantle. Their aluminous phases change with pressure, with plagioclase present at low pressures, spinel at intermediate pressure and garnet at high pressure." (http://www.alexstrekeisen.it/english/pluto/lherzolite(tl).php).

Lithophysae: Radial aggregates of fibrous crystals which have formed around an expanding vesicle in a melt which is capable of flowing (Cas and Wright, 1987, p. 84). Lithophysae are commonly the result of vapor-phase crystallization within a rhyolitic magma. They should not be confused with spherulites, which are similar-shaped structures formed from devitrification of volcanic glass.

Lithic: Fragments of previously-formed rocks or dense fragments that occur within volcaniclastic deposits. Lithic fragments may be accessory fragments, accidental fragments, or juvenile fragments.

Lithospheric plates: The series of rigid slabs that comprise the earth's lithosphere (crust and upper mantle. This term is synonymous with *tectonic plates*.

Littoral: An adjective describing physical features or processes associated with shorelines of oceans, seas, or lakes (Peterson and Tilling, 2000, p. 957).

Lobate lava: A submarine lava comprising elongate, flattish lobes with smooth, outer glassy skins (Batiza and White, 2000, p. 361).

Maar: A type of monogenetic volcano, generally formed by subterranean phreatic or phreatomagmatic eruptions that occur as magma explosively interacts with ground water or subsurface moisture. Maar craters are cut into the surrounding country rock, vary from 10-500 meters deep, and range from a few hundred meters to 3 km in diameter. Maar volcanoes are generally surrounded by low, shallowly outward-dipping beds of well-bedded volcanic ejecta that rapidly decrease in thickness away from the vent. The volcanic deposits are mainly emplaced by base surges and fallout, and commonly contain very little (or in the case of phreatic eruptions, no) juvenile volcanic materials (Vespermann and Schminke, 2000, p. 685: Cas and Wright, 1987, p. 376-377).

Mafic: A compositional term for igneous rocks which contain 45%-55% SiO_2 (by weight). Mafic rocks are generally dark colored, and are characterized by mineralogy including pyroxene and calcium-rich plagioclase, variable amounts of olivine, and accessory minerals such as ilmenite and magnetite. Examples of mafic rocks include basalt and gabbro.

Mafic lava: A lava with a silica content (by weight) ranging from 45-55% (AGI, 1976, p. 447; Peterson and Tilling, 2000, p. 957).

Magma: A term used to describe subsurface molten rock (Jeanloz, 2000, p. 41). Magmas are generally considered to be silicate melts (Grove, 2000, p. 133; Wallace and Anderson, 2000, p. 149), but may also be composed of carbonatitic liquids (Spera, 2000, p. 171). Magmas are composed of up to three components (liquid, crystalline solids, and gas (or supercritical fluid) bubbles; Grove, 2000, p. 133), and may be fully liquid or partially crystalline. Lavas are magmas that have erupted on to a planet's surface.

Magma chamber: A subterranean region composed of magma that may have a conduit or set of conduits leading to a volcanic vent or vents on a planet's surface.

Magnetic polarity: The direction of the magnetic poles (either normal or reversed) that is preserved in igneous rocks after they cool below their Curie temperature (USGS Glossary of Volcano and Related Terminology)

Magnitude: A numerical measure of the size of an earthquake based on the amount of seismic energy released. The magnitude of an earthquake is determined by measuring the highest-amplitude waves and correcting for distance and the type of seismometer used (McNutt, 2000, p. 1015). The seismic magnitude scale is logarithmic, with each increase in one unit on the scale equivalent to a tenfold increase in the wave amplitude.

Mantle: The part of the earth's interior lying above the outer core and below the Mohoroviĉić discontinuity. The mantle is commonly divided into three parts: the upper mantle (depths down to ~400 km), the transition zone (~400-670 km depth), and the lower mantle (~670-2900 km depth).

Mantle bedding: Pyroclastic deposits generated by ash fall which maintain a uniform thickness and drape over all but the steepest topography (Cas and Wright, 1987, p. 96).

Mantle plume: An elliptical, drop-shaped mass of mantle that ascends toward the earth's crust due to its relatively lower density relative to the adjacent mantle. The density contrast is commonly the result of higher heat content of the plume, but may also be the result of chemical anomalies within the mantle (Perfit and Davidson, 2000, p. 89: Sigurdsson, 2000, p. 271). Mantle plumes are associated with intraplate rifting and volcanism. Mantle plumes are the hypothetical cause of hot spots (Hooper, 2000, p. 345).

Melilite: A group of minerals that commonly form in the place of feldspar in silica-deficient, sodium-rich alkalic volcanic rocks (Hazlett and Hyndman, 1996). The melilite group is "A group of tetragonal sorosilicates with a disilicate anion $(Si_2O_7)^{6-}$ or an Al or B-bearing derivative thereof and the general formula given above, where M denotes a small- to medium-sized divalent or trivalent cation (mostly Mg and Al, or rarely Fe, B, Zn, Be, Si, etc.) and X is Si, Al or rarely Be or B. In general, Al or B replace one Si atom when M is a trivalent ion, but the charge can also be balanced by coupled substitution of Ca^{2+} with a monovalent ion, especially Na, and M^{3+} with M^{2+}, such as in Alumoåkermanite, where Al^{3+} is still dominant on the M-site but the mineral is far from end-member composition. In petrology "melilite" usually refers to minerals in the åkermanite-gehlenite series, by far the most abundant members of the group." (https://www.mindat.org/min-29310.html).

Megabreccia: Coarse, heterolithic breccia deposits formed during caldera collapse, which contain fragments which are generally greater than one meter in diameter (Lipman, 1976). Megabreccia fragments may be so large that individual fragments may not be readily recognizable on the scale of an outcrop.

Mesa lava: Generally rhyolitic in composition, a lava flow with an approximately circular plan which forms a biscuit-shaped body (Cas and Wright, 1987, p. 81).

Mesobreccia: Heterolithic breccia deposits formed during caldera collapse which contain fragments that are generally less than 1 meter in diameter (Lipman, 1976).

Metamorphic rock: In the strictest sense, rocks that have formed in the solid state in response to pronounced changes in temperature and/or pressure without any change in the bulk chemical composition of the rock. Metamorphic processes are generally confined to regions within the earth below the zones of weathering, cementation, and diagenesis.

Metamorphism: In the strictest sense (isochemical metamorphism), the process by which consolidated rocks undergo textural and mineralogical changes brought about by changes in temperature and/or pressure. The textural and/or mineralogical changes associated with metamorphism are thermodynamic responses to the physical conditions present in the metamorphic environment. In general, increasing metamorphism results in dehydration of the rocks, as well as an increase in the grain size of the rocks.

Metasomatism: A type of metamorphism characterized by the exchange of chemical species between rocks and their associated altering fluids and/or vapors.

Moat sediments: A general term for sedimentary deposits that occur between the topographic walls and the resurgent central cores of the calderas. In felsic caldera systems, moat sediments are commonly intruded by, and associated with, lava domes.

Monogenetic volcano: A volcano that erupts only once (Walker, 2000, p. 283).

Monolithic: A type of volcaniclastic deposit in which all the clasts present are of the same composition.

Moraine: A topographic feature or landform composed of an accumulation of sediment that has been carried and subsequently deposited by a glacier.

Mudflow: A flowing mixture composed of water and mud (clay- and silt-sized sediments). The term should be used exclusively for mud-dominated mass flows, and should not be used as a substitute for the term “lahar” (Rodolfo, 2000, p. 973-974). Mudflows are common in both volcanic and non-volcanic environments.

Mugearite: An “orthoclase-bearing oligoclase basalt, with major olivine, accessory apatite, and opaque oxides. Pyroxene may or may not be present.” (https://www.mindat.org/glossary/mugearite).

Nested caldera: A type of caldera which is found within a larger, older caldera structure.

Nueés ardente: The term used for a “glowing avalanche” resulting from a small-volume block and ash flow produced by the collapse of an actively growing lava dome (LaCroix, 1904). In recent years, the term has unfortunately been more widely used as a synonym for “ignimbrite”. Its use should be restricted to the original definition of LaCroix (Cas and Wright, 1987, p. 225).

Orogeny: A term which describes the process of forming mountains, particularly by folding and thrusting (AGI, 1976, p. 308).

Outwash: Sediments deposited by glacial meltwater beyond the active glacial ice. Outwash sediments are commonly characterized by poorly bedded gravels interlayered with well-bedded (and commonly cross-bedded) sands.

Pahoehoe lava: A Hawaiian term to describe lava flows with smooth, continuous surfaces (Kilburn, 2000, p. 291). Pahoehoe flows may have a variety of surfaces described as smooth, ropy (characterized by rope-like, commonly braided flow folds on the lava flow's surface) , or shelly (vesicular and cavernous; Cas and Wright, 1987, p. 66-67). Pahoehoe toes and lobes form when largely degassed mafic magma issues from tubes relatively far from the erupting vent.

Palagonite: A yellow clay that forms from the hydration of basalt glass (Hazlett and Hyndman, 1996).

Piecemeal caldera: A type of caldera characterized by an internal structure composed of several individual fault-bounded blocks (Lipman, 1997). Piecemeal calderas may result from non-uniform subsidence of a caldera formed from a single eruption, or may be the result of subsidence following a series of large eruptions (multicyclic; Lipman, 1997; Lipman, 2000, p. 655-656).

Pele's hair: A type of achnelith composed of thin, hair-like strands of volcanic glass. These thin, cylindrical strands of volcanic glass are commonly golden in color, have diameters between 1-500μm in diameter, and may be up to 1 meter in length. They are formed from stretched magma droplets emitted into the atmosphere during fire fountaining and strombolian eruptions (Vergniolle and Mangan, 2000, p. 447).

Pele's tears: A type of achnelith composed of small droplets of shiny black volcanic glass that have been ballistically moulded and quenched during flight into spherical, dumbbell, or tadpole shapes. These droplets generally range from a few millimeters to a few centimeters in size, are generally dense, but locally may be quite vesicular (Vergniolle and Mangan, 2000, p. 447).

Pele: The mythological Polynesian goddess of volcanoes. In Hawaii, this temperamental goddess makes her home in Kilauea's fiery vent, Halema'uma'u (Sigurdsson and Lopes-Gautier, 2000, p. 1297).

Pelean eruption: A type of volcanic eruption characterized by a ground hugging glowing avalanche (pyroclastic flow) resulting from a mixture of hot volcanic gases, ash, and incandescent lava fragments. Pelean eruptions may occur when pyroclasts are blown out of a central volcanic vent and then collapse onto the earth's surface to form a pyroclastic flow (Tilling, 1985). Pelean eruptions may also occur as a result of the explosive disintegration of a lava dome (as was the case for the lava dome on Mt. Pelée, Martinique in 1902).

Peperite: A genetic term for a rock formed by in-situ disintegration and mixing of molten magma or lava with wet, poorly consolidated sediment (Batiza and White, 2000, p. 361). A breccia-like deposit formed from the extrusive or intrusive mixture of lava or magma with wet sediment (Schmidt and Schminke, 2000, p. 383).

Peridotite: "Peridotites are a group of ultrabasic igneous rocks containing more than 40 vol% olivine with or without orthopyroxene and clinopyroxene. Accessory phases include garnet, spinel, plagioclase, ilmenite, chromite and magnetite. Peridotites comprise the bulk of the Earth's upper mantle and are present as xenoliths within a wide range of mantle-derived magmas and within the mantle sequences of ophiolites." (http://www.alexstrekeisen.it/english/pluto/peridotites.php).

Perlite: Hydrated obsidian, generally light grey in color, that is commonly characterized by rounded, onion-skin-like fractures (perlitic cracks). Apache's tears are unhydrated clumps of fresh obsidian that are commonly found within regions containing perlite.

Phreatic eruption: A steam eruption, commonly associated with water, mud, and other earth materials, that is caused when groundwater, heated by a magma, flashes (and explosively expands) into steam (Harris, 2000, p. 1301). Phreatic eruptions expel no juvenile (magmatic) material, and are commonly the precursor to magmatic eruptive activity.

Phreatomagmatic eruption: A type of explosive volcanic eruption that occurs when water (groundwater or surface water) comes in contact with hot magma. The quenching of the magma by the water causes the magma to violently fragment into juvenile (cognate) particles that are bounded by fracture surfaces and by rounded walls of broken vesicles. Due to the moisture present, accretionary lapilli are also common in volcanic deposits resulting from phreatomagmatic eruptions (Williams and McBirney, 1979, p. 247-248).

Pillow breccia: A mixture of coarse, typically glassy fragments and broken to whole pieces of pillow lava formed from the shattering of pillow lava crusts (Batiza and White, 2000, p. 361). Pillow breccias commonly form in areas where pillow lavas are not strong enough to maintain their competence along steep submarine slopes or scarps.

Pillow hyaloclastite: Hyaloclastite deposits immediately surrounding, and intimately associated with, pillow lavas.

Pillow lava: A type of submarine lava flow consisting of interconnected, elongated lava tubes. Cross-sections of individual lava tubes resemble pillows with convex upper surfaces and flat or concave lower surfaces (Schmidt and Schminke, 2000, p. 383). Both radial and concentric cooling fractures may be present along the margins of individual pillows, and these fractures are brought on by thermal contraction during cooling. Growth of the pillow tubes takes place as the outer, commonly striated outer glassy surface of the pillow tube fractures, and a new tube "buds" from the fracture in a manner similar to the way that toothpaste is squeezed out of a tube.

Pipe-like alteration zone: A type of narrow, cylindrical or inverted-cone shaped, discordant hydrothermal alteration zone that is typically confined to a narrow region in close proximity to a synvolcanic structure (e. g. synvolcanic fault). Pipe–like alteration zones are commonly formed by the highest temperature hydrothermal fluids within a hydrothermal cell (Morton and Franklin, 1987).

Plate (piston)-type caldera: A type of caldera in which the caldera floor subsides more or less evenly as one coherent block. Plate-(piston)-type calderas are believed to result from single, large volume pyroclastic eruptions from relatively shallow depth (hypabyssal) magma chambers.

Plinian eruption: Named for Pliny the Younger (who witnessed the destruction of Pompeii by eruptions from Mt. Vesuvius), a type of violently explosive volcanic eruption that ejects large volumes of tephra high into the atmosphere (Harris, 2000, p. 1301).

Pluton: A body of rock which has formed beneath the earth from crystallization and consolidation from a magma (AGI, 1976, p. 334). Plutons may be considered extinct magma chambers (Marsh, 2000, p. 191). Large plutons (>40 square miles in area) are called "batholiths".

Ponded flow: A term used to describe a lava flow that has ponded within a depression or a volcanic vent. A lava lake is a specific type of ponded flow that occurs a volcanic conduit.

Pumice: Solidified fragments of quenched, highly vesicular (>60%) silicic magma or lava (Cashman et al., 2000, p. 421). The highly vesicular nature of pumice results from large volumes of gas rapidly expanding within a rapidly cooling magma. The low density of pumice commonly permits it to float on water for extended periods of time. Hot pumice, however, has been shown experimentally to sink rapidly upon interacting with water (Whitham and Sparks, 1986).

Pyroclastic: Refers to processes resulting from the explosive fragmentation of a magma or lava. May also be used to describe the deposits formed by explosive volcanic activity and directly deposited by transport processes resulting directly from this activity (Cas and Wright, 1987, p. 8). Pyroclastic is a Greek term which means "fire-broken" (Harris, 2000, p. 1301).

Pyroclastic fall: The "rain-out" of pyroclastic material through the atmosphere from an eruption jet or eruption plume during an explosive volcanic eruption (Wilson and Houghton, 2000, p. 545; Houghton et al, 2000, p. 555).

Pyroclastic fall deposit: Volcaniclastic (pyroclastic) deposits formed from the rain-out of clasts through the atmosphere from an eruption jet and/or plume during an explosive eruption (Houghton et al., 2000, p. 555). Fall deposits typically exhibit mantle bedding, are well sorted, and commonly show well-developed planar stratification (Cas and Wright, 1987, p. 95-96).

Pyroclastic flow: A dense, hot, dry, high particle concentration mixture of gas and hot rock fragments (ash, pumice, blocks, etc.) that travels along the ground surface, typically at high velocity (generally on the order of hundreds of feet or meters per second; Harris, 2000, p. 1301) away from a volcano. The high speeds of pyroclastic flows are possible because they flow over a thin layer of hot, commonly expanding and escaping gases. Most of the material within a pyroclastic flow is contained within concentrated particle dispersion located at the flow's base (Wilson and Houghton, 2000, p. 545).

Pyroclastic flow deposit: Pyroclastic (volcaniclastic) deposits that are left by pyroclastic flows (Cas and Wright, 1987, p. 96). The deposits are usually topographically controlled (infilling valleys and topographic depressions), massive, and poorly sorted. Depending upon their thickness and heat retention, pyroclastic flow deposits may coalesce into welded tuffs. Pumice-rich pyroclastic flow deposits are often called "ignimbrites".

Pyroclastic surge: A type of turbulent, low density (low particle concentration) pyroclastic cloud or pyroclastic density current. Being more dilute than pyroclastic flows, surges can sweep over ridges, hills, and other topographic boundaries. Two kinds of surges are known: *wet surges* have temperatures <100°C and contain steam that condenses into water droplets that surge along the ground surface with gas and pyroclasts; and dry surges, which have temperatures >100°C, and form by either hydrovolcanic eruptions with low water/magma ratios, or by magmatic eruptions driven solely by expanding magmatic gases (Valentine and Fisher, 2000, p. 571).

Pyroclastic surge deposit: Pyroclastic deposits that are left by pyroclastic surges. These deposits mantle topographic features but also generally thicken within topographic depressions. These deposits are generally well-sorted, and are enriched in crystals and lithic fragments relatively to pyroclastic flow deposits. Surge deposits commonly exhibit unidirectional sedimentary bedforms, including low angle cross-bedding, dune forms, climbing dune forms, pinch and swell structures, and chute and pool structures (Cas and Wright, 1987, p. 98).

Quenching: The rapid cooling of magma to form glass (Batiza and White, 2000, p. 361). Fuel-coolant interactions commonly lead to quenching. Abrupt quenching may cause a rapid volume decrease which leads to fragmentation of the glass (cooling-contraction granulation).

Reticulite: An exceptionally porous type of scoria containing porosities ranging from 95-99%98% (Vergniolle and Mangan, 2000, p. 447; McPhie et al., 1993, p. 27). Commonly referred to as "thread-lace" scoria, reticulite is made up of a honeycomb-like network of thin glass fibers.

Rhyolite: A volcanic rock containing greater than 68% silica (by weight). Rhyolites are composed primarily of alkali feldspars (sanidine and orthoclase) and quartz (>10% by volume), with lesser amounts of sodic plagioclase (albite, oligoclase), hornblende, or biotite. Accessory minerals include zircon,

apatite, and tourmaline. Due to their high silica content (and thus high degree of polymerization), rhyolite lavas are very viscous and commonly form lava domes, mesa lavas, or coulees. Rhyolitic magmas with high gas contents typically explode violently to form pyroclastic flows, pyroclastic surges, and pyroclastic falls.

Rhyolite magma: A magma which contains greater than 68% silica by weight.

Rift: A linear topographic feature formed by crustal extension. Rift structures associated with volcanism are commonly composed of a graben with a central high region, which is usually the site of active volcanism (for example, along the mid-ocean ridges).

Rift Zone: A zone of fissures and volcanic vents that commonly form along the flanks of volcanoes (Hazlett and Hyndman, 1996).

Ring fracture/Ring fault: The arcuate bounding faults upon which caldera (cauldron) subsidence takes place. Ring fractures (faults) define the structural limits of calderas. Most observed ring faults are nearly vertical or dip steeply inward (toward the center of the caldera), and this is thought to be a result of doming of the caldera structure following its initial formation (Lipman, 2000, p. 649-650).

Ropy Pahoehoe: A type of pahoehoe lava characterized by flexible crusts that are bent into tight folds as lava flows. These tight folds form lava surfaces that appear to be made up of a series of braided ropes (Kilburn, 2000, p. 295).

Satellite vent: A secondary vent on a volcano, commonly located on the volcano's flank.

Scoria: Solidified fragments of quenched, highly vesicular (>60%) mafic magma or lava (Cashman et al., 2000, p. 421). The highly vesicular nature of scoria results from rapid cooling of gas-rich lava.

Scoria cone: Small volcanic landforms formed from focused (single-vent) subaerial strombolian eruptions of basalt or basaltic-andesite magma. These features have an inverted cone-shaped profile and are generally circular in plan, although elongate scoria cones can be formed from multiple-vent volcanic eruptions (Cas and Wright, 1987, p. 371-372).

Seismic wave: A term for elastic earth waves formed by either earthquakes or explosions. Seismic waves include both surface waves as well as body waves.

Seismicity: The phenomenon of earth movement or seismic activity.

Seismograph: A scientific instrument used to detect and record seismic waves.

Semiconformable alteration zone: A regional zone of hydrothermal alteration typically characterized by a sheet-like or cloud-like geometry. Semiconformable alteration zones are generally quite extensive in permeable rock units (e.g., tuffs, medium- to coarse-grained clastic sediments and sedimentary rocks), and are generally patchy in less permeable rock units (e.g., lavas, intrusions). These zones commonly are found along the periphery of "pipe-like" alteration zones, which are generally confined to regions in close proximity to synvolcanic structures (e.g., synvolcanic faults zones) (Morton and Franklin, 1987).

Shelly pahoehoe: A type of pahoehoe lava characterized by highly vesicular, extremely fragile crusts that form over hollow lava blisters. The surfaces of these blisters break easily when stepped upon, giving the impression of walking on eggshells (Kilburn, 2000, p. 295).

Shield volcano: A broad, low-relief volcano constructed by flows of relatively fluid lava (e.g., basalt: Spudis, 2000, p. 698). Flank slopes on shield volcanoes are typically $\leq 5°$ (Zimbelman, 2000, p. 771).

Silica: The chemical compound silicon dioxide, SiO_2.

Silicic: A term used to describe silica-rich volcanic rock or magma (Miller, 1989). A chemical classification for a type of rock or magma containing >62% SiO_2 (Peterson and Tilling, 2000, p. 958) or 63% SiO_2 (Cas and Wright, 1987, p. 16) by weight.

Silicic lava: A lava with a silica content greater than 62% (by weight). Synonymous with the term "felsic lava" (Peterson and Tilling, 2000, p. 957).

Sinter: A type of fragile, commonly white or grey rock formed by precipitation of silica from cooling hydrothermal solutions at or near a hydrothermal vent. Precipitation of siliceous sinter (often with associated sulfide minerals and precious metals) commonly occurs in neutral and acid hydrothermal systems under the influence of biogenic agents such as algae and bacteria (Cas and Wright, 1987, p. 316).

Slabby pahoehoe: A type of pahoehoe lava with a surface composed of slabs of broken lava crust that are up to meters across and up to several centimeters thick (Kilburn, 2000, p. 295).

Solfatara: A type of steam vent or dry fumarole that is characterized by quiet discharge (<20 m/s), and that precipitates a significant amount of sulfur (Hochstein and Browne, 2000, p. 850-851).

Spatter: Fragments of fluid lava that are thrown out of a vent during an eruption (Hazlett and Hyndman, 1996).

Spatter bomb: A glassy pyroclast greater than 64mm in diameter that takes on a fluidal shape by the force of ejection (Vergniolle and Mangan, 2000, p. 447).

Spherulite: Typically rounded, radiating arrays of crystal fibers produced by the high temperature devitrification of volcanic glass. In felsic rocks, the crystal fibers are generally composed of alkali feldspar and a silica polymorph (either quartz or cristobalite), whereas in mafic rocks the fibers commonly consist of plagioclase and/or pyroxene. Spherulites typically have diameters of 0.1-2.0 cm, but can be much larger (commonly up to 20 cm). Isolated spherulites are generally spherical, but adjacent spherulites may impinge upon one another to produce long chains that are often aligned with flow foliation (McPhie et al., 1993, p. 24-25).

Spreading center/Spreading ridge: Places on the ocean floor characterized by active volcanism and where separation of lithospheric plates takes place.

Stratovolcano: A generally steep sided volcano composed of alternating layers of lava flows, pyroclastic deposits, and commonly, volcaniclastic sedimentary deposits (Walker, 2000, p. 283). Stratovolcanoes commonly have increasing slopes toward their summits since they generally have mainly lava flows and sedimentary deposits near their base and pyroclastic (tephra) deposits near their summits. Also called a "composite volcano".

Stony rhyolite: Very finely crystalline rhyolite lava (Cas and Wright, 1987, p. 84).

Strombolian eruption: Volcanic eruptions of basaltic magma, slightly more violent than Hawaiian eruptions, that produce large amounts of scoria and ash around a central vent to form a cone. Strombolian eruptions are typically pulsating and have periods of several seconds (Wolf and Sumner, 2000, p. 321). The deposits consist of lava spatter, vesicular bombs, scoria lapilli, and mafic ash (Vespermann and Schminke, 2000, p. 683). Named after Stromboli, an Italian volcano.

Subduction zone: A sloping region at collisional plate boundaries where one tectonic plate overrides another tectonic plate. In most regions, continental crust overrides oceanic crust which is then consumed in the subduction zone (continental – oceanic plate boundary), but in many areas, oceanic crust may be overridden by another plate of oceanic crust (oceanic – oceanic plate boundaries). Deep

oceanic trenches commonly occur as the surface landform associated with subduction zones. Melting of the subducting slab commonly produces magma which rises to the earth's surface to produce volcanic arcs.

Surtseyan eruption: Hydrovolcanic eruptions dominated by jets of wet tephra (scoria and ash) that result in the formation of tuff cones. The term "surtseyan" is generally used for volcanoes erupting through seawater. Named after Surtsey, a volcano which emerged from the sea off the coast of Iceland in 1963 (Vespermann and Schminke, 2000, p. 683).

Synvolcanic: A term used to describe a process or feature that was active or produced during volcanic activity.

Synvolcanic fault: A fault or geological structure present or produced at the time of volcanic activity.

Tectonic: A general term used to describe the forces involved in the deformation of the earth's crust. Commonly used to also describe the geological structures or features produced by such deformation.

Tectonic plate: One of the large segments of the earth's lithosphere (crust and upper mantle, up to 250km thick) that comprise the earth's outer shell. At the present time, there are 16 major tectonic plates that "float" on top of the asthenosphere, the plastic layer in the earth's mantle.

Tephra: A general term used by volcanologists to describe all fragmental volcanic ejecta produced during explosive volcanic eruptions (Dehn and McNutt, 2000, p. 1271). This includes ash (<2mm diameter fragments), lapilli (2-64 mm diameter fragments and fragments greater than 64 mm in diameter known as bombs (semi-solid or plastic ejecta) or bombs (solid ejecta) (Tilling et al., 1987).

Thread-lace scoria: See "reticulite".

Trap-door caldera: A type of caldera formed when one part of the caldera floor subsides to a greater depth than the other side of the caldera floor. In general, trap-door calderas have a partial ring fracture (associated with the side of greatest caldera collapse) and a hinge area (associated with the side of least collapse). Trap-door calderas may represent either calderas that have undergone incomplete collapse, or calderas formed from eruptions from shallow asymmetrical magma chambers (Lipman, 1997: Lipman, 2000, p. 654.

Tremor: A continuous vibration of the ground around active volcanoes (Vergniolle and Mangan, 2000, p. 447). Tremors defined on seismographs may have either a regular sine-wave appearance (harmonic tremor) or an irregular, pulsating appearance (spasmodic tremor) (McNutt, 2000, p. 1015).

Tuff: A lithified volcaniclastic rock composed primarily of ash, with up to minor volumes of lapilli and/or blocks and bombs (Fisher, 1966). Originally used as a non-genetic rock name, common use today typically implies (incorrectly) that the tephra comprising the rock was deposited while hot. Similar deposits that have no indication of being hot while deposited are commonly referred to as "tuffaceous" (McPhie et al., 1993, p. 8).

Tuff cone: A type of hydroclastic volcano that is generally higher than (generally >50 m high), and has steeper external flanks (commonly >25°) than tuff rings or maars (Vespermann and Schminke, 2000, p. 684). Craters within tuff cones are generally higher in elevation than the adjacent land surface. Tuff cones are made up primarily of juvenile clasts deposited from lateral surges, airfall, and associated volcaniclastic remobilization processes.

Tuff ring: A type of hydroclastic volcano, generally <50m high, defined by craters with low depth/width ratios that sit at or above the elevation of the adjacent land surface. The rims around tuff rings are

composed of juvenile and accidental clasts and are deposited in beds with dips <25° (Vespermann and Schminke, 2000, p. 684).

Tumescence: The doming or uprising of a volcano commonly due to inflation of a shallow magma chamber. Regional tumescence commonly occurs prior to a major pyroclastic eruption, but may also occur following an eruption as less volatile magma is emplaced into the shallow crust (Smith and Bailey, 1968).

Tuya: A flat-topped, steep-sided volcano that erupted into a lake thawed into a glacier by volcanic heat (Smellie, 2000, p. 403). Commonly referred to as a "table mountain".

Unconformity: A surface of erosion that separates younger strata from older rocks (AGU, 1976, p. 448).

Variolite: A spherulite-like radiating aggregate composed of feathery, needle-like crystals of plagioclase and pyroxene that occur in mafic volcanic rocks (typically basalt). Variolites may result from devitrification, but are commonly believed to be formed in subaqueous rocks by quench-induced crystallization (Cas and Wright, 1987, p. 420).

VEI index: The Volcanic Explosivity Index, which is a measure of the size of an eruption based on its magnitude, intensity and destructive power. The VEI is measured on an eight-point scale, where "8" is the most destructive and powerful eruption (Cioni et al., 2000. p. 477).

Vent: A surface opening through which volcanogenic materials are erupted (Davidson and DeSilva, 2000, p. 663). Typically thought of as a hole in a planet from which volcanic products (magma, ash, etc.) are erupted (Spudis, 2000, p. 697).

Vesicle: A frozen bubble in a volcanic rock. Vesicles are formed when magma crystallizes around a gas bubble (Spudis, 2000, p. 697).

Vesicular: A textural term describing volcanic rocks filled with frozen gas bubbles (vesicles).

Vesicular tuff: Tuffs containing millimeter to centimeter-sized, irregular to round vesicles which are interpreted to form during trapping of air or vapor in wet ash deposits (Vespermann and Schminke, 2000, p. 683).

Vesuvian eruption: Commonly used as a synonym for a "Plinian" eruption (e.g., Tilling, 1985), , but also used to describe basaltic eruptions which involve long-sustained gas streaming with little ash being released (as in the 1906 eruption of Vesuvius; Cas and Wright, 1987, p. 130).

Viscosity: A measurement of the ratio of shear stress to the rate of shear strain in a fluid (Williams and McBirney, 1979, p. 20). In common language, how easily a fluid will flow. Considered the most important physical property of a magma because it largely determines eruptive style as well as volcano morphology. Magma viscosity generally increases as the silica content of the magma increases (due to silica polymerization) and as the temperature of the magma decreases. Magma viscosity may also be affected by the presence of trace elements (e.g., Ti) or volatiles (e.g., H_2O, CO_2, SO_2, etc.). In general, common magmas increase in viscosity in the following order: komatiite, basalt, andesite, dacite, rhyodacite, rhyolite.

Volcaniclastic: A non-genetic term used to describe any fragmental aggregate of volcanic parentage (Cas and Wright, 1987, p. 8). Rocks formed by the fragmentation of volcanic materials (either magma or volcanic rocks) irrespective of the method of fragmentation. Pyroclastic rocks and epiclastic rocks are both considered to be "volcaniclastic".

Volcanic bomb: Juvenile fragments of semi-solid or plastic magma ejected during a volcanic eruption. Based on their shapes after they hit the ground and cool, bombs are given various textural names

including breadcrust bombs, cow-dung (cow pie) bombs, spindle bombs (fusiform bombs) and ribbon bombs

Volcanic cycle: A general term used to describe a period of increased volcanic activity.

Volcanic field: A region comprising a large number of volcanic edifices. Volcanic fields are usually associated with basaltic volcanism, and commonly comprise a number of small, monogenetic volcanoes (e.g., cinder cones, maars, tuff cones, tuff rings, small shield volcanoes, lava domes). Fields may form in linear trends associated with tectonic structures (such as faults), on the flanks of larger composite or shield volcanoes, or within calderas (Connor and Conway, 2000, p. 331).

Volcanic landslide: A landslide that occurs along the flank of a volcano.

Volcano: A mound, hill or mountain constructed by the extrusion of lava and/or pyroclastic material from beneath the ground (Fisher et al., 1997, p. 43). A vent in the earth's crust from which molten lava, pyroclastic materials, volcanic gases, etc. issue (AGU, 1976, p. 457).

Vulcanian eruption: An explosive volcanic eruption generally expelling less than $1km^3$ of material, but with an eruption column that may reach heights of up to 10-20km (Nakada, 2000, p. 945). These eruptions last on the order of seconds to minutes (Morrissey and Mastin, 2000, p. 463).

Welding: The sintering together of hot, glassy fragments, irrespective of shape and size, by compactional lithostatic load (Cas and Wright, 1987, p. 165).

Welded tuff: A hard pyroclastic rock compacted by internal heat and pressure from overlying pyroclastic deposits.

4.1. Glossary References

AGI, 1976. Dictionary of Geological Terms: American Geological Institute, Anchor Press, Garden City, New York, 472 pages.

Bardintzeff, J.-M., and McBirney, A, R., 2000. Volcanology, 2nd Edition: Jones and Bartlett Publishers, Sudbury, Massachusetts, 268 pages.

Batiza, R., and White, J. D. L., 2000. Submarine Lavas and Hyaloclastite, *in* Sigurdsson, H., 2000, Encyclopedia of Volcanoes: Academic Press, San Diego, California, p. 361-381.

Carey, S. D., 2000. Volcaniclastic Sedimentation Around Island Arcs, *in* Sigurdsson, H., 2000, Encyclopedia of Volcanoes: Academic Press, San Diego, California, p. 627-642.

Carrigan, C. R., 2000. Plumbing Systems, *in* Sigurdsson, H., 2000, Encyclopedia of Volcanoes: Academic Press, San Diego, California, p. 219-235.

Cas, R. A. F., and Wright, J. V., 1987. Volcanic Successions: Modern and Ancient: Allen and Unwin, London, 529 pages.

Cashman, K. V., Sturtevant, B., Papale, P., and Navon, O., 2000. Magmatic Fragmentation, *in* Sigurdsson, H., 2000, Encyclopedia of Volcanoes: Academic Press, San Diego, California, p. 421-430.

Cioni, R., Marianelli, P., Santacroce, R., and Sbrana, A., 2000. Plinian and Subplinian Eruptions, *in* Sigurdsson, H., 2000, Encyclopedia of Volcanoes: Academic Press, San Diego, California, p. 477-494.

Connor, C. B., and Conway, F. M., 2000. Basaltic Volcanic Fields, *in* Sigurdsson, H., 2000, Encyclopedia of Volcanoes: Academic Press, San Diego, California, p. 331-343.

Davidson, J., and DeSilva, S., 2000. Composite Volcanoes, *in* Sigurdsson, H., 2000, Encyclopedia of

Volcanoes: Academic Press, San Diego, California, p. 663-681.

Dehn, J., and McNutt, S. R., 2000. Volcanic Materials in Commerce and Industry, *in* Sigurdsson, H., 2000, Encyclopedia of Volcanoes: Academic Press, San Diego, California, p. 1271-1282.

Fisher, R. V., 1966. Rocks composed of volcanic fragments and their classification: Earth Science Reviews, v. 1, pp. 287-298.

Fisher, R. V., Heiken, G., and Hulen, J. B., 1997. Volcanoes: Crucible of Change: Princeton University Press, Princeton, New Jersey, 317 pages.

Foxworthy and Hill, 1982. Volcanic Eruption of 1980 at Mount St. Helens: The First 100 Days: USGS Professional Paper 1249.

Gardner et al., 1995. Potential Volcanic Hazards with Regard to Siting Nuclear Power Plants in the Pacific Northwest: USGS Open-File Report 87-297.

Grove, T., 2000. Origin of Magmas, *in* Sigurdsson, H., 2000, Encyclopedia of Volcanoes: Academic Press, San Diego, California, p. 133-147.

Harris, S. L., 2000. Archaeology and Volcanism, *in* Sigurdsson, H., 2000, Encyclopedia of Volcanoes: Academic Press, San Diego, California, p. 1301-1314.

Hazlet, R. W., and Hyndman, D. W., 1996, Roadside Geology of Hawaii: Mountain Press Publishing Company, Missoula, MT, 304 p.

Hochstein, M. P., and Browne, P. R. L., 2000. Surface Manifestations of Geothermal Systems with Volcanic Heat Sources, *in* Sigurdsson, H., 2000, Encyclopedia of Volcanoes: Academic Press, San Diego, California, p. 835-855.

Hooper, P. R., 2000. Flood Basalt Provinces, *in* Sigurdsson, H., 2000, Encyclopedia of Volcanoes: Academic Press, San Diego, California, p. 345-359.

Houghton, B. F., Wilson, C. J. N., Smith, R. T., and Gilbert, J. S., 2000. Phreatoplinian Eruptions, *in* Sigurdsson, H., 2000, Encyclopedia of Volcanoes: Academic Press, San Diego, California, p. 513-525.

Jeanloz, R., 2000. Mantle of the Earth, *in* Sigurdsson, H., 2000, Encyclopedia of Volcanoes: Academic Press, San Diego, California, p. 41-54.

Kilburn, R. J., 2000. Lava Flows and Lava Fields, *in* Sigurdsson, H., 2000, Encyclopedia of Volcanoes: Academic Press, San Diego, California, p. 291-305.

LaCroix, A., 1904. *La Matagne Pelee et ses eruptions*. Paris, Masson.

Lipman, P. W., 1976. Caldera collapse breccias in the western San Juan Mountains, Colorado: Geological Society of America Bulletin, v. 87, p. 1397-1410.

Lipman, P. W., 1997. Subsidence of ash-flow calderas: relation to caldera size and magma chamber geometry: Bulletin of Volcanology, v. 59, p. 198-218.

Lipman, P. W., 2000. Calderas, *in* Sigurdsson, H., 2000, Encyclopedia of Volcanoes: Academic Press, San Diego, California, p. 643-662.

Marsh, B. D., 2000. Magma Chambers, *in* Sigurdsson, H., 2000, Encyclopedia of Volcanoes: Academic Press, San Diego, California, p. 191-206.

McNutt, S. R., 2000. Volcanic Seismicity, *in* Sigurdsson, H., 2000, Encyclopedia of Volcanoes: Academic Press, San Diego, California, p. 1015-1033.

McPhie, J., Doyle, M., and Allen, R., 1993. Volcanic Textures: A guide to the interpretation of textures in volcanic rocks: University of Tasmania Centre for Ore Deposit and Exploration Studies, Hobart, Tasmania, 198 pages.

Miller, 1989. Potential Hazards from future volcanic eruptions in California: United States Geological Survey Bulletin 1847.

Morrissey, M. M., and Mastin, L. G., 2000. Vulcanian Eruptions, *in* Sigurdsson, H., 2000, Encyclopedia of Volcanoes: Academic Press, San Diego, California, p. 463- 475.

Morton, R. L., and Franklin, J. M., 1987. Twofold classification of Archean volcanic-associated massive sulfide deposits: Economic Geology, v. 82, p. 1057-1063.

Nakada, S., 2000. Hazards from Pyroclastic Flows and Surges, *in* Sigurdsson, H., 2000, Encyclopedia of Volcanoes: Academic Press, San Diego, California, p. 945-955.

Perfit, M. R. and Davidson, J. P., 2000. Plate Tectonics and Volcanism, *in* Sigurdsson, H., 2000, Encyclopedia of Volcanoes: Academic Press, San Diego, California, p. 89-113.

Peterson, D. W. and Tilling, R. I., 2000. Lava Flow Hazards, *in* Sigurdsson, H., 2000, Encyclopedia of Volcanoes: Academic Press, San Diego, California, p. 957-971.

Rodolfo, K. S., 2000. The Hazard from Lahars and Jokulhlaups, *in* Sigurdsson, H., 2000, Encyclopedia of Volcanoes: Academic Press, San Diego, California, p. 973-995.

Schmid, R., 1981. Descriptive nomenclature and classification of pyroclastic deposits and fragments: recommendations of the IUGS Subcommission on the Systematics of Igneous Rocks: Geology, v. 9, pp. 41-43.

Schmidt, R., and Schminke, H.-U., 2000. Seamounts and Island Building, *in* Sigurdsson, H., 2000, Encyclopedia of Volcanoes: Academic Press, San Diego, California, p. 383-402.

Sigurdsson, H., 2000a. The History of Volcanology, *in* Sigurdsson, H., 2000, Encyclopedia of Volcanoes: Academic Press, San Diego, California, p. 15-37.

Sigurdsson, H., 2000b. Volcanic Episodes and Rates of Volcanism, *in* Sigurdsson, H., 2000, Encyclopedia of Volcanoes: Academic Press, San Diego, California, 271-279.

Sigurdsson, H., and Lopes-Gautier, R., 2000. Volcanoes and Tourism, *in* Sigurdsson, H., 2000, Encyclopedia of Volcanoes: Academic Press, San Diego, California, pp. 1283-1299.

Smellie, J. L., 2000. Subglacial Eruptions, *in* Sigurdsson, H., 2000, Encyclopedia of Volcanoes: Academic Press, San Diego, California, pp. 403-418.

Smith, R. L. and Bailey, R. A., 1968. Resurgent Cauldrons: Geological Society of America Memoir 116, pp 613-662.

Spudis, P. D., 2000. Volcanics on the Moon, *in* Sigurdsson, H., 2000, Encyclopedia of Volcanoes: Academic Press, San Diego, California, p. 697-708.

Spera, F., 2000. Physical Properties of Magmas, *in* Sigurdsson, H., 2000, Encyclopedia of Volcanoes: Academic Press, San Diego, California, p. 171-190.

Tilling, 1985. Volcanoes: United States Geological Survey General Interest Publication.

Tilling, Heliker, and Wright, 1987. Eruptions of Hawaiian Volcanoes – Past, Present, and Future: United States Geological Survey General Interest Publication.

USGS Glossary of Volcano and Related Terminology: United States Geological Survey / Cascades Volcano Observatory, Vancouver, Washington, http://vulcan.wr.usgs.gov/Glossary/volcano_terminology.html

Vallance, J. W., 2000. Lahars, *in* Sigurdsson, H., 2000, Encyclopedia of Volcanoes: Academic Press, San Diego, California, p. 601-616.

Valentine, G. A., and Fisher, R. V., 2000. Pyroclastic Surges and Blasts, *in* Sigurdsson, H., 2000, Encyclopedia of Volcanoes: Academic Press, San Diego, California, p. 571-580.

Vergniolle, S. and Mangan, M., 2000. Hawaiian and Strombolian Eruptions, *in* Sigurdsson, H., 2000, Encyclopedia of Volcanoes: Academic Press, San Diego, California, p. 447-461.

Vespermann, D., and Schminke, H.-U., 2000. Scoria Cones and Tuff Rings, *in* Sigurdsson, H., 2000, Encyclopedia of Volcanoes: Academic Press, San Diego, California, p. 683-694.

Walker, G. P. L., 2000. Basaltic Volcanoes and Volcanic Systems, *in* Sigurdsson, H., 2000, Encyclopedia of Volcanoes: Academic Press, San Diego, California, pp. 283-289.

Walker, G. P. L., and Croasdale, R., 1972. Characteristics of some basaltic pyroclastics: Bulletin of Volcanology, v. 35, p. 303-317.

Wallace, P., and Anderson, A. T., 2000. Volatiles in Magmas, *in* Sigurdsson, H., 2000, Encyclopedia of Volcanoes: Academic Press, San Diego, California, p. 149-170.

White, J. D. L., and Houghton, B., 2000. Surtseyan and Related Phreatomagmatic Eruptions, *in* Sigurdsson, H., 2000, Encyclopedia of Volcanoes: Academic Press, San Diego, California, p. 495-511.

Whitham, A. G., and Sparks, R. S. J., 1986. Pumice: Bulletin of Volcanology, v. 48, p. 209-223.

Williams, H., and McBirney, A. R., 1979. Volcanology: Freeman, Cooper and Co., San Francisco, California, 397 pages.

Wilson, C. J. N., and Houghton, B. F., 2000. Pyroclastic Transport and Deposition, *in* Sigurdsson, H., 2000, Encyclopedia of Volcanoes: Academic Press, San Diego, California, p. 545-554.

Wolf, J. A., and Sumner, J. M.,2000. Lava Fountains and Their Products, *in* Sigurdsson, H., 2000, Encyclopedia of Volcanoes: Academic Press, San Diego, California, p. 321-329.

Zimbelman, J. R., 2000. Volcanism on Mars, *in* Sigurdsson, H., 2000, Encyclopedia of Volcanoes: Academic Press, San Diego, California, p. 771-783.

5. Field Guide References

Aciego, S.M.; Jourdan, F.; DePaolo, D.J.; Kennedy, B.M. , Renne, P.R.; and Sims, K.W.W. 2010 Combined U-Th/He and 40 Ar/39 Ar Geochronology of Post-shield Lavas from the Mauna Kea and Kohala volcanoes, Hawaii; Geochimica et Cosmochimica Acta, *74*(5), p.1620-1635.

AllTrails website, www.alltrails.com .

Babb, J.L., Kauahikaua, J.P., and Tilling, R.I. 2011. The story of the Hawaiian Volcano Observatory—A remarkable first 100 years of tracking eruptions and earthquakes: U.S. Geological Survey General Information Product 135, 60p.

Big Island Hikes website, www.bigislandhikes.com 135

Clague, D.A. and Dalrymple, G.B. 1987. The Hawaiian-Emperor volcanic chain, Part 1, Geologic Evolution; *in* Decker, R.W., Wright, T.L., and Stauffer, P.H., eds., Volcanism in Hawaii: U.S. Geological Survey Professional Paper 1350, v.1, Chapter 1, p.5-54.

Clague, D.A. and Dixon, J.E. 2000. Extrinsic controls on the evolution of Hawaiian ocean island volcanoes; Geochemistry, Geophysics, Geosystems (G3), v.1, no.4, 1010, 9 p.

Clague, D.A., and Moore, J.G. 1991. Geology and petrology of Mahukona Volcano, Hawaii: Bulletin of Volcanology, v. 53, no. 3, p. 159–172.

Clague, D.A.; Paduan, J.B.; Caress, D.W.; Moyer, C.L.; Glazer, B.T.; and Yoerger, D.R. 2019. Structure of Lōʻihi Seamount, Hawai'i and lava flow morphology from high-resolution mapping; Frontiers in Earth Science 7, Article 58, p.1-17.

Clague, D. R. and Sherrod, D.R. 2014. Growth and Degradation of Hawaiian Volcanoes; *in* Characteristics of Hawaiian Volcanoes, Poland, M.P., Takahashi, T.J., and Claire M. Landowski, C.M., editors; U.S. Geological Survey Professional Paper 1801, p.97-146.

Dana, J.D. 1890. Characteristics of volcanoes, with contributions of facts and principles from the Hawaiian Islands; New York, N.Y., Dodd, Mead; 399p. and Co.

Eakins, B.W.; Robinson, J.E.; Kanamatsu, T.; Naka, J.; Smith, J.R.; Takahashi, E.; and Clague, D.A. 2003. Hawaii's volcanoes revealed: U.S. Geological Survey Geologic Investigations Series Map I-2809, 1 plate, *https://pubs.usgs.gov/imap/2809/*.

Easton, R.M. 1978. Stratigraphy and Petrology of the Hilina Formation: The oldest exposed Lavas of Kilauea Volcano; unpublished M.Sc. Thesis, University of Hawaii at Manoa, Honolulu, Hawaii, 274p.

Easton, R.M. 1987. Stratigraphy of Kilauea Volcano; *in* Decker, R.W., Wright, T.L., and Stauffer, P.H., eds., Volcanism in Hawaii: U.S. Geological Survey Professional Paper 1350, v.1, Chapter 11, p.243-260.

Easton, R.M. and Easton, M.G. 1995. Highway Geology of the Hawaiian Islands; Easton Enterprises; 168p.

Easton, R.M. and Garcia, M.O. 1980. Petrology of the Hilina Formation, Kilauea Volcano, Hawaii; Bulletin Volcanologique 43; p.647-673.

Foulger, G.R. and Anderson, D.L. 2006. The Emperor and Hawaiian Volcanic Chains: How well to they fit the plume hypothesis? www.MantlePlumes.org website.

Frey, F.A. and Clague, D A. 1983. Geochemistry of diverse basalt types from Loihi Seamount, Hawaii: petrogenetic implications; Earth Planet. Sci. Lett. 66, p.337–355.

Garcia, M.O., Hanano, D., Flinders, A., Weis, D., and Kurz, M. 2012. Age, geology, geophysics, and geochemistry of Mahukona Volcano, Hawai'i; Bulletin of Volcanology 74, p.1445-1463.

Garcia, M.O.; Kurz, M.D.; and Muenow, D.W. 1990. Mahukona: the missing Hawaiian volcano; Geology, 18: p.1111-1114.

Garcia, M.O., Muenow, D.W., Aggrey, K.E., and O'Neil, J.R. 1989. Major element, volatile, and stable isotope geochemistry of Hawaiian submarine tholeiitic glasses; J. Geophys. Res. 94, p.10525–10538.

Gazdar, Nasir. 2003. Hawaii's Volcanoes Revealed; PowerPoint Presentation, revise 2018.

Hawai'i Tropical Botanical Garden website – www.htbg.com .

Hazlett, Richard. 2014. Explore the Geology of Kīlauea Volcano; Hawai'i Pacific Parks Association, Revised Edition 2014; 146p.

Hazlett, R.W. and Hyndman, D.W. 2007. Roadside Geology of Hawai'i; Mountain Press Publishing Company, MT, 5th Edition (originally published in 1996), 304p.

Head, J.W. and Wilson, L. 1989. Basaltic pyroclastic eruptions: Influence of gas-release patters and volume fluxes on fountain structure, and the formation of cinder cones, spatter cones, rootless flows, lava ponds, and lava flows; J. Volcanol. Geotherm. Res. 37: p.261-271.

Holcomb, R.T. 1976. Preliminary map showing products of eruptions, 1962-1974 from the upper east rift zone of Kilauea volcano, Hawaii: US Geological Survey Map MF-811, 1:24,000.

Holcomb, R.T. 1987. Eruptive history and long-term behavior of Kilauea volcano; *in* Decker, R.W., Wright, T.L., and Stauffer, P.H., eds., Volcanism in Hawaii: U.S. Geological Survey Professional Paper 1350, v.1, Chapter 12, p.261-350.

Jackson, E.D., Clague, D.A., Engleman, E., Friesen, W.F., and Norton, D. 1981. Xenoliths in the alkalic basalt flows of Hualalai Volcano, Hawaii; U.S. Geological Survey Open File Reports, 81-1031; 33p.

Kirby, S.H. and Green, H.W. 1980. Dunite xenoliths from Hualalai Volcano: Evidence for mantle diapiric flow beneath the island of Hawaii; American Journal of Science, 280-A: p.550-575.

Lockwood, J.P. and Hazlett, R.W. 2010. Volcanoes: Global Perspectives; John Wiley & Sons, 541p.

Love Big Island website, www.lovebigisland.com .

Macdonald, G.A., Abbott, A.T., and Peterson, F.L. 1983. Volcanoes in the Sea – The Geology of Hawaii: Second Edition, University of Hawaii Press, Honolulu, HI, 517p.

MacTavish, A.D. 2019. Unpublished geological field notes, July 30 to August 9, 2019.

MacTavish, A.D. 2020. Unpublished geological field notes, February 11 to 21, 2020.

Malahoff, A. 1987. Geology of the summit of Loihi submarine volcano; *in* R.W. Decker, T.L. Wright, and P.H. Stauffer, eds., Volcanism in Hawaii: USGS Professional Paper 1350, v.1, Chapter 6, p.133–144.

Mattox, S. 1994. A teacher's guide to the geology of Hawaii Volcanoes National Park. (Activity 4.2). Honolulu, HI: Hawai'i Natural History Association.

Merguerian, C. and Okulewicz, S. 2007. Geology of Hawaii; Hofstra University, Geology 280F – Field Trip Guidebook, Summer Session Two – 23 July to 02 August 2007; 137p.

Moore, J.G. and Clague, D.A. 1992. Volcano growth and evolution of the island of Hawaii; Geological Society of America Bulletin 1992; 104, no. 11, p.1471-1484.

Moore, J.G., Clague, D.A., Holcomb, R.T., Lipman, P.W., Normark, W.R., and Torresan, M.E. 1989. Prodigious submarine landslides on the Hawaiian Ridges; Journal of Geophysical Research, 94: p.17465-17484.

Moore, J.G., Normark, W.R., and Lipman, P. W. 1979. Loihi Seamount – a young submarine Hawaiian volcano; *in* Proceedings of the Hawaii Symposium on Intraplate Volcanism and Submarine Volcanism, Hilo, 127p.

Morgan, W.J. 1971. Convection plumes in the lower mantle; Nature 230, p.42-43.

Hawai'i Volcanoes National Park Illustrated Trails Map. 2010. National Geographic Trails Illustrated Map 230.

Peterson, D.W. and Moore, R.B. 1987. Geologic history and evolution of volcanic concepts, Island of Hawaii; *in* Decker, R.W., Wright, T.L., and Stauffer, P.H., eds., Volcanism in Hawaii: U.S. Geological Survey Professional Paper 1350, v.1, Chapter 7, p.149-189.

Pu'u Wa'awa'a Ahupua'a'Ōhi'a Cone Trail System Visitor Guide.

Robinson, J.E. and Eakins, B.W. 2006. Calculated volumes of individual shield volcanoes at the young end of the Hawaiian Ridge; *J. Volcanol. Geotherm. Res.*, 151: p.309-317.

Robinson, R.C. 2010. Illustrated Geological Guide to the Island of Hawaii; Santa Monica College; 287p.

Robinson, R.C. 2012. Hawaii Volcanoes National Park, A Geologic Guide; 70p.

Rowland, S.K. and Munro, D.C. 1993. The 1919-1920 eruption of Maunaiki, Kilauea: chronology, geologic mapping, and magma transport mechanism; Bulletin of Volcanology, v.55, p.190-203.

Schmincke, H-U. 2004. Volcanism; Springer-Verlag, 324p.

Seach, J. 2022. www.volcanolive.com website, list compiled by John Seach.

Stearns, H.T. 1946. Geology of the Hawaiian Islands; Hawaii Div. Hydrogr. Bull. 8: 105p.

Swanson, D.A. and Christianson, R.L. 1973. Tragic base surge in 1790 at Kilauea volcano; Geology, v.1, p.83-86.

Temblor.net Website. 2018. USGS Volcanic Hazard Map from Lava Flows (2010).

Tilling, R.I., Heliker, C., and Swanson, D.A. 2010. Eruptions of Hawaiian Volcanoes – Past, Present, and Future: U.SW. Geological Survey General Information Product 117, 63p.

USGS Hawaiian Volcano Observatory (HVO) Website. Evolution of Hawaiian Volcanoes. www.usgs.gov/observatories/hvo

US National Park Service (NPS), Hawai'i Volcanoes National Park.

- Kīlauea Iki Trail Guide.
- Kipukapuaulu Trail Guide
- Mauna Ulu Eruption Guide.

Will Seaborn, Visualization Artist and Photographer. 2016. www.willseaborn.com website.

Walker, G.P.L. 1990. Geology and volcanology of the Hawaiian Islands; Review Article, Pacific Science, vol. 44, no. 4: p.315-347.

White, J. D. L. and Houghton, B. 2000. Surtseyan and Related Phreatomagmatic Eruptions, *in* Sigurdsson, H., 2000, Encyclopedia of Volcanoes: Academic Press, San Diego, California, p. 495-511.

Wikipedia. 2022. Evolution of Hawaiian Volcanoes; 7p.

Dark Tourism website, www.darktourism.com .